Les relations de phase dans les métapelites de haute pression. Approche expérimentale et naturaliste, conséquences géodynamiques pour les Alpes occidentales.

Christian Chopin

CHOPIN (Ch.)

N° 85 -11

THESE DE DOCTORAT D'ETAT ES SCIENCES NATURELLES

présentée

à l'Université Pierre et Marie Curie - Paris 6 -

par

Christian CHOPIN

pour obtenir le grade de DOCTEUR ES SCIENCES

Sujet de la thèse :

LES RELATIONS DE PHASES DANS LES METAPELITES DE HAUTE PRESSION

Approche expérimentale et naturaliste, conséquences géodynamiques

pour les Alpes occidentales

Soutenue le 15 mars 1985

Devant le jury composé de :

J. KORNPROBST, Président et rapporteur
W. SCHREYER, Rapporteur
B. VELDE, Rapporteur
B.W. EVANS, Examinateur
G. GUITARD, Examinateur
X. LE PICHON, Examinateur
P. VIALON, Examinateur

RESUME

L'étude des métapélites de haute pression des Alpes occidentales révèle une variété considérable de degrés métamorphiques, depuis un domaine à Fe-Mg-carpholite, un domaine intermédiaire à chloritoïde magnésien-talc-phengite, jusqu'à un domaine où sont stables la coesite, le pyrope et l'ellenbergerite, $(Mg,Ti,\square)_2Mg_6Al_6Si_8O_{28}(OH)_{10}$, nouveau mineral du système pélitique.

L'étude expérimentale du système $MgO-Al_2O_3-SiO_2-H_2O$ a permis la synthèse de Mg-carpholite, Mg-chloritoïde et pyrope, et la détermination de leur stabilité et relations de phases entre 480 et 800°C, 15 et 40 kbar.

Appliquées aux systèmes naturels et associées à de nouvelles datations (^{39}Ar-^{40}Ar), ces données sont intégrées dans un schéma évolutif de la chaîne alpine impliquant l'enfouissement de croûte continentale à près de 100 km de profondeur.

MOTS-CLES : métapélites, haute pression, Alpes occidentales, pétrologie, étude expérimentale, système $MgO-Al_2O_3-SiO_2-H_2O$, Mg-carpholite, Mg-chloritoïde, pyrope, coesite, ellenbergerite.

N° 85 -11

THESE DE DOCTORAT D'ETAT ES SCIENCES NATURELLES

présentée

à l'Université Pierre et Marie Curie - Paris 6 -

par

Christian CHOPIN

pour obtenir le grade de DOCTEUR ES SCIENCES

Sujet de la thèse :

LES RELATIONS DE PHASES DANS LES METAPELITES DE HAUTE PRESSION

Approche expérimentale et naturaliste, conséquences géodynamiques

pour les Alpes occidentales

Soutenue le 15 mars 1985

Devant le jury composé de :

J. KORNPROBST, Président et rapporteur

W. SCHREYER, Rapporteur
B. VELDE, Rapporteur
G. GUITARD, Examinateur
X. LE PICHON, Examinateur
P. VIALON, Examinateur

"Je voudrais savoir bien des choses : (...) ce qu'est au juste cette cause occulte que nous appelons métamorphisme et comment des sédiments vils et laids, argiles, sables ou calcaires, sont devenus ces roches somptueusement cristallisées qui alternent, sous nos yeux, avec les granites et leur font cortège. Ah ! mon ami, quelle joie quand nous saurons tout cela !"

Paroles attribuées à Urbain Le Verrier
par Pierre Termier.

Table des matières

DEUXIEME PARTIE

TROISIEME PARTIE

Avant-propos et remerciements

Puis vinrent les derniers bivouacs de la saison. Dans quelques jours les cieux délavés de la Westphalie allaient succéder aux nuits étoilées de la Haute Maurienne. La fin d'une époque, pensais-je, adieu belle pétrographie alpine ! Deux ans plus tard le travail accompli n'avait été, en fait, que le strict prolongement des études alpines, la suite logique de la démarche du pétrographe qui passe de la nature au laboratoire pour éprouver les hypothèses. Puis c'est un nouveau sentiment de rupture. En rentrant en France il me faut délaisser l'expérimentation à haute pression. Avec le recul de trois années, on se demande justement où est la rupture. Par délà les discontinuités subjectives, l'unité du travail existe bien. Si j'ai donc pu poursuivre mes chimères favorites, je le dois à la rencontre de plusieurs génies bienfaisants :

- à toi Bruce Velde, tout d'abord, qui ne t'es pas opposé à ce que le travail que tu dirigeais prenne, à la suite d'une découverte heureuse, un cours bien différent de ce qu'il eût dû être. Les résultats ont dépassé mes espérances ; j'espère que tu peux en dire autant.

- à vous Werner Schreyer, qui m'avez accueilli pendant plus de deux ans dans votre laboratoire en m'y accordant une confiance et une liberté totales. Vous avez suivi l'évolution de ce travail en partageant mon enthousiasme. Vous avez été un interlocuteur privilégié et je suis particulièrement heureux que vous ayez accepté de juger ce mémoire en connaissance de cause.

- à toi Martine, qui m'as accueilli dans ton équipe comme peu de gens savent le faire : chacun ici connaît ton souci d'assurer les meilleures conditions de travail et d'entretenir une ambiance chaleureuse. Pour la vigilance de ton amitié, pour ton constant soutien matériel, sans entrave à mon indépendance, pour avoir su ainsi épanouir ma vocation, tu as toute ma gratitude et mon admiration.

Ma reconnaissance va vers vous aussi, Pierre Vialon, arpenteur de Dora Maira. Ce travail doit beaucoup au vôtre, même si vous vous en défendez, et vous me faites grand plaisir de participer à mon jury.

Je suis heureux, Jacques Kornprobst, que vous ayez accepté d'appliquer votre compétence à l'examen de ce travail. Vous me faites l'honneur d'être le président de ce jury, j'espère que ce sera l'occasion d'établir une solution solide plus continue entre les pôles clermontois et parisien de la pétrographie !

Je ne saurais oublier, professeur Jauzein, que vous avez été un directeur de laboratoire accueillant et bienveillant, et que mon travail a pu se réaliser "chez vous", à l'Ecole, dans d'excellentes conditions. Le Mâconnais n'est pas ennemi du Beaujolais !

Dans vos nouvelles fonctions de directeur du laboratoire, professeur Le Pichon, vous avez accepté de donner votre avis sur un travail a priori éloigné de vos préoccupations scientifiques et je vous en remercie. Bien que nos échelles d'observation soient différentes, c'est la même dynamique du globe que nous cherchons à comprendre.

Un travail scientifique ne peut être que le reflet de multiples influences. Je pense d'abord à toi, Pierre Saliot, avec qui tout a commencé. Tu m'as fait découvrir la géologie alpine et la montagne. Comme tu vois, je n'en suis pas encore lassé.

Ma vocation de pétrographe tient aux journées passées sur le terrain en ta compagnie éclairée, Michel Demange. Elle doit beaucoup aussi à la lecture de vos beaux articles, professeur Guitard ; merci à vous d'être encore une fois l'un de mes juges.

Les joies de la prospection et l'enthousiasme de la découverte, je les ai pleinement partagés avec toi, Bruno (même si curieusement cela n'apparaît guère dans nos publications). Merci de ton amitié et de ton soutien si efficace dans les dernières longueurs de cette course de fond.

Je garde des "années allemandes" un souvenir heureux et c'est à la qualité de votre accueil que je le dois : Irmgard, Dominique et Volker, Conny, Barbara et Peter, Hans-Joachim, Peter encore, quelle amitié que la vôtre !

Que dire de votre merveilleux accueil à Seattle, Sheila et Bernard Evans, sinon que celui qui ne vous a entendu chanter en chœur au petit déjeuner ignore une des joies de l'existence.

Je voudrais vous dire aussi, Henri Maluski et Patrick Monié les "argonautes", Rolf Klaska, Olaf Medenbach, Philippe Gillet, Bill Murphy, quel plaisir c'est de travailler avec vous.

O vous, Jacqueline, déesse aux mille bras et au doux sourire, quels épithètes suffiraient à dire votre célérité et votre enthousiasme à terrasser les manuscrits et à forger les légendes?

Grâce à ta chimie 4 étoiles et 4 pipettes, Nicole, bien des minéraux ont livré leur secret ; grâce à ton art du pointillisme, mes figures se sont vues achevées ; grâce à l'éclat de ton rire et à ta disponibilité, bien des choses se sont réalisées.

Grâce à voûs et votre compétence, Elisabeth, Hélène, Yann, Jacques Cassareuil, la citrouille est devenue carrosse, mes cailloux des lames minces comme on en voit peu, mon manuscrit et mes figures un mémoire de thèse.

Grâce à vous, Doudou et M. Berthet, les photocopies sont parvenues à bon port avant le douzième coup de minuit. Merci à toi, Christian Robert, pour ton aide de la vingt-cinquième heure.

Enfin, merci à toi, Dorothée (10 mois) de ne pas avoir, malgré la grande envie que tu en avais, dévoré tous mes papiers. Quant à vous, mes parents, et toi, mon épouse, ma gratitude va vers vous pour votre aide et à bien des titres encore...

INTRODUCTION

Dans l'étude des terrains métamorphiques, les roches pélitiques et les roches basiques retiennent particulièrement l'attention du pétrographe. Les premières sont originellement un sédiment composé d'argiles et de quartz en proportions variables, les secondes généralement des roches magmatiques intrusives ou effusives. Toutes deux ont l'intérêt d'être abondantes à l'affleurement et surtout de constituer des systèmes chimiques réagissant sensiblement aux variations de paramètres intensifs tels que température et pression.

Ainsi, à basse pression et température croissante, l'apparition, la disparition ou les variations de composition dans les pélites de toute une succession de minéraux ou associations "index", tels que chlorite, cordiérite, silicate d'alumine, grenat, feldspath potassique - sillimanite, etc... a conduit à l'établissement de "grilles pétrogénétiques" très fines. Celles-ci permettent des comparaisons qualitatives extrêmement précises et, en s'appuyant sur des travaux expérimentaux qui ont connu leur apogée dans les années 70, des estimations quantitatives sérieuses.

A haute pression, dans les schistes bleus, les études se sont concentrées sur les roches basiques dont la composition est très favorable à l'apparition d'associations éclogitiques ou de minéraux index comme la glaucophane, la lawsonite ou la jadéite. C'est ainsi que les traités de pétrologie, même les plus récents (Winkler, 1979 ; Turner, 1981), enseignent qu'en l'absence de Na et Ca, nécessaires à l'apparition de ces minéraux, les roches pélitiques ne présentent pas à haute pression de variations minéralogiques significatives. Les résultats exposés dans les pages qui suivent réfutent cette affirmation.

Mes travaux ont pour la plupart déjà été publiés sous forme d'articles qui sont placés en annexe. Ce mémoire n'est donc pas destiné à les présenter de nouveau ; seuls les observations et les résultats expérimentaux inédits sont exposés avec quelque détail. Les articles ayant nécessairement entraîné une fragmentation de l'information, l'esprit de ce bref mémoire est de présenter dans leur ensemble et de manière synthétique les résultats acquis et leurs conséquences.

Dans une première partie pétrographique, il est montré, sur l'exemple des Alpes occidentales, que les minéraux des métapélites présentent dans leur nature, leur composition et leurs associations autant

de diversité à haute pression qu'à basse pression, ceci allant jusqu'à la découverte de nouvelles espèces. A grands traits, leur évolution est présentée à métamorphisme croissant jusque dans le domaine de la coesite.

Dans une deuxième partie, la signification en termes de pression et de température de ces associations nouvelles est abordée par voie expérimentale, par une étude des relations de phases de la carpholite, du chloritoïde et du pyrope dans le système limitant $MgO-Al_2O_3-SiO_2-H_2O$ entre 15 et 40 kbar, 480 et 800°C.

La combinaison de ces approches pétrographique et expérimentale conduit au résultat surprenant que des roches sédimentaires ont pu être enfouies à des profondeurs de 100 km environ avant de revenir à la surface, ce qui double les valeurs de pression envisagées jusqu'alors pour le métamorphisme de telles roches. Dans la troisième partie, les conséquences géodynamiques de ces résultats sont envisagées dans le cadre de la chaîne alpine, à la lumière de nouvelles données radiochronologiques.

Première partie

ETUDE PETROGRAPHIQUE DES METAPELITES DANS LA ZONE PENNIQUE INTERNE DES ALPES OCCIDENTALES

Une caractéristique des domaines métamorphiques de haute pression est qu'une tectonique tangentielle importante les affecte postérieurement à la culmination en pression du métamorphisme. C'est probablement la raison même de la préservation des paragenèses correspondantes (Goffé et Velde, 1984, par exemple). La reconstitution de la progression métamorphique originelle est alors comme la reconstitution d'un vaste puzzle dont les pièces ont été dispersées et certaines irrémédiablement perdues. Le pétrographe glane les éléments d'information d'une unité tectonique à l'autre et, par un raisonnement thermodynamique élémentaire, il les ordonne et essaie de combler les "blancs". Dans cette première approche qui est celle du chimiste, le puzzle n'a que deux dimensions, pression et température. En fait, rien ne prouve que les associations provenant d'unités différentes ont cristallisé au même moment. La considération du facteur temps est donc indispensable pour passer de la chimie à la géologie. Dans les domaines internes où les archives stratigraphiques ont disparu, l'apport de la radiochronologie sera donc essentiel.

Dans cette première partie, l'approche du chimiste est privilégiée : nous nous intéressons à l'évolution purement minéralogique d'un système chimique. Pour la raison évoquée précédemment, seules quelques étapes de cette évolution sont documentées. Elles sont présentées ici à métamorphisme croissant à partir de l'étude pétrographique de trois secteurs du domaine pennique interne des Alpes occidentales : la Haute Maurienne (massif du Grand Paradis), le haut Val d'Ayas (massif du Mont Rose) et le bas Val Pô (massif de Dora Maira). Afin de présenter une image synthétique de cette évolution minéralogique, les résultats obtenus par B. Goffé dans le domaine pennique plus externe (Vanoise et Briançonnais ligure) sont d'abord rappelés succinctement. En effet, ils couvrent les tout premiers stades de cette évolution et fournissent un élément de comparaison important ; de plus, certains des travaux expérimentaux présentés dans la dernière partie s'y appliquent directement. Bien que cette évolution minéralogique ne soit envisagée dans son cadre géologique que dans la troisième partie, la figure 1 permet au lecteur de situer dans la chaîne alpine les régions étudiées.

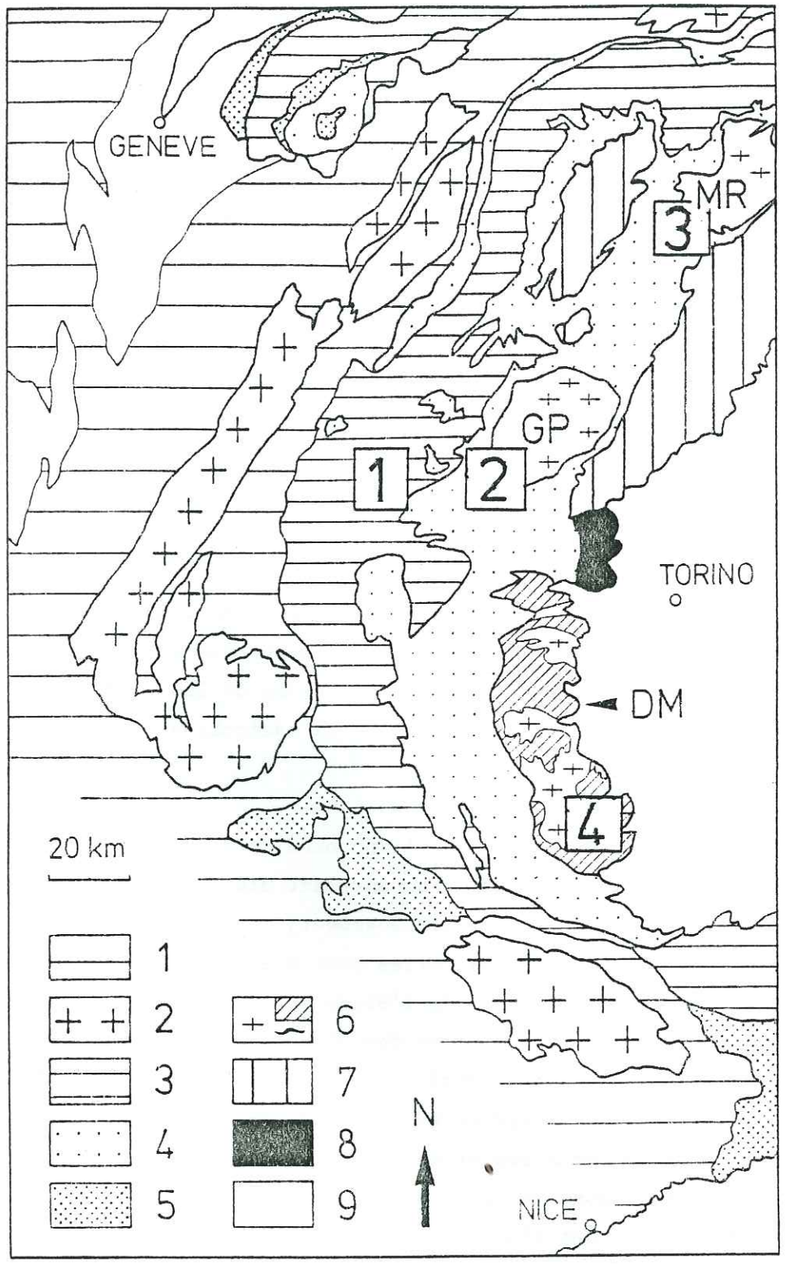

Fig. 1. Localisation dans les Alpes occidentales des principaux domaines étudiés :
Chiffres encadrés. 1 : Vanoise (Goffé, 1982) ; 2 : Haute Maurienne (Chopin, 1979, 1981) ; 3 : haut Val d'Ayas (Chopin et Monié,1984) ; 4 : Val Pô (Chopin, 1984, 1985).
Légende de la carte structurale : Zone externe : (1) chaînes subalpines et avant-pays plissé, (2) massifs cristallins externes. Domaine pennique : (3) Briançonnais, socle et couverture indifférenciés, (4) nappe des Schistes lustrés, (6) massifs cristallins internes, Mont Rose MR, Grand Paradis GP, Dora Maira DM. (5) Flysch à Helminthoïdes. Austroalpin : (7) d'Est en Ouest la zone Sesia, klippe du Mont Emilius et nappe de la Dent Blanche. (8) Massif ultrabasique de Lanzo. (9) bassins molassiques tertiaires.

I - LE SYSTEME D'ETUDE

En renonçant délibérément à l'étude des roches basiques, mon but était de m'affranchir des constituants CaO et Na_2O, afin de limiter la variance des associations étudiées et d'approcher autant que possible certains systèmes expérimentaux. L'application de cette stratégie d'échantillonnage parmi la variété des roches pélitiques s'est révélée très fructueuse ; c'est pourquoi la plupart des échantillons étudiés sont bien représentés par le système K_2O-FeO-MgO-Al_2O_3-SiO_2-H_2O (K-FMASH), quelques uns parmi les plus riches en fer nécessitant l'addition du constituant Fe_2O_3. Le constituant TiO_2 est toujours en excès, exprimé sous forme de rutile ; sauf mention explicite, il en est de même pour la silice, sous forme de quartz.

De plus, j'ai montré (Chopin, 1981 a, Fig. 10) que l'extension à haute pression de la substitution phengitique SiMg = AlAl dans le mica blanc limitait l'apparition de la biotite aux roches très pauvres en aluminium. Ainsi, à la grande différence des métapélites de basse pression, la seule phase potassique présente à haute pression dans les roches pélitiques est la phengite. En l'absence d'une autre phase potassique, la substitution phengitique n'y atteint pas la valeur maximale pour ces conditions de pression et température, mais on peut en déduire une valeur minimale de la pression de formation grâce aux travaux expérimentaux de Velde (1965) et de Massonne (1981). Une fois considéré cet aspect barométrique, la phase phengite et le constituant K_2O peuvent être négligés, ce qui ramène l'étude à celle du système FeO-MgO-Al_2O_3-SiO_2-H_2O.

En termes de phases, la pélite de départ peut s'exprimer simplement comme un mélange d'eau, de quartz, d'illite, de chlorite, éventuellement de kaolinite (par exemple, Fonteilles, 1976). La transformation de l'illite en phengite survient précocement dans l'évolution métamorphique et laisse un résidu essentiellement silico-alumineux. En négligeant la phengite pour nous ramener au système FMASH, nous pouvons donc considérer qu'une fraction de kaolinite était toujours présente initialement. C'est donc l'évolution d'un mélange chlorite-kaolinite-quartz en proportions variables et de rapport Fe/Mg variable qui est envisagée dans ce mémoire. Les principaux minéraux

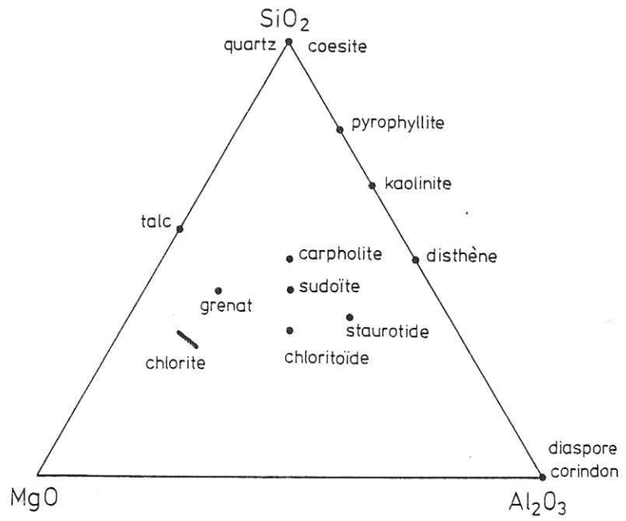

Fig. 2. Les principaux minéraux du système (FeO, MgO) - Al_2O_3-SiO_2 - H_2O rencontrés dans ce travail à partir du constituant H_2O.

Liste des abréviations utilisées :

And	: andalousite	En	: enstatite	Q	: quartz
Car	: carpholite	Jad	: jadéite	Sill	: sillimanite
Chl	: chlorite	Ky	: disthène	Sud	: sudoïte
Ctd	: chloritoïde	Law	: lawsonite	Tc	: talc
Cs	: coesite	Py	: pyrope	V	: fluide H_2O
Dee	:deerite	Pyroph	: pyrophyllite		

rencontrés par la suite sont représentés dans la projection de la figure 2.

II - LE DOMAINE DE LA CARPHOLITE : HAUTE PRESSION ET BASSE TEMPERATURE.

Dans les domaines de haute pression caractérisés par la présence de minéraux de basse température comme lawsonite, pyrophyllite, diaspore, par l'extrême rareté du grenat et par l'absence d'associations éclogitiques dans les roches basiques, la minéralogie des métapélites est dominée par l'importance des carpholites ferro-magnésiennes $(Fe,Mg)Al_2Si_2O_6(OH)_4$, associées ou non au chloritoïde. De découverte récente (De Roever, 1951, pour la ferrocarpholite ; Goffé et al., 1973, pour la magnésiocarpholite), ce minéral n'a vu son importance reconnue que récemment (Goffé et Saliot, 1977 ; De Roever, 1977 ; Viswanathan et Seidel, 1979). On se mit à le chercher et les quelques fins limiers sachant sur le terrain distinguer ce minéral de l'actinote le trouvèrent, cette fois à profusion, que ce soit dans le Briançonnais ou en Oman (Goffé), en Calabre (De Roever), en Crète ou dans le Péloponnèse (Seidel). Une bibliographie exhaustive est donnée dans Chopin et Schreyer (1983, Tableau I). Pour les roches strictement alpines, le lecteur est renvoyé au travail très complet de Goffé (1982).

1 - L'évolution générale

A partir d'une analyse théorique du système, nous avons proposé (Chopin et Schreyer, 1983) les principales étapes suivantes pour l'évolution commençante des métapélites de haute pression :

- apparition de ferrocarpholite et enrichissement progressif en magnésium aux dépens de chlorite + pyrophyllite (ou kaolinite) ; le chloritoïde n'est pas encore stable (Fig. 3a). Cet état paraît documenté dans les Célèbes (De Roever, 1951), le Nord de la Calabre (De Roever et Beunk, 1978), la Crète orientale (Seidel, 1978) et les Schistes lustrés de Haute Ubaye (Steen et Bertrand, 1977).
- apparition de chloritoïde + quartz aux dépens de la ferrocarpholite ; coexistence du chloritoïde toujours ferreux avec une carpholite de plus en plus magnésienne. L'association chlorite-pyrophyllite, si caractéristique à basse pression, n'existe plus (Fig. 3b). Cette situation est la plus fréquemment rencontrée dans les domaines à carpholite (voir

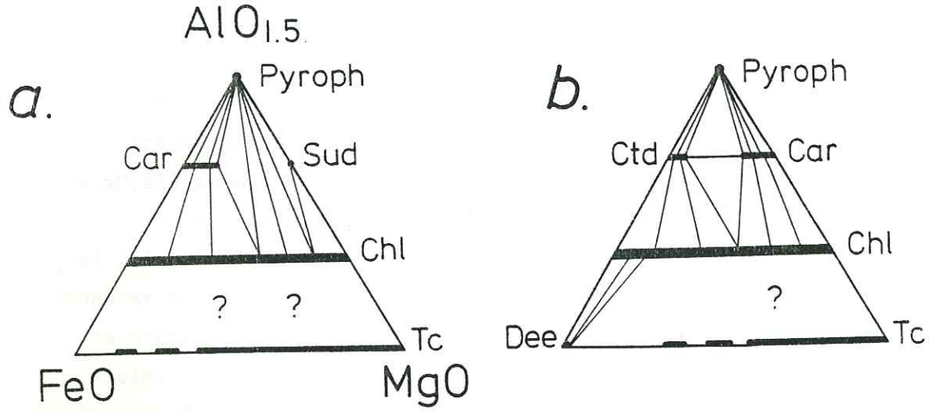

Fig. 3. Relations de phases dans les domaines à carpholite.

a - A faible degré de métamorphisme : le chloritoïde est instable, la ferrocarpholite se forme par la réaction d'hydratation

pyrophyllite + chlorite + H_2O → Fe - carpholite + quartz

qui ne peut être que favorisée par la pression. La sudoïte est probablement présente dans les compositions magnésiennes (ou très oxydées).

b - A degré plus élevé : les carpholites magnésiennes sont devenues stables, les ferreuses se déstabilisent en chloritoïde selon la réaction continue carpholite → chloritoïde + quartz + H_2O
La sudoïte n'est probablement plus stable ; la deerite est présente dans les compositions ferrifères.
SiO_2 et H_2O en excès.

Chopin et Schreyer, 1983), dans les Alpes en particulier.

L'existence dans la nature de domaines à ferrocarpholite sans chloritoïde et d'autres à Fe/Mg-carpholites et chloritoïde démontre la validité de cette analyse. Néanmoins, le travail de Goffé (1982) montre que le deuxième stade peut aussi être atteint sans passer par l'intermédiaire du premier. Dans ce cas, le chloritoïde se forme concurremment à la carpholite à partir de chlorite-pyrophyllite et non à partir de ferrocarpholite. Ce télescopage de réactions peut s'expliquer simplement par une montée en pression et température particulièrement rapide : le champ de nucléation du chloritoïde est alors atteint avant qu'il y ait eu nucléation importante de ferrocarpholite.

2 - Une inversion du fractionnement Fe-Mg

Une conséquence de l'analyse présentée est très remarquable : le passage de la figure 3a à 3b suppose en effet l'inversion du sens de partage Fe-Mg entre carpholite et chlorite, ce qui implique la non-idéalité de l'une ou l'autre de ces solutions solides. Si une telle non-idéalité n'est pas très étonnante dans un minéral comme la staurotide (cf. IV et Grambling, 1983) où fer et magnésium sont accueillis dans des sites octaédriques et tétraédriques, elle est plus surprenante dans les structures carpholite ou chlorite où les sites occupés par Fe et Mg sont plus homogènes car tous octaédriques. Cette inversion est néanmoins réelle puisque Goffé a pu depuis la mettre en évidence en Oman (comm. pers., 1984).

3 - Le rôle de la sudoïte

La découverte d'une association sudoïte-pyrophyllite-quartz, toujours par Goffé en Oman, est venue corroborer une autre de nos anticipations concernant le rôle possible de la sudoïte dans les métapélites (Chopin et Schreyer, 1983, p. 86). Cette chlorite di-trioctaédrique $Mg_2Al_3Si_3AlO_{10}(OH)_8$ (cf. Fig. 2) présente dans des séries pélitiques de basse pression (Ardennes : Fransolet et Bourguignon, 1978 ; Harz : Kramm, 1980) est chimiquement équivalente à la carpholite selon la réaction

sudoïte + quartz = Mg-carpholite (1)

Cette réaction qui fait passer tout l'aluminium en site octaédrique ne libère pas d'eau. Elle se fait avec une diminution de volume considérable,

de plus de 6%, et doit donc être très dépendante de la pression. Ce pouvait être une des réactions limitant inférieurement en pression le champ de stabilité de la Mg-carpholite (Chopin et Schreyer, 1983). L'existence d'un domaine de stabilité pour la sudoïte (Fransolet et Schreyer, 1984) et la découverte de ce minéral dans des régions à carpholite, en Oman (Goffé, comm. pers.) et en Crète (Seidel, cité par Fransolet et Schreyer, 1984), viennent confirmer ce point de vue. Ainsi, pour les compositions les plus magnésiennes (puisque la sudoïte semble être exclusivement magnésienne), chlorite et kaolinite formeront, à pression et température croissantes, d'abord sudoïte + quartz puis carpholite magnésienne (voir figure 3a).

4 - **Les milieux ferrifères**

L'évolution des compositions riches en fer est mal documentée dans ce domaine de pression et température, elle dépend de plus de l'état d'oxydation du système. Dans les milieux oxydés, l'hématite est présente avec, par exemple, chloritoïde et chlorite ferreux (Goffé, 1982). Dans les milieux moins oxydés, la deerite $Fe^{2+}_{12}Fe^{3+}_{6}Si_{12}O_{40}(OH)_{10}$ est stable, comme en témoigne la minéralogie d'un hard-ground de Vanoise où les "longues aiguilles opaques" signalées par Ellenberger (1958) ont été identifiées à la deerite (Bocquet, 1973). Elles sont associées à une chlorite très ferreuse (chamosite). Pour rendre la figure 3 aussi complète que possible, j'ai supposé, par analogie avec les "iron-formations" faiblement métamorphisées (e.g. Gole, 1981), que la solution solide talc-minnesotaïte est presque complète.

Il faut remarquer que le grenat est absent de toute cette évolution, ce qui reflète la faiblesse des températures. Son apparition dans les pélites est néanmoins documentée dans le Péloponnèse où la relative richesse en Mg du chloritoïde (20-25% du pôle magnésien) coexistant avec la magnésiocarpholite est aussi un indice d'évolution plus avancée (Seidel, 1981). Mais la richesse en manganèse du grenat exclut cette phase du système d'étude ; le grenat purement almandin n'est probablement pas stable.

5 - **La réactivité du système**

Comme en témoignent les métabauxites associées, les différentes étapes de l'évolution précédente se déroulent dans le champ de stabilité

de l'association pyrophyllite-diaspore donc à des températures inférieures à 350°C (Halbach et Chatterjee, 1982). Pour des températures allant de 200 (?) à 350°C, la déshydratation progressive de l'association chlorite -kaolinite fait apparaître successivement dans les pélites deux minéraux index,la ferrocarpholite (12% H_2O) et le chloritoïde (7% H_2O); de plus, la composition de la carpholite associée au chloritoïde passe progressivement des plus ferreuses aux plus magnésiennes. Cette combinaison de réactions continues et discontinues fournit d'excellents instruments d'étude et démontre la réactivité du système pélitique à haute pression, dès les basses températures.

Un avant-goût de l'évolution ultérieure nous est donné (hors des Alpes) par l'association réactionnelle chloritoïde-magnésiocarpholite- chlorite-disthène-quartz décrite par Okrusch (1981) à Samos, qui est unique à deux titres. C'est la seule association à carpholite où le silicate d'alumine est le disthène et non la pyrophyllite ; c'est aussi la seule où le chloritoïde est nettement magnésien (plus de 30% du pôle Mg-chloritoïde). On peut donc présumer qu'à métamorphisme croissant la pyrophyllite disparaît dans le champ de la carpholite puis que le joint carpholite-chloritoïde est rompu au profit de chlorite-disthène après un certain enrichissement en magnésium du chloritoïde.

III - LES DOMAINES A TALC-CHLORITOIDE : HAUTE PRESSION ET TEMPERATURE MODEREE

Un stade plus avancé de l'évolution est représenté en Haute Maurienne, dans le massif cristallin interne du Grand Paradis et les Schistes lustrés "océaniques" qui le surmontent directement. Cette région, en dépit de la proximité immédiate de la Vanoise, constitue véritablement un autre monde : les minéraux sont gros, la carpholite, la pyrophyllite, la lawsonite sont absentes, le grenat et le chloritoïde sont abondants, le seul silicate d'alumine est le disthène et des associations éclogitiques sont présentes dans les roches basiques. En quelques kilomètres, on passe donc de schistes bleus de bas degré ou basse température à des schistes bleus de haut degré (Chopin, 1979).

Le trait minéralogique essentiel des métapélites de ce domaine est l'existence de l'association talc-chloritoïde. Cette association est paradoxale puisqu'elle réunit un minéral caractéristique des milieux magnésiens et pauvres en alumine et un minéral considéré comme typique dans les milieux riches en fer et en alumine. Effectivement, cette assocation est complètement inconnue dans les séries métamorphiques classiques de pression basse à intermédiaire. Jusqu'à sa découverte récente en U.R.S.S. dans la chaîne du Tien Shan (Korikovskiy et al., 1983), elle était même exclusivement connue dans le domaine pennique interne des Alpes occidentales (Bearth, 1963, 1967) et orientales (Miller, 1974, 1977). Curieusement, sa signification théorique n'a pas été envisagée par ces auteurs et à peine discutée par Chinner et Dixon (1973), alors qu'elle est la clef de toute l'évolution des métapélites dans les schistes bleus de haut degré (Chopin, 1979, 1981 ; Chopin et Schreyer, 1983 ; Chopin et Monié, 1984). Les paragraphes qui suivent résument ces articles et fournissent quelques indications supplémentaires sur la partie ferreuse du système.

1 - L'instabilité de chlorite + quartz

Dans le domaine envisagé, l'évolution minéralogique repose sur la disparition progressive de l'association chlorite-quartz. Les chlorites les plus ferreuses disparaissent au profit de talc-grenat, puis les chlorites intermédiaires au profit de talc-chloritoïde, alors que les chlorites magnésiennes sont encore stables en présence de quartz. Les

champs divariants caractéristiques qui en résultent sont talc-chloritoïde-grenat et talc-chloritoïde-chlorite (Fig. 4 a) ; ils se déplacent progressivement vers les compositions magnésiennes par le jeu des réactions

chloritoïde + talc --> grenat + quartz + H_2O (2)

et surtout

chlorite + quartz --> talc + chloritoïde + H_2O. (3)

Cette dernière réaction de déshydratation se fait avec diminution de volume et fait donc apparaître talc-chloritoïde comme un équivalent de plus haute température et de plus haute pression que chlorite-quartz. De plus, on peut écrire

chlorite + disthène --> talc + chloritoïde (4)

réaction qui se produit sans libération d'eau mais avec une diminution de volume de 3 à 4% aux dépens d'une association (chlorite-disthène) très commune dans les domaines métamorphiques de pression intermédiaire (Chopin et Schreyer, 1983). Les températures envisagées n'ayant rien d'exceptionnel, la stabilité de l'association "paradoxale" talc-chloritoïde ne peut donc être due qu'à des pressions anormalement élevées.

2 - Les chloritoïdes magnésiens

Au delà de son existence même, un caractère très remarquable de l'association talc-chloritoïde est la richesse en magnésium du chloritoïde qui peut atteindre 50% du pôle magnésien dans le Grand Paradis. Cette richesse reconnue depuis Bearth (1963) est caractéristique de domaines de schistes bleus de haut degré ; elle est complètement inconnue à basse pression mais aussi à haute pression et basse température (cf. II). Ceci m'avait amené à postuler l'existence d'un champ de stabilité à haute pression et température modérée pour un chloritoïde purement magnésien (Chopin, 1979), ce qui a pu être démontré expérimentalement (cf. deuxième partie).

La stabilité de l'association talc-chloritoïde et la richesse en magnésium du chloritoïde ont une conséquence importante et immédiatement perceptible sur le terrain : la présence du chloritoïde n'est plus limitée aux roches très ferreuses et alumineuses, comme c'est

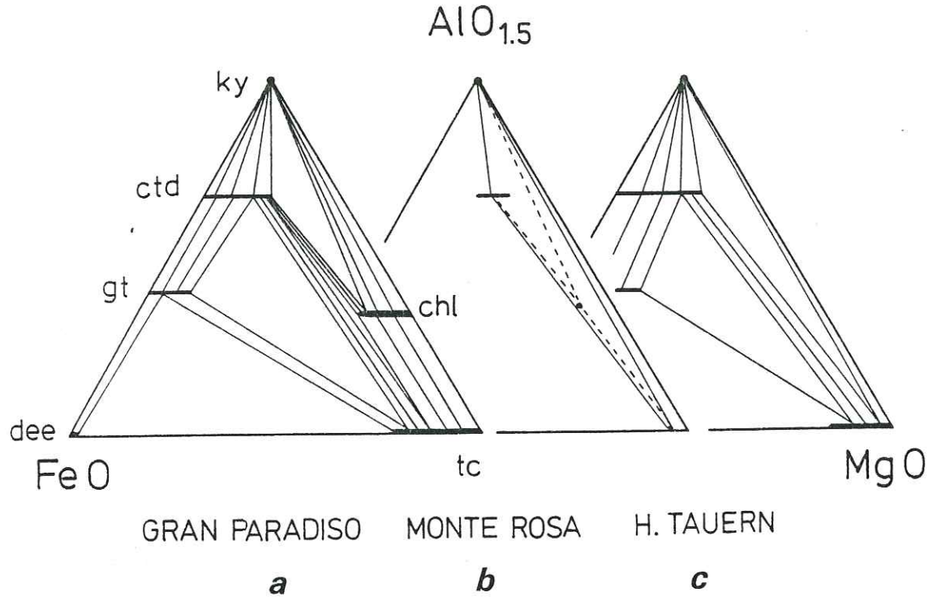

Fig. 4. Relations de phases dans le domaine à talc - chloritoïde. La pyrophyllite a disparu au profit du disthène.
a - Les chlorites magnésiennes sont encore stables.
b - La dernière chlorite disparaît.
c - Stade à talc - disthène - chloritoïde, sans chlorite.
La teneur en Mg du chloritoïde est maximale en b - De a à b elle croît par la réaction continue

chloritoïde + quartz → talc + chloritoïde + H_2O

elle décroît de b à c par la réaction continue

chloritoïde + quartz → talc + disthène + H_2O

En c, il se pourrait déjà que les chloritoïdes les plus ferreux disparaissent au profit de grenat-disthène (non représenté). Le champ du chloritoïde serait donc réduit à la fois du côté ferreux et du côté magnésien. SiO_2 et H_2O en excès.

typiquement le cas à basse pression (Halferdahl, 1961). Bien au contraire : la paire talc-chloritoïde, associée à grenat ou chlorite selon le rapport Fe/Mg du système, couvre un très large domaine de compositions, en particulier celui des pélites les plus banales. Elle doit donc être l'association classique dans ces domaines. Sa découverte ultérieure en divers secteurs du massif du Grand Paradis, dans tout le Val d'Aoste et dans le Mont Rose, est venue confirmer la validité de l'analyse développée initialement sur les pélites de Haute Maurienne.

3 - Les compositions proches du pôle ferreux

Les relations de phases dans la partie la plus ferreuse du système sont établies dans la figure 4 à partir de l'échantillon 8-23, collecté dans les Schistes lustrés de Haute Maurienne (Chopin, 1979). La paragenèse primaire est talc-almandin-deerite-ankérite-magnétite-quartz (Tableau 1). Elle présente la coexistence remarquable d'un silicate de fer (la plus magnésienne des deerites : 2% MgO) avec un silicate de magnésium (le talc, dont les 23% de minnesotaïte représentent le maximum possible pour ces conditions physiques). Dans des systèmes moins oxydés, la grunérite pourrait être stable au pôle Fe comme le montre sa présence dans les concentrations Fe-Mn de la même région (Chopin, 1978). La découverte dans la même unité de pseudomorphoses de howieite $Na(Fe^{2+},Fe^{3+},Mn)_{12}Si_{12}(O,OH)_{44}$ dans un quartzite (ARD 2, avec hématite et grenat riche en caldérite, $Mn_3Fe_2Si_3O_{12}$) montre que dans les systèmes plus oxydés, la howieite peut aussi être stable pourvu que le constituant supplémentaire Na (et Mn ?) soit présent.

4 - l'apparition de talc-disthène

L'évolution immédiatement ultérieure est documentée par des échantillons recoltés dans le massif du Mont Rose. Leur paragenèse à chloritoïde magnésien-talc-disthène-chlorite-quartz a été largement décrite et interprétée (Chopin et Monié, 1984 ; Chopin et Schreyer, 1983, plate 1c ; Chopin, 1983). Elle montre qu'à métamorphisme croissant le champ de la chlorite continue à se réduire du côté ferreux au profit du couple talc-chloritoïde qui devient toujours plus magnésien (réaction 3) : le chloritoïde contient jusqu'à 74% du pôle magnésien ! Mais la nouveauté est l'apparition de l'association talc-disthène qui réduit également du côté magnésien le champ de la chlorite par la réacton

Tableau 1

	Dee	Dee	Ank	Gt c	Gt b	Gt b	Tc	Tc
SiO_2	33,33	33,74		35,80	36,42	36,51	61,37	60,35
TiO_2	4,17	2,69		0,24	0,26	0,23	0,09	0,14
Al_2O_3	0,40	0,47		19,61	20,29	20,10	0,00	0,04
FeO	48,66	50,21	14,37	29,37	33,05	31,27	9,08	12,39
MnO	1,22	1,18	2,71	5,46	1,73	1,16	0,02	0,06
MgO	2,01	1,95	9,62	0,74	1,31	1,60	25,58	23,20
CaO	0,27	0,29	27,20	5,48	4,73	6,52		
Total	90,06	90,53	53,97	96,70	97,80	97,39	96,14	96,18
Si	12,000	12,000		3,006	3,017	3,017	4,004	4,000
Ti	1,129	0,719		0,015	0,015	0,015	0,004	0,007
Al	0,169	0,197		1,943	1,982	1,955		0,003
Fe	14,652	14,935	0,208	2,063	2,290	2,159	0,495	0,687
Mn	0,372	0,355	0,040	0,388	0,119	0,079	0,001	0,003
Mg	1,079	1,033	0,248	0,091	0,159	0,199	2,487	2,292
Ca	0,104	0,110	0,505	0,494	0,418	0,576		
Σ cat.	29,505	29,349	1,000	12,000	12,000	12,000	6,992	6,992
M	0,069	0,065	0,544	0,042	0,065	0,084	0,834	0,769

Minéralogie de l'échantillon 8-23 : paragenèse à talc (Tc) - deerite (Dee) - almandin (Gt) - ankérite (Ank) - quartz - magnétite, dans les Schistes lustrés de Haute Maurienne (Le Vallonet, commune de Bonneval).
La formule de la deerite est calculée sur la base de 12 Si, celle du grenat sur 12 cations, celle du carbonate sur 1 cation, celle du talc sur 11 oxygènes.
M = Mg/(Fe + Mg), c : cœur, b : bord.
Microsonde Cambridge Mark V, programme de correction E.N.S.

divariante

chlorite + quartz --> talc + disthène + H_2O (5)

C'est la réaction classique des "whiteschists" (Schreyer, 1968, 1977) qui, par leur composition purement magnésienne, ne constituent qu'un cas limite du système envisagé ici dans sa généralité. Tout comme la réaction (3), cette réaction est favorisée par l'augmentation de pression et température qui va donc conduire à la disparition de la chlorite en présence de quartz par la réaction univariante "terminale"

chlorite + quartz --> talc + chloritoïde + disthène + H_2O (6)

On notera que la chlorite la plus stable n'est pas la plus magnésienne.

Cette disparition constitue évidemment une étape très importante de l'évolution des métapélites. Elle permet de définir un domaine à talc-chloritoïde-disthène de degré métamorphique si élevé que le seul exemple connu en est la zone à éclogite des Hohe Tauern (Miller, 1977), pour laquelle Holland (1979) propose des pressions approchant 20 kbar en se fondant sur l'étude des éclogites à disthène. Dans les Alpes occidentales, ce domaine est tout juste atteint, comme le montre l'association du Mont Rose où la "dernière chlorite" est encore présente. La présence de talc-chloritoïde-disthène dans certains microsystèmes du gabbro de l'Allalinhorn (Bearth, 1967 ; Chinner et Dixon, 1973), dans l'unité de Schistes lustrés qui surmonte directement le Mont Rose, pourrait ne refléter que des variations locales de l'activité de H_2O.

Il est significatif que la staurotide n'ait jamais été signalée dans ces régions : les paragenèses des pélites ferreuses sont disthène-chloritoïde ou grenat-chloritoïde, selon la richesse en alumine du milieu (Fig. 4). Ceci implique que, même dans ces domaines de très haut degré métamorphique, les températures n'ont pu excéder 550 ou 600°C (cf. Ganguly, 1972).

5 - Une évolution riche mais incomplète

Dans l'évolution de ce domaine à talc-chloritoïde, l'apparition du couple talc-disthène et la disparition de la dernière chlorite constituent des repères faciles dans les compositions relativement magnésiennes. En fait, les variations progressives de composition des minéraux et plus précisément le glissement des champs divariants permettent de suivre cette évolution beaucoup plus finement et dans une

large gamme de composition de roches. Un exemple en est l'enrichissement progressif en magnésium des paragenèses talc-chloritoïde-grenat et talc-chloritoïde-chlorite, qui a permis de mettre en évidence une variation subtile de degré métamorphique entre deux unités structurales dont les associations critiques sont qualitativement identiques (Chopin, 1981 b). Dans pareils cas, il importe d'évaluer précisément l'influence du degré d'oxydation des systèmes.

On notera aussi que la teneur en magnésium du chloritoïde passe par un maximum, à métamorphisme croissant : 50% du pôle magnésien dans le Grand Paradis, 74% dans le Mont Rose, 65% dans les Hohe Tauern. Le travail expérimental en fournit une explication simple (cf. 2ème partie).

Depuis la Haute Maurienne jusqu'aux Hohe Tauern, ces variations sur le thème talc-chloritoïde nous renseignent avec détail sur l'évolution des métapélites vers de très hautes pressions. Il subsiste malheureusement une importante lacune entre ces domaines et ceux à carpholite : nous n'avons pas vu apparaître talc-grenat et talc-chloritoïde, ni disparaître la dernière carpholite, et nous ne savons rien de ce qui sépare ces deux étapes, même si les chaînons manquants peuvent être reconstitués. Ainsi, à partir de la paragenèse décrite par Okrusch (1981) à Samos (cf. II), on imagine aisément la suite :

- rupture du joint carpholite-chloritoïde au profit de chlorite-disthène,
- disparition des dernières carpholites (magnésiennes) par la réaction divariante

carpholite --> chlorite + disthène + quartz + H_2O (7)

- lent déplacement vers des compositions plus magnésiennes du champ divariant chlorite-chloritoïde-disthène.

Entre temps, l'almandin sera apparu à partir de chloritoïde et chlorite dans les roches de rapport Fe/Mg élevé. Les associations talc-grenat puis talc-chloritoïde n'apparaissent que plus tard, aux dépens de Fe-Mg-chlorite + quartz et par rupture du joint chlorite-grenat, respectivement. Entre les domaines à carpholite et talc-chloritoïde, l'association dominante serait donc chlorite-chloritoïde, éventuellement accompagnée de disthène ou grenat selon le rapport Fe/Mg de la roche. Quoi de plus banal ? Si l'on n'a pas observé d'associations

remarquables entre ces deux domaines, c'est peut-être tout simplement qu'il n'y en a pas à observer... De plus, de petites quantités de talc peuvent facilement être confondues avec du mica blanc. C'est pourquoi l'importante lacune d'observation dans notre évolution métamorphique pourrait être plus apparente que réelle.

IV - COESITE ET COMPAGNIE : LES PRESSIONS EXTREMES

Le seul espoir de trouver des associations de plus haut degré que celles du Mont Rose et de l'Allalinhorn semblait être la zone Sesia, dont les magnifiques associations éclogitiques n'avaient pas d'égales dans les Alpes occidentales. Comme de nombreuses équipes s'y bousculaient déjà, je revins à une logique géologique en m'intéressant, après Grand Paradis et Mont Rose, au troisième massif cristallin interne, Dora Maira. A l'affût des roches à talc, j'entrepris une recherche bibliographique sur le massif. La thèse de P. Vialon (1966) fut une révélation. A la simple lecture, j'étais admiratif devant le travail accompli ; la confrontation aux conditions de travail, dans les collines verdoyantes qui dominent la plaine du Pô, n'a fait que renforcer ce sentiment. P. Vialon ne réalise pas seulement la première synthèse géologique sur le massif, il cartographie et décrit un banc à quartz-phengite-disthène-grenat où le grenat peut avoir la taille d'un ballon et serait un pyrope presque pur. C'est plus que je n'en espérais ; c'est même à peine croyable et un nouvel examen s'impose. Avec l'aide de B. Goffé, l'affleurement-clef est retrouvé en octobre 1982. Depuis, je ne fais plus que puiser dans ce merveilleux coffre au trésor, qui a déjà livré le pyrope, la coesite et un silicate inconnu jusqu'alors. L'essentiel des résultats est publié ou en voie de l'être (Chopin, 1984 ; Chopin et al., 1985 ; Chopin, 1985) et sera très brièvement évoqué ici. En revanche, des données nouvelles concernant les compositions plus ferreuses de l'encaissant de cette roche extraordinaire sont exposées avec plus de détail.

1 - Les compositions magnésiennes

Les relations de phases dans les compositions extrêmement magnésiennes sont documentées dans le banc de quartzite signalé par Vialon. La paragenèse typique est quartz-talc-disthène-grenat-phengite. Le

grenat contient de 90 à 98% du pôle pyrope, pas de spessartine et très peu de grossulaire (CaO < 0.3%) ; il est le plus proche du pôle pyrope jamais rencontré dans la nature (Vialon, 1966 ; Chopin, 1984).
L'associaton talc-disthène-grenat du quartzite est divariante dans le système FMASH (en présence de H_2O), elle correspond à la réaction

talc + disthène = pyrope + quartz + H_2O (8)

Cette réaction est favorisée par l'augmentation de température et pression. Elle fournit une limite supérieure de stabilité de l'association critique talc-disthène et tamponne la teneur en pyrope du grenat à sa valeur maximale. L'association réactionnelle correspondante est très rare ; elle n'a été signalée qu'en Tasmanie (Råheim et Green, 1974) et dans le Kazakhstan (Udovkina et al., 1978, 1980). Il est révélateur que le rapport Mg/(Fe + Mg) du grenat n'y atteigne que 0,5 et 0,4, respectivement. La composition du pyrope de Dora Maira implique donc soit une activité de l'eau dramatiquement basse, soit des pressions ou des températures de formation beaucoup plus élevées que dans ces deux cas, pour lesquels l'ordre de grandeur des pressions estimées est 10 kbar.

La coexistence d'un pyrope presque pur avec quartz et talc est en fait très significative. En effet, la combinaison des travaux expérimentaux de Massonne (1983) sur la réaction

enstatite + disthène = pyrope + quartz (9)

et de ceux de Kitahara et al. (1966) sur la limite de stabilité thermique du talc implique pour l'association talc-pyrope-quartz un domaine de stabilité à des températures proches de 800°C si l'activité de l'eau égale 1, et à des pressions minimales de 28 kbar (Chopin, 1984, Fig. 6), ce qui nous place tout près de la transition quartz-coesite ! Rien d'étonnant à ce que l'association talc-chloritoïde magnésien, si caractéristique des domaines précédents, soit nécessairement instable (comme l'indique la coexistence du pyrope avec le disthène : Chopin, 1984, Fig. 5).

2 - Coesite et autres témoins de haute pression

De fait, la coesite a été découverte en inclusion dans les grenats centimétriques de cette roche (Chopin, 1984). Ce polymorphe du quartz stable à des pressions supérieures à 25-30 kbar est typiquement une phase mantellique, comme en témoigne sa présence dans les enclaves de kimberlites diamantifères (Sobolev et al., 1976 ; Smyth et Hatton, 1977).

Sa découverte dans le socle de Dora Maira, dans une roche dérivant selon toute vraisemblance d'une pélite magnésienne (comme il s'en forme dans la sédimentation épicontinentale), est la première de coesite formée lors d'un métamorphisme régional. Elle est lourde de conséquences (Chopin, 1984, et 3ème partie) et n'a pas tardé à faire école (Smith, 1984), alors qu'elle avait été pressentie dès 1965 par Chesnokov et Popov.

Néanmoins, dès qu'une transition polymorphique est en question, il est nécessaire d'envisager l'aspect mécanique du problème. En effet, des contraintes déviatoriques de 10 kbar (!) peuvent abaisser la pression de transition quartz-coesite de plusieurs kilobars (e.g. Green, 1974). Leur influence a été discutée (Chopin, 1984, p. 113) et rejetée dans ce cas précis, pour les raisons suivantes :

- les contraintes déviatoriques dans les phénomènes naturels sont au moins inférieures d'un ordre de grandeur à celles nécessaires pour modifier sensiblement la pression de transition,
- aucune texture ne suggère des déformations exceptionnelles lors de la cristallisation de cette association,
- il ne peut s'agir d'une zone de cisaillement localisée car la coesite est ou a été présente dans tout le banc de quartzite, qui affleure sur une quinzaine de kilomètres, et je l'ai trouvée depuis dans les schistes et roches basiques de l'encaissant, qui ne portent pas plus trace de déformation exceptionnelle.

Enfin, les pressions très élevées correspondant à la stabilité de la coesite sont suggérées indépendamment par d'autres paragenèses: Talc-pyrope-SiO_2 a déjà été signalée pour les compositions pélitiques. Pour d'autres compositions, la présence d'éclogites à disthène-phengite et surtout d'une superbe association à disthène-phengite-jadéite (90% du pôle) dans un quartzite à almandin (et reliques de coesite) montrent que la limite de stabilité de la paragonite a été dépassée. D'après le travail expérimental de Holland (1979 b) sur la réaction

paragonite = jadéite + disthène + H_2O (10)

ceci impose des pressions minimales de 24 à 25 kbar. Une fois de plus, nous nous trouvons dans un nouveau monde.

3 - Les compositions ferreuses et intermédiaires

L'association caractéristique de ces compositions communes est grenat-disthène. Sur le terrain, lorsqu'on vient du Grand Paradis ou du

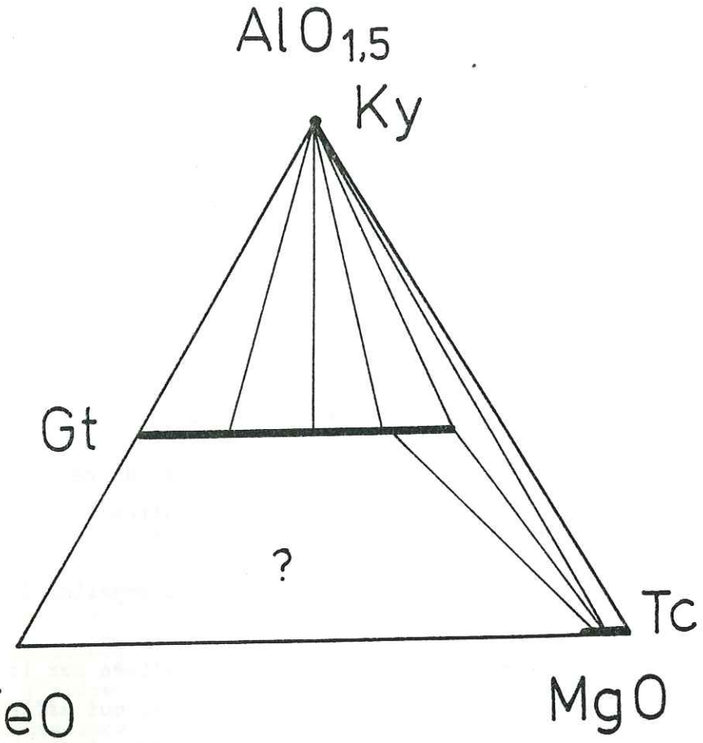

Fig. 5. Relations de phases dans le domaine à coesite.
L'association disthène-grenat est ubiquiste, le chloritoïde a disparu, le talc est limité aux compositions très magnésiennes ou peu alumineuses.

Mont Rose, on ne peut s'empêcher d'être frappé par sa présence et par l'absence du chloritoïde. L'association grenat-disthène paraît en effet stable pour toute la gamme des rapports M = Mg/(Mg + Fe) (Fig. 5, les valeurs rencontrées varient de 15 à 47 et de 80 à 98%), ce qui implique l'instabilité de tout chloritoïde et de toute staurotide en présence de quartz. Il en résulte qu'un observateur non averti pourrait trouver la minéralogie de ces métapélites bien banale et ne rien soupçonner des conditions exceptionnelles de métamorphisme, même si la présence systématique d'associations à grenat-disthène-mica blanc sans biotite ni chlorite primaires est un indice de relativement haute pression.

L'étude des métapélites de l'encaissant du quartzite à pyrope n'est qu'ébauchée mais se révèle déjà prometteuse. Un horizon de schistes à porphyroblastes centimétriques de grenat et de disthène affleure aussi bien en Val Pô (cartographie de Chopin et Monié) qu'en Val Varaita (Lombardo, comm. pers. 1985) et présente un triple intérêt :

- Ce sont des pélites presque idéales, très pauvres en calcium et manganèse puisque dans certains échantillons le grenat contient moins de 0,5% CaO et moins de 0,15% MnO. La seule phase sodique de la matrice est l'albite, associée à une phengite très peu substituée dans des pseudomorphoses prismatiques représentant très vraisemblablement d'anciennes jadéites.
- La partie centrale des grenats contient souvent de nombreuses petites inclusions définissant non pas une texture sigmoïde mais une trace de foliation, dont l'orientation est constante dans chaque grenat mais varie de grenat à grenat. Les inclusions sont monominérales, alors constituées de quartz, parfois de chloritoïde, rarement de disthène, ou composites, contenant staurotide et/ou chloritoïde, paragonite, quelquefois chlorite, jamais de quartz. Staurotide, chloritoïde, paragonite et chlorite sont absents de la matrice quartzeuse.
- La partie corticale des grenats peut être dépourvue d'inclusions ou contenir quelques grosses inclusions de coesite partiellement ou totalement transformée en quartz. Les seules inclusions des porphyroblastes de disthène sont à coesite/quartz.

La paragenèse typomorphe est grenat-disthène-phengite-jadéite(?)-coesite car, pour les raisons mécaniques développées par Gillet et al. (1984), la coesite a nécessairement été présente dans la matrice mais ne peut être conservée qu'en inclusion. Sa présence dans

Tableau 2

	Grenat				Chloritoïde		Chlorite	Parag.	Phengite
	1	2	3	4	2	3	2	4	matrice
Inclusion									
SiO_2	38.78	38.90	38.89	38.71	24.83	25.49	26.48	45.35	51.61
TiO_2	0.02	0.03	0.02	0.04	0.01	0.01	0.10	0.04	0.26
Al_2O_3	22.78	22.66	22.65	22.25	41.82	42.88	23.88	38.43	25.87
FeO	31.74	31.79	30.48	27.92	18.61	18.37	15.67	0.57	1.29
MnO	0.08	0.05	0.08	0.05	0.06	0.00	0.03	0.01	0.01
MgO	7.57	7.39	8.62	9,66	6.32	6.28	21.34	0.20	4.11
ZnO	0.00	0.00	0.00	0.01	0.01	0.02	0.00	0.00	0.00
CaO	0.44	0.36	0.44	0.42	0.01	0.01	0.02	0.08	0.00
Na_2O	0.11	0.06	0.11	0.06	0.00	0.02	0.05	6.96	0.11
K_2O	0.00	0.02	0.00	0.00	0.01	0.00	0.05	0.57	10.60
Total	101.52	101.26	101.29	99.12	91.66	93.08	87.62	92.21	93.86
	24 oxygènes				*12 oxygènes*		*14 ox.*	*11 ox.*	*11 ox.*
Si	5.95	5.98	5.95	5.99	2.00	2.02	2.64	2.99	3.48
Ti							0.01		0.01
Al	4.12	4.11	4.09	4.06	3.98	4.00	2.81	2.99	2.05
Fe + Mn	4.08	4.10	3.90	3.62	1.26	1.22	1.31	0.03	0.07
Mg	1.73	1.69	1.97	2.23	0.76	0.74	3.17	0.02	0.41
Zn									
Ca	0.07	0.06	0.07	0.07			0.01	0.05	0.02
Na	0.03	0.02	0.03	0.02			0.01	0.89	0.91
K									
Σ cat.	15.98	15.96	16.01	15.99	8.00	7.98	9.96	6.96	6.95
M	0.30	0.29	0.33	0.38	0.38	0.38	0.71		0.85

Echantillon 4-30b2 : Schiste à quartz-phengite-grenat-disthène du socle de Dora Maira (Martiniana Po, Italie). Analyses de la phengite de la matrice et des minéraux contenus dans différentes inclusions du grenat.
Microsonde Cameca Microbeam, programme de correction Cameca.

l'encaissant du quartzite à pyrope est capitale ; nous y reviendrons dans la troisième partie. A la différence du quartzite à pyrope qui ne fournit qu'un instantané de l'évolution métamorphique, ces roches ont conservé la mémoire de toute une partie de leur histoire. Ceci peut nous aider à reconstituer la lacune qui sépare ce domaine à pyrope-coesite de celui à talc-chloritoïde.

4 - Les étapes antérieures : le rôle de la staurotide

La présence de reliques de staurotide est remarquable car les seules staurotides connues jusqu'alors dans les Alpes occidentales (Belledonne, Ruitor, gneiss du Sapey) sont des reliques d'un métamorphisme paléozoïque. Une telle origine peut être exclue pour celles qui nous concernent en raison de leur association à un chloritoïde contenant jusqu'à 48% du pôle magnésien, donc typiquement "alpin". Cette découverte de staurotide de haute pression, la première dans les Alpes centrales et occidentales, est d'un grand intérêt théorique. Les autres staurotides de relativement haute pression signalées sont magnésiennes (M = 40-55) et formées à température élevée : plus de 7 kbar et 800°C en Afrique du Sud (Schreyer et al., 1984), 12 kbar et 750°C en Nouvelle Zélande (Ward, 1984), plus de 8 kbar et 700°C en Antarctique (Grew et Sandiford, 1984). Le seul proche équivalent est la roche à talc-disthène-grenat-quartz du Kazakhstan où Udovkina et al. (1978, 1980) décrivent des reliques de staurotide (M = 15-20%), de chloritoïde (M = 35%) et de chlorite (M = 80%) dans le coeur des grenats (M = 20-25%).

La première information que livre l'association de Dora Maira est d'ordre thermique. La présence du couple almandin-staurotide (ZnO < 1%) démontre que des températures dépassant 600°C (cf. Ganguly, 1972 ; Rao et Joahnnes, 1979) ont pu être atteintes dans le métamorphisme alpin. Ceci peut constituer un jalon vers les températures encore plus élevées déduites de la paragenèse talc-pyrope-quartz/coesite.

De plus, le fractionnement Fe-Mg entre les minéraux de cette roche est original (Tableau 2), la succession à rapport M croissant étant staurotide < grenat < chloritoïde < chlorite. Le fait que la staurotide soit nettement plus riche en fer que grenat et chloritoïde est particulièrement intéressant. En effet, on cherche encore à comprendre ce qui gouverne le sens de ces fractionnements. Le problème a été clarifié pour le couple staurotide-chloritoïde (Grambling, 1983), où la staurotide ne peut être plus magnésienne que le chloritoïde que pour

les compositions les plus ferrifères (M < 10). Si, comme le pense Grambling, ceci n'est pas dû à l'incorporation de Fe^{3+} par le chloritoïde, il y a bien inversion du fractionnement entre les deux minéraux pour cette valeur de M. La situation est beaucoup plus confuse pour le couple staurotide-grenat où, quelle que soit la composition de la staurotide, celle-ci est tantôt plus magnésienne tantôt plus ferreuse que le grenat. Nos roches viennent renforcer l'idée que ce partage pourrait s'inverser avec la pression. En effet, la staurotide semble toujours plus magnésienne que le grenat associé à basse pression (e.g. Hietanen, 1969 ; Albee, 1972 ; Guidotti, 1974 ; Demange, 1978 ; Holdaway, 1978 ; Pigage et Greenwood, 1982 ; Grambling, 1983). Or, à haute pression, la staurotide magnésienne décrite par Schreyer et al. (1984) est nettement plus ferreuse que le grenat, ce qui est aussi notre cas et semble également réalisé dans l'échantillon du Kazakhstan. Malheureusement, la staurotide la plus magnésienne (Ward, 1984), légèrement plus magnésienne que le grenat associé, vient ruiner cette hypothèse. Peut-être l'étude du couple staurotide-grenat sur une gamme aussi large que possible de rapports Fe/Mg dans cet horizon pélitique de Dora Maira pourra-t-elle nous fournir de nouvelles hypothèses...

Cette paragenèse pose un autre problème, celui de l'association staurotide-quartz. Cette dernière n'est plus présente dans la roche mais il est légitime de penser qu'elle l'a été puisque la matrice est fort riche en quartz et la staurotide riche en Si (Tableau 2). Or les travaux expérimentaux de Ganguly (1972) et de Rao et Johannes (1979) montrent que, dans le système purement ferreux, cette association est stable à une pression maximale de 15 kbar, vers 600°C. De plus, les fractionnements observés dans la roche réduisent ce champ, aussi bien du côté des basses températures (au profit de chloritoïde-disthène) que de celui des hautes températures (au profit de grenat-disthène), ce qui abaisse encore de plusieurs kilobars la pression maximale de stabilité. Il semblerait donc que cette étape ne puisse pas représenter la suite de l'évolution menant à l'association talc-chloritoïde ; elle traduirait un gradient thermique initialement plus élevé. La présence dans le grenat de chlorite (supposée primaire et initialement associée au quartz) irait également dans ce sens, tout comme l'absence de reliques de talc, en suggérant que le couple grenat-chlorite (+ quartz) était stable au lieu de talc-chloritoïde.

Cependant, je me garderai d'être catégorique sur ce point, pour

plusieurs raisons. Malgré leur cohérence les divers travaux expérimentaux sur la staurotide ferreuse (Richardson, 1968 ; Ganguly, 1972 ; Rao et Johannes, 1979) se révèlent d'application extrêmement délicate (Ferry, 1980 ; Pigage et Greenwood, 1982), probablement en raison du caractère aberrant de la solution solide Fe-Mg. D'autre part, la reconstitution de paragenèses précoces à partir d'inclusions conservées dans le grenat est également délicate (cf. Chopin, 1985). Certes, la préservation de paragonite par le grenat, alors que jadéite-disthène sont devenus stables dans la matrice, s'explique simplement : la différence de compressibilité entre paragonite et grenat fait qu'à pression externe croissante la pression dans l'inclusion de paragonite reste inférieure à celle appliquée sur le grenat (cf. Gillet et al., 1984). Mais que dire de l'absence d'inclusions de talc alors que la phengite, présente dans la matrice pendant toute l'évolution, n'est jamais incluse dans le grenat ? Comment le grenat discrimine-t-il entre phengite et paragonite ? La chlorite est-elle vraiment primaire ? Sa faible teneur en silice ne le suggère pas (cf. Chopin, 1985, p. 13). Il me paraît donc sage d'attendre le résultat d'observations plus nombreuses pour conclure.

5 - Retour sur les phases potassiques

Pour les compositions pélitiques du domaine à coesite, il est remarquable que la phase potassique soit toujours et exclusivement la phengite. Dès le moment où la chlorite commence à disparaître au profit d'associations à talc, le couple talc-phengite devient une paragenèse caractéristique de tout ce domaine de haute pression (Chopin, 1981), jusque dans le quartzite à pyrope et coesite (Chopin, 1984). On remarquera que vers ces pressions extrêmes la présence du talc et donc de talc-phengite est limitée à des compositions de plus en plus magnésiennes ou peu alumineuses, à cause de l'envahissement du champ de composition par l'association grenat-disthène (Fig. 5). Il existe ainsi un domaine privilégié où la paire talc-phengite est présente pour une large gamme de compositions et donc abondante sur le terrain ; c'est le domaine à talc-chloritoïde. A plus basse pression, cette paire n'est pas stable ; à plus haute pression (et température), elle est limitée à certaines compositions. C'est une des raisons pour laquelle cette association a pu rester inconnue jusqu'en 1976 (Abraham et Schreyer).

Son domaine de stabilité est limité en pression mais aussi en température par la réaction

talc + phengite --> phlogopite + disthène + quartz + H_2O (11)

Cette réaction, déduite par Abraham et Schreyer (1976) et confirmée expérimentalement par Schreyer et Baller (1977), a été précisément déterminée par Massonne (comm. pers., 1982 ; voir Chopin, 1984, Fig. 8). Elle est d'un intérêt considérable car elle confine toute l'évolution qui vient d'être décrite à un domaine de pression élevée et de température relativement basse, même pour les termes extrêmes et d'autant plus que l'activité de l'eau est faible (cf. Chopin, 1984).

Digression :

La connaissance de cette courbe de réaction permet de localiser vers 28 kbar, 800°C son intersection avec la courbe de la réaction (8), qui engendre la réaction

phengite + pyrope = phlogopite + disthène + quartz (12)

(Chopin, 1984, Fig. 6). Cette réaction procède avec un changement de volume notable et ne libère pas d'eau, quelle que soit la composition du feuillet des deux micas. Cette réaction est donc faiblement dépendante de la température et de l'activité de l'eau. Or son équivalent ferreux présente les mêmes propriétés mais se situe à des pressions beaucoup plus basses, de l'ordre de 5 kbar (comparer Rao et Johannes, 1979, et Vielzeuf, 1984). Ceci confère à l'association grenat-phengite/muscovite-biotite-silicate d'alumine-quartz un intérêt évident : les valeurs absolues du rapport Mg/Fe dans le grenat et la biotite dépendent de la pression (cf. ci-dessus), le quotient de ces rapports dépend de la température (cf. Ferry et Spear, 1978), et le tout est virtuellement indépendant de l'activité de l'eau. De plus, l'étendue de la substitution phengitique dans le mica blanc est essentiellement et indépendamment une mesure de la pression. De quoi faire rêver les pétrographes... mais dans des domaines de températures plus élevées que celles qui nous concernent. Les premières utilisations barométriques ont été faites avec un inégal bonheur (Robinson, 1983 ; Vielzeuf, 1984).

6 - Un nouveau minéral : l'ellenbergerite

L'étude du quartzite à pyrope de Dora Maira a conduit à la découverte de coesite dans les grenats centimétriques de la lithologie la plus commune. L'étude des grenats décimétriques présents localement a

permis la découverte d'une nouvelle espèce minérale, très spectaculaire par sa couleur pourpre et son pléochroïsme. Ce minéral a été dédié au professeur François Ellenberger, hommage rendu au maître de la géologie alpine qui a ouvert le domaine pennique interne à l'analyse stratigraphique et, même s'il s'en défend, pétrographique. C'est aussi une marque de reconnaissance qui atteste la pérennité et la vitalité d'une équipe alpine à l'Ecole, dans le laboratoire-même où il élabora son grand oeuvre. Le nom et la description du minéral (Chopin et al., 1985) ont été acceptés par la commission compétente de l'I.M.A. Sa formule structurale s'écrit

$(Mg,Ti,Zr,\square)_2\ Mg_6\ Al_6\ Si_8\ O_{28}\ (OH)_{10}$.

Puisque chimiquement équivalente à chlorite + quartz + kaolinite + rutile $\pm$ zircon, il s'agit typiquement d'une nouvelle phase du système pélitique. L'étude de ses relations de phases (Chopin, 1985) montre que cette espèce riche en eau (7,5% H_2O) est un minéral de très haute pression, stable à plus de 20 kbar, qui constitue un peu un équivalent hydraté et de basse température du pyrope.

Au delà de certaines particularités chimiques comme la substitution Ti = Zr et l'incorporation possible de phosphore jusqu'à 8,3% P_2O_5 (Chopin et al., 1985), l'ellenbergerite est remarquable par sa structure. Dans les chaînes d'octaèdres situées sur les axes sénaires comme dans les doubles chaînes situées sur les axes d'inversion d'ordre 2 (Fig. 6), les liaisons entre octaèdres sont réalisées en majorité par mise en commun non d'un sommet ou d'une arête, mais d'une face, ce qui semble être un cas unique parmi les silicates. Il en résulte une compacité de la structure qui approche celle du pyrope (cf. Chopin et al., 1985).

Les sites octaédriques situés sur les axes sénaires sont particulièrement intéressants. Ils sont remplis environ pour un tiers par Mg, un tiers par Ti ou Zr, un tiers restant vacant. La présence d'atomes de fer dans ces sites est à l'origine de la couleur du minéral (Chopin et al., 1985). Il est d'autre part tentant d'imaginer la substitution $Ti\square = 2Mg$, qui conduirait à un pur alumino-silicate magnésien : de quoi faire rêver l'expérimentaliste coutumier du système MASH ! De plus, la structure autour de cet axe, avec un octaèdre régulier entouré de 6 tétraèdres, rappelle celle de la wadéite $K_2ZrSi_3O_9$ (Henshaw, 1955) ou de son homologue $K_2TiSi_3O_9$, où Zr et Ti occupent le site octaédrique. La chose devient piquante si l'on considère l'homologue

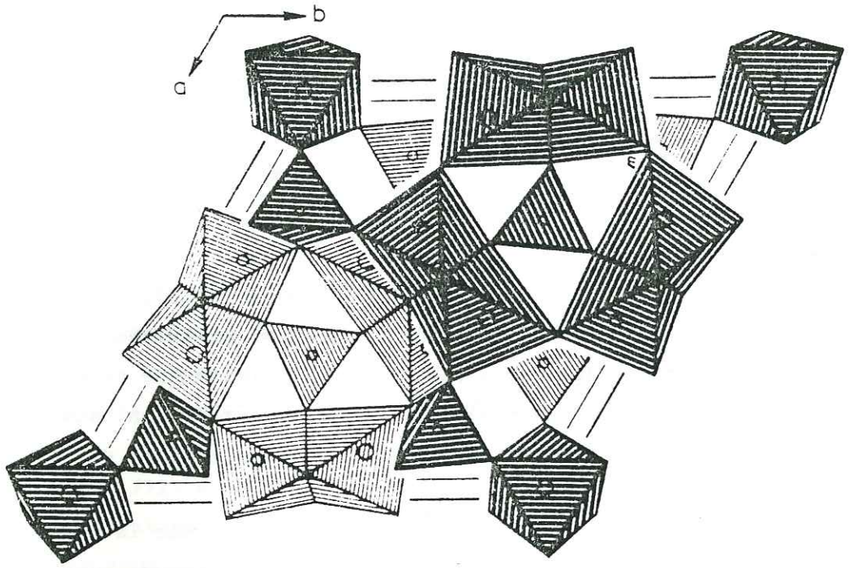

Fig. 6. Vue perspective de la structure de l'ellenbergerite, parallèlement à l'axe c (voir Chopin et al., 1985).

$K_2SiSi_3O_9$ synthétisé à 24 kbar, où un atome Si est hexacoordonné (Swanson et Prewitt, 1982). En effet, les très fortes teneurs en phosphore de l'ellenbergerite s'accompagnent d'un excès de Si + P au delà des 8 sites tétraédriques, suggérant la présence de Si hexacoordonné (Chopin et al., 1985). Sa place dans la structure serait donc toute trouvée, ce qui ferait de l'ellenbergerite le second minéral terrestre (après la stishovite !) à avoir cette particularité qui passe pour caractériser de très hautes pressions.

V - PREMIER BILAN : L'INTERET DES COMPOSITIONS MAGNESIENNES

Cette évolution qui nous a mené jusqu'à des terres inconnues témoigne d'une route originale. Au long de cette route, nous avons vu les paysages minéralogiques se succéder, certains absolument caractéristiques de la contrée traversée, d'autres plus banals, rappelant des domaines connus. Curieusement, plus nous avancions dans les terres nouvelles, moins le paysage était caractéristique. Je m'explique : à faible degré métamorphique, les associations à carpholite $\pm$ chloritoïde couvrent presque toute la gamme des rapports Fe/Mg ; à degré intermédiaire les associations à talc-chloritoïde-phengite couvrent la gamme des valeurs moyennes du rapport Fe/Mg qui sont certes les plus courantes ; les degrés extrêmes ne sont manifestés clairement que dans les compositions les plus magnésiennes.

La logique qui sous-tend ces observations est d'ordre cristallochimique. Pour un alumino-silicate ayant des pôles ferreux, manganeux et magnésien, le domaine de stabilité se trouve à pression d'autant plus élevée que le cation divalent est plus petit. Ceci fournit la succession Mn < Fe < Mg à pression croissante, dont les cordiérites, les grenats ou les staurotides fournissent des exemples. Les systèmes magnésiens sont donc effectivement les plus critiques à haute pression.

A cet égard, une des belles découvertes pétrographiques de ces dernières années, l'une des rares à attester la réalisation dans la nature de conditions insoupçonnées jusqu'alors, me paraît symptomatique : dans les granulites de haute température et relativement haute pression de l'Enderby Land (Antarctique), les paragenèses à osumilite et sapphirine-quartz qui caractérisent un autre extrême de métamorphisme apparaissent exclusivement dans les métapélites magnésiennes (Ellis,

1980).

C'est la raison essentielle pour laquelle un travail expérimental a été entrepris dans le système purement magnésien $MgO-Al_2O_3-SiO_2-H_2O$ (MASH). La première partie de ce mémoire se cantonnait volontairement à ce que l'on peut tirer de l'observation et d'un raisonnement simple, en limitant les estimations thermobarométriques aux évidences. Le but du travail expérimental exposé dans la partie suivante était de fournir des éléments d'appréciation quantitative pour l'évolution minéralogique reconnue. Après avoir touché une terre nouvelle, il s'agissait de la cartographier.

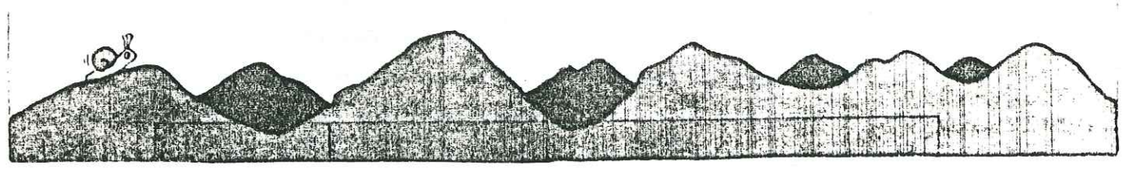

Deuxième Partie

ETUDE EXPERIMENTALE

DU SYSTEME $MgO - Al_2O_3 - SiO_2 - H_2O$

ENTRE 480 ET 800° C, 15 ET 40 KBAR

Contrairement à ce que pourrait laisser croire le plan de ce mémoire, le travail expérimental n'est pas venu couronner une étude pétrographique achevée. Les deux démarches ont été menées conjointement, au plus grand profit de l'une et de l'autre. Initialement, le chloritoïde relativement magnésien de Haute Maurienne et la familiarité avec les recherches de B. Goffé m'ont naturellement orienté vers la synthèse du Mg-chloritoïde et de la Mg-carpholite. Mais la découverte de chloritoïde très magnésien dans le Mont Rose n'est intervenue qu'après la synthèse, venant ainsi justifier le travail expérimental s'il en était besoin. Inversement, la familiarité acquise avec le pyrope et la coesite dans le travail expérimental m'a certainement beaucoup aidé dans leur découverte : la richesse en pyrope des grenats de Dora Maira fut certes une surprise, mais par elle la présence de coesite entrait dans le domaine du possible. Elle fut alors décelée très rapidement. En contre-coup cette découverte a initié un nouveau travail expérimental sur la limite inférieure de stabilité du pyrope ; la découverte de l'ellenbergerite ouvre à son tour un nouveau domaine à l'expérimentation.

Les travaux exposés ci-dessous ont été réalisés à l'Institut de Minéralogie de l'Université de la Ruhr, au cours de deux séjours, l'un de longue durée (1979-1981), l'autre pendant l'hiver 1983. L'essentiel des conséquences pétrologiques et géologiques du travail concernant la carpholite et le chloritoïde a déjà été publié (Chopin et Schreyer, 1983). Les détails expérimentaux et les résultats concernant le pyrope sont encore inédits et sont exposés ici.

I - TECHNIQUES ET STRATEGIES EXPERIMENTALES.

1 - **Technique expérimentale :**

Les presses hydrauliques utilisées sont du type décrit par Boyd et England (1960). La cellule de pression est entièrement réalisée en NaCl avec un four en graphite assurant un comportement quasi-hydrostatique et rendant toute correction de friction négligeable (Mirwald et al., 1975). La température est mesurée par un thermocouple Ni-NiCr dont la soudure est réalisée sous flux d'argon. Le domaine P-T exploré rend minime l'effet de la pression sur la mesure du thermocouple. La correction varierait de 0 à 4°C, elle n'est pas prise en compte dans les tableaux 3 à 5. Pour les

Tableau 3

P H_2O (kbar)	T (°C)	Durée (heures)	Observations	Taux de réaction
Réaction carpholite = chlorite + disthène + quartz + H_2O				
19,9	539	97	carpholite +	+
19,0	564	87	carpholite -	++
17,7	517	182	carpholite +	++
17,5	549	126	carpholite -	+++
15,0	508	236	carpholite -	+
14,9	492	256	pas de réaction	
15,1	482	320	carpholite +	++
6,5	430	2260	carpholite -	+
6,5	400	2260	pas de réaction	
Réaction carpholite = chlorite + pyrophyllite + diaspore + H_2O				
14,0	530	120	carpholite +	++
6,5	430	2260	carpholite -	+
6,5	400	2260	pas de réaction	
6,5	350	2260	pas de réaction	
Réaction carpholite = chlorite + disthène + talc + H_2O				
19,0	535	137	carpholite +	+
19,1	557	119	carpholite -	+
30,0	569	115	carpholite +	+
29,9	587	85	carpholite -	+++
Réaction carpholite + quartz = talc + disthène + H_2O				
20,0	543	94	Car Q +	+
20,0	555	76	pas de réaction	
20,0	561	120	Car Q -	+
25,1	551	72	Car Q +	+
25,0	558	53	pas de réaction	
25,0	568	85	Car Q -	+
30,1	560	83	Car Q +	+
29,9	569	42	pas de réaction	
30,1	580	46	Car Q -	+
Réaction carpholite + diaspore = chlorite + disthène + H_2O				
23,0	500	125	Car Dia +	+
24,5	521	147	Car Dia +	+
32,5	499	170	Car Dia +	+++
31,8	551	139	Car Dia +	+
31,8	569	141	Car Dia -	+

Résultats expérimentaux sur la stabilité de la Mg-carpholite
+ faible réaction ++ réaction forte +++ réaction complète ou presque

"grosses" synthèses, des capsules en or de 5 mm de diamètre et environ 10 mm de long sont remplies d'environ 200 mg de mélange et embouties. Pour la détermination d'équilibres, 8 à 10 mg de réactifs et 1 à 2 mg d'eau sont contenus dans une capsule en or de 2 mm de diamètre et 8 mm de long qui est soudée aux extrémités puis disposée parallèlement à l'axe de la cellule. La géométrie des pièces de sel de la cellule est adaptée aux conditions de pression de l'expérience (c'est à dire au taux de raccourcissement prévisible) afin que la perle du thermocouple se trouve à mi-hauteur de la capsule durant l'expérience. La pression nominale est atteinte à froid, puis la température est amenée au point de consigne, ce qui nécessite en général de compenser l'augmentation de pression résultante. Durant l'expérience, la pression et la température sont maintenues par des régulateurs à $\pm$ 200 bars et $\pm$ 2°C des points de consigne. L'arrêt du chauffage entraîne une chute de la température jusque vers 150°C en moins de deux secondes. La cellule extraite est décortiquée afin de reconstituer la position de la capsule dans le gradient de température et d'intégrer l'influence de ce gradient sur la longueur de la capsule, ce qui entraîne une correction négative de la température de 1 à 4°C. Les valeurs données dans les tableaux 3 à 5 sont corrigées de cet effet. Les conditions expérimentales sont estimées reproductibles à mieux que 5°C et 200 bars près. L'erreur sur la température et la pression est proche de 1%.

2 - **Interprétation des résultats**

La capsule est pesée avant et après expérience pour s'assurer de son étanchéité. Elle est ouverte au rasoir et le produit est déposé sur une lame porte-objet du diffractomètre X sans être étalé en force, point important visant à limiter l'orientation préférentielle des particules. Le diagramme de diffraction est réalisé systématiquement entre 5 et 75°2θ (CuKα). Ceci paraît un domaine plus large que celui utilisé par beaucoup d'expérimentateurs mais la faible orientation des produits permet d'avoir de bonnes réflexions aux grands angles où, de toute manière, des minéraux comme le chloritoïde (69°) ou le disthène (70°) ont des réflexions caractéristiques. La détermination du sens de réaction est faite par comparaison des diffractogrammes obtenus avant et après expérience, en utilisant toutes les réflexions, basales et non basales, de chaque minéral, dans la mesure où elles ne sont pas affectées de superposition. En cas de doute, c'est à dire lorsque ces réflexions

Tableau 4

P H_2O (kbar)	T (°C)	Durée (heures)	Observations	Taux de réaction
Réaction chloritoïde = chlorite + disthène + corindon + H_2O				
19,0	628	154	Ctd -	+++
19,0	615	125	Ctd -	+
19,0	605	159	Ctd -	+
19,0	587	328	pas de réaction	
22,1	643	104	Ctd +	++
22,0	660	86	pas de réaction	
22,0	667	110	Ctd -	+
25,0	690	112	Ctd +	++
25,0	710	60	Ctd -	+++
24,9	725	72	+ staurotide	
27,0	715	49	Ctd +	+
Réaction chloritoïde + talc = chlorite + disthène				
31,7	562	105	Ctd Tc +	+++
31,6	675	63	Ctd Tc +	++
31,3	710	46	Ctd Tc +	+
30,7	716	70	Ctd Tc -	+
26,9	600	162	Ctd Tc +	+
27,5	665	209	Ctd Tc -	++
27,0	715	49	Ctd Tc -	+++
24,9	609	149	pas de réaction	
Réaction chloritoïde = pyrope + corindon + H_2O				
30,1	785	24	+ Stau, + Chl, Ctd -, Pyr Co +	
31,7	752	70	Pyr Co -	+++
32,8	756	51	pas de réaction	
33,9	765	38	Pyr Co +	+
37,1	751	25	pas de réaction	
37,1	764	21	Pyr Co +	++
37,1	782	22	Pyr Co +	++
42,4	736	48	Pyr Co -	++
42,4	747	53	Pyr Co -	+
Réaction chloritoïde + quartz = talc + disthène + H_2O				
29,5	675	63	Ctd Q -	+++
30,0	563	105	Ctd Q -	+++
Réaction diaspore = corindon + H_2O				
25,0	620	41	Co -	+
24,8	640	47	Co +	+++

Résultats expérimentaux sur la stabilité du Mg-chloritoïde

n'indiquent pas toutes croissance ou décroissance, j'estime qu'il n'y a pas eu de réaction. Le quartz n'a cependant jamais été pris en considération dans ces déterminations, l'expérience montrant que les intensités relatives de ses pics ne sont pas reproductibles et qu'il est préférentiellement dissous dans la phase fluide. Une étude optique des produits n'a été réalisée systématiquement que lors des synthèses, pour s'assurer de la pureté du produit.

3 - Synthèses de nouvelles phases

La première synthèse des pôles magnésiens de la carpholite et du chloritoïde a été réalisée au cours de ce travail (Chopin et Goffé, 1981 ; Chopin et Schreyer, 1983). Lors de la rédaction de ces articles, la nucléation de la carpholite en l'absence de germes n'avait pu être obtenue qu'avec des mélanges de départ bien particuliers, mélanges d'oxydes et de cordiérite ou de sudoïte. Plus tard, il est apparu fortuitement que la carpholite pouvait croître spontanément à partir d'un mélange d'oxydes vers 20-25 kbar, 500°C. La synthèse du chloritoïde a été beaucoup plus laborieuse et je n'ai encore jamais observé sa nucléation spontanée. Des conditions de synthèse typiques sont 32-34 kbar, 700-720°C, après une lente montée en température pour éviter la nucléation et la persistance de Mg-staurotide. La taille des produits est de l'ordre du micron, mais une tablette hexagonale de près de 30 microns a été observée.

4 - Les mélanges de départ : stratégie et tactique

Après avoir synthétisé un minéral, on cherche naturellement à déterminer son domaine de stabilité et ses relations de phases. Une méthode logique et élégante consiste à déterminer précisément une réaction mettant en jeu ce minéral et des phases dont les propriétés thermodynamiques sont bien connues. On en déduit alors celles du minéral (cf. Chatterjee, 1975) ce qui permet ensuite de calculer d'autres réactions. Malheureusement, le système MASH ne se prête guère à cette approche en raison des nombreuses substitutions existant en particulier dans la chlorite (MgSi = AlAl) et dans le talc (3 Mg = 2 Al et/ou MgSi = AlAl). L'étendue de ces substitutions peut varier le long d'une même courbe de réaction, modifiant donc la stoechiométrie de la réaction et rendant illusoire toute exploitation thermodynamique simple des résultats expérimentaux.

Tableau 5

P H_2O (kbar)	T (°C)	Durée (heures)	Observations	Taux de réaction
Réaction talc + disthène = pyrope + quartz + H_2O				
28,2	810	43	Tc Ky +	+++
28,7	825	23	+ Enst, + Coes	
Réaction talc + disthène = pyrope + coesite + H_2O				
31,9	762	34	Tc Ky +	+++
32,2	785	40	Tc Ky +	+
32,1	805	29	pas de réaction	
34,9	798	47	pas de réaction	
38,0	769	84	Tc Ky +	+
38,1	780	70	pas de réaction	
38,0	798	47	Tc Ky -	+
Réaction talc + chlorite + disthène = pyrope + H_2O				
20,0	763	71	pyrope -	+
19,9	780	46	pas de réaction	
19,9	794	52	pyrope +	+
20,0	804	71	pyrope +	++
25,0	699	60	pyrope -	+++
24,9	737	39	pyrope -	+
24,9	754	48	pas de réaction	
25,0	770	71	pyrope +	+
30,1	700	73	pas de réaction	
30,1	726	71	pas de réaction	
30,1	738	76	pyrope +	+

Résultats expérimentaux sur la stabilité du pyrope

Dans ce cas, il devient nécessaire de déterminer un plus grand nombre de courbes de réaction. Mon choix s'est orienté vers des réactions qui représentent une limite importante du champ de stabilité, ou qui mettent en jeu un nombre réduit (1 ou 0) de phases à composition variable, avec l'espoir d'utilisation ultérieure à des fins thermodynamiques, ou des réactions qui sont le pôle magnésien d'une réaction importante dans la nature et qui pourraient donc être utilisées directement. La liste de ces réactions et les résultats correspondants sont donnés dans les tableaux 3 à 5.

Pour la détermination de la courbe d'équilibre d'une réaction, il est nécessaire de partir d'un mélange précristallisé des réactifs et des produits de la réaction. A ce point deux stratégies sont possibles :

- soit synthétiser indépendamment chaque minéral dans les conditions optimales, puis réaliser le mélange. Ceci va sans problème pour les phases à composition fixe (quartz, disthène, corindon, carpholite, chloritoïde), mais quelle composition choisir pour la chlorite (et accessoirement le talc) ?

- soit synthétiser ensemble tous les minéraux (sauf un, de composition fixe, que l'on ajoute ensuite) dans des conditions proches de celles de la réaction étudiée. Cette dernière solution a été systématiquement adoptée de façon à ce que la chlorite et le talc du mélange aient des compositions aussi proches que possible des compositions à l'équilibre, le long de la courbe de réaction.

Ce choix ne va pas toujours sans problèmes pratiques, en particulier pour la synthèse d'associations à disthène à partir de gels ou de mélanges d'oxydes. En effet, la Mg-staurotide a une vitesse de nucléation et de croissance bien supérieure à celle du disthène. Ceci fait qu'elle cristallise à la place du disthène dès 600°C, plus de 100° en dessous de sa limite inférieure de stabilité et parfois même en présence de germes de disthène ! Il faut donc ruser, la meilleure technique consistant à introduire des germes de disthène et à élever lentement la température. La synthèse de pyrope, à 900°C et 25 kbar, présente occasionnellement un problème comparable avec la croissance métastable d'enstatite et de corindon.

Par ailleurs, il a été possible de jouer sur la proportion de produits et réactifs : un mélange à parts égales n'est pas toujours le plus favorable, une petite proportion de réactifs (ou de produits) rendant souvent l'effet de faibles degrés d'avancement de la réaction plus évident

sur le diffractogramme.

II - LES RELATIONS DE PHASES DE LA CARPHOLITE MAGNESIENNE

Ce minéral de basse température pose à l'expérimentateur l'éternel problème des barrières cinétiques. Pour des raisons évidentes, une expérience en presse hydraulique ne peut guère durer plus d'une semaine, exceptionnellement deux (quand les collègues sont en vacances !). Ceci fixe vers 500°C la limite de réactivité du système pour des pressions de 15 kbar et plus. Il n'est donc pas question de reproduire les conditions naturelles. On peut alors déterminer à plus hautes pression et température le prolongement (stable ou métastable) d'une courbe de réaction que l'on extrapolera vers les conditions naturelles, ceci arbitrairement, ou par le calcul en faisant une hypothèse sur la composition des phases à stoechiométrie variable (chlorite en particulier). On peut aussi essayer de déterminer un lot de réactions à hautes pression et température, sans intérêt direct pour les associations naturelles, mais pouvant permettre de reconstituer toute la grille pétrogénétique et donc d'imposer des contraintes sur les réactions de basse température. Les deux approches ont été adoptées ; à la première se rattache l'étude des réactions

carpholite = chlorite + disthène + quartz + H_2O (7)

carpholite + diaspore = chlorite + disthène + H_2O (13)

carpholite = chlorite + pyrophyllite + diaspore + H_2O (14)

à la seconde l'étude des réactions

carpholite = chlorite + disthène + talc + H_2O (15)

carpholite + quartz = disthène + talc + H_2O. (16)

Les résultats combinés aux données de Halbach et Chatterjee (1982) sur le sous-système Al_2O_3-SiO_2-H_2O fournissent la grille pétrogénétique représentée dans la figure 5 de Chopin et Schreyer (1983), reproduite ici en figure 7.

Je ne soulignerai que deux conséquences :

- l'existence vers 18 kbar et 540°C d'un point invariant mettant en jeu les phases solides talc, chlorite, disthène, quartz et carpholite. Cette température représente une nouvelle limite inférieure de stabilité à l'association "fétiche" talc-disthène, et la limite supérieure de stabilité de la Mg-carpholite.
- la limite inférieure de stabilité en pression de la Mg-carpholite peut être située vers 7 ou 8 kbar, pour des températures proches de 350°C. La prise en compte de la sudoïte dans le système ne doit guère élever cette valeur de pression. En effet, une série d'expériences à 6,5 kbar sur un mélange de Mg-carpholite, sudoïte naturelle et quartz n'a montré aucune réaction entre 300 et 400°C. Le domaine de stabilité de la Mg-carpholite est entièrement contenu dans celui de la lawsonite, ce qui fait de la carpholite un meilleur indicateur de haute pression et basse température.

III - LES RELATIONS DE PHASES DU CHLORITOIDE MAGNESIEN

Trois réactions mettant en jeu ce minéral ont été étudiées :

chloritoïde = chlorite + disthène + corindon + H_2O (17)

chloritoïde + talc = chlorite + disthène (4)

chloritoïde = pyrope + corindon + H_2O (18)

La première détermine la limite inférieure de stabilité en pression du chloritoïde ; la seconde correspond à une paragenèse naturelle et est d'un grand intérêt barométrique ; la troisième fournit la limite thermique supérieure du chloritoïde et, surtout, est la seule de toutes les réactions étudiées à ne mettre en jeu que des phases à stoechiométrie fixe (au composant hydropyrope du grenat près, cf. Ackermann et al., 1983).

1 - Le champ de stabilité du Mg-chloritoïde

La réaction (17) a pu être déterminée précisément entre 19 et 27 kbar, 600 et 720°C (tableau 4). On notera que la forte concavité de la courbe de réaction ne peut s'expliquer seulement par la variation des

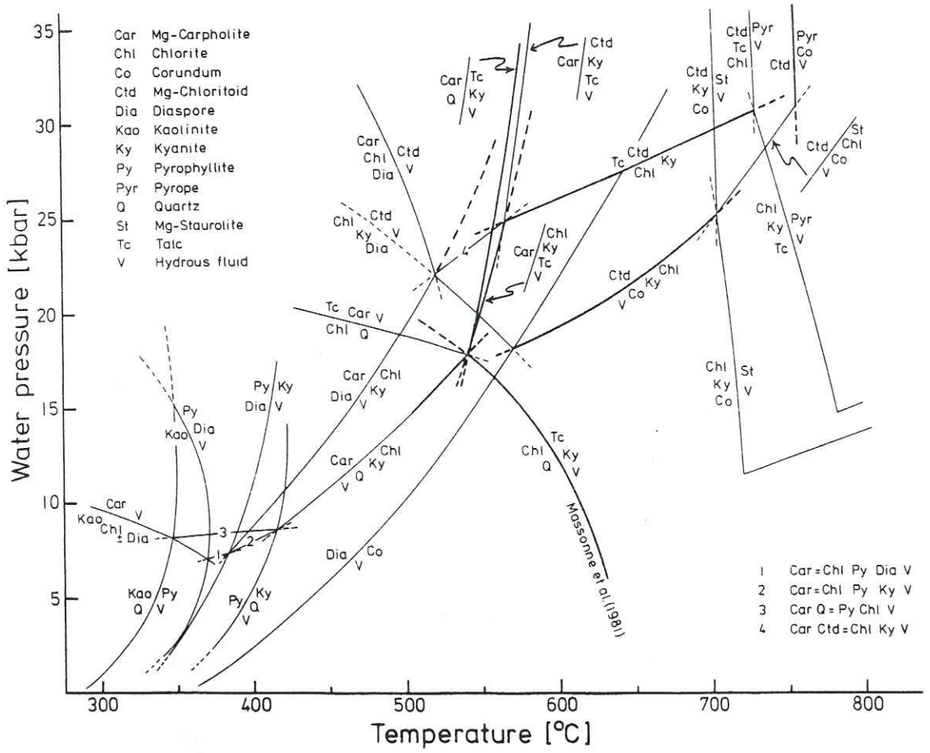

Fig. 7. Relations de phases à haute pression dans le système MASH (tiré de Chopin et Schreyer, 1983) : domaines de stabilité de la Mg-carpholite et du Mg-chloritoïde.
Les courbes en gras ont été déterminées expérimentalement lors de cette étude. Voir texte et tableaux 3 et 4.

propriétés thermodynamiques de l'eau. Il est nécessaire de supposer que la composition de la chlorite change le long de la courbe. Une courte extrapolation de la courbe jusqu'à 570°C lui fait couper celle de la réaction diaspore = corindon + H_2O que j'ai déterminée à 25 kbar (tableau 4). Cette intersection engendre la courbe de la réaction

chlorite + disthène + diaspore = chloritoïde + H_2O (19)

dont la pente calculée est négative (Fig. 7). Ce point invariant situé vers 570°C et 18 ou 19 kbar fixe donc la pression minimale de stabilité du Mg-chloritoïde. Ce dernier apparaît comme une phase de plus haute pression que le pyrope ou la Mg-staurotide dont les limites de stabilité sont proches de 15 kbar (Schreyer, 1968).

La limite thermique supérieure du chloritoïde est donnée par la réaction (18) que j'ai déterminée précisément entre 32 et 42kbar (tableau 4). La composition fixe des différentes phases faisait espérer qu'il serait possible de tirer de la courbe les paramètres thermodynamiques du chloritoïde. Cet espoir est malheureusement déçu car la pente de cette courbe est presque verticale, au point qu'il n'est pas possible d'en préciser le signe malgré des fourchettes expérimentales de moins de 20°C... Elle fixe en tout cas au chloritoïde une limite absolue de stabilité à 750°C. On notera que l'équivalent ferreux de cette réaction a également une pente très raide, vers 600-650°C (Ganguly, 1969). Sa position à plus basse température est conforme au fractionnement Fe-Mg observé dans la nature où le grenat est toujours plus ferreux que le chloritoïde.

2 - L'association talc-chloritoïde

La stabilité à haute pression du pôle magnésien du chloritoïde vient vérifier l'hypothèse faite lors de l'étude des paragenèses naturelles. Il est alors intéressant d'envisager le rôle dans le système magnésien du couple talc-chloritoïde, si caractéristique sur le terrain. Une différence importante apparaît dans le système magnésien : le chloritoïde ne peut coexister avec le quartz (Chopin et Schreyer, 1983), pas même de manière métastable. Il est donc impossible d'étudier directement les pôles des réactions mettant en jeu le quartz dans la nature, comme l'importante réaction (3). Néanmoins, la réaction (4)

chlorite + disthène = talc + chloritoïde

se révèle rapidement capitale pour la topologie du système. Elle impose en effet une limite de pression à l'association chlorite-disthène dont la stabilité ou l'instabilité domine toutes les relations de phases du système à température plus élevée (Schreyer, 1968). De plus, elle est indépendante de l'activité de l'eau (si la chlorite ne présente pas de déficit de remplissage octaédrique) et a priori fortement dépendante de la pression. La réaction a donc été étudiée expérimentalement, avec quelques difficultés. L'absence ou la faible quantité d'eau libérée fait que l'énergie libre mise en jeu est faible, le système est donc peu réactif en particulier à faible température. D'autre part, des superpositions de pics sur le diffractogramme rendent des taux de réactions élevés nécessaires pour l'interprétation du sens de réaction. Pour ces raisons, la courbe de réaction n'a pu être bien encadrée que vers 700°C, 30 kbar, les données de basses températures permettant néanmoins une bonne localisation de la courbe vers 600°C, 25 kbar (Tableau 4).

L'intérêt barométrique de cette réaction est montré par l'étude de l'association du Mont Rose à talc, disthène, chloritoïde, chlorite et quartz : les données expérimentales permettent d'estimer les conditions de formation à environ 16 kbar, 500°C. La présence de quartz réduit la variance du système et permet même de préciser l'activité de l'eau (Chopin et Monié, 1984).

De plus, grâce à la connaissance de cette courbe, la topologie du système peut être entièrement reconstituée (Fig.7), ce qui permet d'estimer la position des courbes métastables où interviennent quartz et chloritoïde (Chopin et Schreyer, 1983, Fig. 7). Ceci donne une idée assez précise des pentes des courbes les plus importantes pour l'évolution des systèmes naturels. Par exemple, le passage par un maximum de la teneur en Mg du chloritoïde à métamorphisme croissant trouve une explication simple : après la disparition de la chlorite au profit de talc-disthène-chloritoïde, la composition du chloritoïde est contrôlée par l'équilibre

chloritoïde + quartz = talc + disthène + H_2O (20)

Chopin et Schreyer (1983, Fig. 7) montrent que la courbe correspondante a une pente si forte que, pour tout chemin métamorphique prograde, l'équilibre est déplacé vers la chlorite, c'est-à-dire vers une diminution de la teneur en Mg du chloritoïde. Cette teneur passe donc bien par un maximum au moment où la chlorite disparaît (Fig. 4 et Chopin, 1983, Fig. 2).

IV - L'APPARITION DU PYROPE

La paragenèse à talc-disthène-pyrope-quartz/coesite découverte dans le quartzite de Dora Maira et celle à chlorite-talc-disthène découverte en inclusion dans les pyropes décimétriques à ellenbergerite (Chopin, 1985) correspondent aux réactions

talc + disthène = pyrope + SiO_2 + H_2O (8)

et chlorite + talc + disthène = pyrope + H_2O (21)

Elles sont univariantes dans le système MASH et représentent l'apparition prograde du pyrope et de pyrope + SiO_2. Les conditions uniques de métamorphisme de ce gisement et le caractère hypermagnésien du système naturel rendaient la détermination expérimentale de ces réactions fort instructive et d'application directe.

Les résultats expérimentaux sont portés dans le tableau 5 et la figure 8. La localisation des deux courbes n'est pas très précise et est souvent fondée sur des taux de réaction faibles. Néanmoins, elle représente un progrès considérable par rapport aux données expérimentales disponibles jusqu'alors (Schreyer, 1968, pour la réaction 21) et même par rapport à des modèles thermodynamiques sophistiqués qui, par exemple, placent la courbe de la réaction (8) 50°C trop bas (Holland, comm. pers. 1983), avec des conséquences dramatiques pour la stabilité de l'association talc-pyrope-quartz. Les deux premières expériences du tableau 5 permettent de localiser à la fois la transition quartz-coesite vers 28,5 kbar et la limite de stabilité thermique du talc vers 815°C (Fig. 8). Il en résulte que l'intersection de ces deux courbes se trouve sur la courbe déterminée par Massonne (1983) pour la réaction

enstatite + disthène = pyrope + quartz. (9)

Cette courbe est donc relayée vers les basses températures par celle de la réaction (8) où la coesite, et non le quartz, figure SiO_2. Ainsi, à l'incertitude analytique près et quelle que soit l'activité de l'eau, l'association talc-pyrope-quartz n'a pas de domaine de stabilité dans le système MASH. Seule l'introduction de fer peut la stabiliser.

Les données du tableau 5 et la figure 8 montrent que le champ de stabilité de l'association talc-pyrope-coesite définit un domaine très étroit de température, centré sur 800°C. Cette association a donc une excellente valeur thermométrique ou "hygrométrique", puisque la position

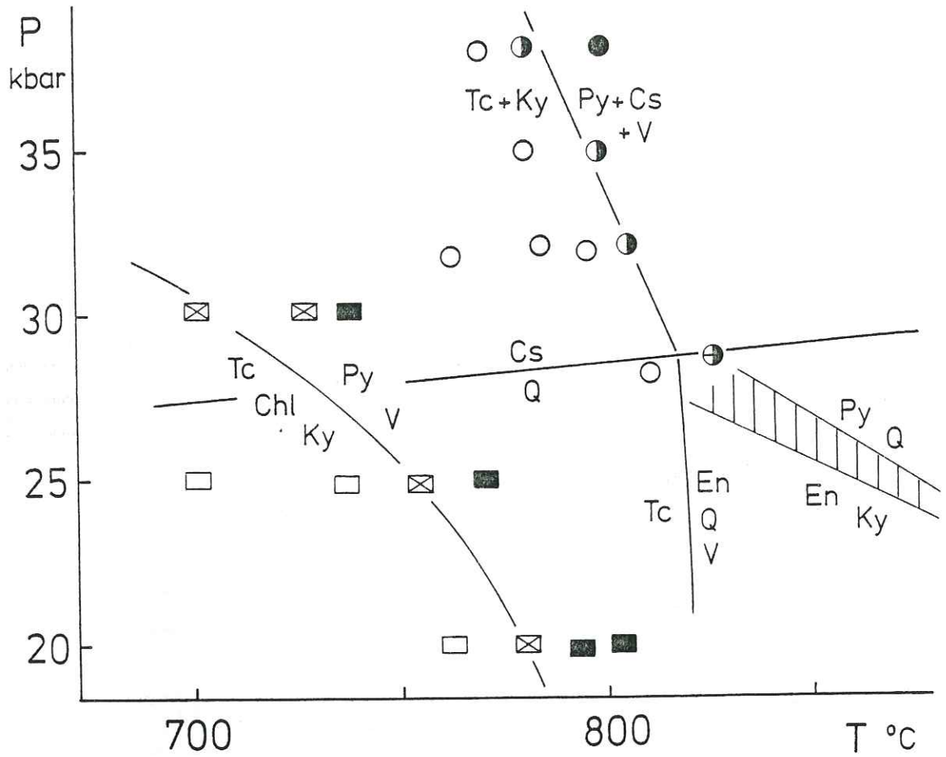

Fig. 8. Résultats expérimentaux portant sur la limite de stabilité inférieure du pyrope.
Les symboles pleins indiquent la croissance du pyrope, les symboles barrés ou à demi remplis indiquent l'absence de réaction observée. Le domaine d'incertitude sur la réaction En + Ky = Py + Q est tracé d'après Massonne (1983 et comm. pers.). Comme la stabilité thermique du talc est encore abaissée dans le champ de la coesite, le domaine à pyrope - coesite - talc est extrêmement étroit.

du domaine correspondant dépend de l'activité de l'eau.

La connaissance des courbes des réactions (8) et (21) permet d'aborder l'histoire du quartzite à pyrope en termes de pression, température et activité de l'eau (Chopin, 1985). Ce dernier paramètre est particulièrement important en l'occurrence, car il est le seul à pouvoir expliquer l'absence de fusion partielle pour les conditions de pression et température déduites (Chopin, 1984). Néanmoins, une activité de l'eau élevée dans les gros grenats (à chlorite, ellenbergerite, amphibole) et faible dans la matrice (à talc, disthène, pyroxène) ne suffit pas à expliquer cette différence de paragenèse. Les inclusions des gros grenats témoignent bien d'un stade un peu antérieur de l'évolution, à température et peut-être pression un peu plus faibles : 700°C environ contre 750°C, pour des pressions de 1'ordre de 25 kbar contre 28 à 30 ensuite (Chopin, 1985).

V - L'ELLENBERGERITE, NOUVELLE PHASE DU SYSTEME MASH

Nous avons déjà évoqué la possibilité d'une ellenbergerite non titanifère impliquant la substitution $Ti\square = MgMg$ et conduisant à la formule

$Mg_2Mg_6Al_6Si_8O_{28}(OH)_{10}$ "Mg-ellenbergerite".

Des expériences préliminaires conduites par W. Schreyer avec cette composition de départ ont rapidement permis la synthèse d'une phase ayant toutes les propriétés cristallographiques de l'ellenbergerite (Schreyer et al., 1985). A 40 kbar et 700°C, cette phase apparaît même spontanément ; à 30kbar et 700°C, elle n'est plus stable (W. Schreyer, comm. pers.).

En se fondant sur des arguments cristallochimiques déjà développés concernant la taille des cations, il est possible de proposer la succession suivante de domaines de stabilité à pression croissante : Zr-ellenbergerite, Ti-ellenbergerite et "Mg-ellenbergerite" (Chopin, 1985). Ce premier résultat expérimental confirme une partie de l'hypothèse puisque la Ti-ellenbergerite naturelle n'a pu se former à plus de 30 kbar (en raison de la stabilité de chlorite-disthène au lieu de Mg-chloritoïde-talc). Mais il est possible d'aller encore plus loin en jouant sur l'analogie de structure avec la wadéite et $K_2SiSi_3O_9$ (cf. 1ère partie, IV-6), en substituant Si à Ti dans

le site octaédrique situé sur l'axe sénaire. Ceci conduit à la formule extrême

$$(Si,\square)_2\ Mg_6\ Al_6\ Si_8O_{28}\ (OH)_{10}$$

la substitution $Si\square$ = MgMg fournissant une série de compositions jusqu'à la "Mg-ellenbergerite". Pour la même raison que précédemment, la composition serait d'autant plus riche en Si que la pression serait élevée.

Tout ceci n'est que spéculation, mais pourrait rendre compte du fait que les synthèses réalisées avec une composition de départ de Mg-ellenbergerite n'ont pas été totales, d'autres phases restant présentes même après 4 jours d'expérience (Schreyer et al., 1985). Quoi qu'il en soit, ceci ouvre à nouveau la possibilité de trouver du silicium hexacoordonné dans cette structure.

VI - CONCLUSION A L'ETUDE EXPERIMENTALE ET PETROGRAPHIQUE

1 - **Le système magnésien**

Il est piquant de constater qu'en moins de cinq ans trois nouvelles phases ont été synthétisées dans un système expérimental qui, modèle par excellence des pélites naturelles, a déjà reçu une attention considérable de la part des expérimentateurs, même à haute pression (Boyd and England, 1959 ; Schreyer, 1968 ; Schreyer et Seifert, 1969 ; Ackermand et al., 1975 ; Gasparik et Newton, 1984, parmi d'autres). Ceci me paraît significatif de l'évolution récente de la pétrologie qui découvre l'intérêt des métapélites de haute pression et basse température (cf. Chopin, 1985, conclusion). Pour un même domaine de pression, mon unique mérite aura été d'avoir travaillé à des températures inférieures à celles qu'affectionnaient mes prédécesseurs et d'avoir su, guidé par l'étude pétrographique, ce qu'on pouvait espérer y trouver.

Le travail expérimental présenté ici renouvelle donc les connaissances dans ce domaine. La succession avec recouvrement à pression et température croissantes des champs de stabilité de la carpholite, du chloritoïde et du pyrope en est la pièce maîtresse. Elle fournit un cadre à l'évolution minéralogique reconnue dans la première partie et confirme largement les hypothèses faites. Le caractère inhabituel des associations rencontrées est bien dû à des gradients thermiques faibles, mais surtout à l'atteinte de degrés métamorphiques élevés le long de tels gradients.

2 - **Passage au système ferro-magnésien**

a) D'un pôle à l'autre :

La comparaison des domaines de stabilité des pôles ferreux et magnésiens du grenat, de la staurotide et du chloritoïde a été esquissée par Chopin et Schreyer (1983, Fig. 6). Le chloritoïde, dont le pôle ferreux est stable dès les très basses pressions, fournit un nouvel exemple de la relation entre taille du cation et stabilité en pression. Cette comparaison rend évident le fait que dans les métamorphismes classiques, de type basse ou moyenne pression, ni les Fe-Mg-carpholites ni les chloritoïdes magnésiens ne peuvent être rencontrés. Au contraire, pour des gradients thermiques faibles, de

l'ordre de 10°C/km ou moins, il est clair que la succession paragénétique doit bien être Fe-Mg carpholite avec ou sans chloritoïde ferreux et sans grenat ; chloritoïde devenant magnésien, sans carpholite mais avec grenat ferreux ; puis possibilité de grenats très magnésiens. Par comparaison avec les autres phases de haute pression, la Mg-staurotide apparaît surtout comme une phase de haute température. On trouve là l'explication à l'apparition des staurotides magnésiennes dans des gradients thermiques plus élevés (cf. Schreyer et al., 1984 ; Ward, 1984 ; Grew et Sandiford, 1984). Un gradient thermique plus faible favorise l'incorporation du magnésium dans le chloritoïde ; une éventuelle staurotide reste alors ferreuse (cf. 1ère partie, IV-4 ; Udovkina et al., 1978) sauf si des températures élevées sont atteintes, ce qui impose d'approcher le champ de la coesite. Ceci fait rêver de rencontrer une roche magnésienne et hyperalumineuse dans Dora Maira, car une telle roche fournirait l'occasion unique de trouver une staurotide proche du pôle magnésien.

b) Vers une grille pétrogénétique

J'ai essayé de résumer l'état des connaissances sur les métapélites de haute pression dans une grille pétrogénétique s'appliquant au système ferromagnésien. L'emploi fait de l'analyse de Schreinemakers généralisée suppose l'analyse préalable des systèmes magnésien et ferreux ; c'est la seule approche rigoureuse, dont Vielzeuf et Boivin (1984) ont précisé récemment le détail.

Dans le système FMASH j'ai donc considéré les phases quartz, disthène, talc-minnesotaïte, grenat (almandin-pyrope), chlorite (Fe-Mg) et chloritoïde (Fe-Mg). J'ai dû renoncer momentanément à inclure dans cette analyse la carpholite et la staurotide, en raison des inversions de fractionnement qu'elles présentent. L'analyse du sous-système magnésien est simple, l'unique difficulté provient de l'instabilité du Mg-chloritoïde en présence de quartz. Néanmoins Chopin et Schreyer (1983, Fig. 7) ont montré que la position des courbes métastables pouvait être déduite des données expérimentales avec une relative précision. Il advient que les points invariants (Mg-chlorite), (Mg-grenat) et (Mg-chloritoïde) sont stables dans l'analyse considérée et les points invariants (Mg-talc) et (Mg-disthène) métastables (Fig. 9). La position du point (Mg-grenat) peut-être estimée vers 500°C, 20 kbar (Chopin et Schreyer, 1983, modifié par Chopin et Monié, 1984), celle du

point Mg-chlorite très grossièrement vers 800°C, 40 kbar. Le point (Mg-chloritoïde), qui est le même que le point (ellenbergerite, rutile) de Chopin (1985), est rejeté vers des pressions négatives car les deux courbes stables qui le déterminent sont quasi parallèles (réactions 5 et 8). L'analyse du sous-système ferreux, en particulier des relations entre chloritoïde et almandin, fournit bien la grille résiduelle où les points invariants (Fe-disthène) et (Fe-talc) sont stables, (Fe-chloritoïde), (Fe-grenat) et (Fe-chlorite) métastables. A partir des travaux expérimentaux déjà cités, seul le point (Fe-talc) peut être localisé, entre 550 et 600°C et à une pression inférieure à 3 kbar.

Les réactions univariantes du système ferromagnésien joignent deux à deux les points invariants homologues des deux systèmes limitants et se coupent en un point invariant d'ordre supérieur (Fig. 10 a). Le long de chacun de ces segments de courbes, la composition des minéraux varie du pôle Fe jusqu'au pôle Mg, avec un fractionnement entre les phases qui reste qualitativement le même dans le cas de solutions solides proches de l'idéal. La préférence du fer va croissant dans l'ordre talc, chlorite, chloritoïde, grenat. L'ordre de préférence détermine la position des courbes univariantes Fe-Mg par rapport à celles des systèmes limitants. La branche partant d'un point stable du système limitant est stable, celle partant d'un point métastable est métastable.

La grille résultante est représentée dans la figure 10 b. Celle-ci met clairement en évidence un domaine à chlorite-quartz, un domaine à talc-chloritoïde et un domaine à talc-disthène-grenat. On vérifie avec intérêt que le domaine à talc-chloritoïde se subdivise en un domaine à chlorite (cf. Grand Paradis) et un domaine à disthène (cf. Hohe Tauern) de plus haut degré. Sur la courbe qui les sépare se trouverait le "point" représentatif de la paragenèse décrite au Mont Rose (à l'activité de l'eau près). Le domaine à talc-chloritoïde est limité vers les basses pressions par la courbe de la réaction

chlorite + grenat + quartz = talc + chloritoïde $\pm$ H_2O (22).

Le sens de la déshydratation dépend de la composition exacte des phases et pourrait varier le long de la courbe, dont la pente est certainement faible. Nous avons vu dans la première partie (III-5) que cette réaction intervient dans la "lacune" qui sépare Vanoise de Grand Paradis. Il n'est malheureusement guère possible de la localiser précisément en pression. Une estimation moyenne de 10 kbar me paraît raisonnable, entre le minimum de 7 kbar imposé par l'absence de cordiérite et le maximum de 15

Fig. 9. Analyse de Schreinemakers des systèmes FeO - Al_2O_3 - SiO_2 - H_2O et MgO - Al_2O_3 - SiO_2 - H_2O. Les phases considérées sont talc, chlorite, chloritoïde, grenat, disthène ; SiO_2 et H_2O sont en excès. Les lignes pleines et les points représentent les courbes et points invariants stables, les lignes en tireté et les cercles représentent les courbes et points invariants métastables. Les points invariants sont désignés par la phase absente.

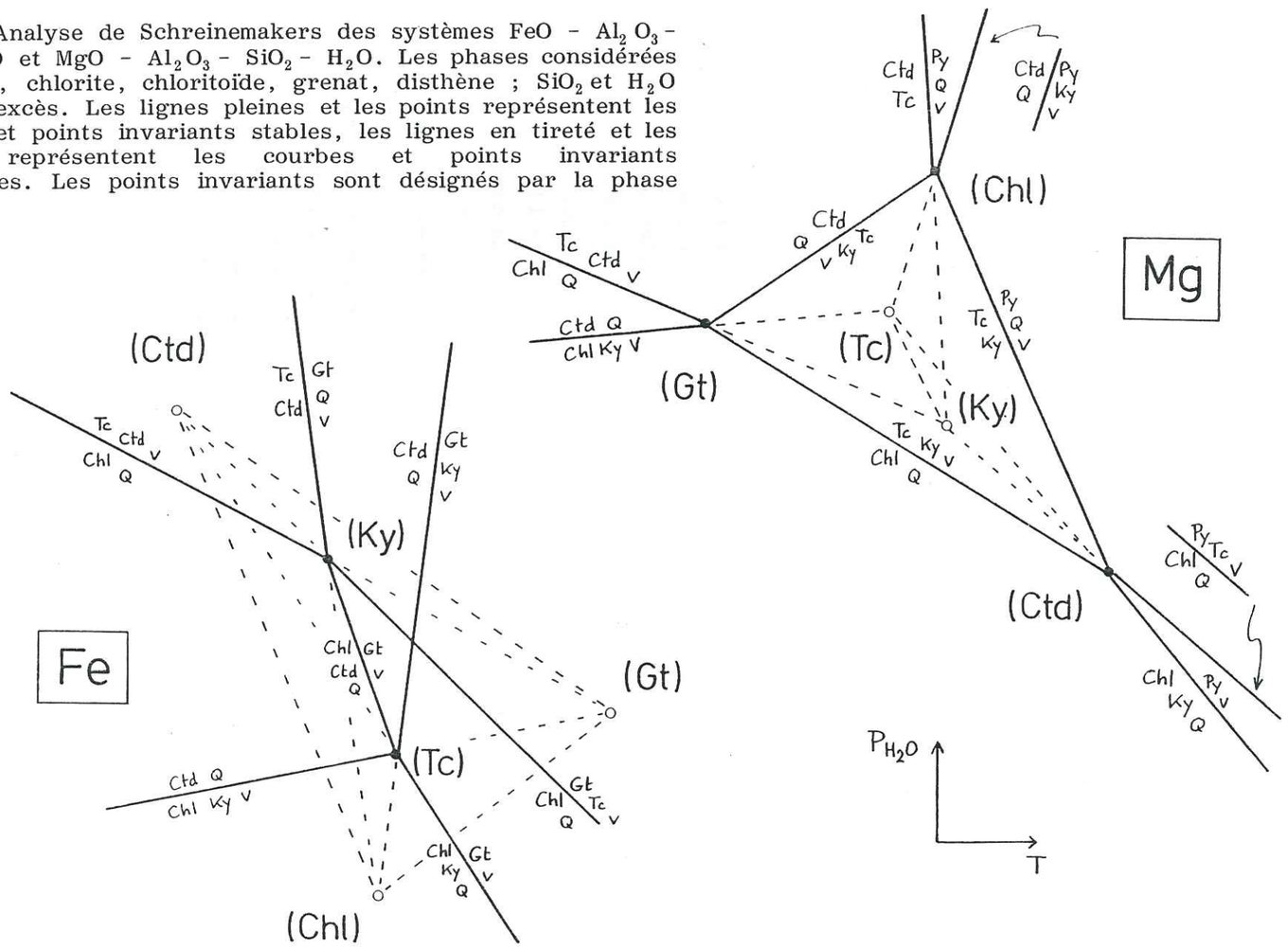

Fig. 10 a

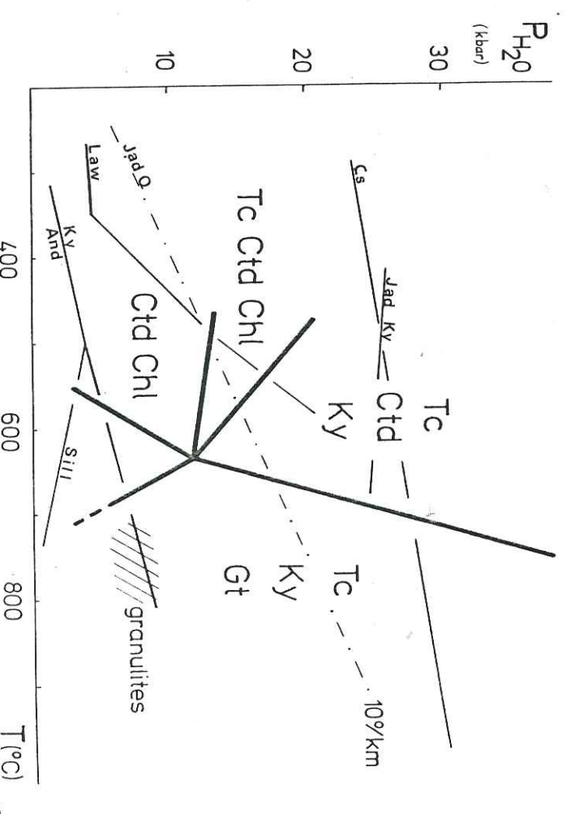

Fig. 10 b

Légende au verso

Univ. J. Fourier - O.S.U.G.
MAISON DES GEOSCIENCES
DOCUMENTATION
B.P. 53
F. 38041 GRENOBLE CEDEX
Tél. 04 76 63 54 27 - Fax 04 76 51 40 58
Mail : platour@ujf-grenoble.fr

Fig. 10 a. Combinaison des deux analyses précédentes, réalisée en imposant un enrichissement en fer croissant dans l'ordre talc, chlorite, chloritoïde, grenat.
Les traits gras représentent les courbes univariantes du système ferro-magnésien, les traits fins et continus, les courbes univariantes stables des systèmes magnésiens et ferreux. La localisation dans le champ P-T est faite en utilisant les données expérimentales de Massonne et Schreyer (1983) et les miennes pour le système magnésien, celles citées dans le texte pour le système ferreux. L'échelle des températures est la même que celle de la figure b.

Fig. 10 b. Domaine de stabilité des principales paragenèses discutées dans cette étude. La construction précédente est réduite aux courbes du système ferro-magnésien. Par comparaison sont indiqués les domaines de stabilité de quelques autres associations ou minéraux caractéristiques Le gradient de 10°/km est tracé pour une densité de 2,7, Il coïncide avec la limite de stabilité de jadéite + quartz. Le domaine des granulites est représenté comme exemple d'un métamorphisme extrême.

kbar imposé par la paragenèse du Mont Rose.

La figure 10 b montre aussi fort bien la signification de l'association talc-disthène-grenat. Celle-ci est surtout révélatrice de températures relativement élevées car elle peut exister pour une très large gamme de pressions. Il s'agit dans tous les cas de pressions se situant au-dessus de 7 kbar. Les trois gisements connus sont effectivement associés à des éclogites. Mais dans deux d'entre eux (Tasmanie et probablement Kazakhstan), l'association critique est formée sans que le domaine à talc-chloritoïde soit traversé. Au contraire, le chemin métamorphique conduisant à la paragenèse de Dora Maira doit presque nécessairement traverser tout le champ à talc-chloritoïde.

Nous arrivons ainsi à la nécessité de distinguer parmi les roches à talc-disthène, les "whiteschists" de Schreyer (1977), certaines formées à relativement basse pression, d'autres à haute ou très haute pression (Chopin et Schreyer, 1983). Ceci se trouve corroboré par le travail expérimental de Massonne et Schreyer (1983) qui montre que le couple talc-disthène peut être stable dès 6,5 kbar. C'est donc uniquement la nature et la composition d'une phase ferromagnésienne éventuellement associée qui peut renseigner sur les conditions de formation : chloritoïde ou grenat, l'un et l'autre plus ou moins magnésiens.

Ce diagramme qui intègre harmonieusement les données expérimentales et les observations couvre exactement mon domaine d'élection, celui des pressions élevées et températures modérées voire fortes. Il demanderait à être complété vers les basses températures par la prise en compte de la carpholite. Il se raccorde directement vers les basses pressions et températures plus élevées avec la construction de Grew et Sandiford (1984, Fig. 6) qui met en jeu cordiérite et staurotide. Une fois surmonté le problème des inversions de fractionnement, c'est donc une image assez complète de l'évolution des métapélites que nous aurons.

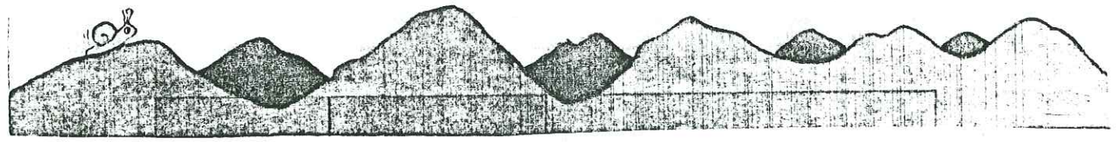

Troisième partie

CONSEQUENCES GEOLOGIQUES

La nouveauté apportée par l'étude pétrographique n'est pas la persistance à grande profondeur de gradients thermiques anormalement faibles, car les modèles thermiques d'enfouissement d'une plaque lithosphérique en montrent la nécessaire existence (Minear et Toksöz, 1970). La nouveauté relative tient à deux choses :

- au fait qu'une paragenèse cristallisée à une profondeur voisine de 100 km peut revenir quasi intacte à la surface.
- au fait qu'une unité continentale semble impliquée dans un enfouissement aussi considérable.

Ces deux points ont des incidences importantes sur la nature des phénomènes mis en jeu lors de l'exhumation et sur le comportement de la croûte continentale dans une zone de collision. C'est ce que nous envisageons dans un premier chapitre, avant de nous intéresser spécifiquement à la chaîne alpine.

I - LA CROUTE CONTINENTALE ENFOUIE A 100 km DE PROFONDEUR ?

1 - Situation et signification de la coesite de Dora Maira

Le rôle possible des contraintes mécaniques dans l'apparition de coesite a déjà été envisagé (1ère partie, IV-2 ; Chopin, 1984) et récusé. De plus, la présence du nouveau minéral ellenbergerite dans une roche de composition commune est sans doute le meilleur argument pour confirmer les pressions très élevées. Une autre hypothèse a priori envisageable était celle de l'introduction tectonique de la roche à coesite dans un encaissant qui n'aurait pas subi les mêmes pressions, à l'instar de certains corps de péridotite à grenat des Alpes centrales (e.g. Evans et al., 1979). L'extension géographique du banc de quartzite à pyrope-coesite (Chopin, 1985, Fig. 1), son association quasi stratigraphique avec un horizon de marbres et éclogites et finalement la découverte de coesite dans cet encaissant réfutent également cette possibilité. Il nous faut donc admettre qu'est passée dans le domaine à coesite toute l'unité encaissante, qui représente un socle paléozoïque polymétamorphique injecté de granite. Il n'y a donc pas de doute sur ce point : un matériel crustal typiquement continental peut être enfoui à près de 100 km de profondeur.

S'agit-il alors simplement d'une écaille ou la totalité du massif

Dora-Maira a-t-elle subi le même sort ? Le socle polymétamorphique constitue près de la moitié du massif à l'affleurement (cf. Vialon, 1966 ; Chopin, 1984, Fig. 1) et s'allonge du Nord au Sud. La présence d'associations de très haute pression n'est pas documentée dans toute la partie nord. Néanmoins, Vialon y décrit et j'y ai observé en Val Germanasca des schistes à porphyroblastes de grenat et grosses pseudomorphoses qui rappellent beaucoup les schistes à grenat, disthène et coesite du Sud du massif ; de petits cristaux de chloritoïde semblent postérieurs au grenat et seraient donc rétrogrades. Une communauté d'histoire avec le socle méridional paraît vraisemblable, avec un stade initial à grenat-disthène. Cette unité affleurant sur près de 20 km d'Est en Ouest et près de 40 du Nord au Sud (voir la figure 1 de Chopin, 1984), il ne peut s'agir d'une modeste écaille, même si nous sommes loin des coupes à travers la croûte inférieure que peuvent livrer la Calabre ou la zone d'Ivrée.

2 - **Conséquences**

On considère généralement qu'en raison de sa densité relativement faible, la croûte continentale n'est pas engloutie lors des processus géodynamiques, en particulier dans les zones de subduction. De fait, pendant longtemps les estimations de pression faite sur des roches métamorphiques n'ont guère dépassé 7-10 kbar, l'équivalent de la base de la croûte continentale. La présence d'une unité crustale continentale entièrement éclogitisée, dans la zone Sesia des Alpes occidentales (cf. Compagnoni et al., 1977), a imposé de nuancer d'autant plus qu'on découvrait la fréquence du charriage de croûte océanique sur des unités continentales. Ceci, en impliquant des enfouissements de l'ordre de 40 à 50 km, restait encore à la mesure des épaississemens crustaux connus dans les zones de collision comme les Alpes ou l'Himalaya.

La découverte de coesite dans le massif cristallin de Dora-Maira impose à plus forte raison de renoncer à l'idée d'une croûte continentale restant en surface. Au même titre que la croûte océanique, elle peut être entraînée à grande profondeur (Chopin, 1984). Le contraste de densité n'est peut-être pas aussi critique qu'il y paraît. Même si elles se produisent à plus grande profondeur que dans les roches basiques, les transitions de phases dans le matériel continental, l'apparition de la coesite en particulier (d = 2,9), viennent réduire la différence de densité. Par ailleurs, l'entraînement en

profondeur de matériel continental est d'autant plus facile que la croûte en question est amincie (Ingrin, 1985). Ceci peut en particulier être le cas pour une marge continentale jusqu'alors passive, comme l'évolution de la sédimentation dans le Briançonnais le suggère (Lemoine, 1975 ; Graciansky et Lemoine, 1980). J'ai évoqué (Chopin, 1984) quelques indices géophysiques suggérant l'existence actuelle d'un enfouissement de croûte continentale en Indonésie (de la plaque australienne sous Timor) et dans le golfe d'Alaska.

II - LES CONDITIONS DU REFROIDISSEMENT ; COROLLAIRES.

La plupart des modèles d'évolution thermique d'une zone d'épaississement crustal (Oxburgh et Turcotte, 1974 ; Draper et Bone, 1981 ; England et Thompson, 1984) montrent que, si l'érosion est le seul facteur entrant en compétition avec la remontée des isothermes, les roches enfouies subissent une notable élévation de température lors de leur retour vers la surface.

Or l'étude pétrographique des roches à coesite montre qu'après la culmination de pression, l'élévation de température a été très limitée. L'argument le plus contraignant est apporté par la stabilité de l'association talc-phengite, qui a été envisagée en termes cinétiques (Chopin, 1984, p. 114-115). De plus, l'étude mécanique du comportement d'une inclusion de coesite dans un pyrope (Gillet et al., 1984) conduit au même résultat par des voies totalement indépendantes. Nous en concluons que le retour de ces roches vers la surface, ou plus exactement leur refroidissement, est essentiellement contrôlé par la tectonique. En effet, c'est bien l'érosion qui permet la remontée des unités vers la surface, mais c'est le charriage d'unités plus froides sous les unités considérées qui ralentit la remontée des isothermes (voir Goffé et Velde, 1984, pour un exemple bien documenté pris dans le cadre alpin). Si un tel rôle de la tectonique n'est guère surprenant dans une zone de collision, ce retour ne peut être que facilité par un contraste de densité entre unité considérée et encaissant. S'il est possible à des corps de péridotite d'être inclus tectoniquement à des niveaux crustaux élevés, ce doit l'être d'autant plus pour des roches "légères", surtout en plus grandes masses.

Ceci nous suggère deux remarques. L'une concerne la structure du

massif de Dora-Maira qui, à côté des grands plis couchés transverses (Vialon, 1966), est dominée par de grands écaillages de plusieurs dizaines de kilomètres de flèche (Michard, 1965). Si le socle polymétamorphique semble bien constituer un tout, il est surmonté par une série siliceuse permienne et permo-triasique en contact souvent anormal et il surmonte lui-même la série carbonifère de Pinerolo qui apparaît en fenêtre. Or rien ne laisse penser que cette série apparemment la plus profonde ait subi un intense métamorphisme alpin. L'abondance du chloritoïde dans la série permienne surmontant le socle pourrait également suggérer une saute de métamorphisme. Cependant Michard (1967, p. 83) signale que le chloritoïde peut être postérieur à des pseudomorphoses de staurotide (?), ce qui laisse ouverte la possibilité d'un métamorphisme précoce comparable à celui du socle. Quoi qu'il en soit, cette structure avec de grandes lames de socle reposant sur une série plus "froide" s'accorde parfaitement avec la nécessité d'un refroidissement d'origine tectonique.

La deuxième remarque concerne le devenir d'unités crustales profondément enfouies dans le cas où la remontée des isothermes serait plus rapide, le système étant, par exemple, tectoniquement bloqué. Nous avons vu que les paragenèses du socle de Dora-Maira indiquaient des conditions proches de la fusion pour la plupart des roches. Dans ce cas la remontée des isothermes va engendrer très rapidement l'apparition d'une phase fondue, ce qui ouvre de nouvelles possibilités pour la genèse des magmas acides. Il devient dès lors important de reconsidérer la géologie régionale avec un oeil neuf, des migmatites ou des granites n'étant plus a priori nécessairement anté-alpins. Peut-être n'est-il pas fortuit que le granitoïde alpin de Biella se trouve dans la même situation que Dora-Maira par rapport à l'anomalie gravimétrique d'Ivrée.

III - L'EVOLUTION DE LA CHAINE ALPINE

1 - Les nouvelles données chronologiques

Le travail du pétrographe va au-delà de celui du chimiste. Il ne suffit pas d'assigner telles conditions de pression et température à tel échantillon ou telle unité, encore faut-il pouvoir préciser quand ces conditions ont été réalisées. Pour cette raison, j'ai poursuivi une collaboration avec Henri Maluski et Patrick Monié, tous deux à Montpellier

et spécialistes des datations par la méthode ^{39}Ar-^{40}Ar, bien adaptée à la résolution des problèmes alpins.

Notre stratégie se fonde directement sur l'expérience pétrographique : dans toute paragenèse de haute pression rétromorphosée le système isotopique a été ouvert ; il nous fallait donc des associations de haute pression indemnes de rétromorphose, ce qui implique aussi indemnes de déformations ultérieures. En pratique c'est un petit nombre d'échantillons très caractéristiques qui a été étudié, en particulier l'échantillon du Mont Rose à chloritoïde magnésien et celui de Dora-Maira à pyrope-coesite.

L'échantillon non déformé du Mont Rose fournit un âge plateau de 110 $\pm$ 3 Ma (Chopin et Monié, 1984). L'échantillon de quartzite à pyrope, où une foliation est à peine ébauchée, fournit un âge plateau à 105 $\pm$ 3 Ma (Chopin et Monié, inédit). Une série d'échantillons du Grand Paradis, foliés en conditions de haute pression et non déformés ultérieurement, fournit des âges plateaux indiquant une fermeture isotopique des systèmes s'étageant entre 75 et 60 Ma environ (Chopin et Maluski, 1980, 1982).

Ces résultats s'éclairent mutuellement. Alors qu'un doute était encore permis sur l'interprétation de l'âge du Mont Rose pris isolément, sa coïncidence avec celui obtenu dans Dora-Maira ne peut être fortuite. Elle indique qu'il s'agit bien d'un âge géologiquement significatif, datant la fermeture du système isotopique. Il semble que seuls les rares systèmes ayant échappé à la déformation puissent conserver l'âge initial. Tout l'art du pétrographe consiste à trouver ces perles rares qui le renseignent à la fois sur l'âge et les conditions du métamorphisme ; ceci n'a pas encore été possible dans le Grand Paradis.

Ces résultats sont très importants car ils reculent considérablement l'âge présumé du métamorphisme de haute pression dans les socles internes, qui passe de 60-80 Ma à 100-110 Ma. Ceci vient conforter les âges Rb-Sr de 130 $\pm$ 20 Ma obtenus sur les associations de haute pression de la zone Sesia par Oberhänsli et al.(1982). L'étude pétrographique avait montré un important contraste de métamorphisme entre le Briançonnais, de relativement bas degré, et les socles penniques internes de haut degré tels Grand Paradis ou Mont Rose. Du fait que la série stratigraphique briançonnaise monte jusque dans l'Eocène inférieur,

voire moyen (Ellenberger, 1958), ces datations soulignent l'énormité du hiatus existant entre les deux domaines continentaux de la zone pennique maintenant juxtaposés. Ils diffèrent par l'intensité mais aussi l'âge de leur métamorphisme : au début du Crétacé supérieur, le Briançonnais interne recevait encore une pluie de sédiment, les futurs "marbres chloriteux" de Vanoise, alors que les futurs massifs cristallins internes étaient profondément enfouis.

2 - **Image générale**

Quelle vision des Alpes nous procurent ces données nouvelles combinées à d'autres plus classiques ? En réalisant une coupe passant par Vanoise et Grand Paradis (cf. Fig. 1) nous voyons se succéder d'Ouest en Est :

- un domaine externe où le métamorphisme, simple réchauffement très lié aux circulations de fluides (Saliot, 1973 ; Saliot et al., 1982), est d'âge oligo-miocène. Des bassins molassiques de même âge contiennent des galets de roches métamorphiques des domaines internes (de Graciansky et al., 1971).

- la zone briançonnaise externe, où la lawsonite finit par apparaître (Saliot, 1973),

- la zone briançonnaise interne avec les massifs de la Vanoise et d'Ambin, où s'exprime typiquement la carpholite dans un métamorphisme postérieur à l'Eocène moyen, dont les conditions typomorphes sont estimées vers 300°C, 6-7 kbar (Goffé et Velde, 1984).

- le domaine piémontais. Les Schistes lustrés comprennent d'abord les unités "pré-piémontaises" qui s'étendent du Trias au Crétacé supérieur (Lemoine et al., 1978), ont été déposées sur une marge continentale et sont faiblement métamorphisées. Puis viennent des unités ophiolitiques dont les premiers termes sont datés de l'Oxfordien (De Wever et Caby, 1981) et dont une, dans le Queyras, contient du Crétacé supérieur fossilifère (Dumont et al., 1984). Le degré métamorphique y est variable mais dans toute la partie interne une unité riche en ophiolites et de degré métamorphique élevé (talc-chloritoïde, etc...) affleure depuis Zermatt au Nord jusqu'au Mont Viso dans les Alpes du Sud. L'âge du métamorphisme de haute pression est crétacé supérieur (Hunziker, 1974 ; Carpena, 1984).

- dans les massifs cristallins internes, le degré métamorphique est encore un peu plus élevé et l'âge un peu plus ancien (100-110 Ma, Crétacé moyen), puis une nouvelle étape est encore franchie en intensité

et en âge dans la zone Sesia (130 Ma).

- par dessus reposent les séries austroalpines de la nappe de la Dent Blanche avec une unité granulitique analogue à la zone d'Ivrée.

- la zone d'Ivrée (voir figure 11) n'est pas affectée par le métamorphisme alpin.

Un des traits les plus caractéristiques de cette succession me paraît être l'augmentation discontinue à la fois de l'âge et de l'intensité du métamorphisme lorsqu'on se déplace vers l'Est, jusqu'au bord interne de la zone Sesia et de Dora-Maira, c'est-à-dire à l'aplomb de l'anomalie gravimétrique d'Ivrée.

Ceci s'accorde parfaitement avec l'idée d'une migration progressive vers l'extérieur des Alpes de grands plans de décollement cisaillant la croûte, voire la lithosphère, postérieurement à l'affrontement des masses continentales. Un modèle expérimental fort simple de chevauchements imbriqués (Malavieille, 1983) en fournit une bonne illustration et présente d'ailleurs une ressemblance frappante avec certains traits de la structure alpine. Peut-être plus réalistes et convaincantes sont les données géophysiques regroupées dans l'excellent article de Perrier (1980). Elles montrent que les taux de surrection élevés des massifs cristallins externes ne représentent que la composante verticale d'un mouvement de translation de ces massifs sur leur avant-pays. C'est à mon avis la même logique qui gouverne l'évolution métamorphique dans les domaines plus internes et plus profonds de la chaîne. L'explication de la préservation des paragenèses de haute pression d'une unité de Vanoise par chevauchement sur la zone houillère, avant-pays plus froid (Goffé et Velde, 1984), en est un premier exemple. Nous avons vu la nécessité, pour expliquer la remontée sans réchauffement de l'unité à coesite, de l'enfouissement sous elle d'unités plus froides qui viennent déprimer les isothermes en contribuant à l'épaississement crustal ; c'est un autre exemple du même phénomène. Il n'est même pas nécessaire que cette montée soit rapide tant que les cisaillements fonctionnent ou sont relayés par d'autres plus externes. L'importance de cet écaillage apparaît aussi dans la structure même des massifs, aussi bien de Dora-Maira (Michard, 1965) que du Grand Paradis (Compagnoni et al., 1974), où des unités plus externes apparaissent en fenêtre. Finalement la géophysique elle-même atteste la matérialité de cet écaillage lithosphérique sous les Alpes, aussi bien dans les domaines externes (cf. Ménard et Thouvenot, 1984) qu'internes où la remontée du manteau est spectaculaire.

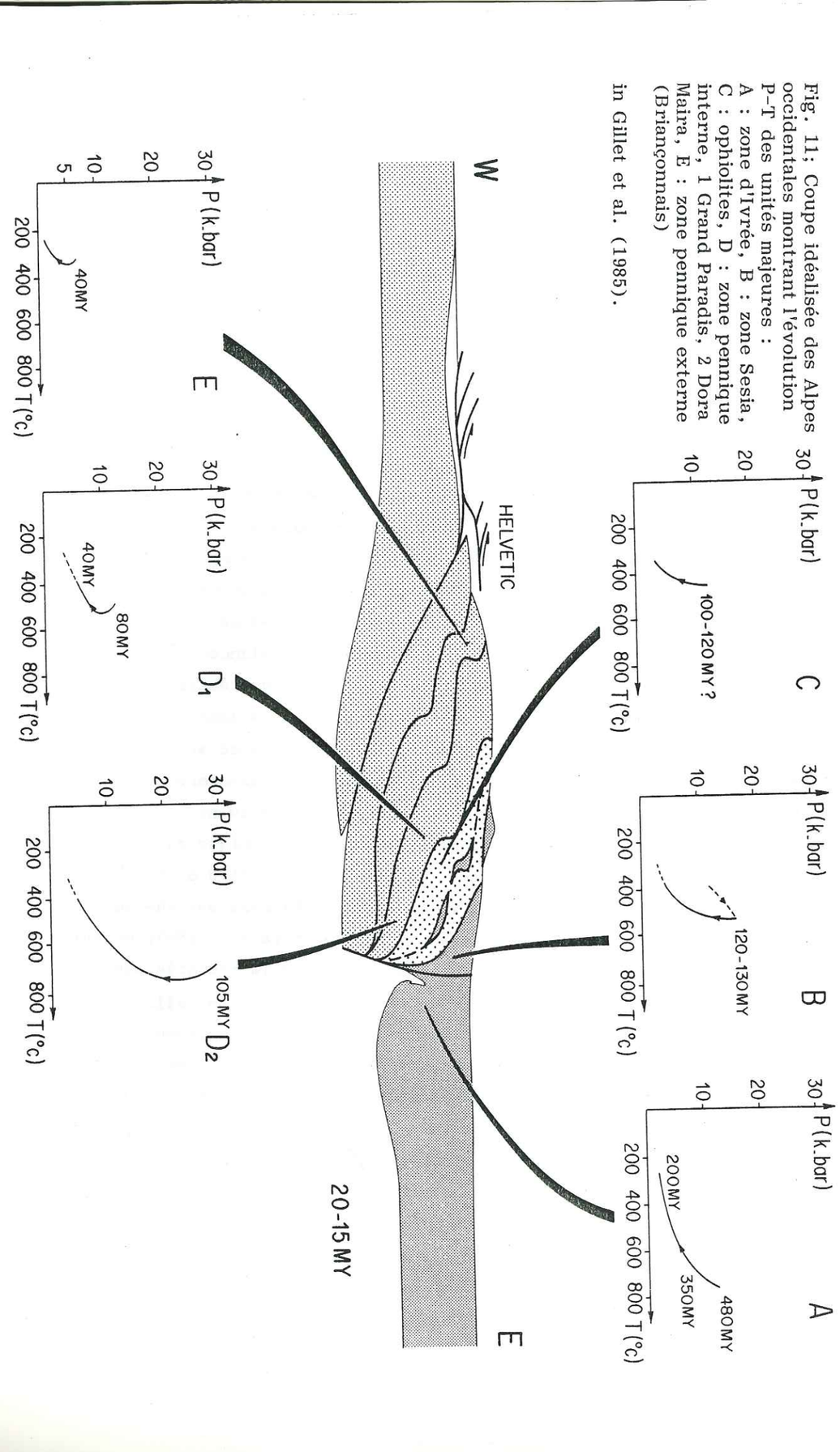

Fig. 11; Coupe idéalisée des Alpes occidentales montrant l'évolution P-T des unités majeures :
A : zone d'Ivrée, B : zone Sesia, C : ophiolites, D : zone pennique interne, 1 Grand Paradis, 2 Dora Maira, E : zone pennique externe (Briançonnais)

in Gillet et al. (1985).

L'importance de ce phénomène de clivage s'oppose un peu à la simplicité des modèles thermiques de zone de collision qui font l'hypothèse d'un chevauchement affectant toute l'épaisseur de la croûte, unique et instantané, le système évoluant ensuite par simple érosion. Ceci a conduit Gillet et al. (1985) à envisager un modèle de chevauchements multiples en utilisant des valeurs moyennes pour tous les paramètres, en fixant l'âge mais en jouant sur le nombre des chevauchements pour obtenir diverses courbes d'évolution de pression et température en fonction du temps. Le modèle n'est pas spécifiquement alpin, mais il lui est possible de rendre compte, avec un, deux ou trois chevauchements selon l'unité, de toutes les données chronologiques et pétrologiques présentées ci-dessus et regroupées dans la figure 11. En particulier l'unité D_2 enfouie à 100 km peut effectivement revenir vers la surface sans échauffement excessif, grâce à l'enfouissement sous elle d'autres unités.

En résumé, nous pouvons admettre pour la formation de la chaîne alpine l'existence d'un mécanisme de type subduction fonctionnant au Crétacé inférieur et moyen. De la croûte continentale (amincie, ou clivée?) est alors enfouie jusqu'à près de 100 km de profondeur. Le métamorphisme résultant s'exprime par des associations à coesite ou talc-disthène-chloritoïde, donc de haute pression et très haut degré, qui ultérieurement seront exclusivement localisées dans les zones les plus internes de la chaîne, en bordure de l'anomalie d'Ivrée. Dans les autres unités le métamorphisme de haute pression, plus classique, n'est pas directement lié à la subduction. Il est plus récent et résulte de cisaillements intracrustaux liés à l'affrontement des blocs continentaux. Ces cisaillements contribuent à l'épaississement crustal qui, en ralentissant la montée des isothermes, peut permettre la préservation d'une partie des associations de très haute pression formées initialement. Une caractéristique de cette évolution est la décroissance à la fois de l'âge et de l'intensité (P et T) du métamorphisme depuis les zones internes vers les zones externes. Cette décroissance procède par discontinuités.

Bref retour aux réalités : la présence de fossiles du Crétacé supérieur dans une unité supra-ophiolitique du Queyras (Dumont et al., 1984) pose un redoutable problème. Si le fait est avéré, ceci implique qu'un domaine océanique existe encore et reçoit une sédimentation alors

que des unités continentales sont déjà engagées dans une subduction. Cela supposerait de curieuses conditions aux limites pour la géométrie du problème mais peut être aussi révélateur de la complexité de l'évolution de la marge européenne de la Thétys. On peut imaginer que cette marge ait été disloquée dans une longue période d'extension, amenant la création de plusieurs bassins. Cette situation se prêterait bien à une évolution ultérieure composite, mais encore faut-il qu'une telle évolution des marges soit possible.

IV - CONCLUSION

A l'issue de cette étude, je ne peux résister au plaisir d'emprunter à Ellenberger (1958) la phrase que Virlet d'Aoust (1844) appliquait à la Savoie et que j'étendrais volontiers à l'ensemble des Alpes :

"(C')est le berceau et la terre classique du métamorphisme, l'une des contrées de l'Europe la plus intéressante à suivre sous ce rapport, et où l'on peut le mieux suivre les modifications du sol, depuis son origine jusqu'aux degrés les plus extrêmes de la transformation."

D'une argile magnésienne aux pyropes géants, il n'a pas été question d'autre chose ici. Nous avons été conduits à repousser loin à l'intérieur du manteau les limites du domaine de transformation métamorphique des roches d'origine supergène, et plus généralement de croûte continentale. Que les découvertes correspondantes aient été faites dans "la terre classique du métamorphisme" montre que la joie de connaître y est toujours donnée et que, même dans la chaîne de montagnes la mieux connue , il est encore possible de labourer des terres vierges.

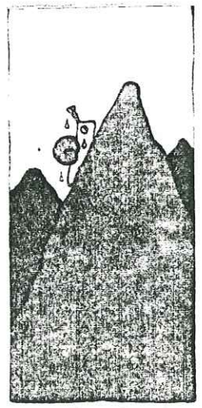

J'AI DÛ M'ÉGARER

BIBLIOGRAPHIE

ABRAHAM K., SCHREYER W. (1976) A talc-phengite assemblage in piemontite schist from Brezovica, Serbia, Yugoslavia. J. Petrol., 17 : 421-439

ACKERMAND D., SEIFERT F., SCHREYER W. (1975) Instability of sapphirine at high pressures. Contrib. Mineral. Petrol., 50 : 79-92

ACKERMANN L., CEMIC L., LANGER K. (1983) Hydrogarnet substitution in pyrope : a possible location for "water" in the mantle. Earth Plan. Sci. Lett., 62 : 208-214

ALBEE A.L. (1972) Metamorphism of pelitic schists : reaction relations of chloritoid and staurolite. Geol. Soc. America Bull., 83 : 3249-3268

BEARTH P. (1963) Chloritoid und Paragonit aus der Ophiolith-Zone von Zermatt-Saas Fee. Bull. suisse Minéral. Pétrogr., 43 : 269-286

BEARTH P. (1967) Die Ophiolithe der Zone von Zermatt-Saas Fee. Beitr. geol. Karte Schweiz., n.F., 132 : 130 p.

BOCQUET J., FORETTE M.C. (1973) Sur une deerite de l'ensemble des calcschistes piémontais, à Troncea (Italie). Bull. Soc. fr. Minéral. Cristallogr., 96 : 314-316

BOYD F.R., ENGLAND J.L. (1959) Pyrope. Carnegie Inst. Washington Yearbook, 58 : 83-87

BOYD F.R., ENGLAND J.L. (1960) Apparatus for phase equilibrium measurements at pressures up to 50 kbar and temperatures up to 1750°C. J. Geoph. Res., 65 : 741-748

CARPENA J. (1984) Contribution de la méthode des traces de fission à l'étude des Alpes franco-italiennes : relation tectonique - métamorphisme. Thèse d'état, Univ. Paris Sud-Orsay, 235 p.

CHATTERJEE N.D. (1975) Calculation of phase diagrams using thermochemical data derived from experimental studies of phase equilibria. Fortschr. Mineral., 52 : 47-60. Sp. Issue IMA Papers 9th Meeting Berlin-Regensburg 1974

CHESNOKOV B.V., POPOV V.A. (1965) Increase in the volume of quartz grains in South Urals eclogite. Doklady Akad. Nauk S.S.S.R., 162 : 176-178

CHINNER G.A., DIXON J.E. (1973) Some high-pressure parageneses of the Allalin gabbro, Valais, Switzerland. J. Petrol., 14 : 185-202

CHOPIN C. (1978) Les paragenèses réduites ou oxydées de concentrations manganésifères des "schistes lustrés" de Haute-Maurienne. Bull. Minéral., 101 : 514-531

CHOPIN C. (1979) De la Vanoise au massif du Grand Paradis : une approche pétrographique et radiochronologique de la signification géodynamique du métamorphisme de haute pression. Thèse 3ème cycle, Univ. Paris 6, 145 p.

CHOPIN C., MALUSKI H. (1980) ^{40}Ar-^{39}Ar dating of high-pressure metamorphic micas from the Gran Paradiso area (Western Alps) : evidence against the blocking-temperature concept. Contrib. Mineral. Petrol., 74 : 109-122

CHOPIN C. (1981 a) Talc-phengite : a widespread assemblage in high-grade pelitic blueschists of the Western Alps. J. Petrol., 22 : 628-650

CHOPIN C. (1981 b) Mise en évidence d'une discontinuité du métamorphisme alpin entre le massif du Grand Paradis et sa couverture allochtone (Alpes occidentales françaises. Bull. Soc. géol. France (7), 23 : 297-301

CHOPIN C., MALUSKI H. (1982) Unconvincing evidence against the blocking temperature concept : a reply. Contrib. Mineral. Petrol., 80 : 391-394

CHOPIN C. (1983) Magnesiochloritoid, a key-mineral for the petrogenesis of high-grade pelitic blueschists. Bull. Minéral., 106 : 715-717

CHOPIN C. (1984) Coesite and pure pyrope in high-grade blueschists of the Western Alps : a first record and some consequences. Contrib. Mineral. Petrol., 86 : 107-118

CHOPIN C., MONIE P. (1984) A unique magnesiochloritoid-bearing, high pressure assemblage from the Monte Rosa, W. Alps : a petrologic and ^{40}Ar-^{39}Ar radiometric study with comments. Contrib. Mineral. Petrol., 87 : 388-398

CHOPIN C. (1985) Phase relationships of ellenbergerite, a new high-pressure Ti-Al-Mg-silicate in pyrope-coesite-quartzite from the Western Alps. Accepté pour publ. Geol. Soc. America Special Papers "Penrose Blueschists Volume".

CHOPIN C., SCHREYER W. (1983) Magnesiocarpholite and magnesiochloritoid : two index minerals of pelitic blueschists and their preliminary phase relations in the model system MgO-Al_2O_3-SiO_2-H_2O. Amer. J. Sci., 283-A : 72-96

CHOPIN C., KLASKA R., MEDENBACH O., DRON D. (1985) Ellenbergerite, a new high-pressure Mg-Al-(Ti,Zr)-silicate with phosphatian varieties and a novel structure based on face-sharing octahedra. Soumis pour publ. à Contrib. Mineral. Petrol.

COMPAGNONI R., ELTER G., LOMBARDO B. (1974) Eterogeneita stratigrafica del complesso degli Gneiss Minuti nel massiccio cristallino del Gran Paradiso. Mem. Soc. geol. Ital., 13 : 227-239

COMPAGNONI R., DAL PIAZ G.V., HUNZIKER J.C., GOSSO G., LOMBARDO B., WILLIAMS P.F. (1977) The Sesia-Lanzo zone, a slice of continental crust with Alpine high-pressure - low-temperature assemblages in the Western Italian Alps. Rend. Soc. ital. Mineral. Petrol., 33 : 281-334

DEMANGE M. (1978) Le métamorphisme progressif des formations d'origine pélitique du flanc sud du massif de l'Agout (Montagne Noire, France). II - Variations de la composition chimique des minéraux. Bull. Minéral., 101 : 350-355

DE ROEVER E.W.F. (1977) Chloritoid-bearing metapelites associated with glaucophane rocks in Western Crete. Some remarks. Contrib. Mineral. Petrol., 60 : 317-319

DE ROEVER E.W.F., BEUNK F.F. (1971) Ferrocarpholite associated with lawsonite-albite facies rocks near Sangineto, Calabria, Italy. Mineral. Mag., 38 : 519-521

DE ROEVER W.P. (1951) Ferrocarpholite, the hitherto unknown ferrous iron analogue of carpholite proper. Amer. Mineral., 36 : 736-745

DE WEVER P., CABY R. (1981) Datation de la base des Schistes lustrés postophiolitiques par des radiolaires (Oxfordien supérieur - Kimméridgien moyen) dans les Alpes Cottiennes (Saint Véran, France). C.R. Acad. Sci. Paris, II, 292 : 467-472

DRAPER G., BONE R. (1981) Denudation rates, thermal evolution, and preservation of blueschists terrains. J. Geol., 89 : 601-613

DUMONT T., LEMOINE M., TRICART P. (1984) Pérennité de la sédimentation pélagique du Jurassique supérieur jusque dans le Crétacé supérieur au dessus de la croûte océanique téthysienne ligure : la série supra-ophiolitique du lac des Cordes (zone piémontaise des Alpes occidentales au SE de Briançon). C.R. Acad. Sci. Paris, II, 299 : 1069-1072

ELLENBERGER F. (1958) Etude géologique du pays de Vanoise (Savoie). Mém. Serv. carte géol. France, 561 p.

ELLIS D.J. (1980) Osumilite-sapphirine-quartz granulites from Enderby Land, Antarctica : P-T conditions of metamorphism, implications for garnet-cordierite equilibria and the evolution of the deep crust. Contrib. Mineral. Petrol., 74 : 201-210

ENGLAND P.C., THOMPSON A.B. (1984) Pressure-temperature-time paths of regional metamorphism. I. Heat transfer during the evolution of thickened continental crust. J. Petrol., 25 : 894-928

EVANS B.W., TROMMSDORFF V., RICHTER W. (1979) Petrology of an eclogite - metarodingite suite at Cima di Gagnone, Ticino, Switzerland. Amer. Mineral., 64 : 15-31

FERRY J.M. (1980) A comparative study of geothermometers and geobarometers in pelitic schists from south-central Maine. Amer. Mineral., 65 : 720-732

FERRY J.M., SPEAR F.S. (1978) Experimental calibration of the partitioning of Fe abd Mg between biotite and garnet. Contrib. Mineral. Petrol., 66 : 113-117

FONTEILLES M. (1976) Essai d'interprétation des compositions chimiques des roches d'origines métamorphique et magmatique du massif hercynien de l'Agly (Pyrénées orientales). Thèse d'état, Université Paris 6, 684 p.

FRANSOLET A.M., BOURGUIGNON P. (1978) Di/trioctahedral chlorite in quartz veins from the Ardenne, Belgium. Canadian Mineral., 16 : 365-373

FRANSOLET A.M., SCHREYER W. (1984) Sudoite, di/trioctahedral chlorite : a stable low-temperature phase in the system $MgO-Al_2O_3-SiO_2-H_2O$. Contrib. Mineral. Petrol., 86 : 409-417

GANGULY J. (1969) Chloritoid stability and related parageneses : theory, experiments and applications. Amer. J. Sci., 267 : 910-944

GANGULY J. (1972) Staurolite stability and related parageneses : theory, experiments and applications. J. Petrol., 13 : 335-365

GASPARIK T., NEWTON R.C. (1984) The reversed alumina contents of orthopyroxene in equilibrium with spinel and forsterite in the system $MgO-Al_2O_3-SiO_2$. Contrib. Mineral. Petrol., 85 : 186-196

GILLET P., INGRIN J., CHOPIN C. (1984) Coesite in subducted continental crust : P-T history deduced from an elastic model. Earth Plan. Sci. Lett., 70 : 426-436

GILLET P., DAVY P., BALLEVRE M., CHOUKROUNE P. (1985) Thermomechanical evolution of a collision zone : example of the Western Alps. Terra Cognita (sous presse)

GOFFE B. (1982) Définition du faciès à Fe-Mg-carpholite-chloritoïde, un marqueur du métamorphisme de HP-BT dans les métasédiments alumineux. Thèse d'état, Univ. Paris 6, 232 p.

GOFFE B., GOFFE-URBANO G., SALIOT P. (1973) Sur la présence d'une variété magnésienne de ferrocarpholite en Vanoise (Alpes françaises). Sa signification probable dans le métamorphisme alpin. C.R. Acad. Sci. Paris, série D, 277 : 1965-1968

GOFFE B., SALIOT P. (1977) Les associations minéralogiques des roches hyperalumineuses du Dogger de Vanoise. Leur signification dans le métamorphisme régional. Bull. Soc. fr. Minéral. Cristallogr., 100 : 302-309

GOFFE B., VELDE B. (1984) Contrasted metamorphic evolutions in thrusted cover units of the Briançonnais zone (French Alps) : a model for the conservation of HP-LT metamorphic mineral assemblages. Earth Plan. Sci. Lett., 68 : 351-360

GOLE M.J. (1980) Mineralogy and petrology of very-low-metamorphic grade Archaean banded iron-formations, Weld Range, Western Australia. Amer. Mineral., 65 : 8-25

GRACIANSKY P.C. de, LEMOINE M., SALIOT P. (1971) Remarques sur la présence de minéraux et de paragenèses du métamorphisme alpin dans les galets des conglomérats oligocènes du synclinal de Barrême (Alpes de Haute Provence). C.R. Acad. Sci. Paris, D, 272 : 3243-3245

GRACIANSKY P.C. de, LEMOINE M. (1980) Paléomarge de la Téthys dans les Alpes occidentales : du Massif central français aux ophiolites liguro-piémontaises. Géol. alpine, 56 : 119-147

GRAMBLING J.A. (1983) Reversals in Fe-Mg partitioning between chloritoid and staurolite. Amer. Mineral., 68 : 373-388

GREEN H.W. (1974) Metastable growth of coesite in highly strained quartz. J. Geoph. Res., 77 : 2478-2482

GREW E.S., SANDIFORD M. (1984) A staurolite-talc assemblage in tourmaline-phlogopite-chlorite schist from northern Victoria Land, Antarctica, and its petrogenetic significance. Contrib. Mineral. Petrol., 87 : 337-350

GUIDOTTI C.V. (1974) Transition from staurolite to sillimanite zone, Rangeley quadrangle, Maine. Geol. Soc. America Bull., 85 : 475-490

HALBACH H., CHATTERJEE N.D. (1982) The use of linear parametric programming for determining internally consistent thermodynamic data for minerals. In : Schreyer W. ed. High-pressure researches in geoscience. Stuttgart, Schweizerbart, 545 p.

HALFERDAHL L.B. (1961) Chloritoid : its composition, X-ray and optical properties, stability and occurrence. J. Petrol., 2 : 49-135

HENSHAW D.E. (1955) The structure of wadeite. Mineral. Mag., 30 : 591-595

HIETANEN A. (1969) Distribution of Fe and Mg between garnet, staurolite, and biotite in aluminum-rich schist in various metamorphic zones North of the Idaho Batholith. Amer. J. Sci., 267 : 422-456

HOLDAWAY M.J. (1978) Significance of chloritoid-bearing and staurolite-bearing rocks in the Picuris Range, New Mexico. Geol. Soc. America Bull., 89 : 1404-1414

HOLLAND T.J.B. (1979 a) High water activities in the generation of high-pressure kyanite eclogites of the Tauern Window, Austria. J. Geol., 87 : 1-27

HOLLAND T.J.B. (1979 b) Experimental determination of the reaction paragonite = jadeite + kyanite + water, and internally consistent thermodynamic data for part of the system Na_2O-Al_2O_3-SiO_2-H_2O, with applications to eclogites and blueschists. Contrib. Mineral. Petrol., 68 : 293-301

HUNZIKER J.C. (1974) Rb-Sr and K-Ar age determination and the Alpine tectonic history of the Western Alps. Mem. Ist. Geol. Mineral. Univ. Padova, 31 : 55 p.

INGRIN J. (1985) Microscopie électronique en transmission de géomatériaux. Thèse 3ème cycle, Univ. Paris 7, 203 p.

KITAHARA S., TAKENOUCHI S., KENNEDY G.C. (1966) Phase relations in the system $MgO-SiO_2-H_2O$ at high temperatures and pressures. Amer. J. Sci., 264 : 223-233

KORIKOVSKIY S.P., TALITSKIY V.G., BORONIKHIN V.A., IVANOV V.P. (1983) Paragenezis talk-khloritoid v metapelitakh i yego petrologicheskoye znacheniye (na primere Makbalskogo antiklinoriya Tyan-Shania). Doklady Akad. Nauk S.S.S.R., 268 : 1454-1457

KRAMM U. (1980) Sudoite in low-grade metamorphic manganese-rich assemblages. Neues Jahrbuch für Mineral. Abh., 138 : 1-13

LEMOINE M. (1975) Mesozoic sedimentation and tectonic evolution of the Briançonnais zone in the Western Alps. Possible evidence for an Atlantic-type margin between the European craton and the Tethys. 9ème Congrès internat. Sédimentologie, Nice : 211-215

MALAVIEILLE J. (1983) Modélisation expérimentale des chevauchements imbriqués : application aux chaînes de montagne. Bull. Soc. géol. France (7), 26 : 129-138

MASSONNE H.J. (1981) Phengite : eine experimentelle Untersuchung ihres Druck-Temperature-Verhaltens im System $K_2O-MgO-Al_2O_3-SiO_2-H_2O$. Dissertation Ruhr-Universität Bochum, 214 p.

MASSONNE H.J. (1983) Experiments on melting to 50 kbar in the system $MgO-Al_2O_3-SiO_2-H_2O$ (MASH) with excess SiO_2 and H_2O (abstr.). EOS Trans. A.G.U., 64 : 875

MASSONNE H.J., SCHREYER W. (1983) Stability of the talc-kyanite assemblage revisited (abstract). Terra Cognita, 3 : 187

MENARD G., THOUVENOT F. (1984) Ecaillage de la lithosphère européenne sous les Alpes occidentales : arguments gravimétriques et sismiques liés à l'anomalie d'Ivrea. Bull. Soc. géol. France (7), 26 : 875-884

MICHARD A. (1965) Une nappe de socle dans les Alpes cottiennes internes ? Implications paléogéographiques et rôle éventuel des mouvements crétacés. C.R. Acad. Sci. Paris, D, 260 : 4012-4015

MICHARD A. (1967) Etudes géologiques dans les zones internes des Alpes cottiennes. Paris, C.N.R.S., 447 p.

MILLER C. (1974) On the metamorphism of the eclogite and high-grade blueschists from the Penninic terrane of the Tauern Window, Austria. Bull. suisse Minéral. Pétrogr., 54 : 371-384

MILLER C. (1977) Chemismus und phasenpetrologische Untersuchungen der Gesteine aus der Eklogitzone des Tauernfensters, Österreich. Tschermaks Min. Petr. Mitt., 24 : 221-277

MINEAR J.W., TOKSÖZ M.N. (1970) Thermal regime of a downgoing slab and global tectonics. J. Geoph. Res., 75 : 1397-1419

MIRWALD P.W., GETTING I.C., KENNEDY G.C. (1975) Low-friction cell for piston-cylinder high-pressure apparatus. J. Geoph. Res., 80 : 1519-1525

OBERHÄNSLI R., HUNZIKER J.C., MARTINOTTI G., STERN W.G. (1982) Mucronites : an example of eo-Alpine eclogitisation of Permian granitoids, Italy (abstract). Terra Cognita, 2 : 325. 1ère Conf. Internat. Eclogites

OKRUSCH M. (1981) Chloritoid-führende Paragenesen in Hochdruckgesteinen von Samos. Fortschr. Mineral., 59 : Beih. 1, 145-146

OXBURGH E.R., TURCOTTE D.L. (1974) Thermal gradients and regional metamorphism in overthrust terrains with special reference to the Eastern Alps. Bull. suisse Minéral. Pétrogr., 54 : 641-662

PERRIER G. (1980) La structure des Alpes occidentales déduite des données géophysiques. Eclogae geol. Helv., 73 : 407-424

PIGAGE L.C., GREENWOOD H.J. (1982) Internally consistent estimates of pressure and temperature : the staurolite problem. Amer. J. Sci., 282 : 943-969

RÄHEIM A., GREEN D.H. (1974) Talc-garnet-kyanite-quartz schist from an eclogite-bearing terrane, Western Tasmania. Contrib. Mineral. Petrol., 43 : 223-231

RAO B.B., JOHANNES W. (1979) Further data on the stability of staurolite + quartz and related assemblages. Neues Jahrbuch für Mineral. Monatsh., 10 : 437-447

RICHARDSON S.W. (1968) Staurolite stability in a part of the system Fe-Al-Si-O-H. J. Petrol., 9 : 467-499

ROBINSON G.R. (1983) Calibration of the muscovite-biotite-quartz-garnet aluminosilicate geothermobarometer (abstr.). EOS Trans. A.G.U., 64 : 351

SALIOT P. (1973) Les principales zones de métamorphisme dans les Alpes françaises. Répartition et signification. C.R. Acad. Sci. Paris, D, 276 : 3081-3084

SALIOT P., GUILHAUMOU N., BARBILLAT J. (1982) Les inclusions fluides dans les minéraux du métamorphisme à laumontite-prehnite-pumpellyite des grès du Champsaur (Alpes du Dauphiné). Etude du mécanisme de circulation des fluides. Bull. Minéral., 105 : 648-657

SCHREYER W. (1968) A reconnaissance study of the system $MgO-Al_2O_3-SiO_2-H_2O$ at pressures between 10 and 25 kbar. Carnegie Inst. Washington Yearbook, 66 : 380-392.

SCHREYER W. (1977) Whiteschists : their compositions and pressure-temperature regimes based on experimental, field, and petrographic evidence. Tectonophysics, 43 : 127-144

SCHREYER W., BALLER T. (1977) Talc-muscovite : synthesis of a new high-pressure phyllosilicate assemblage. Neues Jahrbuch für Mineral. Monatsh., 9 : 421-425

SCHREYER W., BALLER T., CHOPIN C. (1985) High-pressure synthesis of ellenbergerite in the system $MgO-Al_2O_3-SiO_2-H_2O$ (abstract). Terra Cognita, 5 : (sous presse)

SCHREYER W., HORROCKS P.C., ABRAHAM K. (1984) High-magnesium staurolite in a sapphirine-garnet rock from the Limpopo Belt, Southern Africa. Contrib. Mineral. Petrol., 86 : 200-207

SCHREYER W., SEIFERT F. (1969) High-pressure phases in the system $MgO-Al_2O_3-SiO_2-H_2O$. Amer. J. Sci., 267-A Schairer volume : 407-443

SEIDEL E. (1978) Zur Petrologie der Phyllit-Quartzit-Serie Kretas. Habilitationschrift, Braunschweig, 145 p.

SEIDEL E. (1981) Fe-Mg-Verteilung zwischen koexistierenden Karpholithen und Chloritoiden. Fortschr. Mineral., 59 : Beih. 1, 180-181

SMITH D.C. (1984) Coesite in clinopyroxene in the Caledonides and its implications for geodynamics. Nature, 310 : 641-644

SMYTH J.R., HATTON C.J. (1977) A coesite-sanidine grospydite from the Roberts Victor kimberlite. Earth Plan. Sci. Lett., 34 : 284-290

SOBOLEV N.V. et al. (1976) Coesite, garnet and omphacite inclusions in Yakut diamonds - first finding of coesite paragenesis. Doklady Akad. Nauk S.S.S.R., 230 : 1442-1444 (in Russian), abstr. in Mineral. Abstr., 29 : n°78-818

STEEN D., BERTRAND J. (1977) Sur la présence de ferrocarpholite associée aux schistes à glaucophane de Haute Ubaye (Basses Alpes, France). Bull. suisse Minéral. Pétrogr., 57 : 157-168

SWANSON D.K., PREWITT C.T. (1983) The crystal structure of $K_2Si^{VI}Si_3O_9$. Amer. Mineral., 68 : 581-585

TERMIER P. (1928) La joie de connaître. Souvenirs d'un géologue. Paris, Libr. Valois, 333 p.

TURNER F.J. (1981) Metamorphic petrology. 2ème éd. New York, McGraw-Hill, 524 p.

UDOVKINA N.G., MURAVITSKAYA G.N., LAPUTINA I.P. (1978) Phase equilibria in the talc-garnet-kyanite rocks of the Kokchetav block, Northern Kazakhstan. Isvestiya Akad. Nauk S.S.S.R. Geol. Sect., 7 : 55-64 (in Russian)

UDOVKINA N.G., MURAVITSKAYA G.N., LAPUTINA I.P. (1980) Talc-garnet-kyanite rocks of the Kokchetav block, Northern Kazakhstan. Doklady Earth Sci. Sect., 237 : 202-205

VELDE B. (1965) Phengite micas : synthesis, stability, and natural occurrence. Amer. J. Sci., 263 : 886-913

VIALON P. (1966) Etude géologique du massif cristallin Dora-Maira, Alpes cottiennes internes, Italie. Thèse d'état, Univ. de Grenoble, 320 p.

VIELZEUF D. (1984) Relations de phases dans le faciès granulite et implications géodynamiques. L'exemple des granulites des Pyrénées. Thèse d'état, Univ. de Clermont-Ferrand : Annales sci. Univ. Clermont-Ferrand II, 79 : fasc. 36, 288 p.

VIELZEUF D., BOIVIN P. (1984) An algorithm for the construction of petrogenetic grids : application to some equilibria in granulitic paragneisses. Amer. J. Sci., 284 : 760-791

VISWANATHAN K., SEIDEL E. (1979) Crystal chemistry of Fe-Mg carpholites. Contrib. Mineral. Petrol., 40 : 41-47

WARD C.M. (1984) Magnesium staurolite and green chromian staurolite from Fjordland, New Zealand. Amer. Mineral., 69 : 531-540

WINKLER H.G.F. (1979) Petrogenesis of metamorphic rocks. 5ème éd. New York, Springer, 348 p.

LISTE DES PRINCIPALES PUBLICATIONS DE L'AUTEUR

Les articles précédés d'un astérisque sont reproduits à la suite de cette liste

CHOPIN C. (1977) Une paragenèse à margarite dans un domaine de haute pression et basse température (massif du Grand Paradis, Alpes françaises). C.R. Acad. Sci. Paris, série D, 285, 1383-1386

CHOPIN C., MALUSKI H. (1978) Résultats préliminaires obtenus par la méthode ^{39}Ar-^{40}Ar sur les minéraux alpins du Massif du Grand Paradis et de son enveloppe. Bull. Soc. géol. France (7) 20, 745-749

CHOPIN C. (1978) Les paragenèses réduites ou oxydées de concentrations manganésifères des "schistes lustrés" de Haute-Maurienne. Bull. Minéralogie 101, 514-531.

* CHOPIN C., MALUSKI H. (1980) ^{40}Ar-^{39}Ar dating of high-pressure metamorphic micas from the Gran Paradiso area (Western Alps) : evidence against the blocking-temperature concept. Contrib. Mineral. Petrol. 74, 109-122.

* CHOPIN C. (1981) Talc-phengite : a widespread assemblage in high-grade pelitic blueschists of the Western Alps. J. Petrol. 22, 628-650

* CHOPIN C. (1981) Mise en évidence d'une discontinuité du métamorphisme alpin entre le massif du Grand Paradis et sa couverture allochtone (Alpes occidentales françaises). Bull. Soc. géol. France (7), 23, 297-301

* CHOPIN C., GOFFE B. (1981) High-pressure synthesis and properties of magnesiocarpholite : $MgAl_2 Si_2O_6 (OH)_4$ Contrib. Mineral. Petrol. 76, 260-264

* CHOPIN C., MALUSKI H. (1982) Unconvincing evidence against the blocking temperature concept : a reply. Contrib. Mineral. Petrol. 80, 391-394

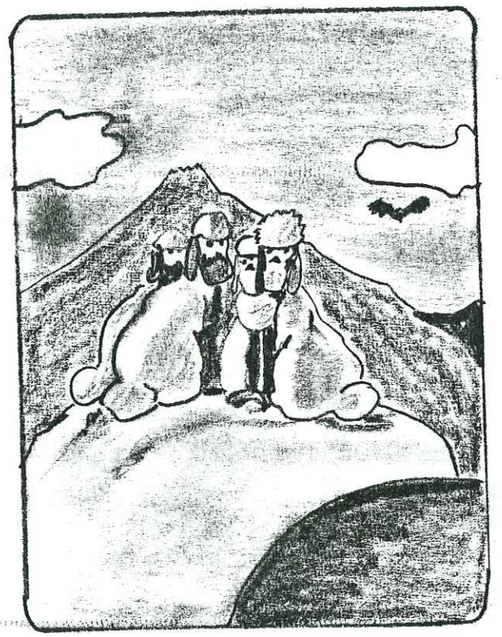

* CHOPIN C., SCHREYER W. (1983) Magnesiocarpholite and magnesiochloritoid : two index minerals of pelitic blueschists and their preliminary phase relations in the model system $MgO-Al_2O_3-SiO_2-H_2O$. Am. J. Sci. 283 A, Orville volume, 72-96

* CHOPIN C. (1983) Magnesiochloritoid : a key-mineral for the petrogenesis of high-grade pelitic blueschists. Bull. Minéral. 106, 715-717

* CHOPIN C., MONIE P. (1984) A unique Mg-chloritoid-bearing, high-pressure assemblage from the Monte Rosa, Western Alps : petrologic and $^{39}Ar-^{40}Ar$ radiometric study. Contrib. Mineral. Petrol. 87, 388-398

* CHOPIN C. (1984) Coesite and pure pyrope in high-grade blueschists of the Western Alps : a first record and some consequences. Contrib. Mineral. Petrol. 86, 107-118

* GILLET , INGRIN J., CHOPIN C. (1984) Coesite in subducted continental crust : P-T history deduced from an elastic model. Earth Plan. Sci. Lett. 70, 426-436

BOYER H., SMITH D.C., CHOPIN C., LASNIER B. (1985) Raman microprobe (RMP) determination of natural and synthetic coesite. Phys. Chem. Minerals (sous presse)

* CHOPIN C., KLASKA R., MEDENBACH O., DRON D. (1985) Ellenbergerite, a new high-pressure Mg-Al-(Ti, Zr)-silicate with phosphatian varieties and a novel structure based on face-sharing octahedra. Soumis pour publ. à Contrib. Mineral. Petrol.

* CHOPIN C. (1985) Phase relationships of ellenbergerite, a new high-pressure Ti-Mg-Al-silicate in pyrope-coesite-quartzite from the Western Alps. Accepté pour publ. Geol. Soc. America Special Papers "Penrose Blueschists volume"

Contrib. Mineral. Petrol. 74, 109–122 (1980)

Contributions to Mineralogy and Petrology

$^{40}Ar-^{39}Ar$ Dating of High Pressure Metamorphic Micas From the Gran Paradiso Area (Western Alps): Evidence Against the Blocking Temperature Concept

Christian Chopin[1] and Henri Maluski[2]

[1*] Laboratoire de Géologie (E.R. 224), Ecole Normale Supérieure, 46 rue d'Ulm, F-75230 Paris Cedex 05, France
[2] Laboratoire de Géologie structurale (L.A. 226), U.S.T.L., place E. Bataillon, F-34060 Montpellier Cedex, France

Abstract. The $^{40}Ar-^{39}Ar$ method has been applied to high pressure (HP) white micas from the Gran Paradiso crystalline massif and from the overthrust Schistes Lustrés of its western slope. Preliminary petrographic and microanalytical investigation of the phengite micas showed that their celadonite-content decreases with time (from $Si_{3.65}$ to $Si_{3.05}$), and that less foliated samples are the most suitable for the metastable persistence of the high celadonite-content of the early HP stage during subsequent metamorphic evolution.

Such samples were investigated together with one where mica is a pure retrogressive product. Two groups of plateau-ages have been found: (a) 60 to 75 Ma on HP phengites and early paragonites of unretrograded HP parageneses, thus dating the early HP metamorphic stage; (b) 38–40 Ma on HP phengites (most often in slightly retrograded HP parageneses) and on the purely retrogressive mica. For the HP phengites in (b), this age is considered to reflect the end of Ar readjustement during the later lower P and/or higher T metamorphic stage, and not their crystallization.

This disparity in plateau-ages for micas sampled within the same area shows that under the same P-T conditions some systems were open while others remained closed. This can be closely related to the mineralogical behaviour: chemically active systems are isotopically active, whereby the reverse is not necessarily true. Thus, although temperature exceeded by far the usually assumed sealing-temperature of white micas, many systems have remained unaffected during the late Eocene event. Therefore, temperature cannot be the determining parameter for the opening of a system. Chemical reactivity, starting mineralogy and, primarily, pervasive deformation and the related fluid behaviour appear to be the effective controls.

This implies that thermally activated diffusion processes (volume diffusion...) cannot be geologically significant. Consequently, the blocking temperature concept which rests on the opposite assumption now appears questionable. The fact that a mica does not necessarily behave as open above its "blocking temperature" necessitates at least a clear distinction between opening- and sealing-temperatures.

* *Present address:* Institut für Mineralogie der Ruhr-Universität, Postf. 102148, D-4630 Bochum 1, Federal Republic of Germany

Introduction

Previous $^{40}Ar-^{39}Ar$ studies of terrestrial samples have shown this method to be a powerful geochronological tool, especially when applied to thermally or tectonically disturbed rocks (Hanson et al. 1975; Dallmeyer 1975a, 1975b; Dallmeyer and Sutter 1976; Maluski 1977, 1978, etc). Our purpose was thus to apply the $^{40}Ar-^{39}Ar$ technique to high pressure (HP) metamorphic minerals of the Western Alps, where the tectonic history and metamorphism have for many years been recognized as being low in temperature, complex and multiphase (Ellenberger 1960; Nicolas 1966; Bearth 1967; Saliot 1973, 1978; Caron 1977; Bocquet(-Desmons) 1974, 1977; Caby et al. 1978, etc). Indeed, mixed ages have been widely assumed after extensive classical $K-Ar$ analysis (Hunziker 1974; Bocquet et al. 1974; Delaloye and Desmons 1976). The scattering of these ages is a problem; although several generations of micas and amphiboles have been commonly recorded in the Central (Steiger 1961) and Western Alps (Nicolas 1966; Bearth 1967; Goffé 1976), little attention has been paid to this point by the above analysts. Mixed ages may result either from the presence of several mineral generations of different ages in the concentrate, from the partial reopening of a single generation, or both. We have therefore attempted a preliminary petrologic and chemical in-

0010-7999/80/0074/0109/$02.80

vestigation of the samples in combination with the $^{40}Ar-^{39}Ar$ stepwise heating technique to allow discrimination between these possibilities, and thus lead to a better understanding of the metamorphic history.

We focused our attention on phengite micas. These minerals are not only very widespread in HP metamorphic terranes, but are also good recorders of tectonic events by their growth in different foliation planes, and of their own metamorphic path by the dependence on P and T of the muscovite-celadonite ($Al^{IV}Al^{VI} \rightleftharpoons Si\ Mg$) and, to a lesser extent, of the muscovite-paragonite ($K \rightleftharpoons Na$) solid solutions (Velde 1967; Chatterjee and Froese 1975). Phengite micas are therefore well-suited to investigations of metamorphic evolution. Two non exclusive procedures are possible for separating different mica generations. On the basis of structural considerations, they may be chosen from different foliation planes, for example, or by choosing samples with only one generation, as Steiger (1964) did with amphiboles. They can also be distinguished on petrographic and chemical grounds, after careful microprobe work, by choosing samples containing either late or early minerals. We chose this latter approach, which had of course to be carried out in a limited area where the tectonic units and the metamorphic evolution had been previously sufficiently well documented in order to allow valid comparison between the samples. This area is the Gran Paradiso massif and the Schistes Lustrés of its western slope (Haute Maurienne in France and Orco valley in Italy).

Geological Setting and Petrological Background

Two subdivisions of the Pennine domain of the Western Alps are commonly made (see Debelmas and Lemoine 1970): the Briançonnais zone, a micaschist Paleozoic basement with a thick detached Mesozoic and Paleocene cover unit, and the more eastern Piémont zone, a series of Mesozoic metasediments and ophiolites (the Schistes Lustrés thrust sheet) overlying a granitogneissic Hercynian basement and its Mesozoic cover, which appear in windows cut through the Schistes Lustrés (these are the Monte Rosa, Gran Paradiso and Dora Maira massifs from north to south – Fig. 1).

The Gran Paradiso massif is an Alpine foliation dome. U–Pb age determinations performed on zircons of a fine-grained metagranite yielded 300–350 Ma (see Chessex et al. 1964). This crystalline basement is overlain by a non-fossiliferous presumably autochtonous cover, 0–20 m thick, consisting of quartzites and marbles. Despite this thinness, the presence of Triassic strata is widely assumed, but the presence of younger ones is also possible (Bertrand 1968).

The Schistes Lustrés in the region studied (Fig. 1) are unusual in that they can be separated on lithological, structural and metamorphic grounds into three superimposed thrust sheets (Chopin 1979). The lowermost lies on the Gran Paradiso massif and is distinctly ophiolite- and eclogite-bearing; it is a southern extension of the Zermatt-Saas Fee zone of Bearth (1967). The present work has been limited to this unit and the Gran Paradiso massif.

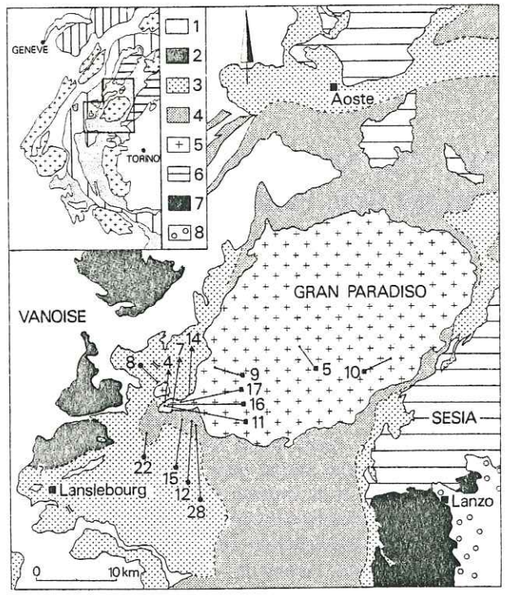

Fig. 1. Geological setting and sample locations. *Inset:* Structural units in the Western Alps. *Crosses:* external and internal crystalline massifs. *Wide vertical ruling:* Briançonnais-Bernhardiner zone. *Narrow vertical ruling:* Chablais thrust sheets. *Dotted:* Schistes Lustrés thrust sheet and Helminthoid flysch thrust sheet. *Horizontal ruling:* Lower Austroalpine units: Sesia zone and Dent Blanche nappe. Legend: *1* Briançonnais zone: cover and basement have not been distinguished; *2* Upper Schistes Lustrés, lying on the Vanoise and partly on 3; *3* Intermediate Schistes Lustrés unit, dipping westward under the Vanoise; *4* Lower Schistes Lustrés unit, lying on the Gran Paradiso Massif; *5* Gran Paradiso Massif; cover has not been distinguished; *6* Lower Austroalpine units (crystalline basement). From north to south: Dent Blanche nappe, Mt Emilius and Mt Rafray klippes, Sesia zone. *7* Lanzo ultramafic body; *8* Tertiary and quaternary post-tectonic deposits of the Po valley.

For the samples, *solid squares* refer to Gran Paradiso basement, *solid triangles* to Gran Paradiso cover and *solid circles* to Schistes Lustrés. AL has been omitted before each sample number for clarity

The area investigated may therefore be briefly described as the eastern margin of the former European plate, overthrust by an ocean-floor unit. In both units "high temperature" blueschist assemblages (glaucophane-chloritoid, talc-chloritoid, metabasic eclogites, etc., without lawsonite) have been produced and then overprinted. Estimated conditions (Chopin 1979) are $P \geqq 7$ kb, $T \simeq 400$–$450°$ C for the HP stage and $P \simeq 4$–6 kb, $T = 470 \pm 20°$ C for the overprinting ("retrogression").

The chemistry of phengite micas supports this evolution of the P-T conditions. In many samples several

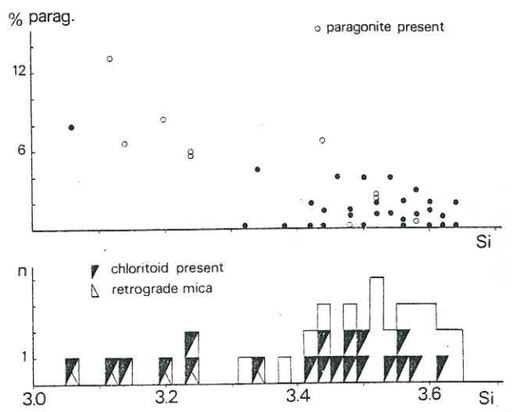

Fig. 2. Phengite chemistry. *Lower diagram:* celadonite content of 39 phengite micas from the studied area. Representative analyses of about 30 samples have been selected and are given in Chopin (1979). Celadonite content is expressed as the number of Si atoms in a 120 molecule. Only micas which were obviously retrograde on textural grounds have been designated as such. Most others are obviously primary but the status of some celadonite-poor micas remains ambiguous. *Upper diagram:* relation between molar paragonite content and celadonite content in the phengite

phengite generations are conspicuous. An early one, where large flakes often outline a foliation, has a high celadonite content ($3.45 \leqq Si \leqq 3.65$ on a 12 0 basis), regardless of the presence or absence of a highly aluminous phase (Fig. 2). A later generation appears among the breakdown products of aluminous minerals such as chloritoid and margarite. Its celadonite content is distinctly lower and its paragonite content higher (Fig. 2). So it may be stated on purely petrographic grounds that phengite evolution with time is marked by a decrease of the celadonite content (and an increase of the paragonite content) as typically exemplified by sample AL 15 (Fig. 3). According to Velde (1967), this behaviour indeed speaks for a temperature increase and/or pressure decrease (Fig. 10), whereby the early HP phengites should have disappeared during subsequent metamorphic evolution to yield a less celadonitic phengite. They should thus be found beside less substituted phengites only in the samples where the reaction was incomplete (as in AL 15) or by themselves as metastable remnants in chemically inert systems (as in samples AL 4, 11, 14...). Interestingly enough, chemical zoning within a single crystal has never been observed (see also Saliot 1978), except for a unique case related to exceptional Ba contents (AL 8, Fig. 4). These features may be evidence for a discontinuous mica growth process together with a lack of long range equilibrium within the samples.

Previous Work

In the Gran Paradiso massif a single K–Ar date (45 Ma) has been obtained on a relict Hercynian biotite (Krummenacher and Evernden 1960). Despite this result, an Upper Cretaceous age is widely assumed for the HP metamorphism in this area, as in the other internal crystalline massifs (Hunziker 1974; Bocquet et al. 1974). The only radiometric support is a 98 ± 18 Ma Rb–Sr age on biotite among younger ones in the basement of the Dora Maira massif (Vialette and Vialon 1964)

In the French-Italian Schistes Lustrés extensive investigations have been performed with the K–Ar method in regions neighbouring the present study area (Bocquet et al. 1974; Delaloye and Desmons 1976). Two sets of true ages were deduced, namely 75–100 and 38–40 Ma, on both micas and amphiboles. Apparent ages between 40 and 54 Ma were interpreted as a "Lepontine" (38 Ma) recrystallization with inherited argon, and those between 60 and 70 Ma as an "Eoalpine" (75–100 Ma) crystallization with a partial reopening at about 38 Ma. Thus, the possibility of mixed ages has been widely recognized, but, as already mentioned, little or no attention has been paid to the mica chemistry and to the existence of several mica or amphibole generations in the same sample. According to Delaloye and Desmons (1976), the Upper Cretaceous event dates the HP metamorphism and affects the innermost Schistes Lustrés (Zermatt-Saas Fee zone s.l.), the internal crystalline massifs, and probably the eastern Briançonnais basement (Desmons 1977). The 38 Ma event dates the general retrogression of the HP parageneses and affects both the Piémont and the Briançonnais zone. In the Zermatt-Saas Fee zone s.l. these authors draw a 350° C isotherm (running SW of the Gran Paradiso massif) to the north of which all micas should have been fully reopened, and to the south of which Upper Cretaceous ages are still to be found beside the 38 Ma ages.

The Material Studied

Preliminary petrologic work showed that the poorly foliated samples generally contained phengites from one generation only. Hence calc-schists, although by far the most abundant material in the Schistes Lustrés, were discarded and attention was focused on quartzites and marbles, which appear to be the most suitable rocks for the metastable persistence of celadonite-rich phengites ($Si_{3.6-3.5}$). In the Gran Paradiso basement, micas of unretrograded glaucophanites were given special attention. Thus the samples studied here display typical HP parageneses. Some of them are slightly overprinted (AL 7, 15, 8?), but even in this case the mica concentrate consists mainly of early HP phengites. AL 28 is the only sample which contains a purely secondary mica, namely paragonite as a breakdown product of chloritoid.

Sample descriptions and chemistry are given in Appendices A and B, and localities in Fig. 1. In the mica concentrate, the polytype has been determined for most samples (Appendix A). The striking abundance of the 3T form is probably a common feature in HP terranes, and may be related to solid solution toward celadonite. However, these data clearly demonstrate that the 3T form is by no means characteristic of typical HP phengites, because they are of the 2M polytype in AL 14, while the retrogressive micas are 3T in AL 15.

Experimental Technique

Minerals were separated by classical means (heavy liquids and Frantz isodynamic separator) and cleaned with ultrasonic generator

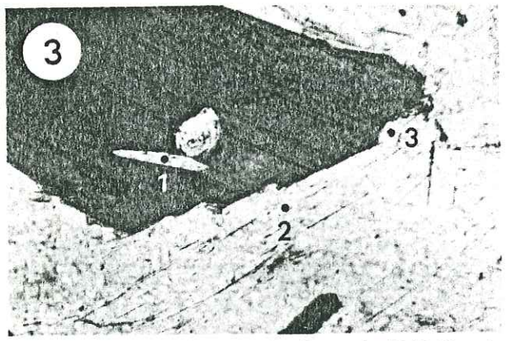

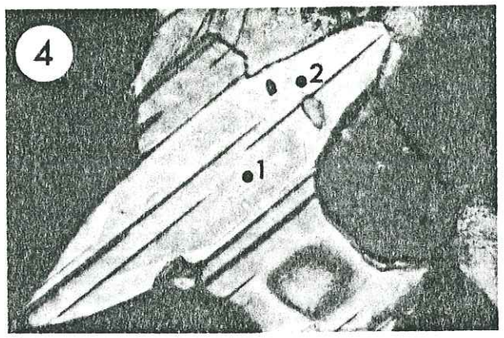

Fig. 3. Successive phengite generations in sample AL 15. Phengite 1 is an armoured relic in chloritoid; the typomorphic mica is phengite 2, determining the foliation, and a late product is phengite 3, corroding the chloritoid crystal. Celadonite content decreases with time: $Si_{3.6}$ in phengite 1, $Si_{3.5}$ in phengite 2, $Si_{3.3}$ in phengite 3. See analyses in Appendix B; for interpretation see Fig. 7. Length of photomicrograph = 700 μm

Fig. 4. In sample AL 7, zoned phengite crystal between phlogopite flakes and carbonate grains. This exceptional feature is related to high Ba-contents (0.7% in the core, 8.5% on the rim). Correlatively celadonite-content sharply decreases from $Si_{3.6}$ to $Si_{3.3}$ (see Appendix B). Crossed nicols, length of photomicrograph: 250 μm

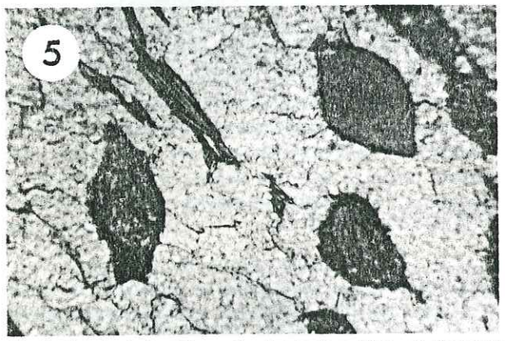

Fig. 5. Petrological evidence for the juxtaposition of chemically active and inert systems: the glaucophane breakdown in the studied area. A crystal (*left*) may be completely retrograded into albite + chlorite, whereas a neighbouring crystal (*right*) remains unaffected. Sample 6-269, glaucophane-chloritoid quartzite from Le Villaron (Bessans). Length of photomicrograph = 1 mm

in ethanol. The pure mineral concentrates were then sealed under vacuum in quartz vials. Each irradiation container was composed of five samples and one standard biotite. Irradiation was carried out in the 10^{14} n/cm².s flux of the C.E.N.G. reactor in Grenoble during 24 h. After two or three weeks, the vials were opened and samples transferred in a high purity Ni-foil-container to the furnace. Heating was performed with an HF generator acting upon a Mo-crucible during one hour. Temperature was measured with an optical pyrometer from 600° C to fusion. Purification of the released gases was made on a SAES Al−Zr getter at 400° C and in a U-tube cooled with liquid nitrogen. A second purification was made in the second part of the line with the same elements. Ar was trapped on activated charcoal and then introduced into the mass spectrometer (a modified THN 206 E). Mass analysis was achieved in the static mode. Mass interferences derived from irradiated Ca and K have been corrected using the a, b, c parameters of Brereton (1970) with values defined in Maluski (1977).

Results and Interpretation

The analytical data and resultant ages are presented in Appendix C and plotted as a function of the accumulative fraction of ^{39}Ar released in Figs. 6, 7, and 8.

The Plateau-Ages and Their Distribution

A main result is that the age-spectra of all potassic micas except AL 5 yield well-defined plateau-ages. With the exception of AL 5, a partial reopening may be ruled out. Furthermore, plotting the data in a $^{40}Ar/^{36}Ar$, $^{39}Ar/^{36}Ar$ diagram yields for each sample a well defined "isochron" with an intercept close to the atmospheric $^{40}Ar/^{36}Ar$ ratio. This, although by no means conclusive (Roddick 1978), does not imply the presence of inherited argon which in any case would have to be equally partitionned between low- and high-temperature sites. Thus, all these plateau-ages are thought to be geologically significant; they represent sealing ages of systems which then suffered no argon loss.

The second feature of these data is the existence of two age-groups in each lithological unit. A first set of young ages points to a well-defined event at 40 ± 2 Ma (AL 8, 12, 15; AL 7; AL 10 phengite). Well represented in the Gran Paradiso basement, the older ages form a second less well-defined group in the range 60–75 Ma, which may include the two old ages (57 Ma) of AL 4 and AL 14 in the Gran Paradiso cover. The Schistes Lustrés sample AL 22, a mixture of primary paragonite and phengite, yields only old ages. These do not form a well-defined plateau-spec-

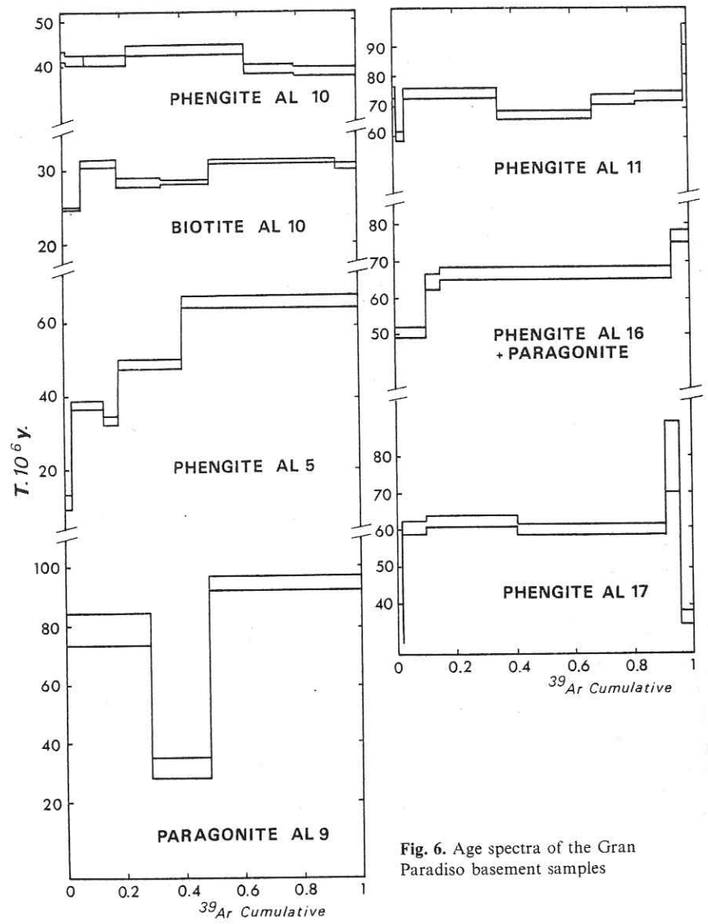

Fig. 6. Age spectra of the Gran Paradiso basement samples

trum, but each step is consistent with the former values which are confirmed in this unit by a glaucophane plateau-age of about 60 Ma (Chopin and Maluski 1978). For the only partially reopened sample (AL 5), the high-temperature step is consistent with these last values and the low-temperature steps may be consistent with a 40 Ma event (their average value is 43 Ma), thus pointing out the true nature of these two age groups.

Significance of the Age Groups

As only typical HP phengites, early paragonites and glaucophanes yield these Upper Cretaceous to Paleocene ages, this older group clearly dates a HP metamorphic event, both in the Gran Paradiso massif and the ophiolite-bearing Schistes Lustrés. The 40 Ma event, first recognized in the Central Alps (Jäger et al. 1967; Jäger 1970) where it dates a relatively HT metamorphism (Ticino thermal high), has subsequently been recognized throughout the Alpine chain (see Jäger 1973) and correlated to the general overprinting of the HP parageneses.

However, in the Briançonnais zone of the Western Alps, HP parageneses have been recorded in the basement (jadeite + quartz: Saliot 1973) as well as in the cover (lawsonite: Goffé 1979). They are necessarily post-Paleocene in age because the stratigraphic sequence ranges from Triassic to Paleocene. Hence this rules out the assumption made by Hunziker (1974) and Desmons (1977) of an Upper Cretaceous HP metamorphism in the Briançonnais basement. Furthermore, the assumption of a Late Eocene HP metamorphism not only involving the Vanoise, but also the area studied, seems a priori possible, as also sug-

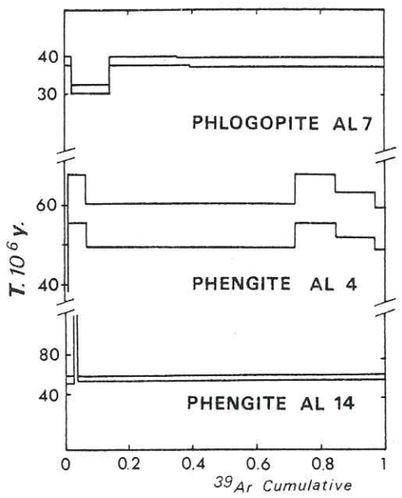

Fig. 7. Age spectra of the Gran Paradiso cover samples

gested by Hunziker (1974): only 39–49 Ma ages have been obtained in the Briançonnais cover (Bocquet et al. 1974), and all phengite samples yielding 40 Ma in the area studied contain HP phengites. This would imply either two successive HP metamorphisms in this area, for which there is no petrographic evidence, or a very long one lasting from late Upper Cretaceous to Late Eocene, that is hardly conceivable on heat conductivity grounds. Moreover, if the 40 Ma event is assumed to be a HP one, a younger age must be assumed for the retrogression of the HP parageneses which occurs both in the Briançonnais and Piémont zones. A quite striking feature of the K–Ar and Ar–Ar data on white micas in the Western Alps is the lack of ages younger than 38 Ma; it should then be assumed that all the phengites investigated thus far are HP ones and that they have remained unaffected. The only evidence of the retrogression would then perhaps be the few 30 Ma ages obtained on biotite in the Gran Paradiso (Al 10), Sesia (Hunziker 1974) and Dora Maira (Vialette and Vialon 1964) massifs.

Thus, to elucidate the significance of this 40 Ma event, samples containing mica only as a retrogressive product had to be searched for. AL 28 is the only one that could be found; however, due to the low K-content of the paragonite, poor precision has been attained. Although no plateau-age has been obtained, four of the six steps (representing 83% of the released ^{39}Ar) are consistent with a 40 Ma value. The total-gas age is 44 Ma. Hence, the retrogression cannot be younger than 38 Ma and our view is that this steep peak around 40 Ma in the age distribution (Fig. 9) records the end of the retrogression and of the metamorphic history. Consequently, all the 40 Ma ages obtained from the HP phengites (AL 7, 8, 10, 12, 15) do not date their crystallization, but their second (?) sealing. The only micas which crystallized at that time were low celadonite-content phengites, muscovites and paragonites, which textural relationships often show to be late products (Fig. 2).

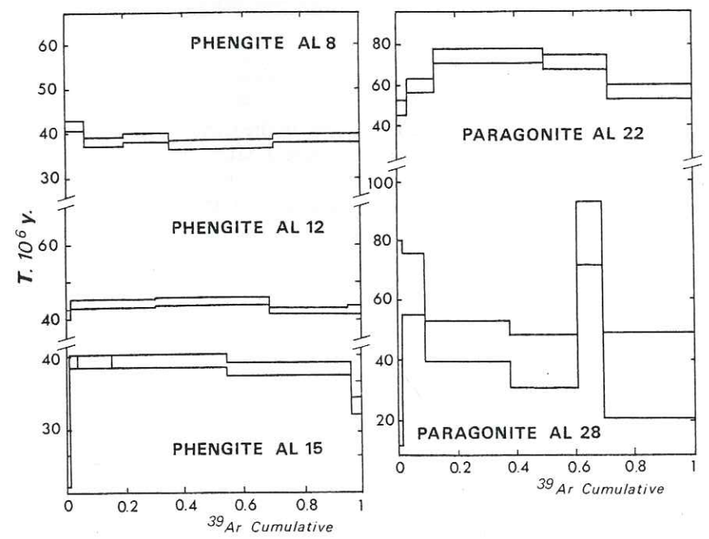

Fig. 8. Age spectra of the Schistes Lustrés samples

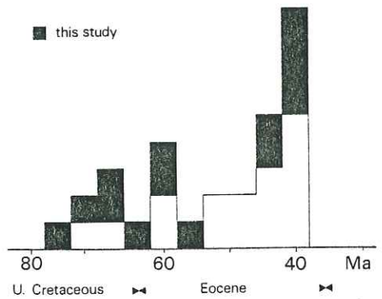

Fig. 9. White mica ages in the French-Italian Western Alps. *Open squares* are K–Ar data from Bocquet et al. (1974) and Delaloye and Desmons (1976). *Solid squares* are $^{39}Ar-^{40}Ar$ plateau-ages of this study. Note the steep peak at 38–40 Ma and the absence of younger ages, suggesting a quenching of the systems by fast uplift

A possible explanation for the lack of ages youger than 38 Ma (Fig. 9) is that the metamorphic pile underwent at this time rather fast cooling, marking the end of the metamorphic evolution. This view is supported by $^{40}Ar-^{39}Ar$ analyses in Alpine Corsica, where the same Late Eocene event has been recognized (Maluski 1977; Maluski and Mayé, in preparation), and where apatites yield 41 ± 2 Ma apparent fission-track ages and the same plateau-ages after stepwise annealing (Carpena and Poupeau, personal communication). This is indeed compelling evidence for a fast uplift and cooling of the metamorphic units. However, the 30 Ma ages on biotite noted above for the most internal parts of the Western Alps (Sesia, Dora Maira and eastern Gran Paradiso) would not fit this convenient explanation. But before an alternative explanation is sought, these ages must be shown to be compatible with fission-track results.

Thus our results are in agreement with those of previous workers insofar as two age groups recording a HP Upper Cretaceous "event" followed by a 40 ± 2 Ma "event" are recognized. The Upper Cretaceous group is even youger (60–75 Ma) than previously suggested (78–100 Ma: Bocquet et al. 1974) from an extrapolation of the data gathered on amphiboles in the northernmost Piémont zone to the central and southern Piémont zone. Indeed, in these regions the few data on micas of these authors and those of Delaloye and Desmons (1976) fall in the range 60–75 Ma, just as those of the Sesia zone do (Hunziker 1974). Our results show that these ages may be true ages as well, and do not need the assumption of a later partial reopening as has been made by Bocquet et al. (1974) by analogy to the Swiss Alps. For the younger group, the great spread of ages between 40 and 54 Ma of these authors has not been corroborated. Although partial reopening cannot be completely ruled out (as shown by AL 5), this simplification of the results shows the usefulness of a sampling based on petrological criteria in a limited area.

Geological consequences will be emphasized elsewhere.

Comparison of Ar-Retention

All samples containing primary paragonite in the concentrate (AL 9, 16, 22) yield Upper Cretaceous ages. Thus paragonite remained unaffected by the 40 Ma event, not only when pure, but also probably when phengite is present. More accurately, it suffered no argon loss, but could yet have suffered some argon redistribution between the different sites, as no perfect plateau has been obtained.

Most of the phengites investigated thus far in the Western Alps have been reopened during the 40 Ma event; biotites, even in textural equilibrium with HP minerals, yield Late Eocene to Oligocene apparent ages, and the presumably early paragonites analysed in the French-Italian Alps all retained their Upper Cretaceous age. There is thus evidence for an increasing retentivity from biotite to phengite and then to paragonite, which may be easily correlated with decreasing basal spacing. This shows that the dating of paragonite may be a powerful tool for investigating the early metamorphic history of an orogenic belt, at least in HP to intermediate pressure metamorphic terranes, where this mica is common. The same might be expected from blue amphiboles, but these have the disadvantage of being strictly limited to HP–LT metamorphic areas and of significant incorporation of non-radiogenic argon, as will be shown elsewhere (Chopin and Maluski, in preparation). Further work is now in progress in order to ensure that the dating of paragonite is not also complicated (to a lesser extent of course) by this latter problem.

The Plateau-Ages Disparity

According to the present study, micas sampled within a small area in the same tectonic unit yield either 40 Ma or 70–60 Ma plateau-ages. Thus, it must be stated that *under the same P–T conditions some systems behaved as fully open while others remained perfectly closed.*

This conclusion may be new for an "isotopist", but not for a petrologist, especially in HP–LT terranes. Indeed, the irregular development of reactions and apparent disequilibrium-parageneses there are common features which are often accounted for by

assuming an open versus closed behaviour of neighbouring systems relative to the fluid, thus also explaining the juxtaposition of otherwise incompatible parageneses (Bearth 1959; Guitard and Saliot 1971; Fry and Fyfe 1971; Chatterjee 1971; etc.). In the investigated area, the random development of the "retrogression" (Fig. 5 for the glaucophane breakdown) and the metastable persistence of HP phengites are actually petrologic evidence for the juxtaposition of chemically active and inert systems.

Moreover, our results demonstrate a close relationship between this peculiar isotopic and chemical behaviour. All Upper Cretaceous ages are yielded by unretrograded HP parageneses (AL 9, 11, 16, 17, 22), whereas the more or less retrograded ones always yield Late Eocene ages (AL 7, 15, 8?). So, as might be expected, an isotopically inert system must be chemically inert and, logically, a chemically active system must be isotopically active (as shown experimentally also by Fructus-Ricquebourg et al. 1963). The reverse may not necessarily be true: AL 12 and AL 5 show once more (cf. Frey et al. 1976) that interlayer positions of micas may be disturbed without affecting the whole framework.

Chemical reactivity is thus an important factor controlling isotopic behaviour, but is itself dependent on the starting mineralogy and whole rock chemistry. For example, an early celadonite-rich phengite will persist metastably for a longer period of time if products of its possible breakdown (K-feldspar and biotite or chlorite) are not already present. Indeed, the most celadonite-rich phengites are to be found in rocks with a simple mineralogy (quartzites, marbles) and not in the metagranites, where the presence of biotite and K-feldspar actually implies the maximum celadonite-content in the phengite for a given P and T. As a further example, the growth of HP phengite in a metashale is a dehydration reaction, whereas granite phengitization is a hydration reaction. Metastable persistence will be more likely in the latter, and in any case reaction rate will be dependent on the fluid behaviour. This leads to variable isotopic behaviour in the same area and could account for the scattering of the older ages.

But the very point is that temperature exceeded by far the usually assumed Ar-retention temperature of white mica (about 350° C, according to Purdy and Jäger 1976). The minimum temperature-estimate during this Late Eocene event is in fact 450° C (Chopin 1979), as indicated by the presence of Alpine corundum in the Gran Paradiso basement and the miscibility gap between Mn–Ca–carbonates in the Schistes Lustrés (Fig. 10). Even at such "high" temperatures, many systems remained unaffected; this implies unequivocally that a purely thermal control of the mica

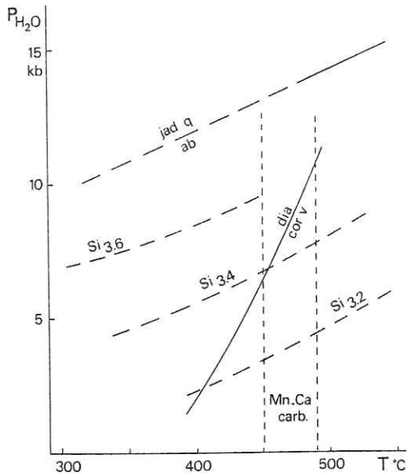

Fig. 10. Main petrological data pertaining to the studied area. Diaspore-corundum transition: Haas (1972); jadeite + quartz ⇌ albite: after Newton and Smith (1967). The lower pressure stability limits of the $Si_{3.6}$, $Si_{3.4}$ and $Si_{3.2}$ phengites are estimates of Velde (1967). The 470 ± 20° C temperature-interval has been deduced from the rhodochrosite-kutnahorite miscibility-gap in the Schistes Lustrés (Chopin 1979), using the experimental data of Goldsmith and Graf (1960)

behaviour can no longer be assumed, and even that temperature is not the primary determining parameter, as far as the opening of the system is concerned.

The same conclusion may be drawn from a magmatic biotite of an undeformed metagranite variety in the Maures massif basement (Maluski and Gueirard 1978). The temperature was higher still (at least 500° C), but this mineral, in contrast to the surrounding deformed variety, retained its crystallization plateau-age (580 Ma) through the Hercynian metamorphism. (A typical feature of the undeformed metagranite samples is the coronitic growth of tiny garnets on the biotite. This most likely results from a pre-Hercynian metamorphism of the basement which approached granulite facies conditions (Gueirard 1976). Then the 580 Ma age of the biotite would be a recrystallisation age as well. In either case the conclusion remains unaffected.)

The first example (Alps) has shown chemical reactivity to be a more important factor than temperature, as already indicated by low-temperature devitrification of basalts (Fleck et al. 1977). The Maures example is evidence for the greater importance of fluid behaviour and above all of deformation. This prominent role of deformation, particularly of the pervasive type, which may allow easier fluid permeation, is also exemplified in the Alps. It has already been mentioned

in conjunction with the metastable celadonite-rich phengites from the less-foliated rocks and is clear from the contrasting behaviour of phengite in AL 5 (a poorly foliated metagranite) and AL 10 (already an orthogneiss). Moreover it has also been recorded by Maluski (1978) in Corsican metagranites and beautifully exemplified by Frey et al. (1976) in the Monte Rosa massif, not only using petrological and K–Ar, but also Rb–Sr and stable isotope data. Again a classical result is outlined: diffusion s.l. and reactivity are strongly dependent on the fluid phase.

Consequences and Conclusions

The isotopic evolution of a system, just as its petrologic one, is of course dependent on migration processes. These are themselves internally and externally controlled. So the isotopic evolution of a system cannot be investigated while disregarding its general evolution. Indeed, sampling made on petrological and deformational criteria demonstrates that, whatever temperature might have been reached during a metamorphic event, it is possible to find systems which remained isotopically closed during this event. Hence the opening of a system is not dictated by the temperature. At first sight, mineralogical reactivity (followed by the bulk chemistry and precursor mineralogy) appears to be an important factor, but this is actually dependent on other migration-controlling parameters. The studied examples show the basic controls to be pervasive deformation and the related fluid behaviour.

This has an important consequence. Temperature not being the determining parameter for the opening of a system implies that thermally activated diffusion processes (volume diffusion, etc; see Mussett 1969) cannot be geologically significant, as tentatively stated by this author. Consequently, the blocking-temperature concept and the wide use made of it (e.g., Clark and Jäger 1969; Dallmeyer 1978) now appear questionable, as they implicitly rest on the assumption of a purely thermally activated diffusion process (e.g., Dodson 1973). Indeed, if the determining process involved was volume diffusion, closure should be strongly dependent on the grain size, which, as pointed out by Dodson, is not the case. We have shown that in general there cannot be a uniform opening temperature in a given area because migration-controlling parameters are variable in space. Logically, if these controls are still operative during cooling, a general closure temperature should not exist. Except in the case of very quick cooling, as suggested for the Western Alps, apparent ages should not be homogeneous in a given area, for a given mineral.

Nevertheless, regular patterns in age distribution have been recorded in several regions, especially the Central Alps (Jäger et al. 1967). These have been convincingly explained by post-metamorphic uplift and cooling, exactly as if closure were only temperature-dependent (or at least determined by highly temperature-dependent parameters). Because pervasive deformation does not equally affect different lithologies, these regular patters would imply that pervasive deformation did not occur during uplift and cooling, a conclusion that is geologically acceptable. Thus a tentative explanation could be as follows: in the absence of pervasive deformation, the last crystallizations or recrystallizations (which are partly temperature-dependent) tend to fill in the pore-system. Fluid mobility then becomes restricted (except along discrete fault or thrust planes), and the rapid attainment of closed systems results, at least as far as major elements are concerned. According to our results, of course bearing in mind that they refer to the K–Ar systematics (but the Rb–Sr one is not basically different), this should then also be generally true from an isotopic point of view. But can in this case the retentivity difference between biotite and muscovite be set forth to account for the systematic age difference between these micas? That is the point...

Thus the problem remains open to debate. On the one hand, the well-documented age distribution pattern of the Central Alps is best accounted for by a cooling-age model supported by fission-track studies and heat-flow data. On the other hand, a combination of isotopic, structural and petrological observations shows that the basic assumption of this model is not fulfilled.

At least, a consequence is that a temperature-determined closure of the isotopic systems cannot be systematically assumed, but must be demonstrated in every case, thus necessitating important analytical work; and even if demonstrated, such temperature-dependence still remains to be explained. This should also lead to a clear distinction between the opening and the sealing temperature, which has not always been made. It has sometimes been assumed that any mica must behave as open above its "closure temperature". We have demonstrated here that this cannot be true, and, for example, that it is basically wrong to draw, as Delaloye and Desmons (1976) and Desmons (1977) did in the Gran Paradiso area, a 350° C isotherm for the Late Eocene event using the persistence or non-persistence of Upper Cretaceous ages.

Remerciements. Pierre Saliot est à l'origine de notre collaboration et de ce travail, pendant lequel il nous a fait bénéficier sans réserve de son expérience du métamorphisme alpin et des phengites en particulier. Des discussions épiques avec Christian Orange et Saint-Clair Dujon ont aussi été une aide précieuse. Les critiques constructives du Professeur B. Grauert ont été également fort appréciées. L'expression anglaise doit beaucoup aux corrections de Walter

Maresch. La détermination du polytype des micas a été faite à Strasbourg grâce à l'intercession de Nicole Bucher et Jean-Michel Caron. De plus, nous avons bénéficié de l'aide matérielle de MM. Guillemin et Bouche pour la séparation des minéraux, de Pierre Blatrix pour la spectrométrie et de Mlles Saint-Raymond et Gaudin pour la frappe du manuscrit. Que tous trouvent ici l'expression de notre gratitude.

Appendix A. Sample description

AL... refers to the laboratory number which is followed by the sampling number in parentheses.

AL 4 (7580): massive phengite marble. Grande Feiche (Bonneval/Arc). Gran Paradiso cover. A single $Si_{3.6}$ phengite generation, 3T polytype.

AL 5 (6-473): fine-grained metagranite. Scalari (Orco Valley). Gran Paradiso basement. Apparently less foliated than the surrounding "augengneisses". Relict magmatic biotites well recognizable. Epitaxial growth of small alpine biotites. $Si_{3.5}$ phengite.

Al 7 (6-242): dolomitic marble. Couloir de la Fontaine (Bonneval/Arc). Gran Paradiso cover. Zoned Ba-rich phengite (Fig. 4 and Appendix B), abundant phlogopite in textural equilibrium with the early $Si_{3.6}$ phengite. The concentrate is a mixture of about 75% 1M-phlogopite and 25% 3T-phengite.

AL 8 (6-402): phengite quartzite. Lenta (Bonneval/Arc). Extension of the dolomite and quartzite beds separating lower and intermediate Schistes lustrés units. Two phengite compositions ($Si_{3.6}$, $Si_{3.35}$; Appendix B) in different layers of the same thin section. Both have the same habit and look primary. 2M and 3T polytypes in the concentrate.

AL 9 (6-456): garnet-paragonite glaucophanite. Carro (Bonneval/Arc). Volcano-sedimentary layer in the Gran Paradiso basement. Typically unretrograded HP paragenesis. Small amounts of quartz have not been removed from the 2M-paragonite concentrate.

AL 10 (6-470): fine-grained gneiss interbedded in the "augengneisses". Fornetti (Orco Valley). Gran Paradiso basement. No relict Hercynian mica. Biotite and $Si_{3.5}$ phengite in textural equilibrium. Small amounts of (retrogressive?) chlorite could not be entirely removed from the biotite concentrate. Phengite is of the 3T polytype.

AL 11 (7-200): micaceous layer with some quartz lenses, interbedded in the upper Bonneval gneisses. Feiche Combe (Bonneval/Arc). Gran Paradiso basement. Pure $Si_{3.6}$ phengite (Appendix B), 3T polytype.

AL 12 (7-152): piemontite-phengite quartzite. Ouille du Midi (Bonneval/Arc). Lower Schistes lustrés unit. A single $Si_{3.5}$ phengite generation, but both 2M and 3T polytypes are present.

AL 14 (6-332): massive dolomitic marble. Ouille des Reys (Bonneval/Arc). Gran Paradiso cover. A single $Si_{3.55}$ phengite generation (Appendic B), 2M polytype. Carbonate has not been completely removed from the concentrate and caused overpressure in the line during degassing (see Appendix C).

AL 15 (6-348): phengite-crossite-garnet-chloritoid quartzite. Ouille

Appendix B. Phengite analyses

Some representative analyses have been selected to illustrate the possible variation of phengite chemistry in one sample and the very high celadonite content of primary phengites. Analyses have been performed with a Cambridge Mark V microprobe, using a procedure detailed elsewhere (Chopin 1979). As correction did not take Ba into account, Al 7 analyses are only approximate. The Fe^{2+}/Fe^{3+} ratio has been chosen on mineralogical criteria (presence of hematite or piemontite...) and in order to approximate the ideal phengite substitution. Chemical formula is calculated on a 11 0 basis. For AL 7 and AL 15 analyses, refer to Figs. 4 and 3

	AL 15			AL 8		AL 11	AL 17	AL 7		AL 14
	Ph 1	Ph 2	Ph 3	Ph 1	Ph 2	Ph	Ph	Ph 1	Ph 2	Ph
SiO_2	53.26	51.50	49.82	54.95	51.34	52.28	52.92	51.72	44.14	53.38
TiO_2	0.14	0.14	0.17	0.27	0.32	0.55	0.27			0.24
Al_2O_3	20.38	24.30	27.60	22.32	28.77	20.53	24.03	20.53	23.54	24.32
Fe_2O_3	3.14	2.51	2.70	0.18	0.36	2.38		3.21	3.34	
FeO	2.80	2.27	2.44	0.39	0.77	3.23	2.18			2.44
MnO						0.02	0.00	0.02	0.01	0.00
MgO	4.17	3.45	2.23	6.30	3.28	3.61	4.27	5.63	4.40	4.18
CaO	0.07	0.01	0.04							
BaO								0.7	8.6	
Na_2O	0.05	0.09	0.31	0.00	0.00	0.14	0.04	0.21	0.09	0.14
K_2O	10.38	10.26	10.19	11.51	11.49	11.05	10.43	10.85	8.20	10.44
Total	94.43	94.53	95.50	95.92	96.33	93.79	94.14	"92.87"	"92.36"	95.14
Si	3.624	3.482	3.342	3.619	3.375	3.602	3.558	3.574	3.260	3.554
Ti	0.007	0.007	0.009	0.013	0.016	0.028	0.014			0.012
Al	1.635	1.937	2.183	1.733	2.23	1.668	1.905	1.673	2.050	1.909
Fe^{3+}	0.161	0.128	0.136	0.009	0.018	0.123		0.167	0.186	
Fe^{2+}	0.162	0.128	0.137	0.021	0.042	0.186	0.123			0.136
Mn						0.001		0.001	0.001	
Mg	0.423	0.348	0.223	0.618	0.321	0.371	0.428	0.580	0.484	0.415
Ca	0.005	0.001	0.003							
Ba								0.019	0.250	
Na	0.007	0.012	0.040			0.019	0.005	0.028	0.013	0.018
K	0.901	0.885	0.872	0.967	0.964	0.971	0.895	0.957	0.773	0.887
Σ cat.	6.925	6.927	6.946	6.981	6.967	6.969	6.926	6.999	7.017	6.931

Appendix C. Analytical data

	Temperature (°C)	$(^{40}Ar^*/^{39}Ar)$st.	$^{40}Ar^*/^{39}Ar$	$^{36}Ar/^{39}Ar$	$^{37}Ar/^{39}Ar$	^{39}Ar % cumul.	Age Ma
AL 4	phengite						
1	635	20.93 ± 0.20[a]	−7.16	0.0172	0	1.0	−123 ± 11
2	760	–	3.952	0.0047	0	6.7	64.5 ± 3.0
3	870	–	3.508	0.0037	0	72.2	57.6 ± 2.9
4	970	–	3.948	0.0029	0	84.8	64.6 ± 2.7
5	1,175	–	3.681	0.0034	0	97.1	60.1 ± 2.8
6	1,575	–	3.454	0.0287	0	100	56.6 ± 5.5
							total-gas age 57.4 ± 3.2
AL 5	phengite						
1	635	26.61 ± 0.25[a]	11.189	0.0006	0.0006	0.6	137 ± 3
2	760	–	0.897	0.0141	0.0637	3.4	11.3 ± 2.1
3	870	–	3.010	0.0036	0.0324	14.0	37.7 ± 1.2
4	970	–	2.661	0.0045	0.0201	19.2	33.4 ± 1.2
5	1,175	–	3.896	0.0020	0.0063	40.5	48.7 ± 1.2
6	1,575	–	5.289	0.0020	0.0181	100	65.8 ± 1.6
							total-gas age 56.4 ± 1.5
AL 7	phengite						
1	635	20.93 ± 0.20[a]	−2.245	0.0697	0.0475	0.3	−36.0 ± 11.4
2	760	–	2.359	0.0099	0.439	1.9	37.6 ± 2.0
3	970	–	1.896	0.0155	0.0201	10.4	31.4 ± 1.9
4	1,075	–	2.435	0.0010	0	40.2	38.8 ± 1.0
5	1,175	–	2.432	0.0069	0	55.5	38.7 ± 1.7
6	1,575	–	2.417	0.0005	0	100	38.5 ± 0.9
							total-gas age 37.8 ± 1.0
AL 8	phengite						
1	760	2.81 ± 0.03[b]	8.506	0.0108	0.0046	6.2	41.8 ± 1.3
2	870	–	7.731	0.0088	0.0026	15.5	38.0 ± 1.1
3	970	–	7.947	0.0033	0	35.0	39.1 ± 1.0
4	1,075	–	7.599	0.0006	0	70.4	37.4 ± 1.0
5	1,575	–	7.875	0.0054	0.0031	100	38.7 ± 1.0
							total-gas age 38.4 ± 1.1
AL 9	paragonite						
1	760	2.81 ± 0.03[b]	3.776	0.0192	0.012	26.8	78.9 ± 6.0
2	1,075	–	1.472	0.0154	0.017	45.6	31.1 ± 4.2
3	1,575	–	4.513	0.020	0.026	100	93.9 ± 2.9
							total-gas age 78.0 ± 4.0
AL 10	biotite						
1	700	2.81 ± 0.03[b]	1.112	0.012	0.012	6.7	23.6 ± 0.3
2	760	–	1.459	0.0026	0	18.5	30.9 ± 0.6
3	870	–	1.288	0.002	0	32.5	27.3 ± 0.7
4	970	–	1.308	0.002	0.0008	49.5	27.7 ± 0.4
5	1,150	–	1.464	0.001	0.0004	93.4	31.0 ± 0.4
6	1,575	–	1.427	0.007	0.0088	100	30.2 ± 0.5
							total-gas age 29.4 ± 0.5
AL 10	phengite						
1	635	2.81 ± 0.03[b]	8.561	0.038	0	1.8	42.1 ± 2.6
2	760	–	8.349	0.0096	0	8.2	41.1 ± 1.3
3	870	–	8.371	0.0019	0.0018	22.3	41.2 ± 1.0
4	970	–	8.804	0.0032	0	62.5	43.3 ± 1.1
5	1,075	–	7.861	0.0035	0.0034	79.6	38.7 ± 1.0
6	1,575	–	7.737	0.0064	0.0408	100	38.1 ± 1.1
							total-gas age 41.0 ± 1.1

Appendix C (continued)

	Temperature (°C)	$(^{40}Ar^*/^{39}Ar)$st.	$^{40}Ar^*/^{39}Ar$	$^{36}Ar/^{39}Ar$	$^{37}Ar/^{39}Ar$	^{39}Ar % cumul.	Age Ma
AL 11	phengite						
1	635	25.06 ± 0.20[a]	5.705	0.0123	0.0098	0.9	75.2 ± 1.7
2	760	–	4.521	0.0032	0.0027	3.9	59.8 ± 1.6
3	870	–	5.647	0.0012	0.0010	35.4	74.4 ± 1.7
4	970	–	5.070	0.0007	0.0001	67.3	66.9 ± 1.5
5	1,075	–	5.463	0.0012	0.0003	82.2	72.0 ± 1.6
6	1,175	–	5.540	0.0012	0.0076	98.6	73.0 ± 1.7
7	1,575	–	7.189	0.0150	0.0293	100	94.2 ± 3.5
							total-gas age 71.3 ± 1.7
AL 12	phengite						
1	635	25.06 ± 0.20[a]	5.155	0	0	0.1	68.0 ± 1.5
2	760	–	3.118	0.0019	0	1.4	41.4 ± 1.0
3	870	–	3.316	0.0016	0	30.3	44.1 ± 1.1
4	970	–	3.349	0.0009	0	69.2	44.5 ± 1.1
5	1,125	–	3.154	0.0007	0	95.8	41.9 ± 1.0
6	1,575	–	3.174	0.0036	0.0015	100	42.2 ± 1.3
							total-gas age 43.6 ± 1.1
AL 14	phengite						
1	635	25.06 ± 0.20[a]	4.358	0.0428	2.0925	0.5	57.7 ± 6.6
2	760	–	4.148	0.0255	3.9490	2.7	54.9 ± 4.2
3	870	–	2.064	0.4244	8.8774	3.9	259 ± 56
4	970	–	lost			...	...
5	1,575	–	4.239	0.0154	0.0015	100	56.1 ± 3.0
							total-gas age 58.5 ± 3.7
AL 15	phengite						
1	635	25.37 ± 0.20[a]	1.829	0.0123	0.0432	0.9	24.2 ± 2.1
2	760	–	2.980	0.0014	0.1014	4.5	39.4 ± 1.0
3	870	–	2.981	0.0005	0.0003	15.5	39.4 ± 0.9
4	970	–	2.985	0.0005	0.0003	54.9	39.4 ± 0.9
5	1,175	–	2.895	0.0005	0.0042	96.8	38.3 ± 0.9
6	1,575	–	2.509	0.0044	0.0148	100	33.2 ± 1.1
							total-gas age 38.6 ± 1.0
AL 16	phengite + paragonite						
1	635	25.37 ± 0.20[a]	−6.186	0.0835	0.5950	0.5	−84.4 ± 12
2	760	–	3.857	0.0031	0.4869	10.8	50.8 ± 1.4
3	870	–	4.920	0.0080	0.9087	15.7	64.6 ± 2.2
4	970	–	5.099	0.0026	0.0205	94.3	66.9 ± 1.7
5	1,125	–	5.863	0	0.0090	"100"	76.7 ± 1.7
6	1,575	–	lost				
							total-gas age 64.9 ± 1.8
AL 17	phengite						
1	635	26.72 ± 0.20[a]	−2.513	0.0377	0.0002	1.5	−32 ± 5
2	760	–	4.874	0.0055	0.0040	9.6	60.7 ± 1.8
3	870	–	5.018	0.0019	0.0017	40.8	62.5 ± 1.5
4	970	–	4.827	0.0017	0.0005	91.2	60.1 ± 1.4
5	1,175	–	6.439	0.0654	0.0259	96.0	79.8 ± 9.6
6	1,575	–	2.876	0.0096	0.0084	100	36.1 ± 1.9
							total-gas age 60 ± 1.9
AL 22	paragonite + phengite						
1	635	26.61 ± 0.25[a]	−8.486	0.0618	0	0.4	−178 ± 13
2	760	–	2.818	0.0074	0.1475	3.0	55.5 ± 2.4
3	870	–	3.239	0.0034	0.0192	13.5	63.6 ± 1.8
4	970	–	3.828	0.0014	0.0008	50.6	75.0 ± 1.8
5	1,075	–	3.672	0.0018	0.0012	72.0	72.0 ± 1.8
6	1,575	–	3.116	0.0017	0.0148	100	61.3 ± 1.6
							total-gas age 67.8 ± 1.8

Appendix C (continued)

	Temperature (°C)	$(^{40}Ar^*/^{39}Ar)$st.	$^{40}Ar^*/^{39}Ar$	$^{36}Ar/^{39}Ar$	$^{37}Ar/^{39}Ar$	^{39}Ar % cumul.	Age Ma
AL 28	paragonite + muscovite						
1	635	16.86 ± 0.18[a]	3.099	0.2969	0.1133	1.6	39.0 ± 41
2	760	–	5.190	0.0717	0.0837	9.0	64.9 ± 10.5
3	870	–	3.612	0.0482	0.0295	38.1	45.4 ± 7.1
4	970	–	3.049	0.0635	0.0255	60.9	38.4 ± 9.1
5	1,075	–	6.580	0.0744	0.0537	69.6	81.9 ± 10.9
6	1,575	–	2.653	0.1051	0.3760	100	33.5 ± 14.7
							total-gas age 43.8 ± 11.0

[a] Age of the standard = 310 ± 10 Ma
[b] Age of the standard = 38 ± 1 Ma

$\lambda = 5.304 \cdot 10^{-10}$ year^{-1}

du Midi (Bonneval/Arc). Lower Schistes lustrés unit. Chemical evolution of the phengites from $Si_{3.6}$ to $Si_{3.3}$ through a main $Si_{3.5}$ stage (Fig. 3 and Appendix B). However, only 3T polytype.

AL 16 (6-04): micaceous glaucophanite interbedded in the upper Bonneval gneisses. Feiche Combe (Bonneval/Arc). Gran Paradiso basement. Glaucophane is strongly oriented in the regional l_1 lineation which is gently folded by a second phase. Unretrograded HP paragenesis. 2M-paragonite and $Si_{3.5}$ 2M-phengite in textural equilibrium.

AL 17 (7-14): quartz-phengite glaucophanite. Lécharenne (Bonneval/Arc). Gran Paradiso basement. Unretrograded HP paragenesis. A single $Si_{3.5}$ phengite generation (Appendix B), but 2M and 3T polytypes.

AL 22 (6-80) paragonite-chlorite-chloritoid-phengite calc-schist. Le Villaron (Bessans). Lower Schistes lustrés unit. 2M-paragonite and $Si_{3.55}$ 3T-phengite both primary minerals.

AL 28 (6-355): chloritoid-quartz glaucophanite. Ouille du Midi (Bonneval/Arc). Lower Schistes lustrés unit. Glaucophane is retrograded into talc + albite (Chopin, in prep.), chloritoid into chlorite + 2M-paragonite with some interlayered muscovite. Mica is purely a retrogressive product.

References

Bearth P (1959) Über Eklogite, Glaukophanschiefer und metamorphe Pillowlaven. Schweiz Mineral Petrogr Mitt 39:267–286

Bearth P (1967) Die Ophiolite der Zone von Zermatt-Saas Fee. Beitr Geol Karte Schweiz 132:130 p

Bertrand JM (1968) Etude structurale du versant occidental du massif du Grand Paradis (Alpes Graies). Géol Alp 44:55–87

Bocquet J (1974) Etudes minéralogiques et pétrologiques sur les métamorphismes d'âge alpin dans les Alpes françaises. Thèse, Grenoble, 489 p

Bocquet J, Delaloye M, Hunziker JC, Krummenacher D (1974) K–Ar and Rb–Sr dating of blue amphiboles, micas and associated minerals from the Western Alps. Contrib Mineral Petrol 47:7–26

Brereton NR (1970) Corrections for interferring isotopes in the $^{40}Ar-^{39}Ar$ dating method. Earth Planet Sci Lett 8:427–433

Caby R, Kiénast JR, Saliot P (1978) Structure, métamorphisme et modèle d'évolution tectonique des Alpes occidentales. Rev Géogr Phys Géol Dyn XX:307–322

Caron JM (1977) Lithostratigraphie et tectonique des Schistes lustrés dans les Alpes cottiennes septentrionales et en Corse orientale. Sci Géol Mem 48:326 p

Chatterjee ND (1971) Phase equilibria in the Alpine metamorphic rocks of the environs of the Dora-Maira Massif, Western Italian Alps. Neues Jahrb Mineral, Abh 114:181–245

Chatterjee ND, Froese E (1975) A thermodynamic study of the pseudo-binary join muscovite-paragonite in the system $KAlSi_3O_8-NaAlSi_3O_8-Al_2O_3-SiO_2-H_2O$. Am Mineral 60:985–993

Chessex R, Delaloye M, Krummenacher D, Vuagnat M (1964) Nouvelles déterminations d'âges "plomb total" sur des zircons alpins. Schweiz Mineral Petrogr Mitt 44:43–60

Chopin C (1979) De la Vanoise au massif du Grand Paradis: une approche pétrographique et radiochronologique de la signification géodynamique du métamorphisme de haute pression. Thèse 3ème cycle. Université Paris VI, 145 p

Chopin C, Maluski H (1978) Résultats préliminaires obtenus par la méthode de datation $^{39}Ar/^{40}Ar$ sur des minéraux alpins du massif du Grand Paradis et de son enveloppe. Bull Soc Géol Fr (7) XX: 745–749

Clark SP, Jäger E (1969) Denudation rate in the Alps from geochronologic and heat flow data. Am J Sci 267:1143–1160

Dallmeyer RD (1975) $^{40}Ar-^{39}Ar$ ages of biotite and hornblende from a progressively remetamorphosed basement terrane: their bearing on interpretation of release spectra. Geochim Cosmochim Acta 39:1655–1669

Dallmeyer RD (1975) Incremental $^{40}Ar-^{39}Ar$ ages of biotite and hornblende from retrograded basement gneisses of the Southern Blue Ridge: their bearing on the age of Paleozoic metamorphism. Am J Sci 275:444–460

Dallmeyer RD, Sutter JF (1976) $^{40}Ar-^{39}Ar$ incremental-release ages of biotite and hornblende from variably retrograded basement gneisses of the Northeasternmost Reading Prong, New-York: their bearing on early Paleozoic metamorphic history. Am J Sci 276:731–747

Dallmeyer RD (1978) $^{40}Ar-^{39}Ar$ incremental-release ages of hornblende and biotite across the Georgia Inner Piedmont: their bearing on Late Paleozoic-Early Mesozoic tectonothermal history. Am J Sci 278:124–149

Debelmas J, Lemoine M (1970) The Western Alps: paleogeography and structure. Earth Sci Rev 6:221–256

Delaloye M, Desmons J (1976) K–Ar radiometric age determinations of white micas from the Piémont zone, French-Italian Western Alps. Contrib Mineral Petrol 57:293–303

Desmons(-Bocquet) J (1977) Mineralogical and petrological investigation of Alpine metamorphism in the internal French Western Alps. Am J Sci 277:1045–1066

Dodson MH (1973) Closure temperature in cooling geochronological and petrological systems. Contrib Mineral Petrol 40:259–274

Ellenberger F (1960) Sur une paragenèse éphémère à lawsonite et glaucophane dans le métamorphisme alpin en Haute-Maurienne (Savoie). Bull Soc Géol Fr 2:190–194
Fleck RJ, Sutter JF, Elliot DH (1977) Interpretation of discordant $^{40}Ar/^{39}Ar$ age-spectra of Mesozoic tholeiites from Antarctica. Geochim Cosmochim Acta 41:15–32
Frey M, Hunziker JC, O'Neil JR, Schwander HW (1976) Equilibrium-disequilibrium relations in the Monte Rosa granite, Western Alps: petrological, Rb–Sr and stable isotope data. Contrib Mineral Petrol 55:147–179
Fructus-Ricquebourg J, Sabatier G, Curien H (1963) Sur le mécanisme structural des changements de phases dans les tectosilicates: échange isotopique d'oxygène et recristallisation des verres. Bull Soc Fr Minéral Cristallogr LXXXVI:90–91
Fry N, Fyfe WS (1971) On the significance of the eclogite facies in Alpine metamorphism. Verh Geol Bundesanst (Austria) 2:257–265
Goffé B (1977) Succession de subfaciès métamorphiques en Vanoise méridionale (Savoie). Contrib Mineral Petrol 62:23–41
Goffé B (1979) La lawsonite et les associations à pyrophyllite-calcite dans les metasédiments alumineux du Briançonnais: premières occurences. CR Acad Sci Paris, D 289:813–816
Goldsmith JR, Graf DL (1960) Subsolidus relations in the system $CaCO_3-MgCO_3-MnCO_3$. J Geol 68:324–332
Gueirard S (1976) Le "Granite de Barral". Un nouveau témoin des conditions sévères de métamorphisme qui ont affecté la région occidentale du Massif des Maures (Var, France). CR Acad Sci Paris, D 283:455–457
Guitard G, Saliot P (1971) Sur les paragenèses à lawsonite et à pumpellyite des Alpes de Savoie. Bull Soc Fr Minéral Cristallogr 94:507–523
Haas H (1972) Diaspore-corundum equilibrium determined by epitaxis of diaspore on corundum. Am Mineral 57:1375–1385
Hanson GN, Simmons KR, Bence AE (1975) $^{40}Ar-^{39}Ar$ spectrum age for biotite, hornblende and muscovite in a contact metamorphic zone. Geochim Cosmochim Acta 39:1269–1277
Hunziker JC (1974) Rb–Sr and K–Ar age determinations and the Alpine tectonic history of the Western Alps. Mem Ist Geol Miner Univ Padova 31:55 p
Jäger E (1970) Radiometrische Altersbestimmungen in der Erforschung metamorpher Prozesse. Fortschr Mineral 47:77–83
Jäger E (1973) Die alpine Orogenese im Lichte der radiometrischen Altersbestimmung. Eclogae Geol Helv 66:11–21
Jäger E, Niggli E, Wenk E (1967) Rb–Sr Altersbestimmungen an Glimmern der Zentralalpen. Beitr Geol Karte Schweiz 134
Krummenacher D, Evernden JF (1960) Déterminations d'âge isotopique faites sur quelques roches des Alpes par la méthode potassium-argon. Schweiz Mineral Petrogr Mitt 40:267–277
Maluski H (1977) Application de la méthode $^{40}Ar-^{39}Ar$ aux minéraux des roches cristallines perturbées par des évènements thermiques et tectoniques en Corse. Thèse, Montpellier, 120 p
Maluski H (1978) Behaviour of biotites, amphiboles, plagioclases and K-feldspars in response to tectonic events with the $^{40}Ar-^{39}Ar$ radiometric method. Example of Corsican granite. Geochim Cosmochim Acta 42:1619–1633
Maluski H, Gueirard S (1978) Mise en évidence par la méthode $^{40}Ar-^{39}Ar$ de l'âge à 580 Ma du granite de Barral (massif des Maures, France). CR Acad Sci Paris, D 287:195–198
Mussett AE (1969) Diffusion measurements and the K–Ar method of dating. Geophys J R Astron Soc 18:257–303
Newton RC, Smith JV (1967) Investigations concerning the breakdown of albite at depth in the earth. J Geol 75:268–286
Nicolas A (1966) Le complexe Ophiolites-Schistes lustrés entre Dora-Maira et Grand Paradis (Alpes piémontaises). Tectonique et métamorphisme. Thèse, Nantes 295 p
Purdy JW, Jäger E (1976) K–Ar ages on rock-forming minerals from the Central Alps. Mem Ist Geol Mineral Univ Padova 30:1–32
Roddick JC (1978) The application of isochron diagrams in $^{40}Ar-^{39}Ar$ dating: a discussion. Earth Planet Sci Lett 41:233–244
Saliot P (1973) Les principales zones de métamorphisme dans les Alpes françaises. Répartition et signification. CR Acad Sci Paris, D 276:3081–3084
Saliot P (1978) Le métamorphisme dans les Alpes françaises. Thèse, Paris Sud, Centre Orsay, 181 p
Steiger RH (1961) Die Hornblende der Tremolaserie. I: Chemismus und Dichte der Hornblende. Schweiz Mineral Petrogr Mitt 41:127–156
Steiger RH (1964) Dating of orogenic phases in the Central Alps by K–Ar ages of hornblendes. J Geophys Res 69:5407–5421
Velde B (1967) Si^{4+} content of natural phengites. Contrib Mineral Petrol 14:250–258
Vialette Y, Vialon P (1964) Etude géochronologique de quelques micas des formations du massif Dora-Maira, Alpes cottiennes piémontaises. Ann Fac Sci Univ Clermont 25:91–99

Received October 31, 1979; Accepted July 10, 1980

Contrib Mineral Petrol (1982) 80:391–394

Contributions to Mineralogy and Petrology

Unconvincing Evidence Against the Blocking Temperature Concept?

A Reply

Christian Chopin[1] and Henri Maluski[2]
[1] ER 224, Laboratoire de Géologie, Ecole normale supérieure, 46 rue d'Ulm, F-75230 Paris Cedex 05, France
[2] LA 226, Laboratoire de Géologie structurale, U.S.T.L., place E. Bataillon, F-34060 Montpellier Cedex, France

One of the purposes of our 1980 paper was to raise a discussion on the use of the blocking temperature concept. This purpose has obviously been achieved. However, we regret that the comment of Desmons et al. is not more constructive. In fact, Desmons et al.'s most serious criticism of our experimental work relies partly on the methodologic misconceptions of these authors, partly on a misprint that could be easily detected and that these authors indeed suspected but preferred to ignore while drawing their figures. They further go on with a discussion in which, beside incorrect statements, our line of argument and conclusions are misquoted and grossly misrepresented. As these authors finally come to "a more satisfying conclusion" which does not substantially differ from our own, one may wonder what the true purpose of their comment is.

Experimental, Comments on Figs. 1, 2, 3

We first would like to apologize for having overlooked a misprint in the column headings of Appendix C where $^{40}Ar/^{36}Ar$ should read $^{40}Ar^*/^{36}Ar$. This could be easily inferred from the negative signs of a few values indicating that correction for atmospheric Ar had been made. Accordingly the zero intercept in the actual ($^{40}Ar^*/^{36}Ar$, $^{39}Ar/^{36}Ar$) plot of Figs. 1 to 3 of Desmons et al. is not really a surprise but just what is expected.

We readily recognize that 5 to 7 degassing steps might appear to be few for a K-rich sample. However it is clear that even 5 steps are in any case more informative than a total fusion. Furthermore, if 3 or 4 contiguous steps with large degassing fractions yield similar apparent ages, fractioning them into numerous steps would not lead to a different pattern. Besides, reproaching with age discrepancy as high as 50% between individual steps, Desmons et al. just show how unfamiliar they are with the ^{40}Ar-^{39}Ar literature. It is well known that the first degassing steps – and sometimes the total fusion step – which represent small percentages of the total argon released often show highly discordant age values. This is the reason why Dalrymple and Lanphere (1974) proposed that one ignore such gas fractions. Later, Roddick et al. (1980) have shown that these fractions might in some cases be the significant ones.

Desmons et al's criticism of our irradiation parameters begins with an erroneous statement. Although J values were not given in our paper, they could be directly obtained from the values of ($^{40}Ar^*/^{39}Ar_{standard}$) which were given in Appendix C (Table of analytical data). The great slope difference in Desmons et al.'s Figure 2 between samples AL 8, 10 and AL 7, 12, 15 indeed reflects different J values, which merely result from the different ages of the irradiation standards used, *as could be read from Appendix C*. For a given standard, the differences in J (or in $^{40}Ar^*/^{39}Ar_{st}$) between different irradiations of course result from variations in the neutron flux; this is the very reason why a standard is used for each irradiation! Perhaps Desmons et al. wanted to demonstrate that the neutron flux was not uniform within the irradiation cannister, but they should then have compared samples (with *presumably* identical ages) from the same irradiation, which is not the case. Briefly, Figure 2 and the whole discussion of Desmons et al. on the control of irradiation parameters make no sense.

Concerning their Fig. 3, we do appreciate that Desmons et al. plot in it sample AL 5 for which we stated that it was a case of partial reopening and would not have expected any "isochron", and sample AL 22 from which we wrote that no well-defined plateau age was obtained. The same holds true for sample AL 28 in their Fig. 1.

Summarizing, the only remaining valid points of Desmons et al. criticism are the low intercept of samples AL 15 phengite (215) and AL 10 biotite (241), and the negative slope of sample AL 9 which would indeed have merited further comments. The case of AL 9 could be best accounted for by the presence in this paragonite sample of "trapped Ar" (in the sense of Roddick 1980) with high $^{40}Ar/^{36}Ar$ ratio and irregularly released between the low- and high-temperature steps. The presence of non-radiogenic argon was suspected for paragonite (Chopin and Maluski 1980, p. 115) but we have no further evidence as yet. The low intercepts are probably due to inadequate blank correction for the two samples in question (AL 15 and AL 10). The correction could have resulted in an underestimation of ^{40}Ar for the degassing steps with a very small gas fraction, which are indeed the ones that determine the intercept value. For example the intercept of sample AL 15 becomes 296 if the two smallest gas fractions (635 °C and 1,575 °C heating steps) are disregarded. These points being cleared up, we leave it to the judgement of the readers whether the spectra *for which we claimed plateau ages* indeed show plateaus.

Next Desmons et al. come to their nicest argument, our "missing samples". As these are actually glaucophanes and Hercynian biotites, we felt that they did not ideally suit a paper devoted to Alpine micas, not to say phengite systematics. Nevertheless, our critics might be usefully referred to Chopin and Maluski 1978.

0010-7999/82/0080/391/$01.00

A Coherent Criticism?

In their following discussion (chapters 4 and 5), Desmons et al. show what they understand under coherent statements and how they have been able to read our paper.

Although they quote in Chapt. 4 that we "assert that only muscovitic mica, phengite low in celadonite and paragonite crystallized at 38 Ma", they reproach us in the same chapter for ignoring the evidence for newly formed micas during that event. Coherence? Again, they write in Chap. 5 that we "wanted to prove that paragonite was a primary Eoalpine mineral that remained unaffected by the Lepontine event", although we presented petrographic and isotopic evidence for the late formation of paragonite (see above quotation!).

Furthermore, in chapter 4, they "quote" twice from our abstract "the micas with younger ages (38 Ma)" which "did not crystallize at that stage but were only readjusted" during that event, and they reproach us with the apparent incoherence between this statement and the actual growth of micas at that stage. Should the reader replace before "micas" the word that Desmons et al. twice omitted, namely *high-pressure,* the incoherence vanishes: high-pressure micas (highly substituted phengites and paragonite) were formed at an early time; lower-pressure micas (less substituted phengites and paragonite) cyrstallized later on, until and during Lepontine times. We see no contradiction between the fact that in most lithological types several phengite generations have grown, often on different foliation planes (Chopin and Maluski 1980, p. 110), and the fact that in most of the samples investigated a high-pressure, early phengite generation was the only present one (this was the actual purpose of our sampling method, p. 111). This single generation could either have remained a closed, metastable system or have been isotopically readjusted, without any further growth process.

In this respect we apparently must stess once again how necessary (but alas not sufficient) the knowledge of the actual composition of the phengite population is for discussing its isotopic evolution. In particular the existence of a single or of several phengite generations in a sample is determining: in the latter case the system must have been chemically active, in the former it might have remain closed after crystallization of the mica. We maintain that wet chemical analyses, as numerous as they might be, do not allow to solve such a problem. The age spread between 54 and 40 Ma found by Bocquet (Desmons) et al. (1974) and Delaloye and Desmons (1976) is certainly an actual fact. The problem is whether or not it has a geological significance. Following Hunziker (1974) these authors assumed the presence of excess argon to account for such ages. We found only one age like these (AL 5 phengite, total-gas age 56 Ma) that we interpreted as resulting from a partial reopening (see age spectrum in Fig. 6). In neither case were these intermediate ages given a geological significance. Therefore, we feel that we can repeat that a sampling method which enables one to avoid such samples is better, as far as geology is concerned.

Chapter 6 of Desmons et al. (1982) provides another example of coherent and pertinent criticism. After having reproached us with the reference to Corsica (where the geological as well as the metamorphic features make definitely the island part of the Western Alps system) and having called upon the Apuane Alps (where the metamorphic history is entirely different in that there is no evidence for a high-pressure, low-temperature phase), Desmons et al. state that the temperature of 450° C we quoted is valid in the Monte Rosa area and can *by no means* be extrapolated to the whole of the Western Alps. We clearly wrote that this temperature estimate had been made on the basis of late assemblages found in the *studied region.* Further, they reproach us for having ignored the fission track data of Wagner et al. (1977) and Deferne (1976), which were obtained in ... the Central Alps and Monte Rosa area, and in the Oligocene intrusives of the Sesia zone and Central Alps, respectively!

Metamorphism in the Briançonnais Unit

In this chapter too, Desmons et al. provide an interesting example of the line of evidence they use, not distinguishing between a necessary condition and a sufficient one.

Desmons et al. present the discrepancy between the *minimum* pressure values yielded by the presence of jadeite in the Vanoise basement and by the presence of lawsonite in the cover rocks as a sufficient condition for a discrepancy in the actual pressures which occurred and thus of the metamorphic history of the two lithological units. This is clearly erroneous since no upper pressure limit is given by the assemblages of the cover rocks. The difference in mineralogy merely results from different lithologies.

Moreover, among the minerals of the cover rocks, Desmons et al. have omitted the most interesting one, magnesiocarpholite, which is found in its type locality (Goffé et al. 1973). Magnesiocarpholite as well as ferrocarpholite are low-temperature phases, exclusively occurring in lawsonite-bearing areas, and ferrocarpholite is generally found in jadeite-bearing areas. Since on crystal-chemical grounds magnesiocarpholite can be expected to be a higher-pressure phase than ferrocarpholite, the presence of magnesiocarpholite in the Vanoise cover sequence provides no upper pressure limit and, on the contrary, magnesiocarpholite could be confidently considered to be a high-pressure phase (which has recently been corroborated by experimental work: Chopin and Goffé 1981; Chopin and Schreyer 1981; Goffé 1982). Therefore, independently of the logical misuse that Desmons et al. made of it, the discrepancy in the minimum pressure estimates between basement and cover rocks in the Vanoise is not as great as supposed.

As far as structural geology is concerned, Platt and Lister (1978) ignore the arguments presented by Goffé (1975) for two successive foliations, both glaucophane-bearing in the basement and both also affecting the cover sequence. The structural evidence is thus, at best, not as clear-cut and convincing as one would let think. Furthermore, to pretend that "the Vanoise cover sequence *as a whole* lies as an overturned thrust sheet upon the basement" can only be based on complete ignorance of geological facts (compare Ellenberger 1958; Goffé 1975; Raoult 1980).

Desmons et al. quote the Northern Briançonnais-St Bernard zone (Barrhorn-Mischabel association) as a similar unsolved problem. However the discovery of Upper Cretaceous and Tertiary wildflysch with microfossils still preserved in the presumably autochthonous cover of the Mischabel (Marthaler and Escher 1980) is strong evidence for the Tertiary age of the metamorphism in the St Bernard zone s.s. In the Upper Val d'Aoste, the same lithological series but without microfossils is clearly autochthonous on the St Bernard basement (Caby 1981). Furthermore, in the Southern Briançonnais zone (Acceglio zone) the Mesozoic sequence has been deeply eroded during Lower Jurassic times, locally down to the Paleozoic basement which was then *transgraded* by an Upper Jurassic to Paleocene sequence and now displays jadeite+quartz (Lefèvre and Michard 1976). The earliest possible high-pressure metamorphism is obviously post-Paleocene.

The Blocking Temperature Concept

The application of this concept to geological problems is what we wish to discuss. Other points of style or grammar are not of great importance. Desmons et al. (1982) recall that *many other factors than temperature* are involved in the opening of a system, even at temperature as high as 400 to 500° C. Evidences are indeed the existence of unreopened mica samples at such temperatures as recorded by, among others, Verschure et al. (1980) and Desmons et al. who quote Eoalpine biotite ages in undeformed samples of the Sesia zone.

A first consequence is of logical nature: the existence of some unreopened systems in a given area is then by no means a *sufficient* condition to state that temperature did not there exceed the "blocking temperature".

A second consequence is of physical nature: these records of some unreopened micas in spite of "high" temperature, the fact that age is not a function of the grain size (see Purdy and Jäger 1976, p. 14), just as the existence of preserved mineral zonation in most of the metamorphic realm, are sufficient conditions to deny the role of thermally activated volume-diffusion as an effective migration process. Again, we maintain that this is evidence against the blocking concept as far as the latter is explicitly or implicitly based on the assumption of the effectiveness of a thermally activated, volume-diffusion-like process – as is actually the case as soon as the blocking concept is used to deduce isotherms without any discussion of other possible migration-controlling factors (e.g. Delaloye and Desmons 1976).

A further consequence is the following: since there is for a given system a priori no reason for all these migration-controlling parameters other than temperature to impose the same control during cooling as during warming, coincidence of actual opening and closure temperature should be the exception rather than the rule. In contrast, coincidence of closure and opening is inherent to the thermally activated volume diffusion model as theoretically developed by Dodson (1973). As they empirically established their blocking temperatures in the Ticino region, Purdy and Jäger (1976) explicitly assumed that opening and closure temperatures coincide, but were aware that this may not be quite correct (p. 19). In this respect we do not understand how Desmons et al. (1982) can write both that "many other factors than temperature are involved" and that "this does not oppose the blocking temperature concept". Indeed, since these other factors are not necessarily all temperature-dependent, the first statement allows for the possibility of different and variable opening and closure temperatures. Interestingly Desmons et al. make then, although incidentally, an important restriction as they precise that they "would ... still assume that mica behave as open above its closure temperature *if fluid mobility allows exchanges in the system*" (italics by Chopin and Maluski). In order for the blocking concept to maintain a meaning, it must be restricted to a group of systems characterized by a certain type of fluid behaviour. However, the practical use of this restriction is questionable since it is hardly possible to define and to quantify the role of the fluid phase. Moreover by doing so one could also obtain for each group of systems (defined by a set of boundary conditions) a blocking temperature or, more probably, a closure and an opening temperature. Depending on the reference system chosen, a variety of temperatures may result. As pointed out by Verschure et al. (1980, p. 251) this is actually the case.

Obviously, the blocking concept remains highly problematic. Each study must accordingly be a case study and no dogmatism is allowed. In this respect we can just refer the reader to Purdy and Jäger (1976) cautions, to our 1980 general discussion (p. 117), to the conclusion of Verschure et al. (1980) which supports our own, and to the fine discussion proposed by Dodson (1981).

Acknowledgements. We express our grateful acknowledgement to F. Albarède for his comments on the manuscript, to B. Velde who tried in vain to let us write a better reply, and to C. Saint-Raymond who cheerfully typed the successive scripts.

References

Bocquet (Desmons) J, Delaloye M, Hunziker JC, Krummenacher D (1974) K-Ar and Rb-Sr dating of blue amphiboles, micas and associated minerals from the Western Alps. Contrib Mineral Petrol 47:7–26

Caby R (1981) Le Mésozoïque de la zone du Combin en Val d'Aoste (Alpes Graies), imbrications tectoniques entre séries issues des domaines pennique, austroalpin et océanique. Géologie Alpine 57:5–13

Chopin C, Maluski H (1978) Résultats préliminaires obtenus par la méthode de datation $^{39}Ar/^{40}Ar$ sur des minéraux alpins du massif du Grand Paradis et de son enveloppe. Bull Soc Geol Fr (7) 20:745–749

Chopin C, Maluski H (1980) ^{40}Ar-^{39}Ar dating of high pressure metamorphic micas from the Gran Paradiso area (Western Alps): evidence against the blocking temperature concept. Contrib Mineral Petrol 74:109–122

Chopin C, Goffé B (1981) High-pressure synthesis and properties of magnesiocarpholite, $MgAl_2[Si_2O_6](OH)_4$. Contrib Mineral Petrol 76:260–264

Chopin C, Schreyer W (1981) Eine experimentelle Untersuchung des MgO-Al_2O_3-SiO_2-H_2O Systems im Hochdruck-Tieftemperatur-Bereich. Fortschr Mineral 59, Beih 1:31–33

Dalrymple GB, Lanphere MA (1974) $^{40}Ar/^{39}Ar$ age spectra of some undisturbed terrestrial samples. Geochim Cosmochim Acta 38:715–738

Deferne J (1976) Essai d'application de la méthode des traces de fission à la datation de quelques massifs éruptifs du Sud des Alpes. Thèse nº 1596 Univ Genève, 70 p.

Delaloye M, Desmons J (1976) K-Ar radiometric age determinations of white micas from the Piemont Zone, French-Italian Western Alps. Contrib. Mineral Petrol 57:297–303

Desmons J, Hunziker JC, Delaloye M (1982) Unconvincing evidence against the blocking temperature concept. Comments on: ^{40}Ar-^{39}Ar dating of high-pressure metamorphic micas ... by C. Chopin and Maluski. Contrib Mineral Petrol

Dodson MH (1973) Closure temperature in cooling geochronological and petrological systems. Contrib Mineral Petrol 40:259–274

Dodson MH (1981) Thermochronometry. Nature 293:606–607

Ellenberger F (1958) Etude géologique du pays de Vanoise. Mém expl Serv Carte géol Fr, 561 p

Goffé B (1975) Etude structurale et pétrographique du versant occi-

dental du massif paléozoïque de Chasseforêt, Vanoise méridionale. Thèse 3ème cycle, Paris Sud-Orsay
Goffé B (1982) Définition du faciès à Fe, Mg-carpholite-chloritoïde: un marqueur du métamorphisme de HP-BT dans les métasédiments alumineux. Thèse Doct Sci, Univ P et M Curie-Paris, 233 p
Goffé B, Goffé-Urbano G, Saliot P (1973) Sur la présence d'une variété magnésienne de ferrocarpholite en Vanoise (Alpes françaises). Sa signification probable dans le métamorphisme alpin. C R Acad Sci Paris D 277:1965–1968
Hunziker JC (1974) Rb-Sr and K-Ar age determination and the Alpine tectonic history of the Western Alps. Mem Ist Geol Mineral Univ Padova 31:55 p
Lefèvre R, Michard A (1976) Les nappes brainçonnaises internes et ultrabriançonnaises de la bande d'Acceglio (Alpes franco-italiennes); une étude structurale et pétrographique dans le faciès des Schistes bleus à jadéite. Sci Géol Bull 29:183–222
Marthaler M, Escher A (1980) Pennique: couverture de la nappe du Grand Saint Bernard dans le Val d'Anniviers (Lac du Toûno-Roc de Boudri). In: Compte rendu de l'excursion de la Société géologique suisse du 1 au 3 octobre 1979: coupe Préalpes-Helvétique-Pennique en Suisse occidentale. Eclogae Geol Helv 73:331–349
Platt JP, Lister GS (1978) Déformation, métamorphisme et mécanismes d'écoulement dans le massif de la Vanoise, Alpes. CR Acad Sci Paris D 287:895–898
Purdy JW, Jäger E (1976) K-Ar ages on rock-forming minerals from the Central Alps. Mem Ist Geol Mineral Univ Padova 30, 32 p
Raoult JF (1980) Interprétation nouvelle de la Vanoise (zone briançonnaise, Alpes françaises). Rev. Géol dyn Géogr phys 22:303–312
Roddick JC, Cliff RA, Rex DC (1980) The evolution of excess argon in Alpine biotites – a ^{40}Ar-^{39}Ar analysis. Earth Planet Sci Lett 48:185–208
Verschure RH, Andressen PAM, Boelrijk NAIM, Hebeda EH, Maijer C, Priem HNA, Verdurmen EAT (1980) On the thermal stability of Rb-Sr and K-Ar biotite systems: evidence from coexisting Sveconorwegian (ca 870 Ma) and Caledonian (ca 400 Ma) biotites in SW Norway. Contrib Mineral Petrol 74:245–252
Wagner GA, Reimer GM, Jäger E (1977) Cooling ages derived by apatite fission track, mica Rb-St and K-Ar dating:nthe uplift and cooling history of the Central Alps. Mem Ist Geol Mineral Univ Padova 30:1–27

Accepted August 3, 1982

Talc–Phengite: a Widespread Assemblage in High-Grade Pelitic Blueschists of the Western Alps

by CHRISTIAN CHOPIN*

Laboratoire de Géologie, Ecole normale supérieure, 46, rue d'Ulm, F–75005 Paris, France

(*Received 25 March 1981; in revised form 25 May 1981*)

ABSTRACT

Talc–phengite, an assemblage hitherto believed to be rare, is found in regional distribution in the Gran Paradiso area, where it occurs in the characteristic mineral association chloritoid–talc–phengite ($Si_{3.4-3.5}$). Talc contains up to 15 mole per cent minnesotaite, and chloritoid up to 45 mole per cent of the magnesium end member. The talc–phengite stability results basically from the disappearance of chlorite + quartz in rocks with low and moderate MgO/FeO ratios through the divariant reactions first recognized here:

$$\text{Fe-Mg-chlorite} + \text{quartz} \rightarrow \text{talc} + \text{garnet} + H_2O$$

$$\text{and Fe-Mg-chlorite} + \text{quartz} \rightarrow \text{talc} + \text{chloritoid} + H_2O.$$

These reactions imply the disappearance of the join biotite–chlorite in the presence of quartz and thus open a talc–phengite stability field (±garnet or chloritoid or Mg-chlorite) which extends, with increasing *P* and *T*, toward Mg-richer compositions. Whether or not it reaches the magnesian subsystem in the Gran Paradiso area cannot be ascertained. However, the sporadic occurrence of the high-pressure assemblage talc–kyanite–chloritoid 50 to 70 km further northeast in the vicinity of the Monte Rosa massif within the same lithological unit (Zermatt–Saas Fee zone *s.l.*) indicates the instability of any chlorite in quartz-bearing rocks, and implies that talc–phengite must also be stable for purely magnesian compositions in that area. This progressive stabilization of talc–phengite with increasing metamorphic grade supports Abraham & Schreyer's (1976) hypothesis of a high-pressure field for this assemblage, and rules out Chernosky's construction (1978) implying a low-pressure field.

The following paragenetic sequence is proposed for pelitic compositions with intermediate Mg/Fe ratios and excess quartz subjected to high-pressure metamorphism with maximum temperatures near 400–500 °C: chlorite–illite → chlorite–phengite → chloritoid–talc–phengite. The absence of biotite is a compositional effect due to the high degree of phengite substitution in the white mica.

INTRODUCTION

DURING a petrological investigation in the internal Penninic zone of the Western Alps, the talc–phengite assemblage was recognized in various lithologies and, in fact, proved to be a characteristic association of the regional high-pressure metamorphism. This assemblage has thus far been considered to be unusual and its significance has been a matter of controversy. Thus this paper is primarily intended to describe the pertinent assemblages in their regional setting and, through phase-relationship analysis, to highlight the talc–phengite significance. This leads to a new analysis of the pelitic system at high pressure, which is also briefly outlined here.

* Present address: Institut für Mineralogie, Ruhr-Universität, Postfach 10 21 48, D–4630 Bochum 1, Federal Republic of Germany.

[Journal of Petrology, Vol. 22, Part 4, pp. 628–650, 1981]

PREVIOUS WORK

Abraham & Schreyer (1976) first described a talc–phengite assemblage in piemontite schist from Serbia. The significance of this assemblage had not been previously recognized. Two possibilities were discussed to account for the appearance of talc–phengite instead of the common alternative assemblages phlogopite–chlorite–quartz, phlogopite–cordierite–quartz or phlogopite–aluminium silicate–quartz (Fig. 1).

Hypothesis 1. The presence of additional components (Fe_2O_3, MnO, CuO, NiO, etc.) in this natural FeO-free system provides additional degrees of freedom, or

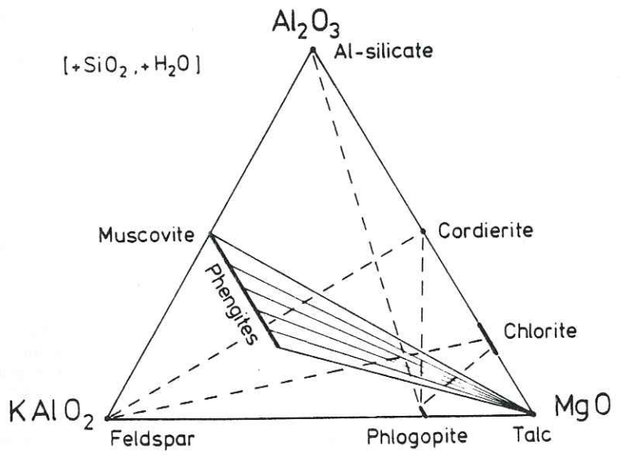

FIG. 1. Projection of the K_2O–MgO–Al_2O_3–SiO_2–H_2O system showing the most important assemblages alternative to the talc–phengite/muscovite pair.

causes shifts of reaction curves from those determined in the model system K_2O–MgO–Al_2O_3–SiO_2–H_2O (Fawcett & Yoder, 1966; Seifert, 1970; Bird & Fawcett, 1973). This could lead to an intersection of the reaction curves

$$\text{chlorite} + \text{quartz} \rightleftharpoons \text{talc} + \text{cordierite} + H_2O \quad (1)$$

$$\text{and chlorite} + \text{muscovite} + \text{quartz} \rightleftharpoons \text{phlogopite} + \text{cordierite} + H_2O \quad (2)$$

thus creating an invariant point and allowing an otherwise forbidden talc–muscovite field (Fig. 2a).

Hypothesis 2. Even in the pure synthetic system, the curves of the reactions

$$\text{chlorite} + \text{muscovite} \rightleftharpoons \text{phlogopite} + \text{kyanite} + \text{quartz} + H_2O \quad (3)$$

$$\text{and chlorite} + \text{quartz} \rightleftharpoons \text{talc} + \text{kyanite} + H_2O \quad (4)$$

intersect, according to the experimental data of Bird & Fawcett (1973) and Schreyer (1968) respectively, to create a new invariant point near 650 °C and 11

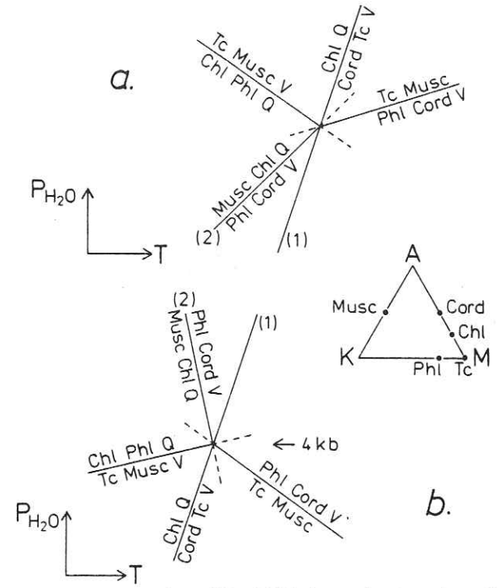

FIG. 2. Two hypotheses for a talc–muscovite stability field in the purely magnesian system. (a) Construction proposed by Abraham & Schreyer (1976, hypothesis 1). (b) Construction proposed by Chernosky (1978). These are mirror constructions. Reactions are numbered as in the text. The *AKM* plot is a projection made onto the Al_2O_3–$KAlO_2$–MgO plane from the SiO_2 and H_2O apices.

kb and produce a talc–'muscovite' stabiiity field confined to high pressures and limited by the reaction.

$$\text{talc} + \text{muscovite} \rightleftharpoons \text{phlogopite} + \text{kyanite} + \text{quartz} + H_2O \quad (5)$$

on the high-temperature side (Fig. 3). Owing to its rigorous derivation, the second hypothesis appeared quite attractive and, although talc–phengite had not been found in a typical high-pressure metamorphic terrane, the presence of kyanite, howieite, calderite and $Si_{3.3}$-phengite in the Serbian occurrence could be indicative of high confining pressures (Schreyer & Abraham, 1977).

The second hypothesis was experimentally confirmed by Schreyer & Baller (1977) shortly therafter. For an appropriate bulk composition of the pure magnesian K_2O–MgO–Al_2O_3–SiO_2–H_2O (*KMASH*) system, talc was found to coexist with a phengitic mica at water pressures between 15 and 25 kb, and the high-temperature breakdown of this assemblage was indeed reaction (5) at about 650 °C.

Shortly afterwards Chernosky (1978) published an experimental redetermination of reaction curve (1) and an analysis of the *KMASH* system in which curves (1) and (2) intersect. This allows a talc–muscovite stability field, as in Abraham & Schreyer's first construction (Fig. 2a), but with a basic difference (Fig. 2b): the two constructions are enantiomorphic and the talc–muscovite and

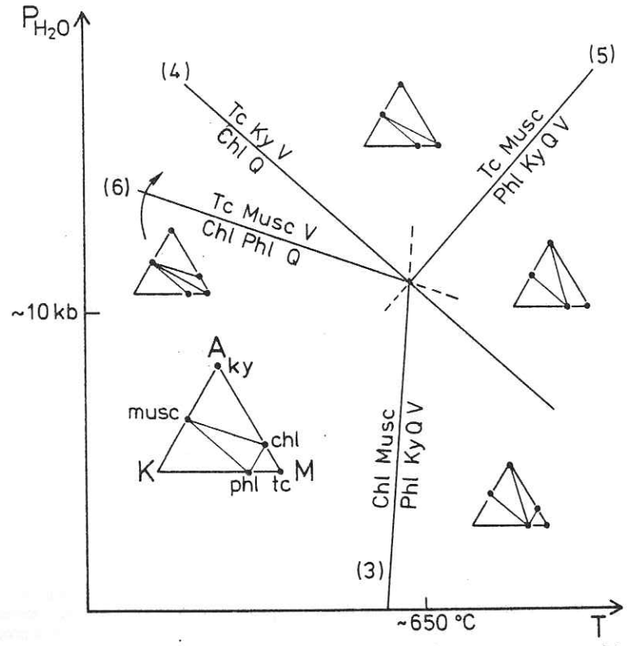

FIG. 3. Analysis of the high-pressure phase relationships in the *KMASH* system as proposed by Abraham & Schreyer (1976, hypothesis 2). The existence of a talc–'muscovite' stability field at high pressure seems inevitable. Reactions are labelled as in the text. Quartz and hydrous fluid are excess phases in the *AKM* plot.

talc–aluminium silicate fields are therefore limited to very low pressures in Chernosky's analysis. Both constructions are chemographically correct, the problem being the relative position and slopes of reaction curves (1) and (2). These curves, as determined by Chernosky (1978) and Seifert (1970) respectively, are in fact nearly parallel and very close to each other. Considering the experimental uncertainty and the possibly different chlorite compositions involved, it is impossible to choose among these two interaction models and the non-intersection scheme implied by hypothesis 2.

In this situation it appears wiser to test these different constructions against natural assemblages and thus to look for talc–muscovite (or phengite) in diagenetic and metamorphosed magnesian sediments, for example in evaporitic sequences. Füchtbauer & Goldschmidt (1959) record talc in the Zechstein formation, but they do not mention if illite (or muscovite) is present in these samples. Perthuisot (1978) describes phlogopite–chlorite–quartz and K-feldspar–chlorite–quartz assemblages in diapirs from Northern Tunisia, but never observed talc + phengite (pers. comm. 1978). In the talc deposits of the Pyrenées, which were also formed at low pressure, muscovite does not occur in contact with talc (Guitard, 1973; pers. comm. 1978). On the other hand, Saliot (1978) mentions a talc–phengite assemblage in evaporitic rocks from Bramans (Savoie) in high-pressure metamorphic terranes of the

Western Alps. It is in a more internal (eastern) part of the Penninic zone (Haute Maurienne valley and Gran Paradiso massif) that I discovered talc–phengite as a regionally widespread metamorphic assemblage.

GEOLOGICAL SETTING AND PETROLOGICAL BACKGROUND

For a geological review of the Western Alps, the reader is referred to Debelmas & Lemoine (1970) or Debelmas (1980), and to Fig. 4. The Alpine metamorphism has been reviewed by Frey *et al.* (1974) and Desmons (1979), while the metamorphic zonation in relation to tectonics is treated by Caby *et al.* (1978).

The Piémont zone, i.e. the eastern part of the Penninic domain, consists of a series of Mesozoic metasediments and ophiolites (the Schistes lustrés thrust sheet) overlying a Paleozoic crystalline basement and its Mesozoic cover which appear in windows cut through the Schistes Lustrés (these are the Monte Rosa, Gran Paradiso and Dora Maira massifs, from North to South—Fig. 4). The area initially investigated includes the Gran Paradiso massif and the Schistes lustrés of its western slope. The Gran Paradiso massif consists mainly of metagranitic basement overlain by a 0–20 m thick Mesozoic cover of quartzites and marbles. The Schistes lustrés can be separated on lithological, structural and metamorphic grounds into three superimposed thrust sheets (Chopin, 1979). The lowermost one lies on the Gran Paradiso massif and is ophiolite- and eclogite-bearing; it consists of a large serpentinite body conformably overlain by a thin volcanosedimentary sequence. It is the southern extension and exact equivalent of the Zermatt–Saas zone of Bearth (1967) around the Monte Rosa, and of the 'unité inférieure' of Kiénast (1973) in the Val d'Aoste (cf. Dal Piaz & Ernst, 1978). The present work has been limited to this unit and to the Gran Paradiso massif. The investigated area may therefore be considered in simple terms as the eastern margin of the former European plate, overthrust by an ocean-floor unit.

During the uppermost Cretaceous (60–75 m.y., Chopin & Maluski, 1978, 1980), high-pressure, low-temperature metamorphism produced the same critical mineral associations in both units: omphacite–garnet-glaucophane, glaucophane–chloritoid, talc–chloritoid, and talc–phengite. Although a very early appearance of lawsonite cannot be precluded, stable calcium silicates in the high-pressure assemblages are zoisite and margarite (Chopin, 1977, 1979). Pure jadeite has been recorded in metagranitoids from the westernmost outcrops of the Gran Paradiso massif (Saliot, 1973, 1979). The phengite substitution in potassic white micas ranges from $Si_{3.4}$ to $Si_{3.65}$ (see Chopin & Maluski, 1980). In primary assemblages, biotite is almost always limited to dolomitic marbles and granitic rock compositions; biotite–kyanite–quartz and biotite–chloritoid–quartz associations, as well as stilpnomelane, are absent.

The high-pressure assemblages have been variably overprinted during the subsequent metamorphic evolution which probably culminated in the Late Eocene (38–40 Ma, Hunziker, 1974; Chopin & Maluski, 1980). In secondary assemblages, phengite substitution ranges from $Si_{3.05}$ to $Si_{3.35}$ and corundum appears in the Gran Paradiso basement. The following P–T estimates have been proposed for this area (Chopin, 1979): $P \geqslant 7$ kb and $T \simeq 400$–450 °C for the high-pressure stage, and P

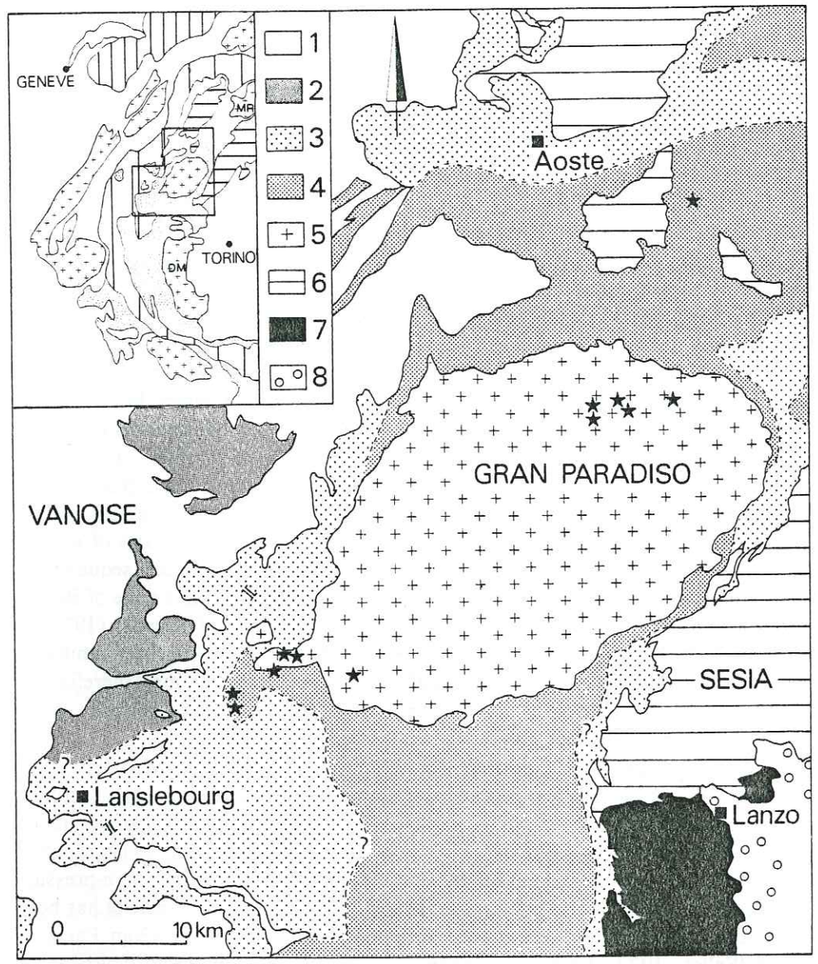

FIG. 4. The talc–phengite assemblage in its geological setting. Legend for inset map: Structural units in the Western Alps. Crosses: external and internal crystalline massifs, MR = Monte Rosa, DM = Dora Maira. Wide vertical ruling: Briançonnais–Grand St. Bernard zone. Narrow vertical ruling: Chablais thrust sheets. Dotted: Helminthoid flysch thrust sheet and Piémont zone (Schistes lustrés thrust sheet). Horizontal ruling: Lower Austroalpine units: Sesia zone and Dent Blanche nappe. Legend for detailed map: Briançonnais zone: (1) Paleozoic basement and Mesozoic cover (not separated). Piémont zone (after Caby *et al.*, 1978, except westward of the Gran Paradiso after Chopin, 1979): (2) Upper Schistes lustrés unit, lying on the Vanoise and partly on 3; (3) Intermediate Schistes lustrés unit, dipping westward under the Vanoise; (4) Lower Schistes lustrés unit, lying on the Gran Paradiso massif; (5) Gran Paradiso crystalline massif. Austroalpine zone (6) Lower Austroalpine units (crystalline basement); from north to south: Dent Blanche nappe, Mt Emilius and Mt Rafray klippes, Sesia zone. (7) Lanzo ultramafic body. (8) Tertiary and quaternary post-tectonic deposits of the Po valley. Stars denote the talc–phengite occurrences discovered during this study.

$\simeq$ 4–6 kb, $T = 470 \pm 20$ °C for the overprinting ('retrogression'). Recent experimental work of Massonne (1981) on the use of phengite substitution as a geobarometer indicates even higher minimum pressures for the early metamorphic stage.

THE TALC–PHENGITE-BEARING ROCKS

The talc–phengite assemblage occurs in the Schistes lustrés as well as in the Gran Paradiso basement and cover (Fig. 4) in various rock compositions. These may or may not be carbonate-bearing; they may be manganiferous (if oxidized) or non-manganiferous (both oxidized and reduced). The most numerous examples are chloritoid-bearing talc or chlorite schists (samples 7-37, 8-27, GP18, etc.) which are specifically found in the Gran Paradiso basement. These 'micascisti argentei' have been interpreted (cf. Compagnoni & Lombardo, 1974) as more or less metasomatic derivatives of granite along shear zones, following Bearth's (1952) interpretation in the Monte Rosa massif. The author's observations in the Gran Paradiso massif do not support the theory of such a genetic relation to deformation but show these 'silvery micaschists' to occur systematically as a thin layer (0–6 m thick) between augengneisses (a former porphyritic Paleozoic granite) and a metavolcanosedimentary series. Whether this layer represents the base of a Paleozoic cover deposited on a granitic basement, or a particular layer in the volcanosedimentary pile at which an intruding granite stopped, is still an open problem. At any rate, this layer is part of the sedimentary sequence (as already proposed by Bertrand, 1968) and crops out together with it throughout the massif.

Other talc–phengite-bearing rocks are blue-amphibole quartzitic schists, which occur both in the Gran Paradiso basement (7-15, 7-172, etc.) and in the Schistes lustrés (7-230). In the westernmost outcrops of the Gran Paradiso massif, a few metres below the Triassic uncomformity, they form decimetre-thick layers intercalated within the upper Bonneval gneisses. The latter may represent a Late Paleozoic volcanosedimentary cover (Bertrand, 1968), whose lithology and exclusively Alpine metamorphic overprint distinguish it from the previously mentioned series. In the Schistes lustrés, a metaradiolarite layer grades, in the vicinity of a metabasaltic sill (?), into interbedded, decimetre-thick layers of chloritoid-bearing chlorite schists and crossite–chloritoid quartzite, the latter containing talc and phengite (7-230).

Furthermore, talc and phengite have also been observed in highly oxidized, manganiferous rocks. These are a piemontite-bearing quartzite (6-255) from a manganese deposit situated in the above-mentioned metaradiolarite layer (cf. Chopin, 1978), and a piemontite-, hematite-, braunite- and barytes-bearing layer of a dolomitic marble (6-242) from the Gran Paradiso autochthonous Mesozoic cover.

Four wet-chemical analyses compiled in table 1 are intended to reflect compositional variations between the talc or chlorite schists (7-37, GP18) and the blue-amphibole-bearing quartzitic schists (7-172, 7-230). Striking common features are the low calcium and alkali contents, and the high magnesium and iron contents with Mg/Mg + Mn + Fe ratios between 0·6 and 0·8. The high H_2O values reflect

TABLE 1

Bulk rock composition of four talc–phengite–chloritoid-bearing samples

	7-37	*GP 18*	*7-172*	*7-230*
SiO_2	43·71	32·36	51·06	70·74
Al_2O_3	24·17	22·32	15·51	9·66
FeO_{total}	7·08	11·24	12·18	8·75
MnO	0·06	0·09	0·11	0·07
MgO	14·67	23·07	10·38	6·11
CaO	0·21	0·11	0·10	0·07
Na_2O	0·16	0·08	1·31	0·08
K_2O	2·64	0·25	0·46	0·31
TiO_2	0·34	0·06	0·31	0·21
P_2O_5	0·29	0·16	traces	0·04
H_2O	6·06	10·13	5·09	2·94
TOTAL	99·71	99·87	99·51	98·98
M	0·79	0·78	0·63	0·64

7-37: Talc–phengite–chloritoid schist. Gran Paradiso basement. Western slope of Mont Séti, about 2800 m in altitude, Bonneval/Arc, France.

GP 18: Chloritoid–chlorite schist. Gran Paradiso basement. Southwestern slope of the Pointe des Eaux Rousses, about 2850 m in altitude. Vallone di Bardonney, Cogne, Italy.

7-172: Galucophane–chloritoid–garnet schist. Gran Paradiso basement. Lécharenne, about 2200 m in altitude, Bonneval/Arc.

7-230: Chloridoid–magnetite–quartzite. Lower Schistes lustrés unit. Le Mollard, about 2100 m in altitude, Bessans, France.

M = Mg/Mg + Fe + Mn after removal of the blue amphibole component in 7-172 and 7-230, and of 20 per cent of the total iron which are assumed to be present as magnetite in 7-230.

Analysts: N. Picot and A. Bérard-Nétillard.

high modal proportions of phyllosilicates and chloritoid. The silica content is quite variable-GP18 is almost quartz-free—but the relative amounts of the other main components show little variation, as evidenced by an 'AKF' projection (Fig. 5). The precursor mineralogy of all these rocks may be expressed as a mixture of chlorite and some illite (±quartz, ±albite), pointing out a basic similarity. Thus, with the possible exception of the manganiferous samples 6-242 and 6-255, the talc–phengite-bearing rocks may be referred to as pelitic in composition, with low alkali contents.

PETROGRAPHY AND MINERAL CHEMISTRY

Textural relationships unambiguously show that both talc and phengite are part of the primary, high-pressure assemblages. In the chloritoid-bearing samples, both phyllosilicates belong to the main rock-forming minerals and the talc–phengite assemblage is most often magnificently developed. In the dolomitic marble 6-242, phlogopite and phengite are abundant, talc extremely rare and quartz absent. A phlogopite crystal has been observed 'sandwiched' between a talc and a phengite flake; the three minerals are in textural equilibrium but talc could not be observed in contact with phengite. In the manganiferous quartzite 6-255, talc occurs mostly in the piemontite- and spessartine-bearing, phengite-free layers, but could also be

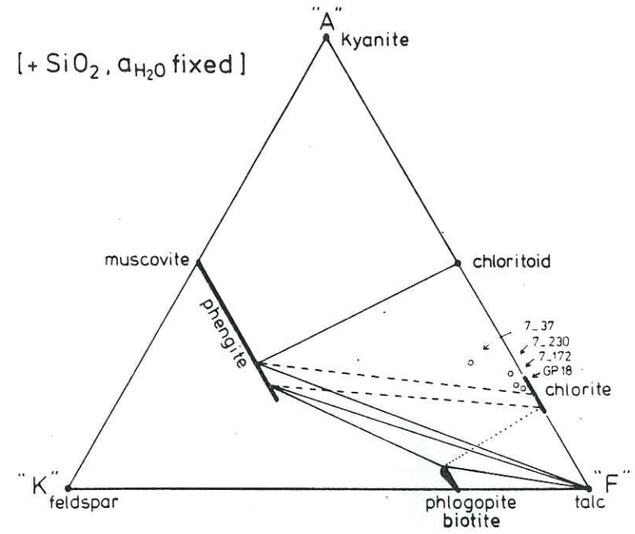

FIG. 5. Rock composition and mineral assemblages. For the rock compositions the projection is made onto the Al_2O_3–(K,Na)AlO_2–(Fe_{total},Mg,Mn)O plane from the H_2O, quartz, rutile, apatite and, if any, blue amphibole apices (using the blue amphibole microprobe analyses), except for 7-230 for which 20 per cent of the total iron has been assumed to be present in magnetite and removed. Mineral assemblages have been drawn using the analyses of Table 3 with $A = (Al,Fe^{3+})_2O_3$, $K = (K,Na)AlO_2$ and $F = (Mg,Fe^{2+},Mn,Co,Ni,Zn)O$, in order to show the main compositional variations between the two paragenetic types distinguished in the text. For ferromagnesian compositions the talc–phengite–chloritoid assemblage has been observed (with or without chlorite, depending upon the bulk Mg/Fe ratio) and the talc–phengite–biotite tie-lines are inferred. For the magnesian subsystem the talc–phengite and talc–phlogopite tie-lines have been observed, but chlorite–phlogopite as well (see text). The chlorite–phengite–kyanite assemblage may be inferred (Fig. 9*a*).

observed in contact with phengite in a phengite-rich layer along with hematite, some chlorite, and rare spessartine and phlogopite.

Talc and phengite have been observed in sharp contact (Figs. 6 and 7) in all the samples reported in Table 2. No reaction rim between them has yet been observed; however, the talc–phengite assemblage may be replaced along discrete shear zones by biotite (growing from phengite) and chlorite (within a finely granulated quartz ground-mass), as in 8-40. In this deformed sample as well as in 8-36, the high-pressure assemblage is conspicuously overprinted. This results in the general development of secondary chlorite, making it difficult to ascertain whether or not a primary chlorite has ever been present in the rock. Actually, the problem also arises for some far less retrograded samples, which have been reported together with 7-37 and GP18 in Table 2.

Mineral analyses

Representative microprobe analyses of coexisting phyllosilicates from talc and phengite-bearing rocks are compiled in Table 3.

Phengite micas. White micas are dioctahedral but deviate considerably from the muscovite end member by a nearly ideal $(Al,Fe^{3+})\ Al \rightleftharpoons (Mg,Fe^{2+})Si$ substitution.

TABLE 2

The talc–phengite-bearing parageneses

Sample number	*Origin*	*Quartz*	*Talc*	*Phengite*	*Chlorite*	*Phlogopite*	*Chloritoid*	*Margarite*	*Garnet*	*Glaucophane*	*Magnetite*	*Hematite*
8-27	GP	+	+	+			+					
7-37, 7-39, 8-28 / 8-29, 8-30, 8-32, 8-33 / 8-44, GP 15. GP 18	GP	+	+	+	+		+					
8-36, 8-40	GP	+	+	+	?		+		+			
GP 12	GP	+	+	+	+		+	(+)				
7-15, 7-172a, b, c	GP	+	+	+	+		+		+	+		
7-230	SL	+	+	+	+		+			+	+	
6-255	SL	+	+	+	+	+			+			+

Except margarite which occurs exclusively as inclusions in chloritoid, the minerals reported are in close association and in textural equilibrium. In any case talc and phengite have been observed in direct juxtaposition. Rutile and apatite are always additional phases. GP = Gran Paradiso basement, SL = lower Schistes lustrés unit.

They are thus typical phengites. The extent of their phengitic substitution is remarkably high, ranging from $Si_{3.4}$ to $Si_{3.6}$ for a 12 (O,OH) formula, but these are normal values for the primary phengites of the area. Likewise, the low sodium content in the phengites (even when coexisting with a sodic phase) is a common feature for the high-pressure assemblages of the area (cf. Chopin & Maluski, 1980).

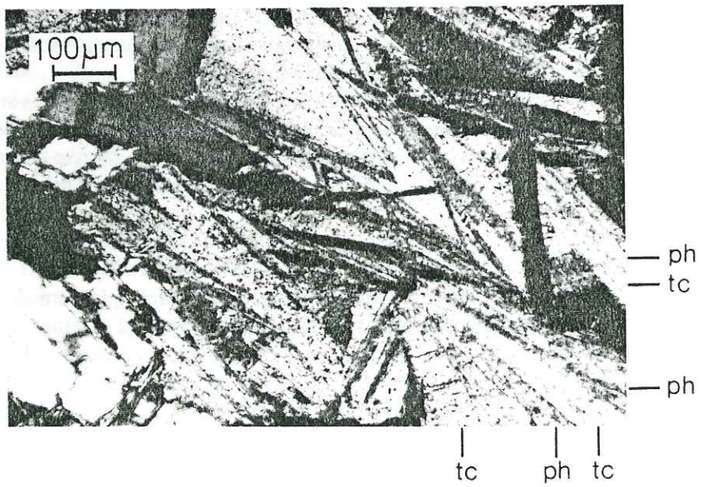

FIG. 6. Intimate intergrowth of talc (tc) and phengite (ph). Talc is seen as the lighest-coloured flakes, phengite as the darker ones. Sample 7-37; crossed nicols.

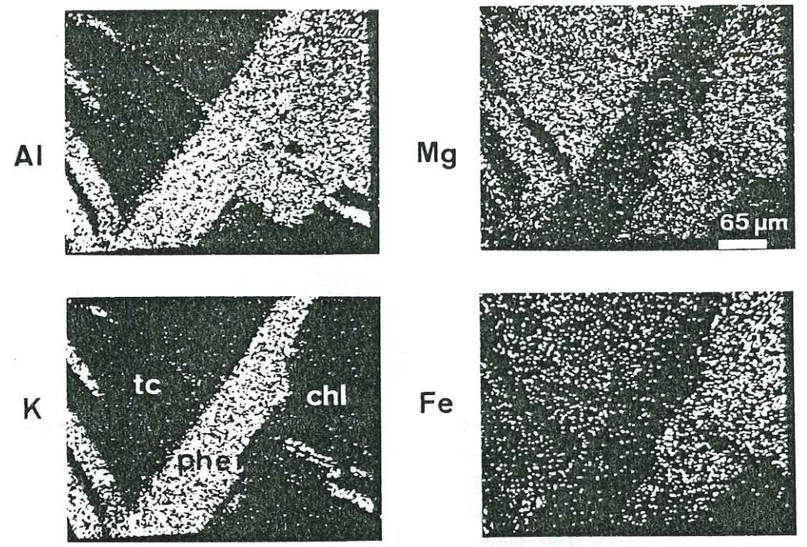

FIG. 7. Characteristic radiation pictures of a talc–phengite–chlorite–quartz assemblage in sample 7-172. Note the iron content of the talc.

Talc. Although analyses are close to the ideal formula $(Mg,Fe^{2+})_3Si_4O_{10}(OH)_2$, the noticeable percentages of Al_2O_3 (0·05–0·40 wt. per cent) remain to be explained. They are not linked with sodium incorporation as in Serbia (Abraham & Schreyer, 1976), in some 'white-schists' (Schreyer & Abraham, 1976) or in a Na-phlogopite-bearing assemblage (Schreyer *et al.*, 1980). Na_2O contents are insignificant, always less than 0·04 wt. per cent. Due to analytical uncertainty, the data do not allow further discrimination between two other possible substitutions: 3 Mg ⇌ 2 Al toward pyrophyllite, or Mg Si ⇌ Al Al. Actually, the most remarkable feature of these analyses is the relatively high percentage of iron, except in the most oxidized assemblages 6-255 and 6-242 where talc is typically iron-free, thus supporting the assumption of a divalent state made for the other assemblages. This leads to molar contents of minnesotaite, $Fe_3Si_4O_{10}(OH)_2$, as high as 15 per cent, which vary with the estimated FeO content of the coexisting phengite. However, considering the uncertainty of the oxidation state of iron and the small iron percentages in phengite, Fe^{2+}/Mg partitioning between the two minerals will not be further considered here. In 6-255, Ni, Co and Zn have been detected in talc, as well as in chlorite and phlogopite, with individual oxide concentrations of about 0·2 wt. per cent. Nevertheless, the talc and chlorite analyses show reproducibly low oxide totals is this sample.

Chlorite. The analysed chlorites deviate from the ideal formula $R^{2+}_{5-x}R^{3+}_{1+x}Si_{3-x}Al_{1+x}O_{10(OH)8}$ by an excess of trivalent cations in the octahedral sites, the resulting charge excess being balanced by octahedral vacancies. This is a general feature for the chlorites of the area. In the less oxidized assemblages

TABLE 3

Chemical composition of coexisting phyllosilicates from various talc–phengite-bearing rocks

	Phengite					*Talc*			*Chlorite*				*Phlogopite*	
Sample	*GP 18*	*7-172*	*7-230*	*6-255*	*6-242*	*7-230*	*6-255*	*'90-99'*	*GP 18*	*7-172*	*7-230*	*6-255*	*6-255*	*6-242*
SiO_2	51·71	51·44	50·94	52·28	51·72	61·25	61·04	61·92	29·20	27·40	27·62	30·52	43·31	42·33
TiO_2	0·24	0·16	0·29	0·06		0·11	0·01	0·0	0·13	0·0	0·15	0·04	0·14	0·61
Al_2O_3	27·37	26·28	22·55	21·86	20·53	0·05	0·22	0·29	21·89	19·92	19·67	19·07	13·54	14·63
Fe_2O_3	0·53	0·77	2·47	3·81	3·21		0·0	0·0				0·55	1·19	1·96
FeO	0·47	0·69	2·23			8·16			10·78	17·04	16·80			
MnO		0·0	0·0	0·0	0·02	0·0	0·07	0·05		0·0	0·06	1·39	1·20	0·25
MgO	4·39	3·87	4·23	4·82	5·63	26·31	29·05	31·34	25·97	21·60	21·75	31·28	24·12	24·90
BaO					0·7			0·0						0·7
Na_2O	0·0	0·28	0·0	0·20	0·21								0·12	0·08
K_2O	10·50	10·56	10·45	10·99	10·85								9·20	9·89
TOTAL	95·21	93·97	93·16	94·02	95·35	95·88	'90·99'	93·60	87·97	85·96	86·05	'83·45'	'93·42'	92·87
Si	3·42	3·45	3·51	3·55	3·57	3·99	4·04	3·98	2·82	2·81	2·83	2·98	3·06	2·96
Al^{IV}	0·58	0·55	0·49	0·45	0·43	0·01		0·02	1·18	1·19	1·17	1·02	0·94	1·04
Al^{VI}	1·55	1·53	1·34	1·30	1·25		0·01		1·31	1·22	1·20	1·17	0·19	0·16
Fe^{3+}	0·03	0·04	0·13	0·20	0·16								0·06	0·10
Fe^{2+}	0·02	0·04	0·13			0·44			0·87	1·46	1·44			
Mn							0·01	0·01				0·11	0·07	0·02
Mg	0·43	0·39	0·43	0·49	0·58	2·56	2·86	3·00	3·74	3·30	3·32	4·55	2·54	2·59
Ti	0·01	0·01	0·01			0·01			0·01		0·01		0·01	0·03
Ba					0·02									0·02
Na		0·04		0·03	0·03								0·02	0·01
K	0·89	0·90	0·92	0·95	0·95								0·83	0·88
Σ cations	6·93	6·95	6·96	6·97	6·99	7·00	'6·95'	7·01	9·93	9·98	9·97	'9·92'	'7·75'	7·81

Analyses have been performed with a Cambridge Mark V microprobe, using a procedure detailed elsewhere (Chopin, 1978). Total iron is expressed as Fe_2O_3 in 6-255 and 6-242, which are hematite- and piemontite-bearing samples. The Fe^{3+}/Fe^{2+} ratio has been arbitrarily chosen in the other samples as 0 in chlorite and talc, as 1 in phengite. Oxide totals of talc, chlorite and phlogopite in 6-255 include 0·2 CoO, 0·2 NiO and 0·2 ZnO. Chemical formulae are calculated on the basis of 22 cation valences for talc, phengite and phlogopite, and of 28 cation valences for chlorite.

(GP18, 7-172) chlorite is by far the most iron-rich phyllosilicate (with respect to absolute iron content as well as to Fe/Mg atomic ratio; see Fig. 7), whereas in the more oxidized ones iron is more abundant in the phengite structure, presumably in the trivalent state. This effect is discernible in the magnetite-bearing sample 7-230 and becomes evident in the most oxidized samples 6-255 and 6-242 in which the highest iron content among the phyllosilicates is found in phengite. It shows that the $Al \rightleftharpoons Fe^{3+}$ substitution is quite limited in biotite and chlorite, at least for the most magnesian members. It may also be noted that the chlorite composition is less siliceous (and fairly constant in this respect) in chloritoid-bearing assemblages (GP18, 7-230, 7-172) than in the phlogopite-bearing one (6-255).

Phlogopite. Just as for the chlorites, phlogopites deviate from the ideal formula by an excess of trivalent cations in octahedral position, which leads to octahedral vacancies. In 6-255, it contains Ni, Co and Zn in amounts similar to those on talc and chlorite.

Other minerals. *Chloritoid* has an unusually high magnesium content in the study area. MgO/FeO substitution toward the magnesiochloritoid end member $Mg_2Al_4Si_2O_{10}(OH)_4$ reaches 50 mole per cent and ranges from 25 to 45 per cent in the talc–phengite-bearing parageneses. This exceptional feature, as well as the high iron content of talc, is related to the stability of the talc–chloritoid pair at high pressure (Chopin, 1979). The petrological significance of the latter assemblage is dealt with in a forthcoming paper in which the chemistry of both minerals, as well as the Fe/Mg partitioning between talc, chlorite and chloritoid, is thoroughly documented. *Garnet* is an almandine–pyrope solid solution with about 5 per cent of other end members in 7-172; it is spessartine (over 80 per cent end member) in 6-255. *Blue amphiboles* labelled as glaucophane in Table 2 are pure glaucophane–riebeckite solid solutions, namely magnesian crossite in 7-230 (about $Na_{1.95}Ca_{0.10}Mg_{2.15}Fe^{2+}_{0.75}Fe^{3+}_{0.80}Al_{1.22}Si_{7.96}O_{22}(OH)_2$ and ferrous glaucophane in 7-172 (about $Na_{1.96}Mg_{2.20}Fe^{2+}_{0.82}Fe^{3+}_{0.10}Al_{1.96}Si_{7.94}O_{22}(OH)_2$).

PETROLOGIC DISCUSSION

In the rocks investigated here, sodium, when present, is concentrated in the blue amphibole (cf. phengite chemistry). Apatite is most often the only calcium-bearing mineral, this element being otherwise incorporated either in margarite or as grossular component in the garnet. Thus, by neglecting these components and phases, one can treat the remaining mineral parageneses in the K_2O–FeO–MgO–Al_2O_3–SiO_2–H_2O (*KFMASH*) system. Fe_2O_3 and MnO are additional components which might have to be taken into account. Quartz is always present as an excess phase (Table 2), and water activity is assumed to be constant in the following discussion.

On paragenetic grounds the talc–phengite-bearing samples fall into two groups, those with chloritoid but no phlogopite and those without chloritoid, but with phlogopite (6-242, 6-255). This mineralogical difference is determined both by the alumina content and by the FeO/MgO ratio of the two rock types. The presence of FeO is, of course, a necessary condition for the appearance of chloritoid, and this is not fulfilled in the highly oxidized, phlogopite-bearing samples in which all the iron

is in the trivalent state. The contrast in FeO/MgO ratio between the two groups is also reflected in the mineral chemistry of talc and chlorite (Table 3). On the other hand, although no analyses of phlogopite-bearing samples are available, a talc–phengite-phlogopite (±chlorite) assemblage is generally less aluminous than talc–phengite–chloritoid assemblages. As shown in Fig. 5, the four analyses of chloritoid-bearing rocks do indeed plot on the Al-rich side of the phengite–chlorite tie-line. This difference in alumina-content is again reflected in the mineral chemistry, here of chlorite and phengite, regardless of the Fe/Mg ratio. Chlorite is rather siliceous ($Si_{3\cdot0}$) in the chloritoid-free, less aluminous assemblages (for example 6-255, but also in talc–chlorite marbles not discussed here where chlorite is very close to clinochlore in composition). On the other hand, the chlorite composition is buffered to a nearly constant $Si_{2\cdot8}$ value by the invariant assemblage talc–chloritoid–chlorite–quartz (Table 3). Similarly, the phengitic substitution is higher ($Si_{3\cdot5-3\cdot6}$) in the chloritoid-free samples than in the chloritoid-bearing ones ($Si_{3\cdot4-3\cdot5}$, Fig. 5 and Table 3).

The consequent distribution of tie-lines between analysed mineral pairs in the projection of Fig. 5 suggests that the K_2O–FeO–MgO–Al_2O_3 volume is subdivided into a sequence of three- and four-phase regions (with excess quartz and H_2O) which are characteristic for the metamorphic conditions endured. In the following discussion these characteristic three- and four-phase assemblages in the iron-bearing system are identified. However, the difficulty arises that the observed tie-lines are either in the ferromagnesian and relatively Al-rich part of the system (chloritoid-bearing samples), or in its FeO-free and Al-poor part (phlogopite-bearing samples). Thus, for the other parts of the system the relevant tie-lines must be inferred. Because of the chemical limitation imposed by sampling, and for the sake of clarity, the following discussion will be subdivided into

(i) *the chloritoid-free rocks*, which represent a close approximation to the purely magnesian subsystem (*KMASH*). Because of the presence of Mn^{3+} (in piemontite and braunite) they are virtually FeO-free, and the additional component Fe_2O_3 is essentially present as hematite. The samples concerned are 6-242 and 6-255.

(ii) *the chloritoid-bearing rocks*, which can only be dealt with in the general *KFMASH* system. Most of the samples are of this type, with the talc-phengite-chloritoid assemblage representing up to 90 per cent of the rock (e.g. 7-37).

Chloritoid-free rocks and relevant phase relations in the system K_2O–MgO–Al_2O_3–SiO_2–H_2O

The piemontite-bearing quartzite 6-255 is very similar to the Serbian sample from which Abraham & Schreyer (1976) first described talc–phengite. Both rocks contain the same minerals (quartz, piemontite, spessartine, hematite, braunite and the four phyllosilicates talc, phengite, chlorite and phlogopite) and they show almost identical compositions for talc, phlogopite and chlorite, as well as similar compositional variations in piemontite (Schreyer *et al.*, 1975: Chopin, 1978). In addition, in both samples Ni and Co are preferentially incorporated into talc, chlorite and phlogopite, and Fe^{3+} into phengite. However, there are significant

differences in phengite composition. In the Alpine sample the white mica is more phengitic ($Si_{3\cdot5}$ *vs.* $Si_{3\cdot3}$) and contains less paragonite component (4 per cent *vs.* 10 per cent for the maximal values), thus pointing to a higher pressure and lower temperature of formation (cf. Velde, 1967; Chatterjee & Froese, 1975). Another important difference is that in 6-255, both the talc–phengite and phlogopite–chlorite–quartz assemblages have been observed less than one millemetre apart within the same layer. The two assemblages are incompatible in the pure magnesian system (Fig. 1); they should thus represent either a reaction assemblage or one of them should be secondary, but textural evidence is inconclusive in this respect. In fact, in each assemblage one of the phases (talc and phlogopite, respectively) appears to be poorly crystallized. At any rate, the presence of additional components such as NiO, ZnO, MnO, etc. in the natural system makes the coexistence of these assemblages possible, as far as the phase rule is concerned. MnO, for example, is strongly partitioned into chlorite and phlogopite (Table 3), and is likely, in the absence of direct contact between spressartine and talc–phengite, to stabilize that pair, talc–phengite then being the stable tie-line in the *KMASH* system. Unfortunately, the latter minerals could not be observed in contact in the other chloritoid-free rock 6-242. Therefore, as long as more decisive evidence is lacking, it remains difficult to establish the phase relations in the model system *KMASH* for the Gran Paradiso area from these rocks.

Nevertheless, the high Si contents encountered in the phengites allow some theoretical considerations regarding the low-pressure stability limit of talc–phengite in the purely magnesian system. After the chemographic analysis developed by Abraham & Schreyer (1976) this limit is given by the hydration reaction

$$\text{talc} + \text{`muscovite'} + H_2O \rightarrow \text{phlogopite} + \text{chlorite} + \text{quartz} \qquad (6)$$

which is generated by the intersection of reaction curves (3) and (4) at the new invariant point (Fig. 3). The slope of this curve should be negative, in order to have the hydrated products on the low-temperature side. As pointed out by these authors, the dioctahedral mica involved in this P–T range is in fact not muscovite but a phengite, the phengitic substitution of which should vary along the reaction curve, namely increase toward lower temperatures (i.e. higher pressures), according to Velde (1965, 1967). But it seems that an important point has been overlooked. With increasing phengitic substitution, the amount of consumed water diminishes and the breakdown of phengite plus talc evolves into a dehydration reaction, as shown by the two end-member reactions

$$3KAl_3Si_3O_{10}(OH)_2 + 8Mg_3Si_4O_{10}(OH)_2 + 4H_2O \rightarrow$$
$$\text{muscovite} \qquad \text{talc}$$
$$3KMg_3Si_3AlO_{10}(OH)_2 + 3Mg_5Al_2Si_3O_{10}(OH)_8 + 23SiO_2$$
$$\text{phlogopite} \qquad \text{clinochlore} \qquad \text{quartz}$$

$$3KAlMgSi_4O_{10}(OH)_2 + 2Mg_3Si_4O_{10}(OH)_2 \rightarrow$$
$$\text{Al-Mg-celadonite} \qquad \text{talc}$$
$$3KMg_3Si_3AlO_{10}(OH)_2 + 11SiO_2 + 2H_2O$$
$$\text{phlogopite} \qquad \text{quartz}$$

For chlorite of clinochlore composition, reaction (6) releases water for phengites having Si $\geqslant 3{\cdot}67$, but with more aluminous chlorites this happens for even lower Si contents, for example between 3·5 and 3·6 for chlorite with $Si_{2{\cdot}8}$. At any rate, the slope of reaction (6) should steadily increase and then become positive with decreasing temperatures. This could allow the stability of talc–phengite at low temperature for pressure values which would not have to be exceedingly high. Experimental studies on these problems are being conducted by H. J. Massonne at Bochum.

Microprobe analyses on Alpine phengites indicate that very high Si contents have indeed been attained during metamorphism. Brown *et al.* (1978) described a $Si_{3.7}$-phengite from the Schistes lustrés on the northern slope of the Gran Paradiso massif in a phlogopite–K–feldspar–quartz assemblage which makes this Si content a maximum value at given P and T. The same $Si_{3.7}$ value has been encountered on the western slope of the Gran Paradiso massif (same outcrop as 6-242; Saliot, 1978) and further south (Monte Viso area; J. R. Kiénast, pers. comm. 1979). These values very probably apply to the early stage of the metamorphic evolution, to which the talc–phengite assemblages are attributed in this paper. However, no coexisting talc has been reported for the $Si_{3.7}$-phengites mentioned. This maybe due to the fact that the phengite coexisting with talc cannot exhibit the maximum Si content for a given P and T (Fig. 5).

Chloritoid-bearing rocks and phase relations in the system K_2O–FeO–MgO–Al_2O_3–SiO_2–H_2O

As previously stated, the samples are essentially composed of talc, phengite and chloritoid (±chlorite, ±garnet; see Table 2), which is a doubly extraordinary assemblage. In addition to the talc–phengite pair discussed here, the even more striking petrological feature of these rocks is the coexistence of talc with chloritoid (±garnet). Its significance is only outlined here, whereas a detailed treatment follows in a subsequent paper. The talc–chloritoid (±garnet) coexistence results from the progressive breakdown, with increasing pressure and temperature, of ferromagnesian chlorites in the presence of quartz, as expressed by the divariant reactions

$$\text{Fe-Mg-chlorite} + \text{quartz} \rightarrow \text{talc} + \text{garnet} + H_2O \qquad (7)$$

and, for less iron-rich compositions,

$$\text{Fe-Mg-chlorite} + \text{quartz} \rightarrow \text{talc} + \text{chloritoid} + H_2O \qquad (8)$$

In the FeO–MgO–Al_2O_3–SiO_2–H_2O (*FMASH*) system, only chlorites with higher Mg/Fe ratios than the talc–chloritoid join may still coexist with quartz. Accordingly, stables assemblages with excess quartz are, among others and in order of increasing Mg/Fe ratio, talc–garnet–chloritoid, talc–chloritoid, talc–chloritoid–chlorite and talc–chlorite (Fig. 8). Evidently, the talc–kyanite pair is not stable under these conditions.

The disappearance of chlorite + quartz for the low and moderate values of the Mg/Fe ratio results in decisive topological changes in the *KFMASH* system,

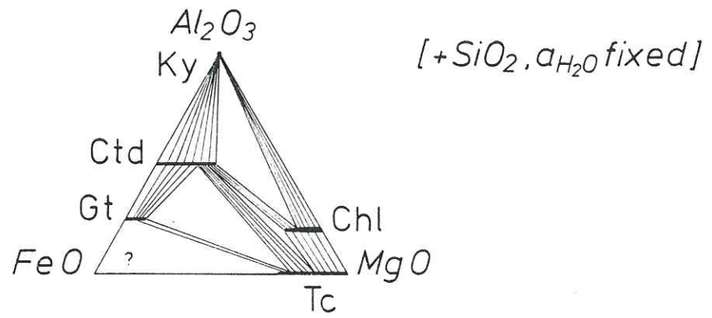

FIG. 8. Phase relations in the FeO–MgO–Al_2O_3–SiO_2–H_2O system as deduced from relevant assemblages in the Gran Paradiso area. The characteristic feature is the existence of a three-phase assemblage talc–chloritoid–magnesian chlorite (+quartz) and the related stability of the talc–chloritoid and talc–garnet tie lines of iron-rich chlorite + quartz. The two- and three-phase assemblages containing talc have all been observed and analysed by the author; the kyanite-bearing assemblages are inferred from the reports of Compagnoni & Lombardo (1974). Chl = chlorite, Ctd = chloritoid, Gt = garnet, Ky = kyanite, Tc = talc.

especially at the low temperatures considered here for which neither the biotite–kyanite nor the biotite–chloritoid pairs are stable. Indeed, the related disappearance of the biotite–Fe–Mg-chlorite join in the presence of quartz makes the coexistence of phengite with talc (±garnet, or chloritoid, or Mg-chlorite) a requirement (Fig. 9a, also Fig. 5). Clearly the chlorite–biotite–quartz assemblage disappears at lower grade in the ferromagnesian systems than in the purely magnesian one, since reaction (7) and (8), and then reaction (9)

$$\text{Fe-Mg-chlorite} + \text{biotite} + \text{quartz} \rightarrow \text{talc} + \text{phengite} + H_2O, \qquad (9)$$

proceed toward magnesium-richer compositions with increasing grade.

Whether or not phlogopite–chlorite–quartz is stable into the magnesian subsystem still remains, as previously stated, a problem as far as the Gran Paradiso area is concerned. However, the talc–kyanite–chloritoid assemblage has been recorded here and there in the same Schistes lustrés unit as the one investigated here, but 50 to 70 km further northeast, in the vicinity of the Monte Rosa massif (from the Allalinhorn, Chinner & Dixon, 1973; from the Valtournanche, Kiénast, 1976, pers comm. 1978). Under these conditions any chlorite is incompatible with quartz and the stability of talc–phengite in place of phlogopite–chlorite–quartz becomes a topological requirement even in the pure magnesian system (Figs. 3 and 9a). The northwestern Alps thus possibly exemplify the successive steps of the talc–phengite appearance which is first limited to the ferromagnesian systems (Gran Paradiso area?) and then extends to the magnesian subsystem with increasing grade (Zermatt area; Fig. 9). A possible cause in the latter area might be that water pressure was locally less than total pressure, but the paragenetic sequence derived still remains unaffected.

The progressive stabilization of the talc–phengite assemblage appears to be closely related to the progressive breakdown of chlorite + quartz into talc + garnet, talc + chloritoid, and talc + kyanite, a basic novel feature of the FMASH system

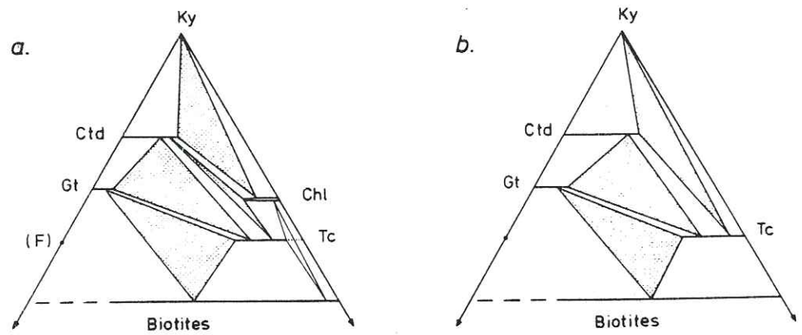

FIG. 9. Thompson's projection illustrating the phase relations as revealed by petrographic and microanalytical work in (a) the Gran Paradiso area (Chopin, 1979), (b) the 'whiteschist' assemblages of the Zermatt area (Chinner & Dixon, 1973; Kiénast, pers. comm.) or of the Hohe Tauern, Eastern Alps (Miller, 1977). (b) represents the higher metamorphic grade and is related to (a) by the development of reactions (8), (4) and possibly (9) among others (see text). Whether chlorite and phlogopite (+quartz) coexist in the Gran Paradiso area is yet questionable (the hypothetical talc–chlorite–phlogopite field has been broadened for the clarity of the picture, which leads to rather unrealistic Fe/Mg partitioning between talc and chlorite and talc and phlogopite). In (a) and (b) the talc–garnet–biotite–'muscovite'–quartz field is inferred from the observation in the Gran Paradiso area of the talc–garnet–quartz, talc–garnet–chloritoid–phengite–quartz and biotite–garnet–phengite–quartz assemblages. Same symbols as in Fig. 8.

which is an essentially pressure-determined process (Chopin, 1979, 1981; Schreyer, 1968, for the magnesian subsystem). This clearly points out the high-pressure character and origin of the talc–phengite assemblage and thus brings the definite support of field evidence to the theoretical and experimental work of Abraham & Schreyer (1976) and of Schreyer & Baller (1977). Chernosky's construction (1978) is not applicable.

CONSEQUENCES: THE HIGH-PRESSURE EVOLUTION OF PELITIC ROCKS

The lower stability limit and first appearance of the talc–phengite assemblage are still a field problem. In this respect the existence of primary biotite–chlorite–quartz assemblages in more external, lower-grade parts of the Alpine chain seems to be a theoretical necessity (Fig. 3). However, in the Western Alps as in other blueschist terranes, this mineral association is exceedingly rare in the metapelites, thus contrasting with its widespread occurrence in the low-grade metapelites for other types of metamorphism. Actually, this does not imply any restriction of the biotite stability field to lower pressure but results from a mere compositional effect. Usual pelitic compositions may be expressed as a mixture of quartz, chlorite and illite, where illite approaches a $Si_{3.5}$-phengite in composition (Fig. 10). In low-pressure metamorphism these rock compositions crystallize into a chlorite-biotite–phengite–quartz assemblage as a result of the limited silica content of the phengite. At high pressure these rock compositions may directly crystallize into chlorite–phengite–quartz owing to the high value of the phengite substitution; biotite occurrence is then restricted to quite alumina-poor compositions (Fig. 10). Such a compositional effect has been well-documented by Mather (1970) in the Dalradian of Scotland,

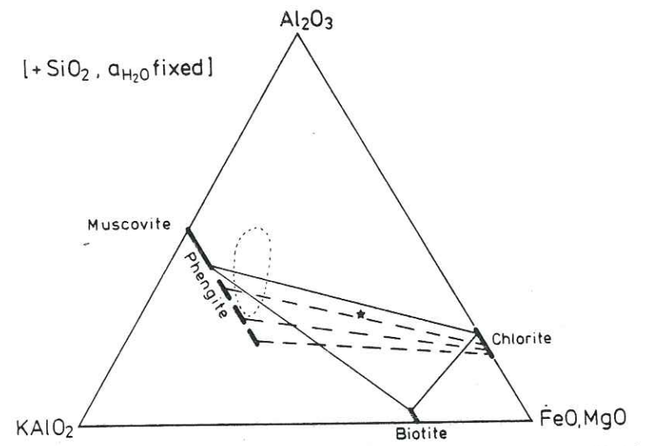

FIG. 10. Projection of the K_2O–MgO–FeO–Al_2O_3–SiO_2–H_2O system illustrating in a simplified fashion the control of biotite appearance in pelitic rocks by the extent of phengitic substituion in the white mica. Solid tie-lines: stable assemblage in low-grade, low-pressure metapelites. Dashed tie-lines: stable assemblage at high pressure, before the beginning of chlorite + quartz breakdown. The star denotes a mean pelitic composition (e.g. Poldervaart, 1955). The illite field is outlined (after Weaver & Pollard, 1973) in order to visualize the possible precursor mineralogy, namely chlorite + illite + quartz.

for example, but the higher pressures involved in the Alps make it much more pronounced: the 'biotite in' isograd is not only delayed but absent in the metapelitic rocks except for the most iron-rich ones (see below).

According to this deduction and the preceding phase relationship analysis, a paragenetic sequence for the high-pressure metamorphism of pelitic rocks with intermediate Mg/Fe ratios may be outlined as follows (Fig. 11):

(1) chlorite–illite–quartz
(2) chlorite–phengite–quartz
(3) talc–chloritoid–phengite ± quartz

The thus far exceptional talc–phengite assemblage, therefore, appears to be in fact the normal and necessary product of the high-pressure evolution in the pelitic system. It becomes a regionally characteristic association for a type of metamorphism which might be labelled 'high-grade blueschist' or even 'high-temperature blueschist'. Indeed, typical low-temperature blueschists as encountered in California or in Queyras (southwestern Alps) are characterized by the ubiquitous occurrence of lawsonite, of jadeite + quartz, the absence of chloritoid and the coexistence of any chlorite with quartz. The area investigated here, although being a blueschist terrane, is basically different. It underwent a metamorphic evolution at pressures at least as high, but at higher temperatures, possibly 400–500 °C as against 250–350° in the former case. According to the preceding analysis, a definition of high-grade blueschists by the presence of talc–chloritoid then implies the talc–phengite stability.

Such high-grade blueschists are thus far known in the northwestern Alps

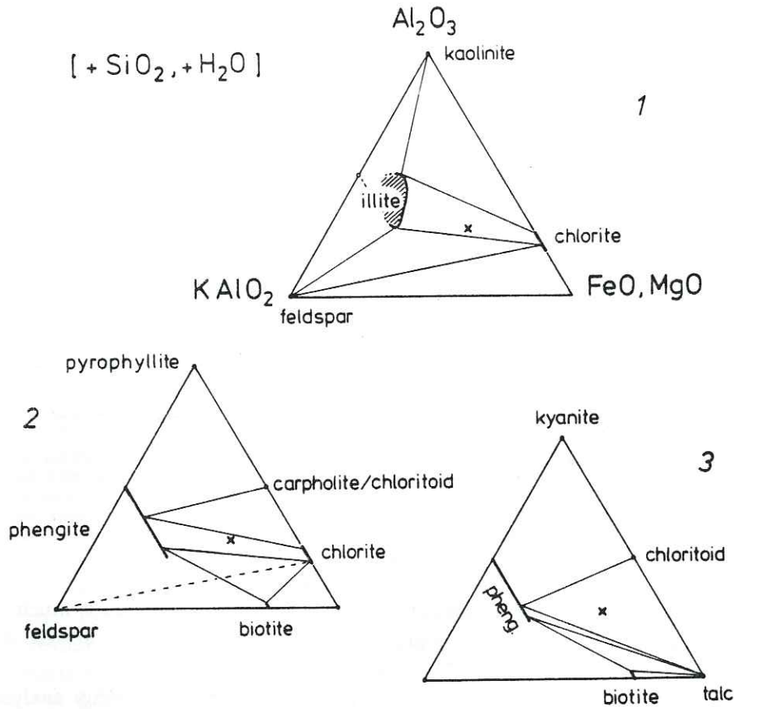

FIG. 11. The high-pressure metamorphic evolution of pelitic rocks with intermediate Mg/Fe ratios. The cross represents a mean pelitic composition. (1) Diagenetic stage: illite–chlorite–quartz. (2) Low-grade blueschist: phengite–chlorite–quartz. (3) High-grade blueschist: phengite–talc–chloritoid ± quartz. The carpholite referred to in stage 2 is a Fe-Mg-carpholite.

and the Eastern Alps (Hohe Tauern), and talc–phengite might indeed be a common assemblage there. Bearth (1963, 1967) reports numerous talc and phengite-bearing rocks from the Zermatt zone, but without specifying the textural relationships. However, a reconnaissance made together with J. R. Kiénast in the southern part of this zone, near Saint-Marcel in the Val d'Aoste, confirmed that talc and phengite are indeed present there in direct contact, in the same chloritoid-bearing assemblages as in the Gran Paradiso area. This occurrence is denoted by the northernmost star in Fig. 4. In the Eastern Alps, Miller (1974), Abraham *et al.* (1974) and Holland (1979) also record talc and phengite-bearing rocks without further textural indication about the two minerals. Nevertheless, the talc–kyanite–chloritoid coexistence is a petrological feature there, which leaves no doubt about the stability of talc–phengite. In effect, it seems that the talc–phengite assemblage simply needs to be searched for in talc–chloritoid-bearing terranes in order to be found, and there is no doubt in the author's mind that it will be reported in these terranes (including the Sesia zone) in the near future.

However, the search in the field also leads back to the problem of the lower

stability and first appearance of the assemblage talc–phengite. Can this pair be found in regions where neither talc–chloritoid nor talc–garnet are stable? Let us consider the two divariant key-reactions in the *KFMASH* system at high pressure

$$\text{chlorite} + \text{biotite} + \text{quartz} \rightarrow \text{talc} + \text{phengite} + H_2O \quad (9)$$

$$\text{chlorite} + \text{quartz} \rightarrow \text{talc} + \text{chloritoid} + H_2O \quad (8)$$

In the latter reaction garnet may replace chloritoid for iron-rich compositions. A topological requirement is that, for a given Mg/Fe ratio of the system, reaction (9) must have already proceeded when reaction (8) proceeds. The present field-investigations confirm this but do not indicate how the two reactions interrelate with varying pressure, temperature, and especially Mg/Fe ratio, i.e. what the relative position of the reaction loops is in, for example, isobaric T–X_{Mg} and isothermal P–X_{Mg} sections. Under certain P–T conditions is it conceivable that reaction (9) goes to completion (i.e. reaches the magnesian subsystem) before reaction (8) becomes effective in the ferromagnesian system. This would indeed allow a broad talc–phengite stability field in which neither talc–kyanite nor talc–chloritoid (±garnet) are stable. The isolated reports of Saliot (1978) and Abraham & Schreyer (1976) might be indications in this direction. In order to shed some new light on this problem a desirable step would be a systematic investigation of alumina-poor rocks in the lower-grade, external part of the Alpine chain, and elsewhere.

Finally, a few words should be said about the upper stability limit of the talc–phengite pair. The garnet–biotite–phengite–quartz assemblage is of common occurrence in the Gran Paradiso basement. The talc–phengite stability is therefore very probably limited on the iron-rich side (Fig. 9) by the divariant reaction

$$\text{talc} + \text{phengite} \rightarrow \text{garnet} + \text{biotite} + \text{quartz} + H_2O$$

which, with increasing grade, can be expected to proceed with increasing Mg/Fe ratio. With further increase of grade along the same metamorphic gradient, one may speculate about the disappearance of talc–phengite–garnet resulting in the new biotite–chloritoid (+quartz) tie-line. However, the critical assemblage biotite–chloritoid–talc–quartz has, to the author's knowledge, never been reported, even in the highest-grade blueschists (Hohe Tauern).

In general, it is hoped that this paper will arouse new interest in the phyllosilicate assemblages of high-pressure, low-temperature metamorphic areas, in order to fill in existing gaps and missing details in the overall mineralogical evolution of this type of metamorphism which is so important for our understanding of subduction mechanisms.

ACKNOWLEDGEMENTS

This paper forms part of a Thèse de troisième cycle prepared in Paris under the guidance of G. Guitard, P. Saliot and J. R. Kiénast. The manuscript has been completed in Bochum during the tenure of a fellowship from the Deutscher Akademischer Austauschdienst, and has benefited from discussions with, and suggestions by W. Schreyer, W. V. Maresch and H. J. Massonne. Helpful criticism

from M. Frey and B. Velde is also gratefully acknowledged, as well as field introduction by R. Compagnoni to the northern Gran Paradiso massif.

REFERENCES

ABRAHAM, K., HÖRMANN, P. K. & RAITH, M., 1974. Progressive metamorphism of basic rocks from the southern Hohe Tauern area, Tyrol (Austria). *Neues. Jb. Miner. Abh.* **122**, 1–35.

—— & SCHREYER, W., 1976. A talc–phengite assemblage in piemontite schist from Brezovica, Serbia, Yugoslavia. *J. Petrology*, **17**, 421–39.

BEARTH, P., 1952. Geologie und Petrographie des Monte Rosa. *Beitr. Geol. Karte Schweiz*, **N.F. 96**, 1–94.

—— 1963. Chloritoid und Paragonit aus der Opiolith-Zone von Zermatt–Saas Fee. *Schweiz. miner. petrogr. Mitt.* **43**, 269–86.

—— 1967. Die Opiolith-Zone von Zermatt–Saas Fee. *Beitr. geol. Karte Schweiz*, **N.F. 132**, 1–130.

BERTRAND, J. M. L., 1968. Etude structurale du versant occidental du massif du Grand Paradis (Alpes Graies). *Géologie Alpine*, **44**, 55–87.

BIRD, G. W., & FAWCETT, J. J., 1973. Stability relations of Mg-chlorite, muscovite and quartz between 5 and 10 kb water pressure. *J. Petrology*, **14**, 415–28.

BROWN, P., ESSENE, E. J., & PEACOR, D. R., 1978. The mineralogy and petrology of manganese-rich rocks from Saint-Marcel, Piémont, Italy. *Contr. Miner. Petrol.* **67**, 227–32.

CABY, R., KIENAST, J. R., & SALIOT, P., 1978. Structure, métamorphisme et modèle d'évolution tectonique des Alpes occidentales. *Rev. Géogr. phys. Géol. dyn.*, **20**, 307–22.

CHATTERJEE, N. D., & FROESE, E., 1975. A thermodynamic study of the pseudobinary join muscovite–paragonite in the system $KAlSi_3O_8$–$NaAlSi_3O_8$–Al_2O_3–SiO_2–H_2O. *Am. Min.* **60**, 985–93.

CHERNOSKY, J. V., 1978. The stability of chlinochlore + quartz at low pressure. *Ibid.* **63**, 73–82.

CHINNER, G. A., & DIXON, J. E., 1973. Some high-pressure parageneses of the Allalin gabbro, Valais, Switzerland. *J. Petrology*, **14**, 185–202.

CHOPIN, C., 1977. Une paragenèse à margarite en domaine métamorphique de haute pression–basse température (massif du Grand Paradis, Alpes françaises). *C.R. Acad. Sci. Paris*, **D 285**, 1383–6.

—— 1978. Les paragenèses réduites ou oxydées de concentrations manganésifères des "schistes lustrés" de Haute Maurienne (Alpes françaises). *Bull. Minéral.* **101**, 514–31.

—— 1979. De la Vanoise au massif du Grand Paradis. *Thèse 3ème cycle, Université Pierre et Marie Curie, Paris* 6.

—— 1981. Talkführende Hochdruckparagenesen aus den Westalpen. *Fortschr. Miner.* **59**, Beih. 1, 30.

—— & MALUSKI, H., 1978. Résultats préliminaires obtenus par la méthode de datation ^{39}Ar–^{40}Ar sur des minéraux alpins du massif du Grand Paradis et de son enveloppe. *Bull. soc. géol. France*, **20**, 745–9.

—— —— 1980. ^{39}Ar–^{40}Ar dating of high-pressure metamorphic micas from the Gran Paradiso area (Western Alps): evidence against the blocking temperature concept. *Contr. Miner. Petrol* **74**, 109–22.

COMPAGNONI, R. & LOMBARDO, B., 1974. The Alpine age of the Gran Paradiso eclogite. *Soc. Ital. Mineral. Petrol.* XXX, 223–37.

DAL PIAZ, G. V., & ERNST, W. G., 1978. Areal geology and petrology of eclogites and associated metabasites of the Piemonte ogphiolite nappe. Breuil-St. Jacques area, Italian Western Alps. *Tectonophysics*, **51**, 99–126.

DEBELMAS, J., & LEMOINE, M., 1970. The Western Alps: paleogeography and structure. *Earth Sci. Rev.* **6**, 221–56.

DEBELMAS, J., & COLL., 1980. Alpes, bassin rhodanien, Provence et Corse. In: *Géologie des pays européens: France, Belgique, Luxembourg.* Paris: Dunod, 263–352.

DESMONS, J., 1977. Mineralogical and petrological investigations of Alpine metamorphism in the internal French Western Alps. *Am. J. Sci.* **277**, 1045–66.

FAWCETT, J. J., & YODER, H. S., 1966. Phase relationships of chlorites in the system MgO–Al_2O_3–SiO_2–H_2O. *Am. Miner.* **51**, 353–80.

FREY, M., HUNZIKER, J. C., FRANK, W., BOCQUET, J., DAL PIAZ, G. V., JÄGER, E., & NIGGLI, E., 1974. Alpine metamorphism in the Alps, a review. *Schweiz. miner. petrogr. Mitt.* **54**, 247–91.

FÜCHTBAUER, H., & GOLDSCHMIDT, H., 1959. Die Tonminerale der Zechsteinformation. *Beitr. Mineral. Petrol.* **6**, 320–45.

GUITARD, G., 1973. Sur la genèse des gisements métasomatiques de talc et de chlorite des Pyrénés et sur les relations entre le talc et la magnésite, In: *Colloque scientifique international E. Raguin.* Paris: Masson, 369–96.

HOLLAND, T. J. B., 1979. High water activities in the generation of high-pressure kyanite eclogites of the Tauern Window, Austria. *J. Geol.* **87**, 1–27.

HUNZIKER, J. C., 1974. Rb–Sr and K–Ar age determinations and the Alpine tectonic history of the Western Alps. *Mem. 1st. geol. min. Univ. Padova*, **31**, 1–55.

KIENAST, J. R., 1973. Sur l'existence de deux séries différentesde l'ensemble "Schistes lustrés–ophiolites" du Val d'Aoste; quelques arguments fondés sur l'étude des roches métamorphiques. *C.R. Acad. Sci. Paris*, **D 276**, 2621–4.

—— 1976. Etude des paragenèses magmatiques reliques, et métamorphiques d'un gabbro lié à la série ophiolitique inférieure du Val d'Aoste (Alpes italiennes). *4ème réunion annuelle des Sciences de la Terre, Paris*, (abstract). 241.

MASSONNE, H. J., 1981. Phengite: eine experimentelle Untersuchung ihres Druck-Temperatur-Verhaltens im System K_2O–MgO–Al_2O_3–SiO_2–H_2O. *Dissertation, Ruhr-Universität Bochum.*

MATHER, J. D., 1970. The biotite isograd and the lower greenschist facies in the Dalradian rocks of Scotland. *J. Petrology*, **11**, 253–75.

MILLER, C., 1974. On the metamorphism of the eclogites and high-grade blueschists from the Penninic terrane of the Tauern Window, Austria. *Schweiz. miner. petrogr. Mitt.* **54**, 371–84.

—— 1977. Chemismus und phasenpetrologische Untersuchungen der Gesteine aus der Eklogitzone des Tauernfensterns, Österreich. *Tschermaks miner. petrogr. Mitt.* **24**, 221–77.

PERTHUISOT, V., 1978. Dynamique et pétrogenèse des extrusions triasiques en Tunisie septentrionale. Thèse d'Etat, Paris, *Trav. Lab. Géol. E.N.S.* **12**, 312 pp.

POLDERVAART, A., 1955. Chemistry of the Earth's crust. Spec. Pap. Geol. Soc. Am. **62**, 119–44.

SALIOT, P., 1973. Les principales zones de métamorphisme dans les Alpes françaises. Répartition et signification. *C.R. Acad. Sci. Paris*, **D 276**, 3081–4.

—— 1978. Le métamorphisme dans les Alpes françaises. *Thèse d'Etat, Université Paris Sud–Orsay.*

—— 1979. La jadéite dans les Alpes françaises. *Bull. Minéral.* **102**, 391–401.

SCHREYER, W., 1968. A reconnaissance study of the system MgO–Al_2O_3–SiO_2–H_2O at pressures between 10 and 25 kb. *Yb. Carnegie Instn. Wash.* **66**, 380–92.

—— ABRAHAM, K., & TROCHIM, H. D., 1975. Piemontitschiefer von Brezovica, Südserbien. *Acta geologica (Zagreb)*, **VIII**, 251–68.

—— —— 1976. Three-stage metamorphic history of a whiteschist from Sar e Sang, Afganistan, as part of a former evaporite deposit. *Contr. Miner. Petrol.* **59**, 111–30.

—— —— 1977. Howieite and other high-pressure indicators from the contact aureole of the Brezovica, Yugoslavia, peridotite. *Neues Jb. Miner. Abh.* **130**, 114–33.

—— & BALLER, T., 1977. Talc–muscovite: synthesis of a new high-pressure phyllosilicate assemblage. *Neues Jb. Miner. Mh.* **9**, 421–5.

—— ABRAHAM, K., & KULKE, H., 1980. Natural sodium phlogopite coexisting with potassium phlogopite and sodian aluminian talc in a metamorphic evaporite sequence from Derrag, Tell Atlas, Algeria. *Contr. Miner. Petrol.* **74**, 223–33.

SEIFERT, F., 1970. Low-temperature compatibility relations of cordierite in haplopelites of the system K_2O–MgO–Al_2O_3–SiO_2–H_2O. *J. Petrology*, **11**, 73–99.

VELDE, B., 1965. Phengite micas: synthesis, stability and natural occurrences. *Am. J. Sci.* **263**, 886–913.

—— 1967. Si^{4+} content of natural phengites. *Contr, Miner. Petrol.* **14**, 250–8.

WEAVER, C. E., & POLLARD, L. D., 1973. *The Chemistry of Clay Minerals.* Amsterdam: Elsevier.

Bull. Soc. géol. France, 1981, (7), t. XXIII, n° 3, p. 297-301.

Mise en évidence d'une discontinuité du métamorphisme alpin entre le massif du Grand Paradis et sa couverture allochtone (Alpes occidentales françaises)

par CHRISTIAN CHOPIN

Mots clés. — Gneiss, Micaschiste, Faciès schiste bleu, Faciès éclogite, Crétacé sup., Métamorphisme régional, Type alcalin, Métamorphisme rétro, Obduction.
Savoie (Massif Grand Paradis).

Résumé. — En dépit de la similitude des paragenèses de HP dans le massif gneissique du Grand Paradis et sa couverture allochtone de Schistes lustrés océaniques, l'étude quantitative de ces associations montre de quatre façons indépendantes une discontinuité du métamorphisme entre les deux unités. La pression plus élevée dans le socle s'explique par un rejeu en sens inverse et post-obduction du contact majeur séparant les deux unités.

Evidence for a discontinuity in the high-pressure metamorphism affecting the Gran Paradiso massif and its allochthonous cover (French Western Alps)

Abstract. — The Gran Paradiso massif (continental unit) and the overthrust Schistes lustrés (oceanic unit) lying on it both have the same Upper Cretaceous HP-LT critical parageneses. However, compositional variation of low-variance assemblages, Al-content of talc, control of garnet occurrence by whole-rock chemistry, and Fe-Mg partitioning between chloritoid and glaucophane point to a higher P in the Gran Paradiso. This pressure gap is accounted for by a reactivation of the thrust plane after the HP-metamorphism in a direction opposite to the initial obduction process during which the HP assemblages have been generated.

L'étude des Schistes lustrés de Haute-Maurienne, dans la zone piémontaise des Alpes occidentales, a permis de distinguer trois grandes unités structurales superposées différant par leur contenu lithologique, l'intensité et peut-être l'âge de leur métamorphisme [Chopin, 1979, et en prép.]. L'unité inférieure est allochtone sur le massif cristallin interne du Grand Paradis. Dans la présente note, seuls sont concernés le massif du Grand Paradis et cette unité inférieure des Schistes lustrés. Celle-ci, grand corps de serpentinite surmonté d'une mince série volcano-sédimentaire, est interprétée comme écaille de plancher océanique tectonisé. Elle constitue le prolongement méridional de la « série inférieure » de Kiénast [1973] en Val d'Aoste et de la zone Zermatt-Saas de Bearth [1967]. Le massif du Grand Paradis est constitué de granites hercyniens *pro parte* [voir Chessex *et al.*, 1964] associés à un matériel paléozoïque de lithologie variée dont probablement une partie seulement a subi un métamorphisme anté-alpin [Bertrand, 1968 ; Compagnoni *et al.*, 1974].

Les deux unités ont été affectées par un métamorphisme alpin d'évolution complexe. Les paragenèses primaires, typomorphes, sont caractéristiques d'un métamorphisme de haute pression et relativement basse température. Elles furent ensuite diversement rétromorphosées dans un gradient géothermique plus élevé, à plus faible profondeur. L'objet de cette étude est de comparer les paragenèses produites par le métamorphisme de haute pression dans ces deux unités, et d'en tirer les conséquences géologiques.

Une approche qualitative : les paragenèses critiques.

Pour chaque lithologie considérée, les associations minérales caractéristiques sont les mêmes dans les deux unités : omphacite-grenat-glaucophane pour les roches basiques ; talc-chloritoïde ± grenat ou chlorite, glaucophane-chloritoïde, talc-phengite... dans des quartzites et roches alumineuses pauvres en calcium (la signification théorique de ces associations typiques de haute pression, en partie nouvelles, est explicitée dans d'autres articles en préparation). La lawsonite est absente des deux unités, les silicates calciques stables sont la zoïsite et la margarite [Chopin, 1977, 1979].

Par ailleurs, une étude radiochronologique des minéraux de haute pression de ces deux unités [méthode ^{39}Ar - ^{40}Ar ; Chopin et Maluski, 1978, 1980] permet de leur attribuer un même âge de cristallisation (75-60 Ma). En première approximation, nous pouvons donc affirmer que le compartiment continental « Grand Paradis » et l'unité océanique charriée sur lui ont été métamorphisés dans les mêmes conditions et à la même époque, et qu'ils constituent ainsi une seule entité métamorphique caractérisée

* Équipe de recherche du C.N.R.S. n° 224, Lab. de géologie, École normale supérieure, 46, rue d'Ulm, 75230 Paris Cedex 05. Présentement : Inst. für Mineralogie, Ruhr - Universität, D-4630 Bochum 1 (R.F.A.).

Note déposée le 22 juillet 1980, présentée à la séance du 27 octobre 1980, manuscrit définitif reçu le 7 novembre 1980.

par la forte intensité et l'âge crétacé supérieur du métamorphisme de haute pression. En fait, une approche plus quantitative des paragenèses va montrer que cette affirmation mérite d'être nuancée.

ÉTUDE QUANTITATIVE DE QUELQUES ASSOCIATIONS.

1) *Chloritoïde-glaucophane.* L'étude du fractionnement de FeO et MgO entre ces minéraux dans des paragenèses semblables des deux unités conduit à la figure 1. Les deux unités se distinguent, le chloritoïde du socle étant comparativement plus magnésien. Chacun des deux groupes définit une nette corrélation et témoigne ainsi d'une bonne approche de l'équilibre chimique. La différence de fractionnement observée résulte alors soit d'une différence des conditions (P et T) du métamorphisme d'une unité à l'autre, soit d'une différence de l'état d'oxydation du fer dans les associations des deux unités. En effet, les coefficients d'activité dans l'amphibole et le chloritoïde ne dépendent, outre P et T, que de la composition de ces phases. Or la seule autre substitution qui affecte ces minéraux est $Fe^{3+} \rightleftharpoons Al$, qui dépend évidemment de la fugacité de l'oxygène (fo_2).

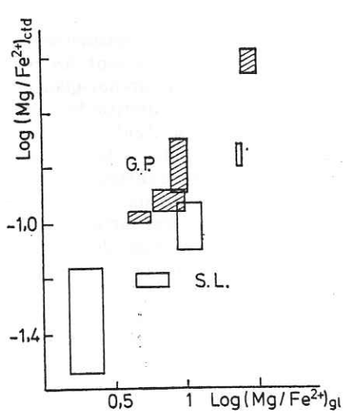

FIG. 1. — Fractionnement de FeO et MgO entre glaucophane et chloritoïde.

Le rapport Fe^{2+}/Fe^{3+} de ces minéraux a été calculé à partir des analyses à la microsonde en posant Si + Al + Fe^{3+} + Ti = 10 et Si + Al + Fe^{3+} + Ti = 6 dans les formules structurales du glaucophane et du chloritoïde calculées sur la base de 24 oxygènes et 8 cations respectivement. Chaque rectangle représente la dispersion des résultats dans un échantillon.

L'analyse des roches et des minéraux montre que les associations du socle sont uniformément peu oxydées et que celles des Schistes lustrés sont très diversement oxydées. Mais comme il n'y a pas entre ces dernières de différence systématique de fractionnement de FeO et MgO, la différence d'oxydation entre les deux unités ne peut être tenue pour responsable de la différence de fractionnement observée.

Nous pouvons donc penser à une différence des conditions métamorphiques entre les deux unités. Les associations naturelles [Chinner et Dixon, 1973 ; Miller, 1977 ; Chopin, 1979] et des expériences menées par l'auteur à Bochum, R.F.A., montrent que le chloritoïde magnésien est une phase de haute pression ; la différence de fractionnement observée d'une unité à l'autre traduirait donc une pression plus élevée dans le socle.

2) *Le contrôle chimique de l'apparition du grenat.* Le contrôle de l'apparition du grenat par le chimisme de l'échantillon peut nous permettre d'éprouver cette dernière hypothèse. Le pyrope étant une phase de haute pression [Schreyer, 1968], le grenat peut en effet apparaître dans des roches d'autant plus magnésiennes que le métamorphisme est de plus haute pression. La comparaison du chimisme de roches à grenat et sans grenat de la zone à grenat de divers domaines métamorphiques permet ainsi d'y comparer les conditions de métamorphisme [Fonteilles et Guitard, 1971]. Il faut bien sûr pour cela tenir compte du constituant MnO et travailler sur des paragenèses comparables, pauvres en CaO. Les roches étudiées s'y prêtant bien, les analyses disponibles ont été reportées dans la figure 2 qui

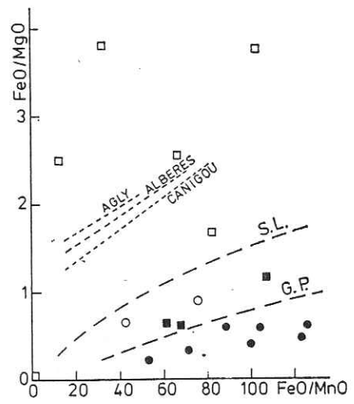

FIG. 2. — Le contrôle de l'apparition du grenat par le chimisme de la roche.

Les coordonnés sont des rapports de teneurs pondérales de l'échantillon, qui comporte (carré) ou non (cercle) du grenat. Les symboles vides renvoient à l'unité inférieure des Schistes lustrés, les pleins au Grand Paradis. Pour comparaison figurent les limites d'apparition déterminées dans trois massifs des Pyrénées Orientales par Fonteilles et Guitard [1971].

permet de définir la limite chimique de l'apparition du grenat dans les deux unités (lignes SL et GP). Elles sont distinctes, le grenat apparaît dans le socle pour des compositions plus magnésiennes que dans les Schistes lustrés. C'est un nouvel argument pour une différence du métamorphisme qui serait de plus haute pression dans le socle. La simplicité apparente de la méthode ne doit cependant pas faire oublier que la comparaison des analyses dans la représentation utilisée n'est rigoureusement correcte que pour des roches sans calcium dont le rapport $Si/Al/R^{2+}$ est identique, la discrimination se faisant uniquement sur les proportions de Fe, Mn et Mg dans R^{2+}. Ce n'est bien évidemment pas le cas ; pris isolément, cet argument reste donc de portée limitée.

3) *L'association talc-chloritoïde-grenat.* Étant toujours observée en présence du quartz, cette association est divariante dans le système réduit FeO-MgO-Al_2O_3-SiO_2-H_2O si l'activité de H_2O est fixée. A pression et température fixées, la composition des minéraux est alors complètement déterminée, en particulier leur rapport Fe^{2+}/Mg. Or le chimisme de cette association diffère d'une unité à l'autre (fig. 3). Avant d'en conclure à une différence de métamorphisme, nous devons cependant nous assurer de la validité des hypothèses faites lors de la réduction des paragenèses au système FeO-MgO-Al_2O_3-SiO_2-H_2O.

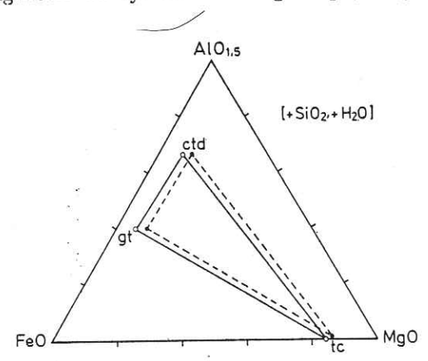

FIG. 3. — L'association talc-chloritoïde-grenat-quartz dans l'unité inférieure des Schistes lustrés (traits pleins) et le massif du Grand Paradis (tiretés) : projection sur le plan Al_2O_3-FeO-MgO à partir des constituants H_2O (voir texte) et SiO_2. Dans le socle et les Schistes lustrés respectivement, les teneurs en composants secondaires du grenat sont Gro : 2 et 6 %, Spe : 2 et 4 %, And : 1 et 2 %. CaO est exclusivement présent dans le grenat, MnO surtout dans le grenat (0,15 et 0,20 % MnO dans le chloritoïde) et Fe_2O_3 surtout dans le chloritoïde (0,4 et 3 %). La projection a donc été faite aussi à partir de grossulaire, spessartine et ferrichloritoïde ; les teneurs en Mn-chloritoïde et andradite sont certes faibles, mais font qu'elle n'est pas absolument rigoureuse. Les deux paragenèses contiennent aussi glaucophane et phengite, mais les constituants Na_2O et K_2O étant *exclusivement* localisés dans *chacun* de ces minéraux, la réduction au système précédent garde la même valeur.

Nous avons ainsi négligé le paramètre fo_2 qui influence aussi le rapport Fe^{2+}/Mg des minéraux, du talc tout particulièrement [Forbes, 1971]. A pression et température constantes, l'association envisagée doit être d'autant plus magnésienne que le système est plus oxydé. Or les analyses montrent que, dans les Schistes lustrés, l'association est plus oxydée que dans le socle ; elle y est cependant moins magnésienne. La variation de chimisme de cette association d'une unité à l'autre, tout en étant réduite par cet effet, a donc nécessairement une autre cause.

Celle-ci pourrait être une valeur variable de la pression partielle de H_2O (p_{H_2O}), la différence de chimisme observée s'expliquant alors par une p_{H_2O} plus faible dans le socle [Chopin, 1979]. Les échantillons étudiés dans le socle sont des roches paradérivées qui ont peut-être subi le seul métamorphisme alpin ; il n'y a donc pas lieu de les croire *a priori* moins hydratées que les échantillons des Schistes lustrés, également paradérivés. D'autre part, c'est dans les Schistes lustrés où les calcschistes abondent, plutôt que dans le socle où les carbonates sont quasi absents, que l'on pourrait attendre une plus faible p_{H_2O}. Enfin, plus décisive, l'existence d'inclusions fluides d'eau pure dans les minéraux des deux unités semble bien y justifier l'hypothèse p_{H_2O} égale pression totale. Il devient alors légitime de penser à une différence de métamorphisme. Le caractère plus magnésien du talc, du chloritoïde et du grenat de cette association dans le socle y indique alors à nouveau un métamorphisme plus intense et en particulier une pression plus élevée.

4) *La teneur en alumine du talc.* Un autre caractère distinctif des deux unités est la teneur en Al_2O_3 du talc (fig. 4). Dans les associations à talc-chloritoïde ± grenat, la moyenne est 0,05 % dans les Schistes lustrés (10 analyses), et 0,45 % dans le socle (9 analyses). Si les travaux expérimentaux [Newton, 1972] permettent mal de distinguer les rôles respectifs de la pression et de la température dans l'incorporation d'Al_2O_3 par le talc, ils montrent néanmoins que celle-ci traduit des conditions (P et T) plus sévères. Dans la nature, les associations

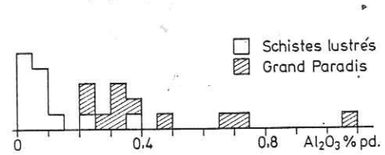

FIG. 4. — Histogramme des teneurs en alumine du talc dans les deux unités. Remarque générale : le lecteur intéressé trouvera l'ensemble des analyses utilisées dans la thèse de troisième cycle de l'auteur [Chopin, 1979].

des « whiteschists » [Mc Kie, 1959 ; Schreyer et Abraham, 1976, etc.] conduisent à la même conclusion. Ainsi l'étude du chimisme du talc fournit un nouvel argument en faveur d'un métamorphisme plus intense dans le socle.

Interprétation et conséquences.

Chacun des arguments précédents peut paraître insuffisant pour une démonstration sans équivoque. La convergence de quatre méthodes indépendantes vers le même résultat permet cependant de conclure qu'en dépit de la minéralogie similaire des paragenèses critiques des deux unités le métamorphisme était plus sévère dans le socle, la pression en particulier y étant plus élevée.

Cette différence de métamorphisme doit être estimée à sa juste valeur ; elle est par exemple négligeable vis-à-vis de celle existant entre ces deux unités et le massif de la Vanoise, immédiatement voisin. Il s'agit plutôt d'une nuance de métamorphisme. Elle ne traduit pas un régime thermique bien différent d'une unité à l'autre, sinon les paragenèses critiques y seraient distinctes. Elle ne résulte pas non plus de la superposition normale de ces séries dans une même séquence métamorphique puisque la dispersion verticale des échantillons est, à l'intérieur d'une unité, du même ordre de grandeur que d'une unité à l'autre et que cependant chacune des unités fournit un lot distinct de valeurs homogènes. Il y a donc une discontinuité des conditions métamorphiques. Celle-ci ne peut résulter que du rapprochement tectonique de deux ensembles métamorphisés dans des conditions légèrement différentes. Mais dans quelles circonstances ? En particulier, ce rapprochement peut-il être contemporain du métamorphisme de haute pression ou lui est-il postérieur ?

Le massif du Grand Paradis représente au Crétacé supérieur la bordure orientale du continent européen engagée dans un charriage profond, à pendage est, sous des unités océaniques (« obduction »). De ce stade datent les paragenèses de haute pression. Il est difficile d'y voir alors l'origine de la différence de métamorphisme observée puisque, à tout moment, arrive au-dessus d'un point donné de la surface du socle un matériel océanique situé peu avant à plus grande profondeur que lui, donc *a priori* davantage affecté par le métamorphisme.

Lors du blocage de la « subduction », des paragenèses de haute pression peuvent avoir scellé le contact entre les deux unités ; elles sont alors identiques de part et d'autre d'un point donné de ce contact, mais, au long de ce contact, leur degré métamorphique augmente avec la profondeur (vers l'Est donc). Un tel épisode, quasi statique, ne permet cependant pas non plus d'expliquer la différence observée puisque celle-ci ne résulte pas *(cf. supra)* de la superposition de ces unités dans une même séquence métamorphique.

En revanche un rejeu tardif (postérieur à l'épisode de haute pression) de ce contact, et en sens inverse, c'est-à-dire déplaçant relativement l'unité océanique vers l'Est, rendrait parfaitement compte de la différence observée (quel que soit alors le pendage du contact, qui est actuellement ouest dans le secteur considéré). Or les flancs des hautes vallées de l'Arc et de l'Isère offrent les preuves tangibles d'un tel phénomène, trait classique de la géologie des Alpes occidentales : « rétrocharriage » des unités briançonnaises sur les unités piémontaises [*cf.* le « sous-charriage » de Caby *et al.*, 1978] ou, en l'occurrence, des unités de Schistes lustrés au-dessus des structures tardives du socle Grand Paradis [*cf.* Bertrand, 1968]. La corrélation de ces observations pétrologiques et structurales ainsi que leur attribution au même phénomène devient alors l'hypothèse logique. Une localisation plus précise dans le temps de ce phénomène reste à faire, en particulier par rapport à l'événement situé vers 38-40 Ma qui traduit peut-être la fin de l'évolution métamorphique régionale [Chopin et Maluski, 1980].

Références

Bearth P. (1967). — Beiträge geol. Karte Schweiz., n° 132.

Bertrand J. M. L. (1968). — Étude structurale du versant occidental du massif du Grand Paradis. *Géol. alpine*, 44, p. 55-87.

Caby R., Kiénast J. R. et Saliot P. (1978). — Structure, métamorphisme et modèle d'évolution tectonique des Alpes occidentales. *Rev. Géogr. phys. Géol. dyn.*, 20, p. 307-322.

Chessex R., Delaloye M., Krummenacher D. et Vuagnat M. (1964). — Nouvelles déterminations d'âges « plomb total » sur des zircons alpins. *Schweiz. Min. Petr. Mitt.* 44, p. 43-60.

Chinner G. A. et Dixon J. (1973). — Some high-pressure parageneses of the Allaline gabbro, Valais, Switzerland. *J. Petrol.*, 14, p. 185-202.

Chopin C. (1977). — Une paragenèse à margarite en domaine métamorphique de HP-BT (massif du Grand Paradis, Alpes françaises). *C. R. Acad. Sc.*, Paris, D, t. 285, p. 1383-1386.

Chopin C. (1979). — De la Vanoise au massif du Grand Paradis. Thèse 3e cycle, Univ. P.-et-M.-Curie (Paris VI).

Chopin C. et Maluski H. (1978). — Résultats préliminaires obtenus par la méthode de datation $^{39}AR/^{40}Ar$ sur des minéraux alpins du massif du Grand Paradis et

de son enveloppe. *Bull. Soc. géol. Fr.*, XX, p. 745-749.

Chopin C. et Maluski H. (1980). — $^{39}Ar/^{40}Ar$ dating of high pressure metamorphic micas from the Gran Paradiso area (Western Alps) : evidence against the blocking-temperature concept. *Contrib. Mineral. Petrol.*, 74, p. 109-122.

Compagnoni R., Elter G. et Lombardo B. (1974). — Eterogeneità stratigrafica del complesso degli « gneiss minuti » nel massicio cristallino del Gran Paradiso. *Mem. Soc. Geol. Ital.*, 13/1, p. 227-239.

Fonteilles M. et Guitard G. (1971). — Sur les conditions de formation du grenat almandin et de la staurotide dans les métapélites mésozonales hercyniennes des Pyrénées Orientales : mise en évidence de variations mineures du type de métamorphisme. *C. R. Acad. Sci.*, Paris, D, t. 273, p. 659-662.

Forbes W. C. (1971). — Iron content of talc in the system $Mg_3Si_4O_{10}(OH)_2$-$Fe_3S_4O_{10}(OH)_2$. *J. Geol.*, 79, p. 63-74.

Kiénast J. R. (1973). — Sur l'existence de deux séries différentes au sein de l'ensemble « Schistes lustrés-ophiolites » du Val d'Aoste ; quelques arguments fondés sur l'étude des roches métamorphiques. *C. R. Acad. Sci.*, Paris, D, t. 276, p. 2621-2624.

McKie D. (1959). — Yoderite, a new hydrous magnesium iron aluminosilicate from Mautia Hill, Tanganyika. *Mineral. Mag.*, 32, p. 282-307.

Miller C. (1977). — Chemismus und phasenpetrologische Untersuchungen der Gesteine aus der Eklogitzone des Tauernfensters, Österreich. *Tsch. Min. Petr. Mitt.*, 24, p. 221-177.

Newton R. C. (1972). — An experimental determination of the high-pressure stability limits of magnesian cordierite under wet and dry conditions. *J. Geol.*, 80, p. 398-420.

Schreyer W. (1968). — A reconnaissance study of the system MgO-Al_2O_3-SiO_2-H_2O at pressures between 10 and 25 kb. *Carnegie Inst. Washington, Yearb.*, 66, p. 380-392.

Schreyer W. et Abraham K. (1976). — Three-stage metamorphic history of a whiteschist from Sar e Sang, Afganistan, as part of a former evaporite deposit. *Contrib. Mineral. Petrol.*, 59, p. 111-130.

Contrib Mineral Petrol (1981) 76:260–264

Contributions to Mineralogy and Petrology

High-Pressure Synthesis and Properties of Magnesiocarpholite, $MgAl_2[Si_2O_6]\ (OH)_4$

Christian Chopin[1] and Bruno Goffé[2]

[1] Institut für Mineralogie, Ruhr-Universität, D-4630 Bochum 1, Federal Republic of Germany
[2] Laboratoire de Géologie (E.R. 224), Ecole normale supérieure, 46 rue d'Ulm, F-75005 Paris, France

Abstract. Magnesiocarpholite has been synthesized on its own composition between 15 and 25 kb water pressure and 415°–600° C. Best conditions are 25 kb–550° C, starting from a mixture of oxides and synthetic cordierite. Within the MgO-Al_2O_3-SiO_2-H_2O system, possible substitutions appear to be very limited in magnesiocarpholite. Cell-parameters are a = 13.706(3), b = 20.075(3), c = 5.107(1) Å, space group Ccca. The larger cell, as compared with the most magnesian natural carpholites, is tentatively ascribed to structural disorder. Preliminary stability data confirm the low-temperature character of this mineral which is shown to be a high-pressure equivalent of sudoite + quartz.

Introduction

Carpholites with the general formula $(Mn^{2+}, Fe^{2+}, Mg)\ (Al, Fe^{3+})_2\ [Si_2O_6]\ (OH, F)_4$ may be considered as solid solutions between the three end-members manganocarpholite (i.e. carpholite s.s.), ferrocarpholite and magnesiocarpholite (Mottana and Schreyer 1977; Viswanathan and Seidel 1979). Natural crystals approach these ideal compositions by 92, 82 and 96 mole percent, respectively. While manganese-rich members are known since the early nineteenth century, the iron and magnesium homologues have only recently been described (De Roever 1951; Goffé et al. 1973, respectively). Yet, the rapidly increasing number of known occurrences (Steen and Bertrand 1977; Seidel and Okrusch 1977; Briggs 1978; Viswanathan and Seidel 1979; Goeffé 1980; for earlier references see Mottana and Schreyer 1977, for a Mg–Mn-carpholite, Kramm 1980) leaves no doubt that the iron-magnesium members are in fact regionally widespread minerals in high pressure-low temperature metamorphic terranes, but are probably most often mistaken for actinolite. Owing to their chemical composition (cf. Fig. 1), Fe–Mg-carpholites are indeed likely to occur, given the appropriate $P-T$ conditions, in quite common pelitic or alumina-rich rock composition and are there a most important index-mineral (Goffé et al. 1973; Dubois and Kiénast 1975; Goffé and Saliot 1977; De Roever 1977; Seidel and Okrusch 1977; Viswanathan and Seidel 1979).

Previous Work

Much experimental work has been devoted to the carpholite group during the last years. Dasgupta et al. (1974), and Mottana and Schreyer (1977) report unreversed breakdown experiments on natural manganocarpholite in the pressure range 0.5–16 kb, but they failed to synthesize the pure Mn-end-member. Similarly, attempts by one of us (B.G.) to synthesize magnesiocarpholite between 1 and 11.5 kb remained unsuccessful; breakdown experiments on natural material will be reported elsewhere. F. Beunk (personal communication) also failed to synthesize ferrocarpholite and intermediate members of the Fe–Mg series at 6 and 25 kb on the magnetite-iron buffer. This note reports the first successful synthesis of a carpholite end-member, namely magnesiocarpholite.

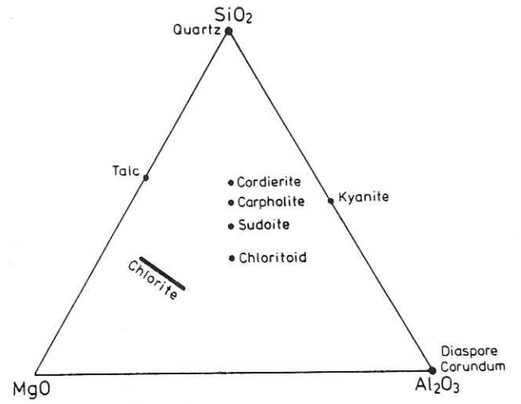

Fig. 1. Projection of the $MgO-Al_2O_3-SiO_2-H_2O$ system onto the waterfree plane showing the phases involved in this study and schematically depicting possible phase relationships between carpholite, chloritoid, sudoite and quartz, among others

Experimental Procedure

Four different starting materials of $MgO \cdot Al_2O_3 \cdot 2SiO_2$ composition were used for synthesis: (i) gel, (ii) oxides, (iii) oxides with cordierite, (iiii) "sudoite" with quartz. The gel was prepared following Luth and Ingamells (1965). The oxides used were SiO_2-glass (Aerosil), synthetic γ-Al_2O_3, and MgO obtained from certified reagent-grade $Mg(CH_3COO)_2 \cdot 4H_2O$; all were either fired or corrected for their water content. Synthetic Mg-cordierite was crystallized from glass at 1,300° C. Natural sudoite (i.e. di/trioctahedral chlorite) is that from Ottré described by Fransolet and Bourguignon (1978); it is very close to $Mg_2Al_3Si_3AlO_{10}(OH)_8$ in composition, the main impurity being 2.7% Fe_2O_3. A 66% Mg-end-member carpholite (sample Chan764, analysis in Goffé 1980) was used as natural seed.

A conventional piston-cylinder apparatus using NaCl cells (Mirwald et al. 1975) was employed for the experiments. The experimental uncertainty for the reported runs is assumed to be within ±10° C

0010-7999/81/0076/0260/$01.00

Table 1. Experimental results. Oxide mix and gel are of $MgO \cdot Al_2O_3 \cdot 2SiO_2$ composition, except CA34 which contains 6 weight percent excess Al_2O_3·CA31 contains 4 weight percent excess SiO_2. Products are listed in order of decreasing abundance. Car: carpholite (clear growth for the seeded runs), Chl: 14 Å chlorite, Co: corundum, Dia: diaspore, Ky: kyanite, Sud: sudoite, Tc: talc

Run	P (kb)	T (°C)	Duration	Starting material	Products	Interpretation
CA 7	25.6	415	133 h.	ox. mix	Q, Dia, Chl	Car more stable than Q+Dia+Chl
CA 6	25.6	415	133	ox. mix + nat. seed	Car, Q, Dia, Chl?	
CA 9	24.9	500	71	ox. mix + 10% CA 6	Car	Car more stable than Sud+Q
SU 1	28.5	505	65	sudoite	Car, Dia, Chl, Sud−	
CA 12	25.0	515	87	ox. mix + 5% CA 9	Car, Q, Dia, Tc	Car more stable than Q+Dia+Tc
CA 15	25.1	540	60	gel + 10% nat. seed	Car, Q, Dia, Tc	
CA 27	25.5	550	69	ox. mix	Q, Dia, Tc, Ky, Car	
CA 30	25.1	550	50	CA 27	Car+, Ky+; Q−, Dia−, Tc−	
CA 29	25.1	550	50	ox. mix + 10% CA 12	Car	Best synthesis procedures
CA 31	25.1	550	50	cordierite + oxides	Car, Q	
CA 34	25.7	550	63	ox. mix + 10% CA 12	Car, Dia	
SU 2	28.5	505	65	sudoite + Q + CA 12	Car, Tc	
CA 24	25.0	605	59	ox. mix	Tc, Ky, Chl	Car less stable than Tc+Ky+Chl
CA 19	25.0	605	45	gel + 10% CA12	Car, Tc, Ky,?	
CA 23	25.0	605	59	CA 19	Tc, Ky, Chl	
CA 22	14.9	555	118	gel + 10% CA 12	Car, Tc, Co, Chl,?	Car less stable than Q+Ky+Chl
TKC 8	15.0	550	103	Car + Q (+Tc+Ky)	Chl, Ky+, Q+, Tc, Car−	

for the temperature and ±500 bars for the pressure. About 10 mg of the starting material along with 3 mg of deionized water were welded into a small gold capsule, except for run CA12, for which a gold capsule containing about 70 mg starting material was used.

Standard optical and X-ray techniques were employed for phase identification. Lattice constants were determined from X-ray diffractograms using Ni-filtered CuKα radiation and Si (SRM 640 of the National Bureau of Standards, $a_o = 5.43088 \pm 0.000035$ Å) as internal standard. A complete oscillation was made between 12 and 78° 2θ and 52 to 73 peaks were measured near their maxima. Cu Kα_1 wavelength (1.54040 Å) was used in the refinements. Relative peak intensities reported are based on peak-height measurements averaged from two charts run under different conditions.

Infrared absorption spectra were obtained with a Perkin-Elmer spectrophotometer 325, using 1 mg samples dispersed in 580 mg RbI pellets.

Experimental Results

Table 1 summarizes the significant runs. At 25 kb, a carpholite phase (see Fig. 2) nucleates spontaneously between about 500° and 570° C. However, reaction only goes to completion within a few days if a low-pressure mineral such as cordierite (or possibly sudoite) is present in the starting material, or if the oxide mix or the gel are seeded (compare runs SU1, CA27, CA30, CA31, CA29). In order to produce *pure* Mg-end-member also from the seeded runs, the first synthetic carpholite obtained (CA6, with natural seeds) was in turn used as seed and the procedure repeated. The third generation carpholite (CA12) thus contains less than 0.03 mole percent Fe-end-member, and the forth generation (CA29) reaches reagent-grade purity. Some preliminary data on carpholite breakdown and metastable growth are also reported in Table 1. According to these data, the best conditions for *direct* synthesis of *pure* magnesiocarpholite are 550° C–25 kb with a mixture of oxides and synthetic cordierite as starting material.

Physical Properties

The synthetic magnesiocarpholite obtained is white in colour and very fine-grained. It forms tiny elongated prisms, 1–4 μm long (Fig. 3). This habit is, indeed, typical for minerals of the carpholite group and related to their single-chain structure (Mc Gillavry et al. 1956; Naumova et al. 1975). Parallel extinction is discernable for bigger crystals; mean refractive index is 1.599 ± 0.002.

X-Ray Data

For a correct indexing of the X-ray pattern, a theoretical powder pattern was computed for a magnesiocarpholite end-member in the Ccca space group, using the LAZY PULVERIX program (Yvon et al. 1977). The atomic parameters of manganocarpholite reported by Naumova et al. (1975) and the cell-parameters extrapolated by Viswanathan and Seidel (1979) for pure magnesiocarpholite were used as input data. The calculated intensities allowed unequivocal allocation of most peaks to a unique reflection (see Table 2). This together with a remarkable agreement between calculated and measured peak intensities seems to confirm the space group chosen and thus the isostructural nature of the whole carpholite group.

This indexing was also used for least square refinements of cell-parameters. The data reported in Table 2 are from a "third generation" carpholite (CA12) which still coexists with small amounts of quartz, diaspore and talc, but for which the greatest number of reflections was measured. Cell parameters were additionally determined from three other synthesis products (CA29, CA31, CA34; see Table 3), for which the carpholite-forming reaction went to completion. In order to investigate possible substitution mechanisms, the starting material had, relative to stoichiometric composition, 4 weight percent excess SiO_2 in CA31 and 6 percent excess Al_2O_3 in CA34. The three runs yielded carpholite, carpholite + quartz and carpholite + diaspore, respectively. Yet the cell parameters of these carpholites show very little variation (they remain within 1σ) and no systematic trend. It is therefore concluded that, within the $MgO-Al_2O_3-SiO_2-H_2O$ system, the extent of possible substitutions in carpholite is extremely limited. Likewise, tetrahedral substitution has not been recorded from natural magnesiocarpholites, not even in diaspore-bearing parageneses (Viswanathan and Seidel

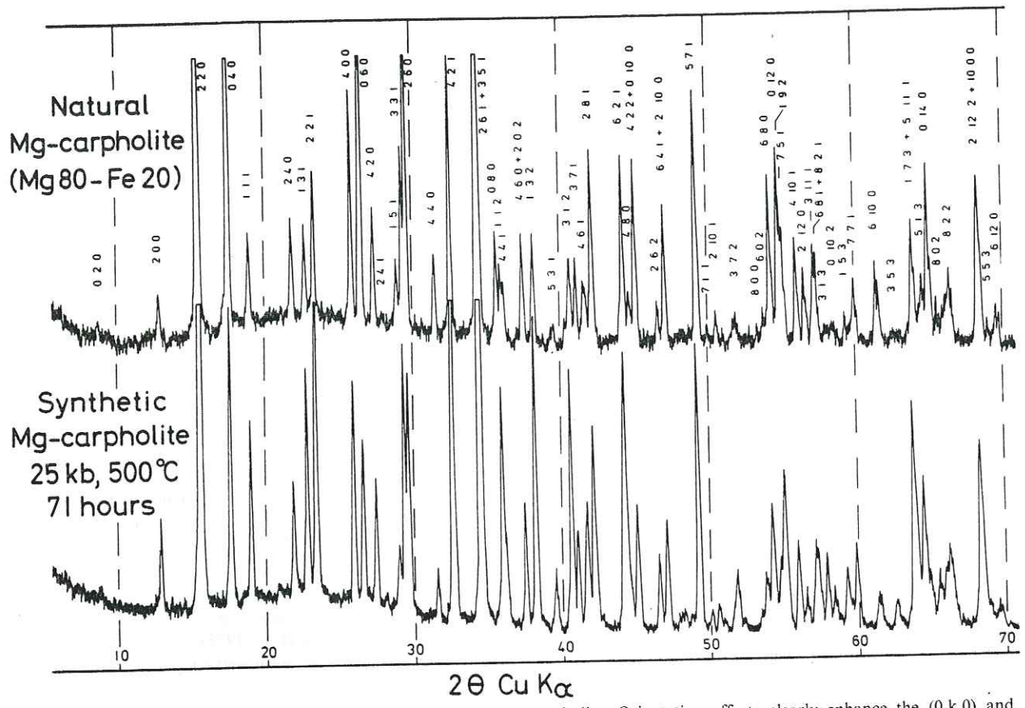

Fig. 2. X-ray powder patterns of natural and synthetic magnesiocarpholite. Orientation effects clearly enhance the (0 k 0) and, to a lesser extent, the (h k 0) reflections in the natural sample (KHR 2 from Crete, described by Viswanathan and Seidel 1979); the smaller particle size of the synthetic material reduces these effects

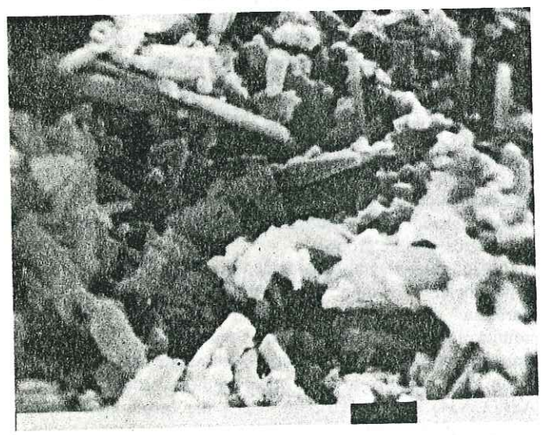

Fig. 3. Scanning electron photomicrograph of synthetic magnesiocarpholite (grown at 25 kb, 550° C in 50 h). The *solid mark* in the *right bottom corner* is 1 μm long

1979; Goffé, unpublished data), and is indeed unlikely to be favoured at high pressure.

However, these cell parameters, especially the *b* parameter, are noticeably larger than those expected for the pure Mg-end-member from the regression curves that Viswanathan and Seidel (1979) obtained from natural material (see Table 3); they approach those of a natural magnesiocarpholite containing about 20 mole percent Fe-end-member. As significant substitutions in the synthetic carpholite have been ruled out, such a discrepancy deserves further attention.

One might assume that the relations established by Viswanathan and Seidel (1979) are biased by the presence of accessory components in the natural material. However, the two main impurities being F and Fe_1^{3+}, which have an opposite effect on the cell-volume, such an assumption appears to be unlikely. On the other hand, in spite of the finegrained nature of the synthetic material, there is no evidence for particle-size effects (e.g. Ross 1968) biasing our cell parameter determination. Even line-broadening is not observed (Fig. 2).

Therefore the only other explanation we could propose would be a disordered structure for the synthetic material. A first possibility would be an Al-Mg disorder in the octahedral beam linking the neighbouring $Si_4Al_2O_{12}(OH)_4$ pyroxene-like slabs parallel to the (100) plane. Natural ferro-, mangano- and magnesiocarpholite are fully ordered in this respect (Mc Gillavry et al. 1956; Naumova et al. 1975, and Viswanathan, personal communication 1981, respectively): Fe, Mn and Mg occupy the outer larger octahedron of the beam (cf. *M*2 site in the pyroxene structure), whereas the smaller Al ions occupy the smaller inner octahedron (cf. *M*1 site in the pyroxene structure). Considering the crystal-chemical similarity between carpholites and pyroxenes (Viswanathan and Seidel 1979) and the dependence of the *c* parameter on the size of the cation occupying the *M*1 site in pyroxenes (Clark et al. 1969), such an Al−Mg disorder in carpholite would be expected to affect noticeably the *c* parameter, which is not the case.

Table 2. X-ray powder diffraction data for synthetic magnesiocarpholite (CA12, see Table 1). "Uncertainties" are 1σ values. Diffraction lines with I_{cal} and I_{obs} less than unity (for example (020), compare Fig. 2) have not been listed.

h	k	l	d_{cal}(Å)	d_{obs}(Å)	I_{cal}	I_{obs}
2	0	0	6.854	6.86	13	8
2	2	0	5.661	5.66	100	100
0	4	0	5.020	5.02	21	22
1	1	1	4.656	4.66	10	13
2	4	0	4.050	4.05	7	8
1	3	1	3.894	3.894	17	16
2	2	1	3.792	3.793	24	26
4	0	0	3.427	3.427	12	17
0	6	0	3.347	3.346	7	13
4	2	0	3.243	3.243	6	9
1	5	1	3.077	3.076	4	5
3	3	1	3.035	3.035	13	19
2	6	0	3.007	3.007	12	17
4	4	0	2.830	2.832	2	4
4	2	1	2.738	2.738	25	33
3	5	1	2.597	2.594	33	62
2	6	1	2.592	2.594	26	
0	8	0	2.510	2.511	2	3
1	1	2	2.492	2.491	11	16
4	4	1	2.476	2.477	2	7
2	0	2	2.393	2.394	2	8
4	6	0	2.394	2.394	2	
2	8	0	2.357		1	21
1	3	2	2.351	2.351	14	
5	3	1	2.272	2.274	1	4
3	1	2	2.216	2.216	10	17
3	7	1	2.194	2.194	4	7
4	6	1	2.168	2.167	2	7
2	4	2	2.160	2.161	5	9
2	8	1	2.140	2.140	8	14
4	0	2	2.048		6	20
6	2	1	2.042	2.043	11	
0	6	2	2.030	2.031	2	5
4	8	0	2.025	2.026	1	4
4	2	2	2.0066	2.0071	3	9
0	10	0	2.0081	2.0071	2	
2	6	2	1.9468	1.9464	4	6
6	4	1	1.9260	1.9267	4	8
2	10	0	1.9271	1.9267	3	
5	7	1	1.8478	1.8477	15	20
6	6	1	1.7700	1.7696	1	2
7	3	1	1.7639	1.7634	1	3
3	7	2	1.7604	1.7599	2	4
8	0	0	1.7135	1.7131	1	2
6	0	2	1.7028	1.7028	3	4
6	8	0	1.6896	1.6895	4	10
8	2	0	1.6891		1	
1	1	3	1.6838		1	
0	12	0	1.6734	1.6736	3	5
1	9	2	1.6679	1.6684	3	6
7	5	1	1.6642	1.6642	9	11
4	10	1	1.6408	1.6402	5	6
2	12	0	1.6257	1.6256	1	2
3	11	1	1.6090	1.6086	3	6
8	2	1	1.6037		1	5
6	8	1	1.6041	1.6045	2	
3	1	3	1.5906	1.5901	4	4
0	10	2	1.5786	1.5783	2	2
1	5	3	1.5575	1.5573	4	4
7	1	2	1.5495	1.5491	1	2
7	7	1	1.5419	1.5420	3	6
6	10	0	1.5083	1.5085	3	3
3	5	3	1.4828	1.4822	2	2
1	7	3	1.4560	1.4561	11	14
5	11	1	1.4564		4	
5	1	3	1.4428	1.4427	9	10
0	14	0	1.4344	1.4345	3	4
8	0	2	1.4230	1.4231	3	4
8	8	0	1.4152	1.4151	2	4
3	11	2	1.4125	1.4125	2	5
8	2	2	1.4089	1.4090	3	6
9	5	1	1.3718		2	
2	12	2	1.3714	1.3714	7	13
10	0	0	1.3708		4	
5	5	3	1.3609	1.3609	1	2
6	12	0	1.3500	1.3502	2	2
1	13	2	1.3157	1.3157	5	4
9	1	2	1.3054	1.3054	5	5
4	14	1	1.2809	1.2812	3	4
1	1	4	1.2690	1.2692	3	2
2	0	4	1.2555	1.2557	1	1
10	6	1	1.2311	1.2312	1	2

a = 13.7081 ± 0.0010 Å, b = 20.0808 ± 0.0014 Å, c = 5.1083 ± 0.0004 Å, V = 1406.2 ± 0.2 Å³
Space group Ccca, Z = 8

Table 3. Unit-cell parameters of synthetic magnesiocarpholites. Uncertainties (in parantheses) are 2σ and refer to the last digit given. The data extrapolated by Viswanathan and Seidel (1979) for a natural Mg-end-member are given for comparison (V.S.)

Run	a (Å)	b (Å)	c (Å)	V (Å³)	Remarks
CA 29	13.707(2)	20.076(3)	5.107(1)	1405.4(3)	
CA 31	13.705(3)	20.074(3)	5.107(1)	1405.1(3)	+quartz
CA 34	13.706(3)	20.073(4)	5.107(1)	1404.9(4)	+diaspore
V.S.	13.693	20.034	5.105	1400.5	extrapolated

A second disorder possibility might arise from the presence in the synthetic crystals (as, for example, in synthetic amphiboles, see Maresch and Czank 1981) of defects involving other chain-silicate units. Such pyriboles being off carpholite composition, their presence should result in additional phases in the product, which have not been observed. If in very small amounts, these could indeed have remained undetected but then, they might as well result from a slight uncertainty in the starting composition or from differential leaching of the components by the vapor phase.

These explanations therefore remain speculative as long as experimental support is lacking. Unfortunately, the excellent agreement in calculated and measured peak intensities obtained for the synthetic material provides few evidence in this respect, as Al and Mg have similar scattering factors. Infra-red data (see below) also prove inconclusive. Time studies to ascertain wether increased run duration will reduce the cell parameters have not yet been completed. Perhaps noteworthy in this respect are the slightly larger cell parameters in CA12, for which the carpholite-producing reaction remained incomplete, than in CA29, CA31 and CA34 (compare Tables 2 and 3). However, only high resolution transmission electron microscopy could provide a more definite evidence.

IR Data

The near-identity of natural and synthetic magnesiocarpholite spectra (Fig. 4) further confirms the close structural similarity of the two. The simpler chemistry of the synthetic product results in a better resolution of the spectrum and could counteract the effect of a structural disorder, if any, so that these IR data cannot yield any definite answer to our problem. At any rate, they yield no evidence for structural disorder.

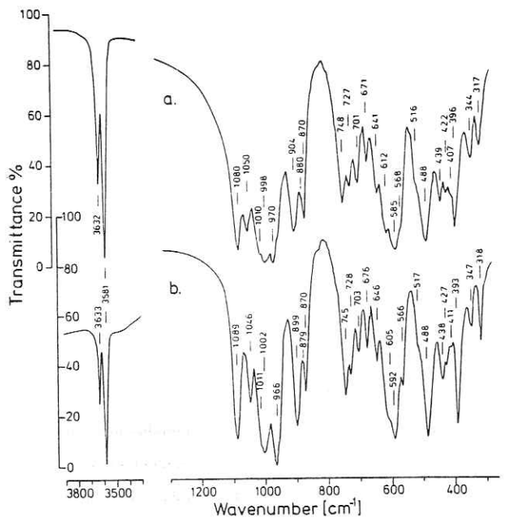

Fig. 4a, b. Infrared absorption spectra of **a** natural sample KHR 2 and **b** synthetic magnesiocarpholite, both recorded under the same conditions. Comparing the spectra of natural magnesiocarpholite and of ferro- and manganocarpholite (cf. Fransolet 1972) shows few, if any, systematic shifts of absorption bands, but an increasing resolution from mangano- to ferro- to magnesiocarpholite

Conclusion

The data presented confirm the low-temperature and probably high-pressure character of magnesiocarpholite, but additional data about its stability field and its crystal-chemistry are clearly needed. The stability of magnesiocarpholite in the $P-T$ range investigated remains to be demonstrated; we merely show this mineral to be more stable than various phyllosilicate-bearing assemblages (Table 1). Actually, magnesiochloritoid + quartz (Fig. 1) might be the most stable assemblage in part of this field. Further experimental work is in progress.

Acknowledgements. This work was carried out while the first author was a guest of Professor W. Schreyer in the Institut für Mineralogie, Ruhr-Universität Bochum, supported by a fellowship from the Deutscher Akademischer Austauschdienst. He benefited there by the permanent help and advice of I. Abs-Wurmbach, D. Lattard, H. Leistner, H.J. Massone, and P. Mirwald, who introduced him to the high pressure techniques. Earlier versions of this paper have been improved by the comments of W. Maresch, B. Velde and especially P. Mirwald and W. Schreyer; a later one by a discussion with K. Viswanathan. O. Medenbach kindly performed the optical measurements and G. Werding assisted in the IR technique. A.M. Fransolet and E. Seidel provided high quality samples of natural sudoite and magnesiocarpholite as well as unpublished data. To each of these persons we express our grateful acknowledgement.

References

Briggs RM (1978) Ferrocarpholite associated with low low-grade blueschists, northern New Caledonia. Mineral Mag 42:147

Clark JR, Appleman DE, Papike JJ (1969) Crystal-chemical characterization of clinopyroxenes based on eight new structure refinements. Mineral Soc Am, Sp Pap 2:21–50

Dasgupta HC, Seifert F, Schreyer W (1974) Stability of manganocordierite and related phase equilibria in part of the system $MnO-Al_2O_3-SiO_2-H_2O$. Contrib Mineral Petrol 43:365–373

Dubois R, Kiénast JR (1975) La Mg–Fe-carpholite de Gimigliano (Calabre) dans le métamorphisme alpin. 3ème Réunion annuelle des Sciences de la terre, Montpellier (Abstr)

Fransolet AM (1972) Données nouvelles sur la carpholite de Meuville (vallée de la Lienne, Belgique). Bull Soc Fr Mineral Cristallogr 95:84–97

Fransolet AM, Bourguignon P (1978) Di/trioctahedral chlorite in quartz veins from the Ardenne, Belgium. Can Mineral 16:365–373

Goffé B, Goffé-Urbano G, Saliot P (1973) Sur la présence d'une variété magnésienne de ferrocarpholite en Vanoise (Alpes françaises). Sa signification probable dans le métamorphisme alpin. CR Acad Sci Paris, D 277:1965–1968

Goffé B, Saliot P (1977) Les associations minéralogiques des roches hyperalumineuses du Dogger de Vanoise. Leur signification dans le métamorphisme régional. Bull Soc Fr Mineral Cristallogr 100:302–309

Goffé B (1980) Magnesiocarpholite, cookéite et euclase dans les niveaux continentaux métamorphiques de la zone briançonnaise. Données minéralogiques et nouvelles occurences. Bull Mineral 103:297–302

Kramm U (1980) Sudoite in low-grade metamorphic manganese rich assemblages. N Jahrb Mineral Abh 138:1–13

Luth WC, Ingamells CO (1965) Gel preparation of starting materials for hydrothermal experimentation. Am Mineral 50:255–258

Mac Gillavry CH, Horst WL, Weichel Moore EJ, Van der Plas HJ (1956) The crystal structure of ferrocarpholite. Acta Crystallogr 19:718–721

Maresch WV, Czank M (1981) Crystal chemistry of Mn-antophyllite: are synthetic amphiboles suitable for stability studies? European Union of Geosciences, 1st meeting, Strasbourg (Abstr)

Mirwald PW, Getting IC, Kennedy GC (1975) Low-friction cell for piston-cylinder high-pressure apparatus. J Geophys Res 80:1519–1525

Mottana A, Schreyer W (1977) Carpholite crystal chemistry and preliminary experimental stability. N Jahrb Mineral Abh 129:113–138

Naumova IS, Pobedimskaya EA, Belov NV (1975) Crystal structure of carpholite $MnAl_2Si_2O_6(OH)_4$. Sov Phys Crystallogr 19:718–721

Roever EWF de (1977) Chloritoid-bearing metapelites associated with glaucophane rocks in Western Crete. Some remarks. Contrib Mineral Petrol 60:317–319

Ross M (1968) X-ray diffraction effects by non-ideal crystals of biotite, muscovite, montmorillonite, mixed-layer clays, graphite and periclase. Z Kristallogr 126:80–97

Seidel E, Okrusch M (1977) Chloritoid-bearing metapelites associated with glaucophane rocks in western Crete, Greece. Additional comments. Contrib Mineral Petrol 60:321–324

Steen D, Bertrand J (1977) Sur la présence de ferrocarpholite associée aux schistes à glaucophane de Haute-Ubaye (Basses Alpes, France). Schweiz Mineral Petrogr, Mitt 57:157–168

Viswanathan K, Seidel E (1979) Crystal chemistry of Fe–Mg carpholites. Contrib Mineral Petrol 70:41–47

Yvon K, Jeitschko W, Parthé E (1977) LAZY PULVERIX, a computer program for calculating X-ray and neutron diffraction powder patterns. J Appl Crystallogr 10:73–74

Accepted March 12, 1981

[American Journal of Science, Vol. 283-A, 1983, P. 72-96]

MAGNESIOCARPHOLITE AND MAGNESIOCHLORITOID: TWO INDEX MINERALS OF PELITIC BLUESCHISTS AND THEIR PRELIMINARY PHASE RELATIONS IN THE MODEL SYSTEM $MgO-Al_2O_3-SiO_2-H_2O$

CHRISTIAN CHOPIN* and WERNER SCHREYER

Institut für Mineralogie, Ruhr-Universität,
D-4630 Bochum 1, West Germany

ABSTRACT. Metapelitic rocks from blueschist-facies terranes, hitherto considered to be devoid of critical mineral assemblages, are in fact not. Recently described rocks from the Alps and the Mediterranean contain two index minerals for blueschist metamorphism: carpholite, $(Mg,Fe^{2+})Al_2[Si_2O_6](OH)_4$, with compositions varying from the Fe to the Mg endmember, and Mg-rich chloritoid, $(Mg,Fe^{2+})Al_2O[SiO_4](OH)_2$, containing up to 74 mol percent Mg endmember. On the basis of their assemblages, four different grades of blueschist metamorphism can be distinguished in simple AFM-plots (in the order of increasing grade): (1) only Fe-rich carpholite present; (2) Mg-rich carpholite coexisting with Fe-rich chloritoid; (3) intermediate Fe–Mg chloritoid with talc and chlorite; (4) Mg-rich chloritoid with talc and kyanite.

High-pressure experimentation in the system $MgO-Al_2O_3-SiO_2-H_2O$ in the range 15 to 35 kb water pressure and 400° to 800°C led to the synthesis of both magnesiocarpholite and magnesiochloritoid. The preliminary petrogenetic grid derived from a limited number of bracketing runs shows both minerals to be typical high-pressure phases with stability fields limited by minimum pressures of about 7 kb for Mg–carpholite and 18 kb for Mg–chloritoid. The less hydrous Mg–chloritoid is stable at higher temperatures, but its stability range overlaps with that of the carpholite phase.

As a result of the relative locations of the stability fields of the Fe and Mg endmembers of both the carpholite and the chloritoid series, FeMg–carpholites and Mg-rich chloritoids can form only under metamorphic conditions characterized by low geothermal gradients (about 8°-15°C/km). The four consecutive metamorphic grades of blueschist metapelites outlined above can be rationalized by mineral reactions occurring in the petrogenetic grid of the Fe-free model system, although for Mg–chloritoid its metastable phase relations with quartz have to be taken into account. The two metapelitic index minerals and their varying parageneses and Mg/Fe ratios may become useful geobarometers and thermometers for different types and grades of blueschist metamorphism in complex areas of subduction.

INTRODUCTION

Until very recently, petrologic studies in blueschist metamorphic terranes concentrated strongly on basic igneous rocks and graywackes, which — due to their bulk chemistry — may develop characteristic blueschist in-

* Present address: Laboratoire de Géologie, Ecole normale supérieure, 46 rue d'Ulm, F-75005 Paris, France

dex minerals such as glaucophane, jadeite, lawsonite, and aragonite, all being Na- or Ca-bearing phases. Indeed, a set of new hydrous calcium silicates was detected through such studies: they are rosenhahnite (Pabst, Gross, and Alfors, 1967; Pabst, 1977), vuagnatite (Sarp, Bertrand, and McNear, 1976), and chantalite (Sarp, Deferne, and Liebich, 1977), among which at least rosenhahnite may be confined in its pressure temperature stability to the blueschist environment (Leistner and Chatterjee, 1978). Mineralogical work on iron-rich metasediments within blueschists had revealed the existence of three new hydrous iron silicate minerals: deerite, howieite, and zussmanite (Agrell, Brown, and McKie, 1965), which later on turned out to represent additional index minerals for this metamorphic facies (Muir Wood, 1979a,b, 1980; Lattard and Schreyer, 1981).

On the other hand, rocks of pelitic compositions appeared to be free from minerals or mineral assemblages diagnostic for blueschist metamorphism (compare Miyashiro, 1973; Turner, 1981; Winkler, 1979), if one ignores the common but not spectacular occurrence of Si-rich phengites instead of muscovite (Ernst, 1963). The surprising discovery of phengite coexisting with talc (Abraham and Schreyer, 1976) initiated more detailed studies of the blueschist phyllosilicate assemblages, especially after it was shown experimentally that the assemblage phengite–talc does indeed form at high pressures (Schreyer and Baller, 1977). Recently Chopin (1981) demonstrated that this pair is of widespread occurrence in high-grade pelitic blueschists of the Western Alps. Independently, it was shown by several authors who will be quoted in the next section that pelitic blueschists carry Mn-poor, *(Mg,Fe)-rich carpholites* which have never been found in metapelites of low- and medium-pressure metamorphism. In the latter environments carpholite is predominantly a manganese mineral with the formula $(Mn^{2+},Mg,Fe^{2+})(Al,Fe^{3+})_2[Si_2O_6](OH)_4$ (Mottana and Schreyer, 1977). Finally and significantly, *Mg-rich chloritoids* ("sismondines"), $(Mg,Fe^{2+})(Al,Fe^{3+})_2O[SiO_4](OH)_2$, have thus far been found only in areas where glaucophane occurs (Bearth, 1963). Thus it would seem that, despite classical prejudice, metapelites in blueschist environments are not necessarily devoid of critical mineral assemblages.

In the present paper we attempt to approach the problem of the behavior of metapelitic rocks under blueschist facies conditions from two different ends:

First, the mineral assemblages as described in the petrographic literature on relevant natural rocks are reviewed, and a subdivision relating to different metamorphic grades within the blueschist facies is proposed, also trying to define the interconnecting mineral reactions.

Second, new experimental results in the simplest model system for metapelites, that is $MgO–Al_2O_3–SiO_2–H_2O$, are presented that define, in a preliminary fashion, phase relations at high water pressures and low temperatures thus extending the work of Schreyer and Seifert (1969a,b) toward lower temperatures, where previously no reactions had been achieved. The incentive for this study was the surprising success of Chopin and Goffé (1981) to synthesize pure magnesiocarpholite, $Mg_4Al_2[Si_2O_6](OH)_8$, and more recently, also pure magnesiochloritoid (Chopin, in preparation).

TABLE 1

Mineralogy of high-pressure, low-temperature metapelites
(Fe–carpholite: < 50 mol% Mg endmember; Mg–carpholite: > 50 mol% Mg endmember; Fe–chloritoid: < 25 mol% Mg endmember; Fe–Mg–chloritoid: 25-50 mol% Mg endmember; Mg–chloritoid: > 50 mol% endmember)

Locality	Mineral contents in metapelitic rocks	Type of occurrence	Index minerals or parageneses in neighboring rocks; additional remarks	References
Eastern Central Sulawesi (Celebes, Indonesia)	Fe–carpholite, quartz, white mica, chlorite, hematite	Quartz veins, metaconglomerate mesostasis, blastopsammitic quartzite	Lawsonite, jadeite–quartz, crossite, Mg–riebeckite, aragonite. No chloritoid	W. P. de Roever, 1947, 1951; W. P. de Roever and Beunk, 1978
Haute Ubaye (Piemont zone, Western Alps, France)	Fe–carpholite, quartz, calcite	Vein in calc–schist	Lawsonite, jadeite–quartz, glaucophane. No chloritoid, no garnet	Scaini, Mottana, and Abraham, 1976
Amorgos island (Greece)	Fe–carpholite	Vein in metabauxite	Blue amphibole? Probably no chloritoid, no garnet	Minoux, Bonneau, and Kienast, 1981
Eastern Crete (Greece)	Fe–carpholite, quartz, calcite, pyrophyllite, chlorite	Pyrophyllite schist, segregations in sheared zones of quartzites and phyllites	Riebeckite/crossite, aegyrine–augite, lawsonite. No garnet, no chloritoid	Seidel, 1978 Viswanathan and Seidel, 1979
Central Crete	Fe–carpholite, Fe–chloritoid, pyrophyllite or chlorite, white micas, hematite, quartz	Phyllites, vein fillings	Remnants of blue amphiboles (glaucophane, crossite)	Seidel, 1978 Viswanathan and Seidel, 1979
	Mg–carpholite, pyrophyllite, diaspore, (Fe–chloritoid)	Metabauxites		
Western Crete	Mg–carpholite, Fe–chloritoid, chlorite, white micas, hematite	Schists, vein fillings	Glaucophane, omphacite, lawsonite, aragonite. No garnet	Seidel, 1978 Viswanathan and Seidel, 1979
Southern Briançon zone (Western Alps, Italy)	Fe–carpholite, Fe–chloritoid, chlorite, white micas, lawsonite, quartz	Schists	Lawsonite, jadeite–quartz, glaucophane — No garnet	Chopin and Goffé, unpub. data
	Mg–carpholite, quartz	Vein filling in phengite–chlorite schists		
Peloponnesus (Greece)	Mg–carpholite, Fe–chloritoid, quartz, chlorite	Schists, vein fillings	Glaucophane, lawsonite, garnet	Skarpelis and Seidel, in preparation
Northern Calabria (Italy)	Fe–carpholite	Veins in phyllite	Lawsonite, albite, pumpellyite, chlorite	E. W. F. de Roever and Beunk, 1971

		Glaucophane, ferroglaucophane, crossite, jadeite–quartz, lawsonite, aragonite. No chloritoid	E. W. F. de Roever and Beunk, 1971 W. P. de Roever and others, 1967; W. P. de Roever and Beunk, 1978
		Greenschist parageneses but remnants of lawsonite, blue amphibole, and green sodic pyroxene. No Fe–carpholite	Dubois, 1976; Dubois and Kienast, 1975; E. W. F. de Roever and Beunk, 1971
		Lawsonite No garnet?	Goffé, Goffé-Urbano, and Saliot, 1973; Goffé and Saliot, 1977; Goffé, 1979, 1980, 1982
		Albite, epidote, chlorite, glaucophane, diaspore, garnet	Okrusch, 1981
		Glaucophane, lawsonite, garnet, green Na–pyroxene. Kyanite? No carpholite	W. P. de Roever, 1947, 1956
		Omphacite–garnet, jadeite–quartz, margarite, zoisite. No carpholite	Chopin, 1979, 1981
		Omphacite–garnet, zoisite. No carpholite	Bearth, 1963, 1967 Chinner and Dixon, 1973
		Omphacite–garnet, zoisite, margarite. No carpholite	Chopin, unpub. data
		Omphacite–garnet, glaucophane, zoisite, margarite. No carpholite	Miller, 1974, 1977
	Fe–carpholite, quartz, calcite, white micas, chlorite, vermiculite	Veins in phyllite, marble, quartzite	
Central Calabria	Mg–carpholite, Fe–chloritoid, quartz, calcite, chlorite	Quartzite	
Vanoise and Liguria (Western Alps, France and Italy, respectively)	Mg–carpholite, Fe–chloritoid, quartz, pyrophyllite, diaspore, chlorite, white micas, cookeite	Aluminous metapelite, metabauxite, quartz veins	
Samos island (Greece)	Mg–carpholite, Fe–Mg–chloritoid, chlorite, quartz, kyanite, pyrophyllite, white micas	Phyllite	
Western Central Sulawesi, Southeast Sulawesi and Kabaena (Indonesia)	Fe–Mg–chloritoid, quartz, garnet, white mica, Mg–chlorite	Schists	
	Fe–Mg–chloritoid, garnet, lawsonite, glaucophane, chlorite, white mica	Schists	
Gran Paradiso area and Aosta valley (Western Alps, France and Italy)	Fe–Mg–chloritoid, quartz, garnet, talc, Mg–chlorite, glaucophane, white micas, epidote	Quartzite, schist	
Zermatt area (Western Alps, Switzerland)	Fe–Mg–chloritoid, talc, garnet, glaucophane, quartz, epidote	Metabasite, schist	
	Mg–chloritoid, talc, kyanite, garnet, Mg–chlorite, omphacite	Mafic microsystems within unfoliated metagabbro	
Monte Rosa area (Western Alps, Italy)	Mg–chloritoid, talc, Mg–chlorite, quartz, kyanite, phengite	Talc–chloritoid quartzite	
Hohe Tauern (Eastern Alps, Austria)	Mg–chloritoid, talc, kyanite, either quartz or Mg–chlorite	Pelitic pods within eclogite	

While the detailed experimental data will be published elsewhere, we wish to emphasize, in this homage to the late P. M. Orville, the application of our results to a kind of progressive metamorphism that seems to be typical of subduction zones along Alpine-type plate boundaries. We hope that Phil, who had developed a keen interest in the metamorphism of the Alps as well as of other Alpidic Mediterranean areas, would have appreciated this contribution.

MINERALS AND MINERAL ASSEMBLAGES OF HIGH-PRESSURE, LOW-TEMPERATURE METAPELITES

The main results of recent petrographic work on metapelites and related rocks from blueschist terranes, largely of the Alps and the Mediterranean, are summarized in table 1. Only assemblages of regional significance are mentioned. This compilation shows that, indeed, FeMg–carpholite and chloritoid are common mineral constituents which may coexist with quartz, pyrophyllite, diaspore, chlorite, and, possibly, garnet, talc, and/or kyanite, as far as alkali- and Ca-free phases are concerned. A brief survey of the chemical variations of both carpholite and chloritoid (fig. 1) confirms that in the blueschist facies these minerals are virtually confined to ferromagnesian compositions. Low-pressure metamorphic environments carry *only* Mn-dominant carpholites; Fe-rich chloritoids may appear both in blueschist and low-pressure regimes.

On the basis of the mineral contents given in table 1, both of metapelites and of neighboring rocks with different chemistry, all the blueschist environments listed can readily be subdivided into two groups:

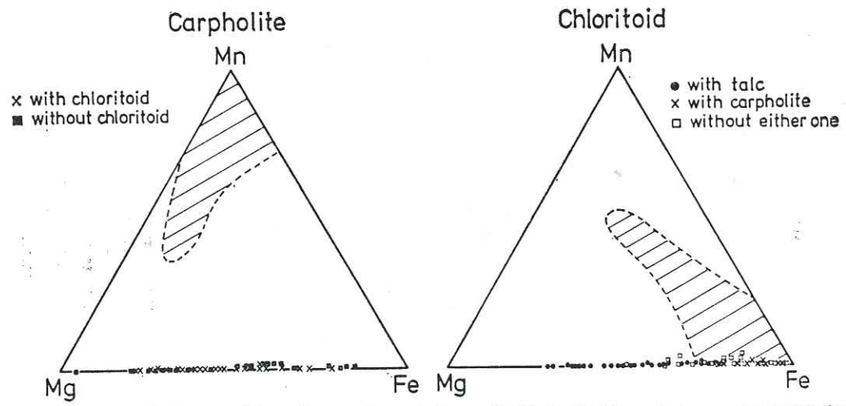

Fig. 1. Chemical composition of natural carpholite and chloritoid. The ruled areas represent the compositional ranges in the low- to intermediate-pressure metamorphic areas. Blueschist-facies carpholite and chloritoid are shown individually, indicating their parageneses by different symbols. Data for carpholite were taken from Goffé (ms), Kramm (1980), Viswanathan and Seidel (1979) and from the compilation of Mottana and Schreyer (1977); for chloritoid from Bearth (1963), Chopin (ms, and unpub. data), Fransolet (1978), Goffé (ms), Halferdahl (1961), Kramm (1980), and Miller (1977).

1. Those exhibiting a relatively low grade of metamorphism indicated by the occurrence of pyrophyllite, diaspore, and lawsonite. Typical mafic phases of the metapelites are here carpholite and chlorite. This group includes about the first dozen localities of table 1.
2. Other environments which, due to the appearance of kyanite, margarite, and zoisite, represent a higher grade of metamorphism. They carry Mg-rich chloritoid, talc, and garnet as mafic phases.

The phyllite from Samos, in which Okrusch (1981) found coexisting magnesiocarpholite, Mg-rich chloritoid, and kyanite may be taken as a transitional type between the two groups. The above grouping can be further refined, if the mineral chemistry of the mafic metapelite phases is taken into account. Ferrocarpholite occurs largely in regions where neither chloritoid nor garnet is known. Eastern Crete, Haute Ubaye, Northern Calabria, and the Celebes occurrence are examples of what is considered here to represent the lowest grade of metamorphism amongst the

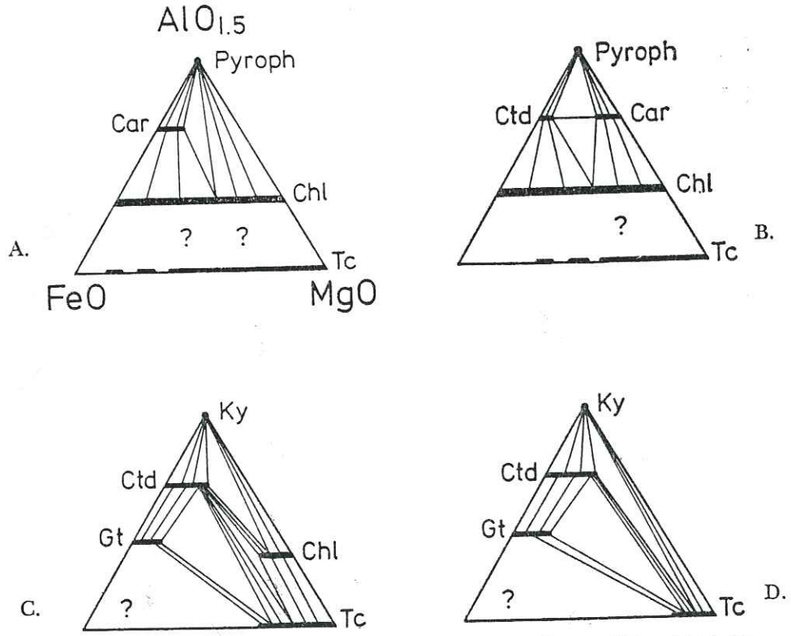

Fig. 2. Four characteristic stages in the mineralogical evolution of blueschist facies metapelites, as represented by AFM-type plots with excess quartz. The sequence A to D indicates principally increasing metamorphic grade. For further discussion see text. Abbreviations: Car = carpholite, Chl = chlorite, Ctd = chloritoid, Gt = garnet, Ky = kyanite, Pyroph = pyrophyllite, Tc = talc.

PLATE 1

Microphotographs of some important assemblages in blueschist metapelites (abbreviations as in figure 2; q = quartz).

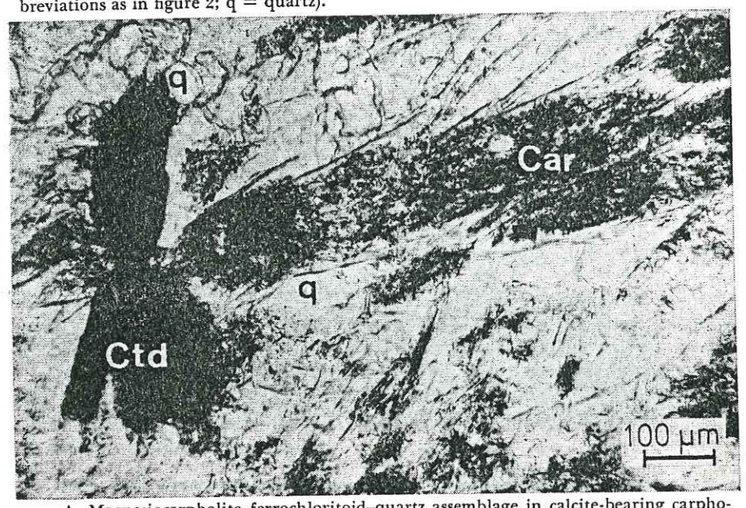

A. Magnesiocarpholite–ferrochloritoid–quartz assemblage in calcite-bearing carpholite schist from the Vanoise area, France (specimen courtesy of B. Goffé). Plane polarized light.

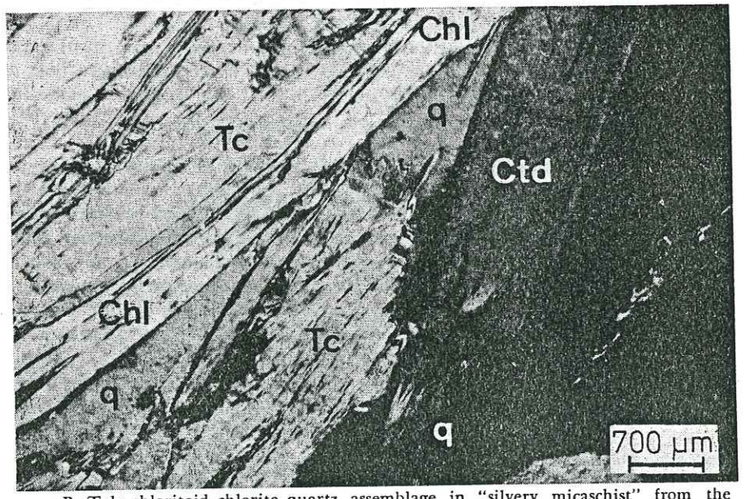

B. Talc–chloritoid–chlorite–quartz assemblage in "silvery micaschist" from the Gran Paradiso area, France. Crossed nichols.

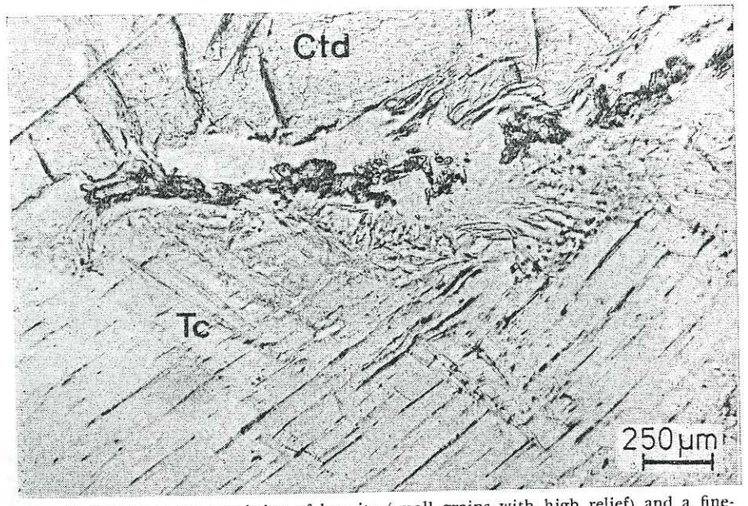

C. Reaction zone consisting of kyanite (small grains with high relief) and a fine-grained chlorite groundmass (white) between magnesiochloritoid (upper portion) and talc (lower portion). Chloritoid quartzite from the Monte Rosa area, Italy. Plane polarized light.

localities of table 1. The AFM-type plot of figure 2A depicts schematically the characteristic phase relations, which involve the coexistence of chlorite and pyrophyllite (Seidel, 1978, p. 112).

As a next step toward higher grade, iron-rich chloritoid appears and may coexist with a more Mg-rich ferrocarpholite (Central Crete, southern Briançon zone) and, subsequently, even with magnesiocarpholite (Western Crete; Vanoise, see pl. 1-A; Liguria; Southern Calabria; Peloponnesus). In 1977 E. W. F. de Roever recognized the significance of carpholite–chloritoid coexistence, in which both phases become increasingly rich in Mg with rising grade. Seidel (1981) and Goffé (ms) confirmed this to be one of the key features of the low grades in the high-pressure metamorphic evolution of pelitic rocks. It should be emphasized, however, that the Mg contents of the chloritoid are still relatively low and fall into the same range as for chloritoids of "normal," low-pressure metamorphic terranes (fig. 1). Figure 2B illustrates the paragenetic relationships indicating that, in the presence of quartz, the carpholite–chloritoid assemblage prohibits the coexistence of chlorite and pyrophyllite, which form a typical pair in lower-pressure metamorphic terranes (for example, Tobschall, 1969; Frey, 1978), but probably also in the lowest grades of the high-pressure evolution (compare fig. 2A). In the higher-grade assemblages with Mg-rich chloritoid, but without carpholite, the common characteristic is the appearance of the pairs FeMg garnet–talc and chloritoid–talc which are due to a progressive restriction of the stability of chlorite in the presence of quartz.

First, talc, chloritoid, and quartz may still coexist with Mg-rich chlorite as in the Gran Paradiso area (pl. 1-B; fig. 2C). At a still more advanced stage chlorite disappears from the assemblage in favor of the pair talc–kyanite (Zermatt area; Hohe Tauern; fig. 2D), leading to kyanite–talc whiteschists in highly magnesian rocks, as described by Schreyer (1977).

Obviously, the evolutionary sequence presented in figure 2, A to D, is by no means complete, and it may indeed be questioned as to whether or not the different stages recognized from different areas do belong to a *single trend* of increasing metamorphic grade. However, this sequence appears reasonable, if one emphasizes the stepwise dehydration of the mineral assemblages that is so characteristic in progressive metamorphism. Thus the following general conclusions about mineral stabilities seem justified and should be compared with the results of the experimental work to be reported later:

1. The long-standing question of the relative stabilities of chloritoid and carpholite, first posed for the Mn-rich members carpholite sensu stricto and ottrelite (Mügge, 1918), finds a clear answer from figure 2 with chloritoid being the high-temperature mineral. For any given intermediate Mg/Fe ratio carpholite breaks down with rising temperature into the less hydrous alternative assemblage according to the reaction:

$$\text{MgFe carpholite} \rightarrow \text{MgFe chloritoid} + \text{quartz} + H_2O \qquad (1)$$

2. Since, in the above divariant breakdown reaction, Mg is preferentially incorporated in carpholite, magnesiocarpholite must be stable, for a given water pressure, toward higher temperatures than ferrocarpholite.
3. The relative stabilities are similar in the MgFe–chlorite series, in the presence of quartz, with the following breakdown reactions taking place at increasing grade:

$$\text{Fe-rich chlorite} + \text{quartz} \rightarrow \text{garnet} + \text{talc} + H_2O \qquad (2)$$

$$\text{FeMg–chlorite} + \text{quartz} \rightarrow \text{FeMg chloritoid} + \text{talc} + H_2O \qquad (3)$$

$$\text{Mg–chlorite} + \text{quartz} \rightarrow \text{kyanite} + \text{talc} + H_2O \qquad (4)$$

4. The formation of very Mg-rich chloritoid, in the presence of quartz, does not seem to be due to the breakdown of preexisting Mg-rich carpholites but rather follows the reactions

$$\text{chlorite} + \text{kyanite} + H_2O \rightarrow \text{chloritoid} + \text{quartz} \qquad (5)$$

$$\text{talc} + \text{kyanite} + H_2O \rightarrow \text{chloritoid} + \text{quartz} \qquad (6)$$

both of which require the addition of water. This seems anomalous for progressive metamorphism, and the PT slope of the requisite reaction curves will be of particular interest.

All these mineral reactions derived from petrologic observation would obviously require experimental investigations in the system MgO–FeO–Al_2O_3–SiO_2–H_2O. The results to be discussed in the following section

from the system $MgO–Al_2O_3–SiO_2–H_2O$ can, therefore, only represent a limiting case, which may, or may not, be a model for the phase relations deduced from natural blueschist metapelites.

EXPERIMENTAL RESULTS IN THE SYSTEM $MgO–Al_2O_3–SiO_2–H_2O$

A systematic study of phase relations in the system $MgO–Al_2O_3–SiO_2–H_2O$ at water pressures in excess of 10 kb has thus far not been undertaken. However, the reconnaissance study of Schreyer (1968) had revealed a fascinating set of new high-pressure phases like yoderite, Mg–staurolite, and kornerupine that were characterized in more detail by Schreyer and Seifert (1969a). Although a few experiments had also been performed at relatively low temperatures, the phase magnesiocarpholite was not encountered, and the appearance of small amounts of magnesiochloritoid could only be suspected (Schreyer, 1968). In the present study experiments were conducted at water pressures between 15 and 35 kb and in the temperature range from 400° to 800°C. Figure 3 depicts all the crystalline phases encountered or considered relevant for the phase relations to be discussed in this PT-range.

Synthesis of magnesiocarpholite and magnesiochloritoid.—The first synthesis of a phase with a *carpholite* structure of the endmember composition $MgAl_2[Si_2O_6](OH)_4$ was recently reported by Chopin and Goffé (1981): Synthesis conditions were 25 kb water pressure and temperatures between 415° and 600°C. Like natural carpholite the synthetic phase is orthorhombic, space group Ccca, and the cell parameters are a = 13.706; b = 20.075; c = 5.107 Å.

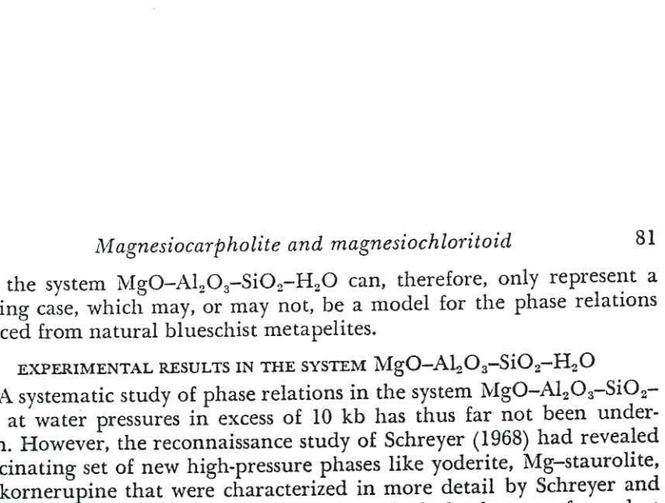

Fig. 3. Selected crystalline phases of the system $MgO–Al_2O_3–SiO_2–H_2O$ projected onto the water-free plane.

TABLE 2

Stable and metastable reactions investigated in the system $MgO–Al_2O_3–SiO_2–H_2O$

A. Stable reactions	
Carpholite $\rightleftharpoons$ chlorite + kyanite + quartz + H_2O	(8)
Carpholite $\rightleftharpoons$ chlorite + kyanite + talc + H_2O	
Carpholite + quartz $\rightleftharpoons$ kyanite + talc + H_2O	
Carpholite + diaspore = chlorite + kyanite + H_2O	(7)
Chloritoid $\rightleftharpoons$ chlorite + kyanite + corundum + H_2O	
Chloritoid $\rightleftharpoons$ pyrope + corundum + H_2O	
Chloritoid + talc $\rightleftharpoons$ chlorite + kyanite	(10)
B. Metastable reactions	
Carpholite $\rightleftharpoons$ chloritoid + quartz + H_2O	(1)
Chloritoid + quartz $\rightleftharpoons$ talc + kyanite + H_2O	(6)

Numbers refer to reactions discussed in the text.

Magnesiochloritoid, $MgAl_2O[SiO_4](OH)_2$, could be synthesized from the anhydrous composition $MgO \cdot Al_2O_3 \cdot SiO_2$ (fig. 3) only at water pressures in excess of 30 kb and at temperatures between 600° and 750°C. Powder X-ray diffraction patterns of the synthetic products indicate that both the monoclinic and the triclinic chloritoid polytypes are present, with the triclinic one dominating and increasing in amount at rising tem-

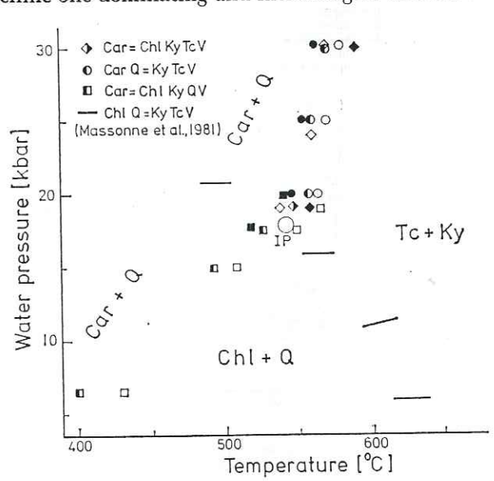

Fig. 4. Results of bracketing runs conducted to define the location of the invariant point IP involving the phases magnesiocarpholite (Car), chlorite (Chl), talc (Tc), kyanite (Ky), quartz (Q), and fluid (V) near 18 kb, 540°C. Filled symbols show reaction proceeding to left or right as indicated, half-filled symbols no reaction. Bars represent brackets obtained by Massonne, Mirwald, and Schreyer (1981) on the reaction as given in the inset leading to the pairs shown by large letters in the lower and upper right portion. The large field of the assemblage Car–Q is indicated crudely on the left.

perature, as one would expect from entropy considerations. The cell parameters of the triclinic form are a = 9.43; b = 5.44; c = 9.13 Å; and α = 96.4°; β = 101.1°; γ = 90.0°; space group C 2/c.

Preliminary phase relations.—A limited number of reactions that were considered appropriate to constrain the topology of the system have been investigated experimentally thus far (table 2). For each reaction a mixture of presynthesized, crystalline reactants and products in nearly stoichiometric proportions was used as starting material. The curves of those reactions which turned out to be stable were determined reversibly in the range 15 to 30 kb, some of them also along their metastable extensions.

For the present purpose, the experimental results were used in combination with a chemographic analysis of the system to construct a preliminary petrogenetic grid that encompasses primarily the phase relations of the synthetic phases magnesiocarpholite and magnesiochloritoid. The detailed experimental results will be published elsewhere (Chopin, in

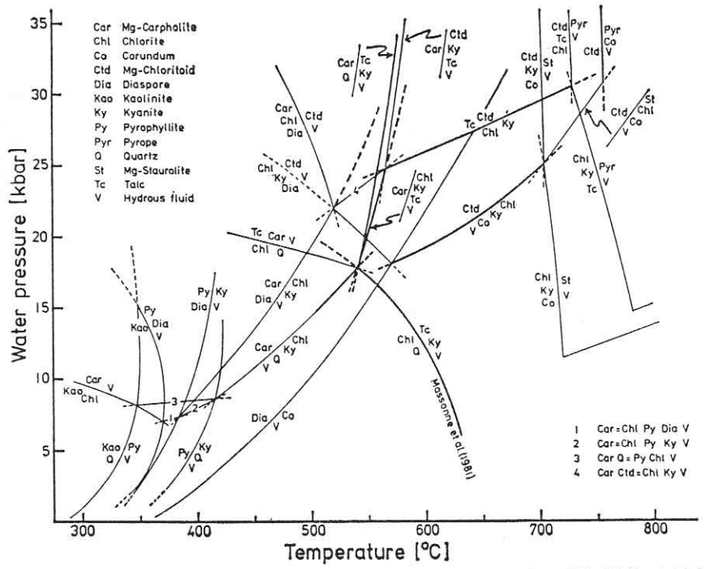

Fig. 5. Selected stable phase relations in the system MgO–Al_2O_3–SiO_2–H_2O at high water pressure and low to moderate temperature. The position of the heavy curves is based upon experimental equilibrium determinations (see table 2). The light curves are either calculated (in the system Al_2O_3–SiO_2–H_2O; Halbach and Chatterjee, 1982b), extrapolated, or estimated. The data concerning the stability of Mg–staurolite and pyrope are adapted from Schreyer and Seifert (1969a), and, for clarity, the stability field of pyrope has been chosen to lie entirely within that of Mg–staurolite. The quartz–coesite transition is ignored in this representation. Numbers 1 to 4 refer to the reactions which for clarity reasons are given in the lower right hand corner of the figure but do not correspond to the reaction numbers used in the text.

preparation), but some critical run data bearing on carpholite stability above 15 kb are given in figure 4 and table 3. Figure 4 also shows brackets reported by Massonne, Mirwald, and Schreyer (1981). For pressures below 15 kb the phase relations shown in the grid of figure 5 have been deduced by extrapolating the curves of the reactions

$$\text{carpholite} + \text{diaspore} = \text{kyanite} + \text{chlorite} + H_2O \quad (7)$$

and

$$\text{carpholite} = \text{kyanite} + \text{chlorite} + \text{quartz} + H_2O \quad (8)$$

established at higher pressures and considering their intersections with the reaction curves of the system Al_2O_3–SiO_2–H_2O as calculated by Halbach and Chatterjee (1982b). This extrapolation is loosely constrained by unreversed experimental data at 6.5 kb for reaction (8) and at 14 kb for the reaction (see table 3)

$$\text{carpholite} = \text{chlorite} + \text{pyrophyllite} + \text{diaspore} + H_2O. \quad (9)$$

The petrogenetic grid of figure 5 also takes into account that, according to the experimental results of Goffé (ms), natural magnesiocarpholite (66 mole percent Mg endmember) is unstable at and below 4 kb water pressure at all temperatures. The resulting low-pressure topology, provided no additional phase is considered (see below), represents a unique solution, although the exact locations and slopes of the different curves (for example 1, 2, 3 in fig. 5) are still unknown. Their overall uncertainty on the low-pressure stability limit of magnesiocarpholite is thought to be

TABLE 3

Results of critical runs bearing on the stability of magnesiocarpholite. Symbols for reaction rate are: + weak reaction, ++ strong reaction, +++ complete or nearly complete reaction. Abbreviations as in figure 5

P_{H_2O} (kbar)	T (°C)	Duration (hours)	Solid phases	Reaction rate
Reaction	carpholite = chlorite + kyanite + quartz + H_2O (8)			
19.9	539	97	Car +, Chl Ky Q −	+
19.0	564	87	Car −, Chl Ky Y +	++
17.7	517	182	Car +, Chl Ky Q −	++
17.5	549	126	Car −, Chl Ky Q +	+++
15.0	508	236	Car −, Chl Ky Q +	+
6.5	430	2260	Car −, Chl Ky Q +	+
Reaction	carpholite = chlorite + pyrophyllite + diaspore + H_2O (9)			
14.0	530	120	Car +, Chl Py Dia −	++
Reaction	carpholite = chlorite + kyanite + talc + H_2O			
19.0	535	137	Car +, Chl Ky Tc −	+
19.1	557	119	Car −, Chl Ky Tc +	+
30.0	569	115	Car +, Chl Ky Tc +	+
29.9	587	85	Car −, Chl Ky Tc +	+++
Reaction	carpholite + quartz = talc + kyanite + H_2O			
20.0	543	94	Car Q +, Tc Ky −	+
20.0	561	120	Car Q −, Tc Ky +	+
30.1	560	83	Car Q +, Tc Ky −	+
30.1	580	46	Car Q −, Tc Ky +	+

± 2 kb. In its high-temperature portion the grid utilizes earlier data of Schreyer and Seifert (1969a).

The salient features of the new grid (fig. 5) may be enumerated as follows:

1. Magnesiocarpholite and magnesiochloritoid are indeed high-pressure phases with stability fields limited by minimum pressures of about 7 and 18 kb, respectively. Compared with magnesiocarpholite, the pressure uncertainty for the magnesiochloritoid stability is smaller (± 1 kb).
2. Magnesiocarpholite is, relatively speaking, the low-temperature phase. Its stability field lies entirely within the diaspore field, with an upper temperature stability near 580°C for 30 kb water pressure.
3. Both magnesiocarpholite and magnesiochloritoid also exhibit low-temperature stability limits, along which they break down into more hydrous assemblages.
4. Mg–chloritoid displays phase relations with Mg–carpholite in the low-temperature part of its stability field and with Mg–staurolite as well as pyrope near its high-temperature end at about 750°C and high water pressures.
5. This indicates that, at pressures of 20 kb and more, the entire subsolidus range of the system $MgO–Al_2O_3–SiO_2–H_2O$ is continuously covered by overlapping stability fields of high-pressure MgAl silicates. The Fe analogues of most of these phases are well-known minerals stable at low pressures.
6. Mg–chloritoid does not seem to display stable phase relations with boron-free kornerupine, because this phase forms only at higher temperatures (Seifert, 1975). The same appears to hold for yoderite, especially as this phase may show an upper pressure limit near 25 kb (Schreyer and Seifert, 1969a, p. 423).
7. Mg–chloritoid cannot coexist with quartz over the entire area of the stability range investigated, alternative assemblages like talc–kyanite or just carpholite alone being stable up to the quartz–coesite transition. However, Mg–chloritoid might well coexist with coesite at still higher pressures.
8. Mg–carpholite, on the other hand, may appear in the presence of quartz over most of its stability field except probably for a small area near the low-pressure end.
9. The invariant point located near 18 kb, 540°C and involving the solid phases chlorite, quartz, talc, kyanite, and Mg–carpholite terminates the reaction curve

$$\text{chlorite} + \text{quartz} \rightarrow \text{talc} + \text{kyanite} + H_2O \qquad (4)$$

which is considered to represent the lower temperature stability limit of whiteschists (Schreyer, 1977) and, equally, the upper thermal stability of the chlorite–quartz pair (fig. 4). At pressures higher and at temperatures lower than that of the invariant point the chlorite–quartz stability is even more restricted due to its breakdown into the assemblage talc + Mg–carpholite. Moreover, at pressures above that of the invariant point, the whiteschist assemblage talc–kyanite is limited, toward lower temperatures, by a reaction to form carpholite + quartz. The temperature of the invariant point (540°C) thus represents the absolute temperature minimum for the appearance of talc + kyanite in the presence of excess water vapor.

10. The assemblage chlorite + kyanite, which was found unstable in nearly all experiments conducted by Schreyer (1968) thus leading to a drastic rearrangement of tie lines (for example, talc–corundum, talc–Mg staurolite) at higher temperatures, can be seen in figure 5 to be limited toward higher pressures by a sequence of breakdown reactions. They cause the appearance of the following alternative pairs, beginning at high temperatures and pressures: Mg–chloritoid + talc; Mg–chloritoid + Mg–carpholite; and Mg–carpholite + diaspore. All these pairs have Mg–Fe-bearing analogues in blueschist metapelites (see table 1). The reaction

$$\text{chlorite} + \text{kyanite} = \text{talc} + \text{Mg–chloritoid} \qquad (10)$$

releases no, or only very little, water, depending on the exact compositions of the chlorite and talc phases participating, thus resulting in a rather flat PT slope (see fig. 5). Therefore, the high-pressure pair chloritoid–talc is restricted, in the purely magnesian system, to astonishingly high water pressures of at least 25 kb.

Finally, it should be noted that the phase relations near the low-pressure end of the magnesiocarpholite stability field may yet have to be modified drastically upon further experimentation. Fransolet and Schreyer (ms in preparation) have found that the di/trioctahedral chlorite *sudoite* (fig. 3), $Mg_2Al_3[AlSi_3O_{10}](OH)_8$ (see also Fransolet and Bourguignon, 1978), has a low-pressure, low-temperature stability field extending at least to some 7 kb water pressure and 350°C. Therefore a reaction relationship

$$\text{sudoite} + \text{quartz} = \text{magnesiocarpholite} \qquad (11)$$

may exist which, importantly, does not involve loss or gain of water and shows a strong volume decrease (> 6 percent) toward the formation of Mg–carpholite. Thus the requisite reaction curve must be strongly pressure-dependent. It would lead to still another low-pressure equivalent of magnesiocarpholite (see also Chopin and Goffé, 1981). If the sudoite/Mg–carpholite reaction is indeed stable, the lower pressure limit of magnesiocarpholite would be raised against that shown in figure 5 thus making this mineral an even more pronounced high-pressure phase.

APPLICATION AND DISCUSSION

As indicated before, the phase relations depicted in figure 5 for the pure magnesian system can only be considered as a limiting case for the metapelite reactions deduced from natural assemblages. Perhaps the most severe deviation of the synthetic system from the natural one is the incom-

patibility of Mg–chloritoid with quartz. Thus two of the outstanding natural reactions, namely

$$\text{carpholite} = \text{chloritoid} + \text{quartz} + H_2O \quad (1)$$

$$\text{chlorite} + \text{quartz} = \text{chloritoid} + \text{talc} + H_2O \quad (3)$$

do not appear in the petrogenetic grid of figure 5. For due comparison, therefore, the metastable locations of these reaction curves in the pure magnesian system will have to be employed.

As a first approach figure 6 summarizes the known and estimated stability limits of the Mg- and Fe-endmembers of the carpholite, chloritoid, and staurolite mineral series. The stability limits of ferrocarpholite, $FeAl_2[Si_2O_6](OH)_4$, which thus far could not be synthesized despite considerable efforts by Beunk and Maresch (personal commun., 1978), were estimated in accordance with the data of table 1 and figure 2,A and B. The result turns out to be basically consistent with the pressure-temperature behavior of Fe–chloritoid and Fe–staurolite relative to their Mg endmembers. However, both the ferrocarpholite stability and the low-temperature end of the Fe–chloritoid field might actually lie as much as 100°C lower than drawn in figures 6 and 7.

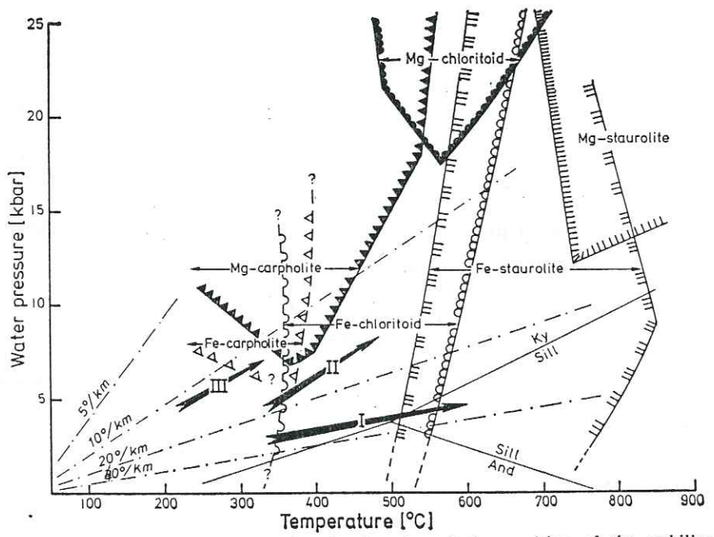

Fig. 6. Pressure-temperature plot showing the relative position of the stability fields of the Mg and Fe endmembers of carpholite, chloritoid, and staurolite as compared with possible metamorphic P,T trajectories (I-III). See text for discussion. The Mg- and Fe–staurolite fields are after Schreyer (1968) and Ganguly (1972), respectively; the Fe–chloritoid upper stability (for NNO-QFM buffer) is taken from Ganguly (1969), its lower stability limit is hypothetical, just as the field of ferrocarpholite. Aluminum silicates phase relations are after Holdaway (1971).

It can be appreciated immediately from figure 6 that along "normal" low- to intermediate-pressure, metamorphic gradients such as from greenschist to granulite approximated by arrow I Fe–Mg carpholites cannot appear, and chloritoid, limited to low and medium grades, must be very iron-rich. Similar relations hold for staurolite which makes its appearance at medium grades. Increasing Mg-contents in staurolite could be expected in rocks formed at high temperatures (700°-800°C), provided that pressures typical for the lower continental crust are prevailing and that there is no quartz present which is known to limit staurolite stability (Richardson, 1968; Schreyer, 1968; Ganguly, 1972). However, Mg-rich staurolites are not known thus far, possibly due to the chemical restriction.

Turning to the other end of the terrestrial pressure-temperature scale with low geothermal gradients near 10°C/km (fig. 6) as typical for many blueschist environments, it is also obvious why Fe–Mg carpholites must appear as the first index minerals in metapelitic compositions (arrow III). Following such gradient toward higher metamorphic grades it is understandable that carpholites give way gradually to chloritoid, and that the latter will show a tendency toward Mg–chloritoid (compare fig. 2,A and B). If the stability range of Mg-rich chloritoid is to be attained without previously entering the field of Mg–Fe carpholite, as might possibly have been the case for rocks characterized by the assemblages of figure 2,C and

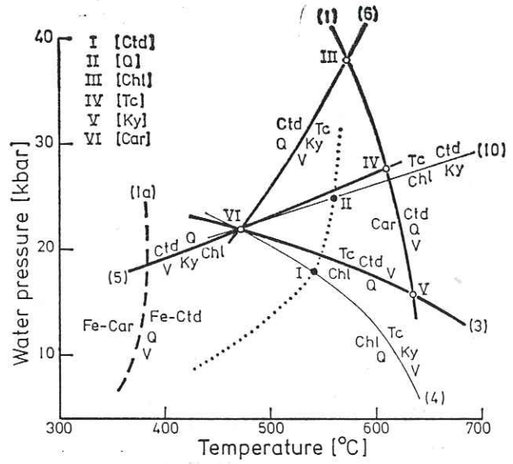

Fig. 7. Approximate location of the most important metastable reaction curves (heavy lines) involving the phases carpholite, chlorite, chloritoid, kyanite, quartz, talc and vapor, in the system $MgO–Al_2O_3–SiO_2–H_2O$. For comparison with figure 5, the upper stability limit of Mg–carpholite is indicated by a dotted line, and the two stable reactions (4) and (10) by light lines. Solid circles are stable, open circles are metastable invariant points defined by Roman numbers. The heavy dashed line is the hypothetical upper stability limit of Fe–carpholite as shown in figure 6. Abbreviations as in figure 5. Reactions are numbered as in the text.

D, PT paths such as that indicated by arrow II must be assumed. A geologic model for verifying such PT trajectory will be discussed in the final section.

After this rather general picture an attempt is made in the following to elaborate in greater detail on the reaction relations leading to the appearance, or disappearance, of the two index minerals of blueschist metamorphism discussed here. Wherever the univariant reaction curves are not known from experiment, their approximate slopes were estimated using known volume data for the solid phases and, for H_2O, the new PVT data of Halbach and Chatterjee (1982a).

Magnesiocarpholite.—The reactions limiting the field of Mg–carpholite (fig. 5) are most likely to occur in highly magnesian and/or highly oxidized metapelitic rocks. The direct formation of magnesiocarpholite in quartz-free rocks such as metabauxites might occur according to the reaction

$$\text{kaolinite} + \text{chlorite} \rightarrow \text{Mg–carpholite} + H_2O \qquad (12)$$

In this reaction the chlorite phase is assumed to be sufficiently aluminous to be colinear with kaolinite–carpholite and thus allow the degeneracy shown in figure 5. If this is not the case, diaspore should participate on the low-temperature side of the reaction that is shifted toward slightly lower pressures.

At higher temperature, that is within the pyrophyllite field, the carpholite-forming reaction, in the presence of quartz, becomes

$$\text{chlorite} + \text{pyrophyllite} + H_2O \rightarrow \text{Mg–carpholite} + \text{quartz} \qquad (13)$$

Due to small amounts of water participating in this reaction and because of a negative volume change of about 3 to 4 percent the slope must be relatively flat (see 3 in fig. 5). This represents a useful pressure indication and defines the common chlorite–pyrophyllite pair as a low-pressure assemblage (see also Dubois and Kienast, 1975; Viswanathan and Seidel, 1979). Alternatively, with retrograde pressure decrease, or isobaric temperature increase, reaction (13) may also proceed in the opposite direction causing the breakdown of Mg–carpholite. This very relationship was recently observed by Goffé (ms) in rocks from the Vanoise area, where in quartz-bearing assemblages magnesiocarpholite (80 percent Mg endmember) is partly or totally replaced by chlorite with pyrophyllite and/or cookeite, whereas it remained stable in the quartz-free, diaspore-bearing parageneses.

Despite this apparently satisfactory applicability of the low-pressure reactions of figure 5 the reader should be reminded once again of the unknown role of the di/trioctahedral chlorite sudoite on the low-pressure phase relations of Mg–carpholite (see p. 86), which may lead to another strongly pressure-dependent low-pressure limit of magnesiocarpholite following the reaction

$$\text{sudoite} + \text{quartz} \rightleftharpoons \text{magnesiocarpholite}. \qquad (11)$$

For more information from natural systems a careful search for sudoite,

which is difficult to distinguish from normal Mg-rich chlorite, in pelitic rocks of very low grade is highly desirable.

In more iron-rich pelitic rocks of the low-grade blueschist facies *ferrocarpholite* develops as the first carpholite phase, and its formation follows principally similar reaction relations as those shown in figure 5 for the magnesian system. Therefore, in these rocks, the formation of *magnesiocarpholite* is different from that in Mg-rich rocks, because — as outlined in a previous section (see p. 80) — ferrocarpholite reacts, with rising grade, continuously toward more magnesian carpholites while the ferrous component breaks down in favor of Fe-rich chloritoid (E. W. F. de Roever, 1977).

Regarding the final disappearance of magnesiocarpholite with increasing metamorphic grade the situation in nature is not clear as yet. In principle, it should be possible that the well-known greenschist-facies assemblage chlorite + kyanite + quartz represents the breakdown product of magnesiocarpholite at pressures as high as 18 kb (fig. 5) according to the reaction

$$\text{magnesiocarpholite} \rightarrow \text{chlorite} + \text{kyanite} + \text{quartz} + H_2O. \qquad (8)$$

In iron-bearing rocks, the prerequisite for reaction (8) to take place is the previous disappearance of the chloritoid–carpholite assemblage (see fig. 2B) according to the reaction

$$\text{ferrochloritoid} + \text{magnesiocarpholite} \rightarrow \text{chlorite} + \text{kyanite} + H_2O. \qquad (14)$$

This will limit the range of bulk compositions in which reaction (8) occurs to high Mg/Fe ratios. Because of the rather "normal" nature of the chlorite–kyanite–quartz assemblage to most petrologists, its significance in blueschist metamorphic terranes may have been overlooked thus far. The unique association of magnesiocarpholite with kyanite, chlorite, quartz, and chloritoid from Samos (Okrusch, 1981; and table 1) may be considered as the relevant assemblage corresponding to reaction (14), the presence of quartz making it univariant.

Magnesiochloritoid.—The second index mineral magnesiochloritoid, containing up to 74 mol percent Mg endmember as known thus far, is of particular significance for blueschist metamorphism inasmuch as its appearance is possible over a rather wide range of rock compositions. While the common Fe-rich chloritoid of low-pressure metamorphism, and also of low-temperature blueschist metamorphism (see preceding section), is confined to strongly Al-rich rocks (see also fig. 2B), the magnesiochloritoid of higher-grade blueschist terranes may also appear in much Al-poorer environments because of its characteristic association with the virtually Al-free mineral talc. The role that magnesiochloritoid plays in high-temperature blueschist facies is best demonstrated by figure 2,C to D.

The following attempts to decipher reaction relationships in the development of Mg-dominant chloritoids cannot be based on the grid of figure 5, because the natural Mg-rich chloritoid–talc parageneses are com-

monly stable in the presence of quartz, a feature that is not verified in figure 5. Therefore, figure 7 presents a simplified grid of the type of figure 5 but with the important *metastable reactions* indicated as deduced chemographically. All these reactions are the pure magnesium equivalents of divariant assemblages occurring in nature.

The metastable reaction

$$\text{Mg carpholite} \rightarrow \text{Mg chloritoid} + \text{quartz} + H_2O \qquad (1)$$

has a steep slope as is to be expected for a strong dehydration reaction. Using a similar slope the equivalent reaction for the breakdown of pure ferrocarpholite,

$$\text{Fe–carpholite} \rightarrow \text{Fe–chloritoid} + \text{quartz} + H_2O, \qquad (1a)$$

is also shown in figure 7. Thus the continuous breakdown of Fe–Mg carpholites into more and more Mg-rich chloritoids as described before must essentially be a temperature-dependent process. However, due to the vastly different pressure locations of the stability fields of the endmember chloritoids relative to those of the carpholites (see fig. 6), a pressure influence on the Fe/Mg partitioning between the two minerals can be expected as it was also predicted by Seidel (1981) from volume considerations for the exchange reaction.

On the other hand, the initial reaction allowing the coexistence of chloritoid and talc, that is in the pure magnesian system

$$\text{chlorite} + \text{quartz} \rightarrow \text{magnesiochloritoid} + \text{talc} + H_2O \qquad (3)$$

has, again as a *metastable* curve, a much flatter and negative slope (fig. 7) that lies intermediate between the slopes of the chlorite + quartz breakdown curves into kyanite + talc and into magnesiocarpholite + talc (see fig. 5). There is a negative volume change toward chloritoid and talc of about 3 to 4 percent. This metastable curve and its expected more iron-rich and, thus, lower-pressure equivalents in the Fe–Mg system lie more or less at right angles to the PT-trajectories of increasing metamorphism. Therefore, the progressive gliding of the 3-phase field talc–chloritoid–chlorite of figure 2C (in the presence of quartz) toward the Mg-side is both a pressure and temperature dependent process. Such reaction relationships are typical for the Gran Paradiso area (see pl. 1-B and Chopin, ms and 1981).

Likewise, the progressive Mg-enrichment of chloritoid coexisting with chlorite and kyanite, in the presence of quartz (fig. 2C) with increasing grade, is a result of the reaction

$$\text{chlorite} + \text{kyanite} + H_2O \rightarrow \text{magnesiochloritoid} + \text{quartz} \qquad (5)$$

which is linked with a volume decrease of about 3 percent. Once again, this reaction is metastable in the model system, but its location is shown in figure 7, where it exhibits a flat, but positive slope. Thus, any progressive metamorphism leading to Mg-rich chloritoid according to reaction (5) must be characterized by very low geothermal gradients. At still higher

grades, in the absence of chlorite (fig. 2D), further Mg-enrichment in chloritoid would imply the reaction relationship

$$\text{talc} + \text{kyanite} + H_2O \rightarrow \text{magnesiochloritoid} + \text{quartz}. \qquad (6)$$

In the model system this reaction involving hardly any volume change is also metastable with a fairly steep, positive slope (fig. 7). It seems doubtful that any progressive metamorphic PT path would intersect such reaction curve in the direction toward the more hydrated assemblage. This may account for a limit in the Mg-contents of chloritoid with rising grade in quartz-bearing assemblages. The highest percentage of Mg endmember chloritoid (up to 74 mol percent) known thus far was recently found (Chopin, unpub. data) in a chlorite–talc–kyanite–chloritoid–quartz–phengite rock from the Monte Rosa area (table 1). The apparently higher-grade, chlorite-free assemblage from Hohe Tauern (table 1) carries a Mg–chloritoid with only 65 percent endmember (Miller, 1977).

In quartz-free environments the important reaction relationship becomes

$$\text{chlorite} + \text{kyanite} \rightarrow \text{magnesiochloritoid} + \text{talc}. \qquad (10)$$

This reaction involving also a 3 to 4 percent volume decrease is a *stable* one in the pure system $MgO–Al_2O_3–SiO_2–H_2O$, and its curve is located, with a rather flat slope (see p. 86), at very high water pressures of at least 25 kb (figs. 5 and 7). The four coexisting phases were recorded previously (table 1) from rocks of the Zermatt area (Chinner and Dixon, 1973) and the chloritoid contains about 65 mol percent of the Mg endmember. As reaction (10) does not involve practically any change in water content (see p. 86), it will be rather insensitive to water activity and could thus provide a very useful geobarometer for high-grade blueschist terranes. Direct textural evidence for reaction (10) is presented in plate 1-C from the Monte Rosa rock, where secondary chlorite and kyanite appear as retrograde products in a local quartz-free environment.

Considering the primary bulk mineralogy of the Monte Rosa rock which includes quartz (table 1), this assemblage must be univariant. An attempt was made to estimate pressures for this rock from reaction (10) using an ideal ionic solution model. For a temperature of about 500°C this led to pressures between 15 and 18 kb (Chopin, unpub. data).

Whiteschists of different pressure regimes.—As reactions (6) and (10) involve both talc and kyanite the rocks discussed in the preceding paragraph might be called whiteschists in the sense of Schreyer (1977). Clearly, for the Zermatt and Hohe Tauern rocks the assemblage Mg–chlorite + quartz is no longer stable. However, as can be seen from figure 5 the assemblage talc–kyanite covers a wide pressure range beginning at some 6 kb (Massonne, Mirwald, and Schreyer, 1981) and extending to at least 35 kb above a minimum temperature of about 540°C. For the pure model system a subdivision of this range is only possible when additional, less siliceous mineral phases such as Mg–carpholite, chlorite, or Mg–chloritoid are coexisting. Whereas rocks of such extreme MgAl-rich compositions are

not known as yet, a subdivision of the more siliceous natural occurrences seems feasible when a coexisting iron-bearing mafic phase is considered.

In this respect the index mineral magnesiochloritoid coexisting with talc and kyanite is of prime interest (fig. 2D). As discussed previously this assemblage indicates pressures of considerable magnitude (15-20 kb), while the talc–kyanite pair alone requires at least 540°C for water pressure equalling total pressure. Thus this high-temperature blueschist facies assemblage is, at the same time, a *high-pressure whiteschist.*

On the other hand, the more common whiteschists appearing in amphibolite-facies terranes as layers of highly magnesian, meta-evaporitic rocks must have formed at much lower pressures (Schreyer, 1977). PT trajectories near gradients of about 20°C/km may lead to these whiteschists that, upon further increase in grade, can develop yoderite at temperatures near 700°C. Such whiteschists should thus be termed *low-pressure whiteschists.*

The one and only occurrence recorded thus far, in which the talc–kyanite pair coexists with a Mg-rich garnet may be of an intermediate nature. This whiteschist occurs in an eclogite terrane in Tasmania (Råheim and Green, 1974). The talc–kyanite–garnet assemblage clearly precludes the coexistence of Mg-rich chloritoid with talc and kyanite as found in the blueschist terranes (see fig. 2D) and must, therefore, belong to a different PT-regime. More experimental and theoretical work, especially on garnet activity/composition relations, is necessary to define this environment more closely.

GEOLOGIC ASPECTS

It is now commonly accepted that the realm of blueschist metamorphism characterized by high confining pressures and low temperatures is best explained geologically as a result of subduction of lithospheric plates, or platelets, in collision zones. Nevertheless, many different kinds of subduction processes seem possible. Thus the subducted, "down-going" slab may not always be of oceanic origin; indeed, in continent/continent collisions clearly continental crust may be subducted as well.

In the orogenic region of the Alpine and Mediterranean System a great many different events of local collisions and subductions have occurred, which may have led to different types of subduction-zone, blueschist metamorphism, with variable PT-trajectories. Even if the PT-gradients during the subduction process were alike or similar (see arrows II and III of fig. 6), this complicated collision system between the European and African continents may have provided a series of platelets with different initial temperatures that would, during subduction, create different series of progressive blueschist metamorphism. In this picture, arrow II of figure 6 could simply be due to a higher heat content of the plate prior to subduction relative to arrow III that may be valid for initial near-surface conditions. Indeed higher initial temperatures may prevail in slabs of lower or middle continental crust or even in freshly produced slabs of oceanic crust.

The results presented in this paper can only be considered as a first step, and much more experimental work aimed at calibrating mineral reactions and the resulting Mg/Fe partitioning will be necessary. However, it seems that, for an important and hitherto in blueschist terranes rather neglected group of rocks, the metapelites, new avenues for geobarometry and -thermometry can be opened. This is particularly important, because future views on the geodynamics of subduction processes in zones of plate collision will depend largely on the success of depth/temperature analyses as a function of geologic time.

ACKNOWLEDGMENTS

The present study was undertaken while the first author held a fellowship of Deutscher Akademischer Austauschdienst. During the experimental work helpful advice was offered by D. Lattard, H. J. Massonne, and P. Mirwald, all at Bochum. B. Goffé, Paris, provided samples and many unpublished results, which promoted the application of the experimental data. Our review of natural assemblages owes much to the generous help offered by E. W. F. de Roever and E. Seidel. Comments by M. Frey, critical reviews by J. Ganguly and F. Seifert, and the editorial support of H. J. Greenwood are also gratefully acknowledged.

REFERENCES

Abraham, K., and Schreyer, W., 1976, A talc–phengite assemblage in piemontite schist from Brezovica, Serbia, Yugoslavia: Jour. Petrology, v. 17, p. 421-439.

Agrell, S. O., Brown, M. G., and McKie, D., 1965, Deerite, howieite and zussmanite, three new minerals from the Franciscan of the Laytonville district, Mendocino Co., California: Am. Mineralogist, v. 50, p. 278.

Bearth, P., 1963, Chloritoid und Paragonit aus der Ophiolith-Zone von Zermatt-Saas Fee: Schweizer min. pet. Mitt., v. 43, p. 269-286.

———— 1967, Die Ophiolithe der Zone von Zermatt-Saas Fee: Beitr. geol. Karte Schweiz, Neue Folge, v. 132, p. 1-130.

Chinner, G. A., and Dixon, J. E., 1973, Some high-pressure parageneses of the Allalin gabbro, Valais, Switzerland: Jour. Petrology, v. 14, p. 185-202.

Chopin, Christian, ms, 1979, De la Vanoise au massif du Grand Paradis: Thèse de 3ème cycle, Univ. Paris 6.

———— 1981, Talc–phengite: a widespread assemblage in high-grade pelitic blueschists of the Western Alps: Jour. Petrology, v. 22, p. 628-650.

Chopin, Christian, and Goffé, B., 1981, High-pressure synthesis and properties of magnesiocarpholite, $MgAl_2Si_2O_6(OH)_4$: Contr. Mineralogy Petrology, v. 76, p. 260-264.

Dubois, R., ms, 1976, La suture Calabro-Apenninique Crétacé-Eocène et l'ouverture Tyrrhénienne Néogène: étude pétrographique et structurale de la Calabre centrale: Thèse d'état, Univ. Paris 6.

Dubois, R., and Kiénast, J. R., 1975, La Mg–Fe–carpholite de Gimigliano (Calabre) dans le métamorphisme alpin [abs.]: réunion annuelle des sci. de la terre, 3ème, Montpellier.

Ernst, W. G., 1963, Significance of phengite micas from low-grade schists: Am. Mineralogist, v. 48, p. 1357-1373.

Fransolet, A. M., 1978, Données sur l'ottrélite d'Ottré, Belgique: Bull. Minéralogie, v. 101, p. 548-557.

Fransolet, A. M., and Bourguignon, P., 1978, Di/trioctahedral chlorite in quartz veins from the Ardenne, Belgium: Canadian Mineralogist, v. 16, p. 365-373.

Frey, Martin, 1978, Progressive low-grade metamorphism of a black shale formation. Central Swiss Alps, with special reference to pyrophyllite- and margarite-bearing assemblages: Jour. Petrology, v. 19, p. 95-135.

Ganguly, J., 1969, Chloritoid stability and related parageneses: theory, experiments and applications: Am. Jour. Sci., v. 267, p. 910-944.

———— 1972, Staurolite stability and related parageneses: theory, experiments and applications: Jour. Petrology, v. 13, p. 335-365.

Goffé, B., 1979, La lawsonite et les associations à pyrophyllite–calcite dans les métasédiments alumineux du Briançonnais — Premières occurrences: Acad. Sci. Paris Comptes rendus, v. 289 D, p. 813-816.
———— 1980, Magnésiocarpholite, cookéite et euclase dans les niveaux continentaux métamorphiques de la zone briançonnaise. Données minéralogiques et nouvelles occurrences: Bull. Minéralogie, v. 103, p. 297-302.
———— ms, 1982, Définition du faciès à Fe–carpholite–chloritoïde, marqueur du métamorphisme de haute pression — basse température: Thèse d'état, Univ. Paris 6.
Goffé, B., Goffé-Urbano, G., and Saliot, P., 1973, Sur la présence d'une variété magnésienne de ferrocarpholite en Vanoise (Alpes françaises) — Sa signification probable dans le métamorphisme alpin: Acad. Sci. Paris Comptes rendus, v. 277 D, p. 1965-1968.
Goffé, B., and Saliot, P., 1977, Les associations minéralogiques des roches hyperalumineuses du Dogger de Vanoise — Leur signification dans le métamorphisme régional: Soc. franç minéralogie cristallographie Bull., v. 100, p. 302-309.
Halbach, H., and Chatterjee, N. D., 1982a, An empirical Redlich-Kwong-type equation of state for water to 1000°C and 200 kbar: Contr. Mineralogy Petrology, v. 79, p. 337-345.
———— 1982b, The use of linear parametric programming for determining internally consistent thermodynamic data for minerals, *in* Schreyer, W., ed., High-pressure researches in geoscience: Stuttgart, Schweizerbarth, 545 p.
Halferdahl, L. B., 1961, Chloritoid: its composition, X-ray and optical properties, stability and occurrence: Jour. Petrology, v. 2, p. 49-135.
Holdaway, M. J., 1971, Stability of andalusite and the aluminum silicate phase diagram: Am. Jour. Sci., v. 271, p. 97-131.
Kramm, U., 1980, Sudoite in low-grade metamorphic manganese-rich assemblages: Neues Jahrb. Mineralogie Abh., v. 138, p. 1-13.
Lattard, D., and Schreyer, W., 1981, Experimental results bearing on the stability of the blueschist-facies minerals deerite, howieite, and zussmanite, and their petrological significance: Bull. Minéralogie, v. 104, p. 431-440.
Leistner, H., and Chatterjee, N. D., 1978, Wasserhaltige Minerale im System $CaSiO_3$–Al_2O_3–H_2O: Rosenhahnit $Ca_3Si_3O_5(OH)_2$, Vuagnatit $CaAlSiO_4(OH)$ und Chantalit $CaAl_2SiO_4(OH)_4$: Fortschr. Mineralogie, Bd. 46, Beih. 1, p. 79-80.
Massonne, H. J., Mirwald, P. W., and Schreyer, W., 1981, Experimentelle Überprüfung der Reaktionskurve Chlorit + Quarz = Talk + Disthen im System MgO–Al_2O_3–SiO_2–H_2O: Fortschr. Mineralogie, Bd. 59, Beih. 1, p. 122-123.
Miller, C., 1974, On the metamorphism of the eclogite and high-grade blueschists from the Penninic terrane of the Tauern Window, Austria: Schweizer min. pet. Mitt., v. 54, p. 371-384.
———— 1977, Chemismus und phasenpetrologische Untersuchungen der Gesteine aus der Eklogitzone des Tauernfensters, Österreich: Tschermaks min. pet. Mitt., v. 24, p. 221-277.
Minoux, L., Bonneau, M., and Kiénast, J. R., 1981, L'île d'Amorgos, une fenêtre des zones externes au coeur de l'Égée (Grèce), métamorphisée dans le faciès schistes bleus: Acad. Sci. Paris Comptes rendus, v. 291 D, p. 745-748.
Miyashiro, A., 1973, Metamorphism and metamorphic belts: New York, John Wiley & Sons, 492 p.
Mottana, A., and Schreyer, W., 1977, Carpholite crystal chemistry and preliminary experimental stability: Neues Jahrb. Mineralogie Abh., v. 129, p. 113-138.
Mügge, O., 1918, Ottrelith- und Karpholithschiefer aus dem Harz: Neues Jahrb. Mineralogie Geologie Paleontologie, 1918, p. 75-98.
Muir Wood, R., 1979a, The iron-rich blueschist facies minerals: 1. Deerite: Mineralog. Mag., v. 43, p. 251-259.
———— 1979b, The iron-rich blueschist facies minerals: 2. Howieite: Mineralog. Mag., v. 43, p. 363-370.
———— 1980, The iron-rich blueschist facies minerals: 3. Zussmanite and related minerals: Mineralog. Mag., v. 43, p. 605-614.
Okrusch, M., 1981, Chloritoid-führende Paragenesen in Hochdruckgesteinen von Samos: Fortschr. Mineralogie, Bd. 59, Beih. 1, p. 145-146.
Pabst, A., 1977, Über einige besonders dichte, wasserhaltige Calcium-bzw. Barium–Silikate aus der Franciscan-Formation, California (Lawsonit, Vuagnatit, Rosenhahnit, Cymrit): Neues Jahrb. Mineralogie Abh., v. 129, p. 1-14.
Pabst, A., Gross, E. B., and Alfors, J. T., 1967, Rosenhahnite, a new hydrous calcium silicate from Mendocino County, California: Am. Mineralogist, v. 52, p. 336-351.
Råheim, A., and Green, D. H., 1974, Talc–garnet–kyanite–quartz schist from an eclogite-bearing terrane, Western Tasmania: Contr. Mineralogy Petrology, v. 43, p. 223-231.

Richardson, S. W., 1968, Staurolite stability in a part of the system Fe–Al–Si–O–H: Jour. Petrology, v. 9, p. 467-488.
Roever, E. W. F. de, 1977, Chloritoid-bearing metapelites associated with glaucophane rocks in Western Crete. Some remarks: Contr. Mineralogy Petrology, v. 60, p. 317-319.
Roever, E. W. F. de, and Beunk, F. F., 1971, Ferrocarpholite associated with lawsonite–albite facies rocks near Sangineto, Calabria, Italy: Mineralog. Mag., v. 38, p. 519-521.
Roever, W. P. de, 1947, Igneous and metamorphic rocks in eastern Central Celebes, *in* Brouwer, H. A., ed., Geological exploration in the island of Celebes under the leadership of H. A. Brouwer: Amsterdam, North-Holland Publishing Co., p. 65-173.
———— 1951, Ferrocarpholite, the hitherto unknown ferrous iron analogue of carpholite proper: Am. Mineralogist, v. 36, p. 736-745.
———— 1956, Some additional data on the crystalline schists of the Rumbia and Mendoke Mountains, southeast Celebes: Royal Dutch Geol. Min. Soc. Trans., pt. 16, p. 305-393.
Roever, W. P. de, and Beunk, F. F., 1978, Ferrocarpholite and its mode of occurrence (in Russian), *in* Problems of the petrology of the Earth's crust and upper mantle: Akad. Nauk. SSSR, Siberian Branch Inst. Geol. Geophysics Proc., v. 403, p. 237-245.
Roever, W. P. de, Roever, E. W. F. de, Beunk, F. F., and Lahaye, P. H. J., 1967, Preliminary note on ferrocarpholite from a glaucophane- and lawsonite-bearing part of Calabria, Southern Italy: Kon. Nederl. Akad. Wet. Proc., v. B70(5), p. 534-537.
Sarp, H., Bertrand, J., and McNear, E., 1976, Vuagnatite, $CaAl(OH)SiO_4$, a new natural calcium aluminium nesosilicate: Am. Mineralogist, v. 61, p. 825-830.
Sarp, H., Deferne, J., and Liebich, B. W., 1977, La Chantalite, $CaAl_2SiO_4(OH)_4$, un nouveau silicate naturel d'aluminium et de calcium: Schweizer min. pet. Mitt., v. 57, p. 149-156.
Scaini, G., Mottana, A., and Abraham, K., 1976, Ferrocarpholite from Colle Ciarbonet (Cottian Alps): Mineralog. Mag., v. 40, p. 900-902.
Schreyer, W., 1968, A reconnaissance study of the system MgO–Al_2O_3–SiO_2–H_2O at pressures between 10 and 25 kb: Carnegie Inst. Washington Year Book, v. 66, p. 380-392.
———— 1977, Whiteschists: their compositions and pressure-temperature regimes based on experimental, field, and petrographic evidence: Tectonophysics, v. 43, p. 127-144.
Schreyer, W., and Baller, T., 1977, Talc–muscovite: synthesis of a new high-pressure phyllosilicate assemblage: Neues Jahrb. Mineralogie Mh., v. 9, p. 421-425.
Schreyer, W., and Seifert, F., 1969a, High-pressure phases in the system MgO–Al_2O_3–SiO_2–H_2O: Am. Jour. Sci., v. 267-A (Schairer v.), p. 407-443.
———— 1969b, Compatibility relations of the aluminum silicates in the system MgO–Al_2O_3–SiO_2–H_2O and K_2O–MgO–Al_2O_3–SiO_2–H_2O at high pressures: Am. Jour. Sci., v. 267, p. 371-388.
Seidel, E., 1978, Zur Petrologie der Phyllit-Quarzit-Serie Kretas: Braunschweig, Habilitationsschr., 145 p.
Seidel, E., 1981, Fe–Mg-Verteilung zwischen koexistierenden Karpholithen und Chloritoiden: Fortschr. Mineralogie, Bd. 59, Beih. 1, p. 180-181.
Seidel, E., and Okrusch, M., 1977, Chloritoid-bearing metapelites associated with glaucophane rocks in Western Crete, Greece. Additional comments: Contr. Mineralogy Petrology, v. 60, p. 321-324.
Seifert, F., 1975, Boron-free kornerupine: a high-pressure phase: Am. Jour. Sci., v. 275, p. 57-87.
Steen, D., and Bertrand, J., 1977, Sur la présence de ferrocarpholite associée aux schistes à glaucophane de Haute Ubaye (Basses Alpes, France): Schweizer min. pet. Mitt., v. 57, p. 157-168.
Tobschall, H. J., 1969, Eine Subfaziesfolge der Grünschieferfazies in den mittleren Cévennes (Dép. Ardèche) mit Pyrophyllit aufweisenden Mineralparagenesen: Contr. Mineralogy Petrology, v. 24, p. 76-91.
Turner, F. J., 1981, Metamorphic petrology 2d ed.: New York, McGraw-Hill, 524 p.
Viswanathan, K., and Seidel, E., 1979, Crystal chemistry of Fe–Mg carpholites: Contr. Mineralogy Petrology, v. 40, p. 41-47.
Winkler, H. G. F., 1979, Petrogenesis of metamorphic rocks, 5th ed.: New York, Springer, 348 p.

Bull. Minéral.
(1983), **106**, 715-717

Magnesiochloritoid, a key-mineral for the petrogenesis of high-grade pelitic blueschists

by CHRISTIAN CHOPIN

Laboratoire de Géologie (ER 224), Ecole normale supérieure - 46, rue d'Ulm, 75005 Paris, France.

Key words : chloritoid, metapelite, blueschist, eclogite.

Le chloritoïde magnésien, un minéral-index dans les séries pélitiques de haut degré du faciès schistes bleus.

Mots-clés : chloritoïde, métapélite, schiste bleu, éclogite.

EXTENDED ABSTRACT

The main feature of the mineralogical evolution of pelitic rocks in eclogite-bearing blueschist terranes is the progressive breakdown of chlorite + quartz with increasing grade and Mg/Fe ratio into talc + garnet, talc + chloritoid and talc + kyanite. The most important assemblage is talc + chloritoid + phengite which, in association with garnet or kyanite or Mg-rich chlorite + quartz, covers almost the whole spectrum of pelitic rock compositions. In this unusual assemblage the magnesium content of chloritoid is characteristically high. The molar content of the Mg-end member $Mg_2Al_4Si_2O_{10}(OH)_4$ ranges from 25 up to 74 per cent, as exemplified in the internal Penninic domain of the Western and Eastern Alps (Bearth, 1963 ; Chinner and Dixon, 1973 ; Miller, 1977 ; Chopin, 1979, 1981 ; Chopin and Schreyer, 1983).

Chloritoid displays characteristic zonation patterns in given assemblages and its maximum Mg content in the talc-chloritoid pair is not a monotonic function of metamorphic grade. The latter increases from Gran Paradiso to Hohe Tauern (Figure 1) through Monte Rosa. The Mg content of chloritoid reaches a maximum (74 mole %) in Monte Rosa in the talc-chloritoid-chlorite-kyanite-quartz assemblage, against 50 mole % in Gran Paradiso (tc-ctd-chl-q) and 63 mole % in Hohe Tauern (tc-ctd-ky-q). The most important divariant reactions responsible for the chloritoid composition in the higher grades are :

chlorite + quartz $\rightleftharpoons$ talc + chloritoid + H_2O (1)
chlorite + kyanite + $H_2O \rightleftharpoons$ chloritoid + quartz (2)
talc + kyanite + $H_2O \rightleftharpoons$ chloritoid + quartz (3)

The synthesis of pure Mg-chloritoid and of pure Mg-carpholite allowed an experimental determination (performed in Bochum, W. Germany) of the high-pressure, low-temperature phase relations in the MgO-Al_2O_3-SiO_2-H_2O system (Chopin and Goffé, 1981 ; Chopin and Schreyer, 1981, 1983). It was demonstrated that pure Mg-chloritoid is stable only at water pressure in excess of 18 kbar and is incompatible with quartz, which is at variance with the behaviour of the Mg-rich chloritoid from blueschist terranes. The univariant Mg end-members of the reactions relevant to natural systems (1, 2 and 3) are therefore metastable. Their P-T curves, however, can be chemographically deduced from the experimental data. They show characteristic slopes which allow discussion of the changing Mg/Fe ratio in natural chloritoid with increasing metamorphic grade (Figure 2). This accounts for the zonation patterns of chloritoid in different assemblages.

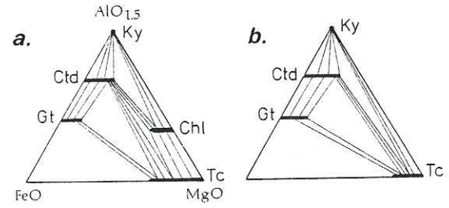

FIG. 1. — *Phase relations in magnesian pelitic rocks from the Gran Paradiso massif* (a) *and the Hohe Tauern* (b, after Miller, 1977). The projection is made from SiO_2 and H_2O.

Comparaison des relations de phases dans les métapélites du massif du Grand Paradis (a) *et des Hohe Tauern* (b, d'après Miller, 1977). La projection est faite depuis les pôles SiO_2 et H_2O. Les associations critiques sont respectivement talc-chloritoïde-chlorite-quartz (± phengite) et talc-chloritoïde-disthène-quartz (± phengite).

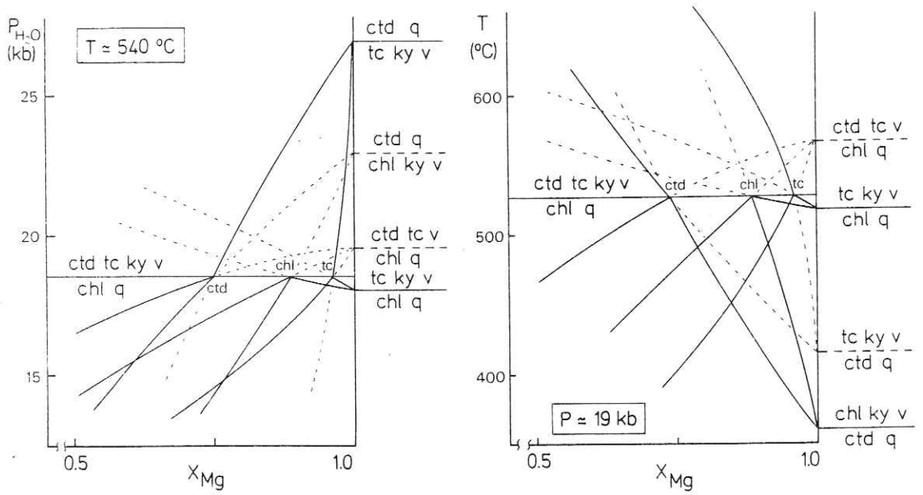

FIG. 2. — *The talc-chloritoid pair and the chlorite + quartz breakdown : tentative isothermal P-X_{Mg} and isobaric T-X_{Mg} sections for the Mg-rich part of the FeO-MgO-Al_2O_3-SiO_2-H_2O system at high water pressure*. The construction relies on analytical data from natural assemblages and on deductions from experimental data for the end-member reactions. The assumption is made throughout that no reversal exists in the Fe-Mg distribution between talc and chlorite. Temperature and pressure are only indicative.

L'association talc-chloritoïde et la déstabilisation de la chlorite en présence de quartz : diagrammes P-X_{Mg} isotherme et T-X_{Mg} isobare pour la partie magnésienne du système FeO-MgO-Al_2O_3-SiO_2-H_2O à pression d'eau élevée. Cet essai de construction est fait à partir d'analyses de minéraux naturels et de données expérimentales pour les pôles magnésiens des réactions ; il repose sur l'hypothèse qu'il n'existe pas de renversement du partage Fe-Mg entre talc et chlorite. Les valeurs de pression et de température restent indicatives.

In contrast to classical prejudice, the pelitic system now appears to be a sensitive metamorphic indicator also at high pressure. In particular, the wide range of Mg/Fe ratio in chloritoid and the progressive shifting of the chloritoid-talc-chlorite (+ quartz) field allow subtle distinctions between blueschist terranes which otherwise do not differ in their eclogitic assemblages.

REFERENCES

BEARTH, P. (1963). — Chloritoid und Paragonit aus der Ophiolith-Zone von Zermatt-Saas Fee. *Schweiz. Mineral. Petrogr. Mitt., 43*, 269-286.

CHINNER, G.A. and DIXON, J.E. (1973). — Some high-pressure parageneses of the Allalin gabbro, Valais, Switzerland. *J. Petrol., 14*, 185-202.

CHOPIN, C. (1979). — De la Vanoise au massif du Grand Paradis. *Thèse 3e cycle*, Univ. P. et M. Curie, 145 p.

CHOPIN, C. (1981). — Talc-phengite : a widespread assemblage in high-grade pelitic blueschists of the Western Alps, *J. Petrol., 22*, 628-650.

CHOPIN, C. and GOFFÉ, B. (1981). — High-pressure synthesis and properties of magnesiocarpholite, $MgAl_2Si_2O_6(OH)_4$. *Contrib. Mineral. Petrol., 76*, 260-264.

CHOPIN, C. and SCHREYER, W. (1981). — Eine experimentelle Untersuchung des MgO-Al_2O_3-SiO_2-H_2O Systems im Hochdruck-Tieftemperatur-Bereich. *Fort. Mineral., 59*, Beih. 1, 31-33.

CHOPIN, C. and SCHREYER, W. (1983). — Magnesiocarpholite and magnesiochloritoid : two index minerals of pelitic blueschists and their preliminary phase relations in the model system MgO-Al_2O_3-SiO_2-H_2O. *Amer. Journ. Science*, Orville vol., 72-96.

MILLER, C. (1977). — Chemismus und phasenpetrologische Untersuchungen der Gesteine aus der Eklogitzone des Tauernfensterns, Österreich. *Tschermaks Mineral. Petrol. Mitt., 24*, 221-277.

Contrib Mineral Petrol (1984) 87:388–398

Contributions to Mineralogy and Petrology

A unique magnesiochloritoid-bearing, high-pressure assemblage from the Monte Rosa, Western Alps: petrologic and $^{40}Ar-^{39}Ar$ radiometric study

Christian Chopin[1] **and Patrick Monié**[2]

[1] Laboratoire de Géologie (ER 224), Ecole normale supérieure, 46 rue d'Ulm, 75005 Paris, France
[2] Laboratoire de Géologie structurale (LA 266), U.S.T.L., Place E. Bataillon, 34060 Montpellier Cedex, France

Abstract. A phengite-talc-chloritoid-chlorite-kyanite-quartz assemblage is reported from a nearly undeformed quartz-rich metapelite found in the Monte Rosa massif (Western Alps). Chloritoid contains up to 74 mol % of the Mg end member and is the most magnesian ever reported. Textural relationships and mineral compositions suggest equilibrium and therefore a low-variance assemblage which represents the high-pressure stability limit of chlorite + quartz according to the terminal reaction

chlorite + quartz ⇄ talc + chloritoid + kyanite + H_2O.

Mineral compositions combined with new experimental data on the stability of the Mg-chloritoid end member lead, for a temperature close to 500° C, to a pressure estimate of 16 kbar and a water activity of 0.6 which is supported by fluid inclusions study. Chloritoid composition is in fact a fine metamorphic indicator which opens new ways for barometry in high-grade blueschists. It demonstrates here the existence of a high-pressure metamorphism in the Monte Rosa massif. The assemblage remained mineralogically unaffected during the subsequent lower-pressure evolution.

Two size fractions of the single phengite generation were analysed by the $^{39}Ar-^{40}Ar$ incremental release method. Both spectra are identical with a plateau at 110 ± 3 Ma representing over 96% of the ^{39}Ar degassed. The ages of the first heating steps are discordant and increase with increasing temperature from values near 70 Ma to the plateau age. Isotope correlation diagrams show two ^{36}Ar components, one released at high temperature and correlated with ^{40}Ar and ^{39}Ar, the other released at low temperature in a mixture of atmospheric argon and of a loosely held argon of 70 Ma apparent age.

The 110 Ma plateau age may reflect the presence of homogeneously incorporated excess argon, the 70 Ma value might then be a true age. However we favour the alternative hypothesis that the 110 Ma plateau age is a true age, implying that the internal crystalline massifs of the Western Alps have endured high-pressure metamorphism as early as mid-Cretaceous. Whatever the interpretation chosen, the preserved high-pressure mineral assemblage remained isotopically unaffected during the low-pressure mid-Tertiary event which is recorded by the 37 Ma plateau age of phengite from a foliated, recrystallised quartzite collected in the same, westernmost part of the massif. The contrasting behaviour of the two samples shows that even at temperatures as high as 400–450° C deformation and recrystallisation are also major controlling factors of isotope mobility.

Offprint requests to: C. Chopin

Introduction

The recent discovery by one of us of an exceptionally well preserved high-pressure mineral assemblage, to be described here, in metapelitic rocks from the Monte Rosa arouses new interest in the problem of high-pressure metamorphism in the internal crystalline massifs of the Western Alps.

The three massifs (Monte Rosa, Gran Paradiso and Dora Maira, from north to south) represent a crustal segment structurally intermediate between the Briançon-St Bernhard zone to the west and the Sesia zone to the east. In the former, paleontological criteria (Ellenberger 1958) point to a post-Paleocene age for the high-pressure metamorphism, of rather low grade. In the latter Rb–Sr whole-rock isochrons of 130 ± 20 Ma are interpreted as dating the beginning of the high-pressure, high-grade "Eoalpine" event, while younger Rb–Sr mineral isochrons as well as K–Ar mica ages would reflect the subsequent cooling and complex mineral evolution continuing until 60 Ma ago (Hunziker 1974, Oberhänsli et al. 1982).

Between these very different units, the status of the internal crystalline massifs is not quite clear as yet. The existence of an Eoalpine (late Cretaceous?) high-pressure metamorphism is widely accepted but is not equally well documented in the different massifs and particularly poorly in the Monte Rosa. Relic eclogites and Alpine kyanite have been found in the three massifs (Bearth 1952, Dal Piaz 1971, Compagnoni and Lombardo 1974, Vialon 1966) and blueschist assemblages in the Gran Paradiso and Dora Maira massifs (Chopin 1979, 1981, Vialon 1966, Michard 1967). Isotopic data to support their Eolpine age are: a 60–75 Ma group of $^{40}Ar-^{39}Ar$ ages on phengites of well preserved high-pressure assemblages from the Gran Paradiso massif (Chopin and Maluski 1980, 1982); a single 98 ± 18 Ma Rb–Sr biotite apparent age among younger ones in the Dora Maira massif (Vialette and Vialon 1964); and a 125 ± 20 Rb–Sr whole-rock isochron in albitized granitic gneisses and schists of the Monte Rosa massif (Hunziker 1970). However, in a thorough investigation of the Monte Rosa metagranites (Frey et al. 1976), further petrologic or isotopic evidence for such an early metamorphism was not found.

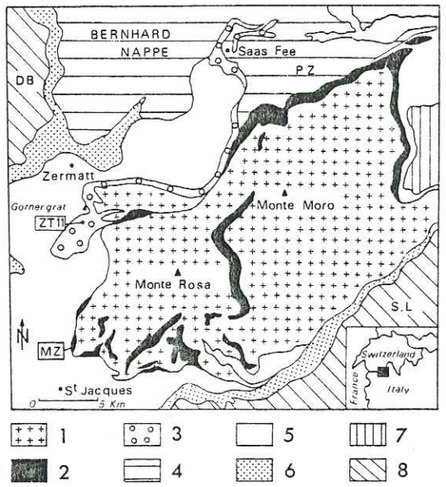

Fig. 1. Geological setting and sample location. Legend: 1. crystalline basement of the Monte Rosa nappe. 2. Furgg zone. 3. Permo-Liassic cover of the Monte Rosa nappe (Gornergrat cover). 4. Bernhard nappe; including the Portjengrat zone (PZ) which is usually considered as the frontal part of the Monte Rosa nappe. 5. Zermatt – Saas Fee ophiolite complex. 6. Combin zone. 7. Lower Pennine units. 8. Lower Austroalpine units: DB Dent Blanche nappe, SL Sesia Lanzo zone. After Bearth (1952); Wetzel (1972); Milnes et al. (1981)

On the basis of the experience gained by Chopin and Maluski (loc. cit.) in the Gran Paradiso, it was thought that the new mineral assemblage found in the Monte Rosa represented a unique opportunity to find a preserved isotopic composition which would make possible the dating of the high-pressure metamorphism in spite of the later, lower-pressure overprint. Besides, this sample is of considerable petrologic interest since it contains the most magnesium-rich chloritoid ever reported. Attention had been recently drawn to magnesiochloritoid (Chopin 1983), and this finding seemed to be a good opportunity to apply the experimental data obtained by Chopin and Schreyer (1983) on the Mg-chloritoid end member, $MgAl_2SiO_5(OH)_2$.

Therefore, it was hoped that a combined petrologic and isotopic study of this exceptional sample would give a better knowledge of both the conditions and the age of high-pressure metamorphism in the Monte Rosa, and also of argon behaviour in mineralogically frozen systems.

Geological and petrological setting

The Monte Rosa massif is composed of a Paleozoic crystalline basement and a thin, discontinuously preserved Permo-Liassic cover series. In the basement metagranites are the dominant rock type. They are emplaced into a highly metamorphosed paragneiss series, and both are discordantly overlain by the Furgg formation, a sedimentary and volcanic sequence of presumably Permo-Carboniferous age. The Permo-Liassic sediments of the cover series are again discordant on all these series. For further geological details the reader is referred to Fig. 1 and to Bearth (1952, 1958), Dal Piaz (1964, 1966), Wetzel (1972) and Klein (1978).

According to Hunziker (1969, 1970), the Monte Rosa granite intruded its high-grade country rocks 310 Ma ago. A 260 Ma whole-rock isochron has been related to younger granite intrusions, possibly contemporaneous with gneissification of a part of the former granite and crystallisation or recrystallisation of muscovite. The 260 Ma age, as well as other Permian Rb–Sr mica ages obtained in different parts of the massif, is interpreted by Hunziker as dating a late Hercynian metamorphism, although pre-Alpine relics are absent in the Furgg zone.

The whole massif underwent a complex Alpine metamorphic evolution which left a variable imprint throughout the massif. Some less deformed parts remained apparently unaffected while some others were mineralogically and isotopically much reworked (see Bearth 1952, Frey et al. 1976, Klein 1978). The late stages of this evolution, in the higher greenschist facies, are mineralogically and isotopically the most apparent and are well documented (Bearth 1952, 1958, Laduron 1976). They are ascribed to a mid-Tertiary event about 38 Ma old (Hunziker 1969, Hunziker and Bearth 1969, Frey et al. 1976). Estimated conditions for the latter metamorphic stage are near 5 kb and 450° C (Frey et al. 1976). Evidences for earlier, high-pressure stages in the metamorphic evolution are scarce. Eclogites are known in the pre-granitic basement (Dal Piaz 1966). Optically and/or chemically zoned phengites have been found in Valle d'Anzasca (Laduron and Wittock 1982) and in orthogneiss near the Monte Rosa Hütte. There, Si-content varies from $Si_{3.45}$ to $Si_{3.15}$ from core to rim and the zoned phengites sometimes coexist with newly formed muscovites and $Si_{3.3}$ phengite (Monié, unpubl. data). According to the experimental work of Velde (1965) and Massonne (1981) on phengite in the buffering assemblage K-feldspar – biotite – quartz, which is the one encountered in the metagranites, such phengite compositions testify for a metamorphic evolution from higher pressure toward lower pressure and/or higher temperature conditions, with partial reequilibration of the early phengites while new phengites and muscovites were formed. It should be stressed that this reequilibration, or even the Alpine overprint as a whole, is strongly dependent on the deformational state of the rock (Frey et al. 1976; compare Chopin and Maluski 1980, in the Gran Paradiso massif).

Given the poor mineralogical constraints, the conditions of the early metamorphic evolution could hardly be estimated. In a comparative study of the mineral chemistry of Monte Rosa and Gran Paradiso eclogites, Dal Piaz and Lombardo (1982) concluded that the early high-pressure metamorphic conditions were very similar or the same in both massifs.

The high-pressure assemblage studied here (sample MZ) has been found in the southwestern Italian part of the Monte Rosa massif (upper Val d'Ayas). There the following upward sequence has been observed:

– Orthogneiss (metagranites) of the Paleozoic basement, with the characteristic assemblage biotite + phengite + K-feldspar + quartz + albite. The foliation is crosscut by shear-zones now occupied by phengite schists (± quartz ± epidote ± tourmaline ± sphene) similar to those described by Dal Piaz (1971) as "micascisti argentei'.

– A thin layer (up to one metre) of silvery talc – phengite – chloritoid schist (± quartz ± chlorite) represents the first deposit of the post-granitic cover series assigned here to the Furgg zone. These schists are the exact stratigraphic equivalent of those described by Chopin (1981) in the Gran Paradiso massif and, although often referred to as "micascisti argentei", they should not be mistaken for those mentioned in the preceding paragraph. Perhaps because of the misleading terminology the assignment of a given lithologic marker to a Furgg zone equivalent in the Gran Paradiso massif has not been made so far, but it opens new ways for deciphering the structure of the massif.

– A few tens of metres of quartzite, phengite – garnet – chloritoid ± biotite schist with marble and metabasite lenses complete the lithologic sequence and are there directly overlain by the Schistes lustrés ophiolitic nappe (see Dal Piaz 1965, 1966).

The sample studied (MZ) was collected as a moraine block on the western side of the Ghiacciaio di Verra, about 2,900 m in altitude, east of the Mezzalama refuge. From lithologic and topographic considerations, it certainly originates from the basal layer of the Furgg zone. It represents a quartz-rich variational type of the talc–phengite–chloritoid schist described above, but

has escaped penetrative deformation as expressed by its unoriented texture.

Structural indications on this area and adjacent ones are given in Klein (1978), Mattauer (1981) and Lacassin (1983). Chronological indications from the immediately underlying gneissic basement are Rb – Sr apparent ages of biotites at 33.2 ± 1.2 and 32.6 ± 2.8 Ma (Hunziker and Bearth 1969, KAW 411 and KAW 412 ages recalculated with $\lambda = 1.42.10^{-11}$ year^{-1}). They have been interpreted as a lower limit to the age of the last phase of Lepontine metamorphism that reached its climax approximately 38 Ma ago.

For comparison, we also investigated a Triassic foliated phengite quartzite (ZT 11) of the cover series sampled to the south of the Gornergrat station (Fig. 1). So, samples MZ and ZT 11 both originate from the westernmost part of the massif, in which the "Lepontine" metamorphism is of lower grade than in its eastern, structurally lower part (Bearth 1952).

Petrology of the high-pressure assemblage

Petrography

Sample MZ is a massive, light-coloured, coarse-grained rock with an equant texture. Large (up to 4 mm in size) dark-blue chloritoid crystals together with centimetre size colourless flakes are embedded without preferred orientation in a colourless groundmass mainly composed of quartz. Under the microscope the chloritoid sections are colourless, the large flakes appear to be talc and magnesian chlorite, while the groundmass consists of quartz and small (up to 300 µm) phengite flakes. The rock also contains large (up to 4 mm), often poekilitic kyanite crystals. Accessory minerals are rutile, apatite, florencite (a La-bearing Ce – Al-phosphate) and zircon. The occurrence of florencite, also recorded from the equivalent schist in the Gran Paradiso massif (Chopin 1979), seems to be characteristic for the basal layer of the Furgg zone *s.l.* and might be of geochemical interest.

The textural relationships suggest that all the minerals were stable together and form a single paragenesis. The only retrogressive effects observed are the occasional formation of a chlorite + kyanite reaction rim between talc and chloritoid (see illustration and discussion in Chopin and Schreyer 1983) and the formation of a narrow rim of secondary chlorite on some chloritoid crystals. It must be emphasized that these secondary reactions are very limited both in occurrence and development. A few deformation effects are evident on the microscopic scale. They are kink bands in the large talc flakes and, to a lesser degree, in the large primary chlorite crystals. Quartz grains which may formerly have been several millimeters in size now consist in their central part of large subgrains with some dislocation bands, and are finely granulated on their margins. There, the subgrain size is about 200–300 µm and the subgrain boundaries are polygonal or lobate. The small phengite flakes are apparently undeformed and their recrystallisation might be coeval with that of quartz grains. Chloritoid and kyanite show no evident deformation features.

Mineral chemistry (Table 1)

Analyses were obtained at the Institut für Mineralogie, Bochum, with a Camebax microprobe operated at 15 kV, 14 nA. Standards used were synthetic pyrope (Mg, Al, Si), Na- and K-bearing glasses, wollastonite (Ca), rutile, magnetite and metallic Mn.

Phengite composition is rather homogeneous with molar paragonite contents between 5 and 7% and Si contents between 3.35 and 3.42 per 12 (O, OH). The slight excess of octahedral filling, although effectively possible (Massonne 1981), is here probably a normalisation artifact linked with a slight deficiency in the interlayer occupancy.

Talc contains 3.5 to 4.5 mol per cent of the iron end member; the lowest Fe-content was measured on crystals associated with kyanite, the highest in crystals associated with chloritoid. Within the large crystals the Fe/Mg ratio shows slight but systematic variations which will be dealt with elsewhere together with zonation patterns in chloritoid. Al_2O_3 content varies between 0.25 and 0.50 weight per cent and, considering the very low Na_2O contents, probably results from the Si Mg ⇄ Al Al substitution or from the 3 Mg ⇄ 2 Al substitution which, with regard to aluminium coordinance, is more likely to be favoured at high pressure (see Newton 1972).

Chlorite: only analyses of large, primary chlorite crystals are given in Table 1. The variation of the molar Fe/Fe + Mg ratio is quite limited, it remains in the range 12–14 per cent. Al/Si variations are also quite restricted ($Si_{2.72-2.77}$), the more Si-rich chlorite being found in association with talc. Secondary chlorites are more Al- and Fe-rich.

Kyanite is nearly pure with Fe_2O_3 contents of about 0.05 weight per cent and still lower Mn_2O_3 values.

Chloritoid composition is exceptional. The molar contents of Mg end member, $MgAl_2SiO_5(OH)_2$, range from 50 to 74% and are thus extremely high. Furthermore they are quite variable within a single crystal. The zonation pattern of the crystals is complex. From core to rim the Mg/Fe + Mg ratio first increases from about 50 to 70 or 75 mol % and then decreases to a typical rim value of about 60 to 65%. For comparison the most Mg-rich chloritoid reported so far contains 63 to 65 mol % of the Mg end member (Bearth 1967, Chinner and Dixon 1973, Miller 1977). Judging from the structural formulas and the absence of any pleochroism the Fe^{3+} contents must be very low.

Discussion

Considering the presence of rutile, the fact that Ca and Ce are only present in apatite and florencite, respectively, the MZ sample may be well approximated by the system $K_2O - MgO - FeO - Al_2O_3 - SiO_2 - H_2O$. The relevant assemblage observed is phengite – talc – chloritoid – chlorite – kyanite – quartz, which has never been described so far. It can be considered as intermediate between the phengite – talc – chloritoid – chlorite – quartz assemblage characteristic for the Gran Paradiso and Valle d'Aosta (Chopin 1979, 1981), and that of talc – chloritoid – kyanite – quartz ± phengite reported from the Hohe Tauern (Miller 1977). As shown in the projection of Fig. 2, the transition from the Gran Paradiso to the Hohe-Tauern assemblage is characterised by the disappearance of chlorite (in the presence of quartz) and the appearance of the talc – kyanite pair. The main interest of the MZ sample is to show how this transition might proceed, particularly how the last chlorite disappears.

In the Gran Paradiso assemblages that are virtually free of Fe^{3+}, chlorite is slightly more Mg-rich than the talc-chloritoid join (Fig. 2). Therefore, with increasing metamorphic grade and especially temperature, the composition

Table 1. Microprobe mineral analyses

Sample	MZ										ZT 11		
	Chloritoid			Talc		Chlorite		Phengite			Phengite		
	core	→	*rim*										
SiO_2	25.38	26.01	25.73	60.93	61.19	28.31	27.95	51.52	50.07	50.09	48.69	48.75	48.63
TiO_2	0.00	0.00	0.00	0.00	0.00	0.00	0.01	0.08	0.18	0.18	0.30	0.43	0.42
Al_2O_3	42.60	43.57	43.29	0.24	0.38	22.17	22.46	27.74	27.62	28.71	25.14	25.24	25.10
Fe_2O_3[a]	–	–	–	–	–	–	–	–	–	–	4.00	4.06	4.02
FeO[a]	15.18	9.02	12.17	2.27	2.54	6.69	7.36	0.52	0.49	0.62	1.80	1.82	1.81
MnO	0.09	0.03	0.05	0.00	0.00	0.00	0.02	0.05	0.00	0.06	0.01	0.04	0.00
MgO	8.22	12.32	10.56	29.28	29.28	28.26	28.41	4.19	3.75	3.53	2.57	2.55	2.59
CaO	0.01	0.01	0.00	0.00	0.00	0.00	0.00	0.00	0.00	0.00	0.01	0.03	0.01
Na_2O	0.00	0.01	0.00	0.03	0.03			0.37	0.50	0.55	0.11	0.10	0.11
K_2O	0.00	0.00	0.01	0.02	0.00			10.22	10.24	10.07	11.23	10.99	11.45
Total	91.48	90.97	91.81	92.77	93.42	85.43	86.21	94.69	92.85	93.81	93.86	94.01	94.14
Si	2.015	2.013	2.005	3.993	3.987	2.761	2.715	3.418	3.394	3.360	3.359	3.355	3.351
Ti							0.001	0.004	0.009	0.009	0.016	0.022	0.022
Al	3.988	3.976	3.977	0.019	0.029	2.549	2.572	2.170	2.207	2.270	2.045	2.048	2.039
Fe^{3+}											0.208	0.210	0.208
Fe^{2+}	1.008	0.584	0.793	0.124	0.138	0.546	0.598	0.029	0.028	0.035	0.104	0.105	0.104
Mn	0.006	0.002	0.003				0.002	0.003		0.003	0.001	0.002	
Mg	0.973	1.421	1.226	2.860	2.843	4.108	4.112	0.414	0.379	0.353	0.264	0.262	0.266
Ca	0.001	0.001									0.001	0.002	0.001
Na		0.002		0.004	0.004			0.048	0.066	0.072	0.015	0.013	0.015
K			0.001	0.002				0.865	0.886	0.862	0.989	0.965	1.007
Σ cat.	7.991	7.999	8.007	7.001	7.001	9.964	9.999	6.950	6.969	6.963	7.000	6.983	7.014
M	0.49	0.71	0.61	0.96	0.95	0.88	0.87	0.93	0.93				

[a] Fe^{3+}/Fe^{2+} is fixed to 0 in MZ, to 2 in ZT 11. The chloritoid, talc, chlorite and phengite formulae are calculated on a 12, 11, 14 and 11 oxygens basis, respectively. $M = Mg/Mg + Fe + Mn$

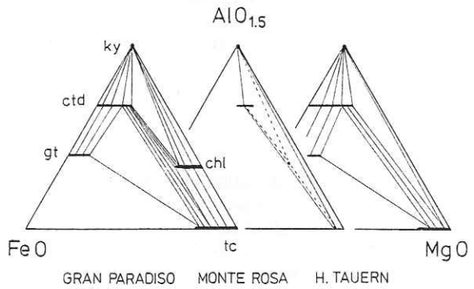

Fig. 2. Phase relationships in high-pressure metapelitic rocks from the Gran Paradiso, Monte Rosa and Hohe Tauern massifs. The projection is made through SiO_2, H_2O and a phengite component. Metamorphic grade increases from Gran Paradiso to Hohe Tauern, the critical assemblages being respectively talc–chloritoid–chlorite–quartz (±phengite) and talc–chloritoid–kyanite (±phengite). The Monte Rosa assemblage represents an intermediate step showing how the last chlorite disappears. In this assemblage, chloritoid shows large compositional variations and tie lines are drawn using its rim composition which is thought to have equilibrated with the nearly homogeneous chlorite and talc. Chl, chlorite; Ctd, chloritoid; Gt, garnet; Ky, kyanite; Tc, talc

of chlorite coexisting with quartz is progressively restricted toward the Mg-side through the divariant reaction

chlorite + quartz → talc + chloritoid + H_2O (1)

(Chopin 1979, 1981, Chopin and Schreyer 1983).

In the Monte Rosa assemblage the join talc-kyanite exists and chlorite is definitely more Fe-rich than this join. This implies that with increasing grade chlorite composition is also restricted on the Mg-side toward the Fe-side according to the divariant reaction

chlorite + quartz → talc + kyanite + H_2O. (2)

Therefore, with increasing P and T the next step will be the disappearance of the last chlorite, through the univariant, terminal reaction

chlorite + quartz → talc + chloritoid + kyanite + H_2O. (3)

This disappearance of chlorite and the incoming of the talc–chloritoid–kyanite assemblage is one of the most important steps in the evolution of the high-grade pelitic blueschists.

In the MZ sample, the very narrow compositional range of chlorite and talc regardless of the mineral in contact (kyanite or chloritoid) and the fact that chlorite lies inside the compositional field defined by talc, kyanite, and the chloritoid rim strongly suggest that the univariant MZ assemblage represents frozen equilibrium conditions very close to those corresponding to the disappearance (or reappearance) of chlorite in the talc–chloritoid–kyanite–quartz assemblage.

The MZ assemblage is univariant in the system MgO–FeO–Al_2O_3–SiO_2–H_2O and defines a P_{H_2O}–T relation. The univariant reaction curve emanates from the invariant point of the system MgO–Al_2O_3–SiO_2–H_2O involving the solid phases chlorite, chloritoid, talc, kyanite and

quartz. Two of the reactions intersecting at this invariant point have been experimentally investigated in the pure magnesian system, namely reaction (2) by Massonne et al. (1981) and the water-conserving reaction

chlorite + kyanite ⇄ talc + chloritoid (4)

by Chopin and Schreyer (1983).

Accordingly, the (metastable) invariant point had been approximately located near 22 kbar water pressure and 470° C by the latter authors but should lie closer to 20 kbar, 500° C according to new experimental data obtained by Chopin (see Appendix). The reader is referred to Fig. 6 of Chopin and Schreyer (1983) showing the chemographic relations around this invariant point in the purely magnesian system, and to Fig. 2 of Chopin (1983) for the relevant isothermal P–X_{Mg} and isobaric T–X_{Mg} sections in the Fe–Mg system. Assuming that solid solutions between Fe and Mg end members do not depart from ideality, the composition of the natural minerals and the two experimentally determined reaction curves make possible an estimate of the crystallisation conditions; more exactly they yield an univariant P–T–a_{H_2O} relation (see Appendix). For unit water activity, estimated conditions are about 18.5 kbar, 560° C. In fact, the stability of iron-rich chloritoid and the absence of staurolite in the Monte Rosa massif imply that temperature cannot have exceeded 500–550° C, according to the experimental work of Ganguly (1972). This suggests that water activity was less than one. A temperature of 500° C, closer to commonly admitted values, implies a water activity of 0.6 and a total pressure close to 16 kbar. Interestingly, a preliminary investigation of fluid inclusions in this sample has shown that trails of tiny, secondary-looking inclusions in quartz are purely aqueous while larger, primary-looking, three-phase inclusions contain both H_2O and CO_2. This definitely supports the assumption of low water activity and the latter P–T estimate.

Such high pressure values are surprising and may seem unrealistically high in view, for instance, of the absence of jadeite in metagranites, even in undeformed ones. However such pressures are at the measure of the unusual chloritoid composition and compare well with estimates independently obtained in other Mg–chloritoid-bearing terranes (e.g. Holland 1979). They are also supported by the composition of white mica. Among the different quartz-bearing assemblages which may buffer the phengitic substitution, for instance talc–phlogopite–quartz or K-feldspar–phlogopite–quartz, talc–kyanite–(chloritoid)–quartz is the one which buffers it to the lowest Si value, according to the reaction

talc + muscovite = phengite + kyanite + quartz + H_2O. (5)

Nevertheless, the Si-content of phengite in MZ sample is rather high (3.36–3.42). According to preliminary experimental data on the talc–phengite–kyanite–quartz assemblage, it would indicate pressures in the range 15–20 kbar (Massonne, pers. comm., 1982). In the case of lowered water activity, this pressure range represents a maximum value. At any rate the existence in the Monte Rosa of a typical high-grade, high-pressure, low-temperature metamorphism is demonstrated. The latter occurred prior to the main, lower-pressure "Lepontine" stage, as shown by the secondary formation of the low-pressure assemblage chlorite + kyanite from talc + chloritoid in the MZ sample.

Obviously Mg-rich metapelites are a sensitive metamorphic indicator also at high pressure, owing in particular to the wide range of Mg/Fe ratio in chloritoid. They allow subtle distinction between blueschist terranes which otherwise do not differ in their eclogitic assemblages. For example, the absence of the talc–kyanite pair and the more Fe-rich mineral composition of the four-phase assemblages talc–chloritoid–chlorite–quartz in the Gran Paradiso as compared to Monte Rosa point to more severe high-pressure P–T conditions in Monte Rosa than in Gran Paradiso.

The Triassic foliated quartzite (ZT 11)

This quartzite layer belongs to the post-Hercynian stratigraphic cover of the Monte Rosa nappe. In the sampling area, all the rocks exhibit a well-expressed foliation plane which supports a strong NW-SE stretching lineation interpreted in terms of a bulk shear context with a NW sense of thrusting (Mattauer 1981, Lacassin 1983). The fabric of the rock is evident from the well pronounced preferred orientation of quartz and micas which can be ascertained as recrystallised phengites. A late phase of non-penetrative deformation can also be observed. However, the phengite composition is remarkably homogeneous, as shown by the analyses of Table 1 which represent extreme values. Because phengite + quartz are the only mineral phases, the phengitic substitution is not buffered and the $Si_{3.35}$ value, although close to that in MZ, may have a different significance. For comparison, $Si_{3.5-3.6}$ values are found in quartzites of the Gran Paradiso cover series (Chopin and Maluski 1980).

$^{40}Ar-^{39}Ar$ experimental procedure

The phengites studied were concentrated by classical separation techniques up to 99% purity as controlled optically and by X-ray diffraction. Purification was achieved by ultrasonic cleaning in ethanol, and the minerals finally rinsed in distilled water. Different size-fractions were irradiated for 24 h by a fast neutron flux in the core of the CENG reactor at Grenoble, France, along with the interlaboratory standard MM Hornblende I (520 ± 2.5 Ma – Alexander et al. 1978). The integrated neutron flux is about 10^{13} n./cm^2 s. As a control of irradiation parameters, a recent age determination of the standard biotite Bern 4B has yielded an age of 18.4 ± 0.3 Ma, in agreement with its conventional age (Jäger 1969). After irradiation, samples were wrapped in high-purity nickel foils and loaded in the vacuum extraction system. Analyses were performed using standard $^{40}Ar-^{39}Ar$ techniques, details of which are given by Mitchell (1968), Brereton (1970), Dalrymple and Lanphere (1971) and Maluski (1977). Stepwise argon extractions were carried out in a Mo crucible using a radiofrequency induction heating. Each heating step was maintained for one hour, except fusion (30 min). Temperatures were monitored using an optical pyrometer; uncertainty is about ± 5° C. The extracted gases were purified on Zr–Al getters at 400° C and by dry ice-acetone mixture at – 75° C; argon was trapped on active charcoal fingers at liquid nitrogen temperature. Argon isotopic compositions were measured with a modified THN – 205E mass spectrometer operated in a static mode.

The data as given in Table 2 are corrected for the following effects:

a. Mass discrimination: the $^{40}Ar/^{36}Ar$ ratio of atmospheric argon has been regularly measured; it is in the range 295.4–298.9. Mass discrimination parameters were subsequently calculated for the $^{40}Ar/^{39}Ar$, $^{36}Ar/^{39}Ar$ and $^{37}Ar/^{39}Ar$ ratios.

b. Irradiation interferences: factors used to correct the effects of interfering neutron reaction are $(^{39}Ar/^{37}Ar)_{Ca} = 0.00202$, ($^{40}Ar/$

Table 2. Results of the argon analysis

Step	T°C	^{40}Ar blank (10^{-14} mole)	$^{40}Ar_{rad}/^{39}Ar$	$^{37}Ar_0/^{39}Ar$	$^{36}Ar/^{40}Ar \times 10^3$	$^{36}Ar/^{39}Ar \times 10^2$	Cum. ^{39}Ar (%)	Age (Ma)
MZ Phengite[a] (125–200 μm) 90.54 mg								
1	513	6.59	2.930	0.2319	1.990	1.413	0.06	67.9±4.5
2	565	7.41	3.032	0.6974	2.135	1.758	0.27	71.5±5.4
3	619	8.51	3.403	0.1977	0.538	0.218	0.40	80.1±2.1
4	668	8.78	2.918	0.1364	1.255	0.582	0.66	68.9±2.6
5	717	9.06	3.845	0.0624	0.613	0.288	1.74	90.2±2.4
6	761	9.06	4.257		0.359	0.171	3.41	99.6±2.5
7	805	9.61	4.616	0.0095	0.209	0.103	6.19	107.7±2.5
8	845	10.16	4.560	0.0058	0.218	0.107	14.20	106.9±2.5
9	886	12.63	4.497	0.0062	0.169	0.080	32.56	105.1±2.4
10	902	13.72	4.601	0.0097	0.195	0.095	45.51	107.4±2.5
11	922	15.10	4.818	0.0033	0.100	0.050	58.26	112.3±2.6
12	940	16.19	4.782	0.0092	0.173	0.087	65.53	111.5±2.6
13	975	18.94	4.833	0.0027	0.079	0.039	79.35	112.7±2.6
14	1008	22.51	4.638		0.110	0.052	89.73	108.2±2.5
15	1042	27.45	4.683		0.019	0.009	94.77	109.3±2.4
16	1097	35.68	4.633		0.078	0.037	98.66	108.1±2.4
17	1248		4.884		0.243	0.128	100	113.8±2.7
Total $^{39}Ar_K = 4.2224\ 10^{-11}$ mole						Total age:		108.3±2.5
						Plateau (7→17):		108.9±2.5
MZ Phengite[a] (200–250 μm) 40.41 mg								
1	457	6.04	3.181		2.549	3.283	0.03	74.9±9.3
2	565	7.41	3.087		2.403	2.558	0.22	72.7±7.5
3	619	8.51	3.086		1.935	1.395	0.37	72.7±4.6
4	668	8.78	3.434		1.183	0.625	0.74	80.8±2.9
5	717	9.06	4.020		0.784	0.411	1.67	94.2±2.8
6	761	9.06	4.857		0.309	0.165	3.27	113.2±2.8
7	805	9.61	4.884	0.0877	0.481	0.274	5.51	113.8±2.9
8	845	10.16	4.799		0.494	0.277	11.97	111.9±2.9
9	886	12.63	4.711		0.202	0.101	44.80	109.9±2.6
10	922	15.10	4.726	0.2171	0.239	0.121	63.33	110.2±2.6
11	958	17.84	5.070		0.178	0.095	78.52	118.0±2.8
12	992	21.41	4.903		0.105	0.053	88.50	114.2±2.6
13	1026	24.70	4.544		0.244	0.119	95.24	106.1±2.6
14	1060	29.65	4.486		0.350	0.175	98.28	104.8±2.6
15	1248		4.333	0.0676	0.579	0.303	100	101.3±2.7
Total $^{39}Ar_K = 1.6394\ 10^{-11}$ mole						Total age:		110.9±2.7
						Plateau (6→15):		111.4±2.6
ZT 11 Phengite[b] (100–125 μm) 178.91 mg								
1	445	1.23	4.876		1.477	1.278	0.02	81.9±3.6
2	520	1.40	5.469	0.2009	1.029	0.809	0.20	91.7±3.0
3	590	1.56	3.885	0.0245	0.454	0.204	0.47	65.6±1.7
4	655	1.75	2.533		0.409	0.118	1.51	43 ±1.1
5	715	1.98	2.230		0.151	0.035	5.58	37.9±0.9
6	770	2.20	2.150		0.119	0.027	14.23	36.6±0.8
7	825	2.47	2.091	0.0125	0.318	0.073	22.73	35.6±0.9
8	875	2.74	2.133	0.0030	0.394	0.095	38.79	36.3±0.9
9	875	2.74	2.128	0.0277	0.167	0.037	41.27	36.2±0.8
10	965	3.65	2.199	0.0008	0.344	0.084	66.55	37.4±0.9
11	1010	4.80	2.204		0.369	0.091	81.22	37.5±0.9
12	1050	7.14	2.248		0.197	0.047	96.21	38.2±0.9
13	1095	9.61	2.109		0.147	0.032	99.93	35.9±0.8
14	1510		3.032		3.054	9.483	100	51.4±18.0
Total $^{39}Ar_K = 4.8781\ 10^{-11}$ mole						Total age:		37.7±0.9
						Plateau (5→14):		37.3±0.9

[a] J=0.013333 [b] J=0.009532

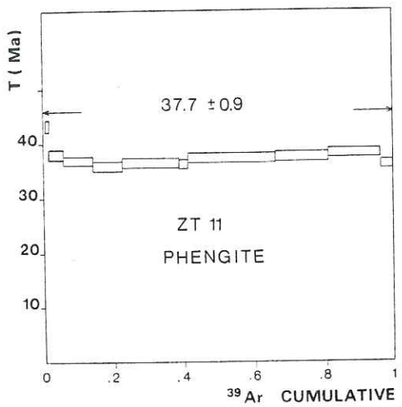

Fig. 3. Age spectrum of phengite from the foliated quartzite ZT 11 (Gornergrat cover). Total gas age: 37.7±0.9 Ma; plateau age: 37.3±0.9 Ma

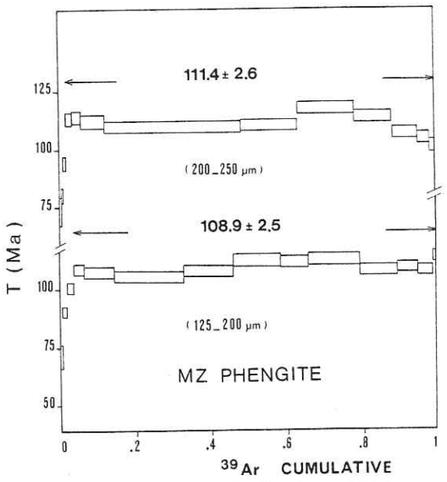

Fig. 4. Age spectra for two size fractions of high-pressure phengite from the undeformed MZ sample

$^{37}Ar)_{Ca} = 0.0216$ and $(^{40}Ar/^{39}Ar)_K = 0.00085$, as determined by analysis of irradiated pure CaF_2 and K_2SO_4 salts.

c. Radioactive decay of ^{37}Ar since irradiation.

d. Blanks: prior to the age measurements, a series of blanks were run through the whole extraction system at increasing temperatures, using the same extraction procedure as for a sample analysis. The results for ^{40}Ar indicate that blank contribution increases from 6×10^{-14} mole at 450° C up to 8.5×10^{-13} mole at 1,250° C for MZ phengites (Table 2). For the fusion step, the blank is typically higher than the ^{40}Ar measured for the sample. Therefore no blank correction is applied to the last step of MZ and ZT 11 phengites. Blanks are lower for ZT 11 phengites as they have been performed after a long baking (48 h at 200° C) of the entire extraction-purification system, in addition with pumps. Repeated determinations show that blank uncertainty is about 50%. As the higher blanks agree with an atmospheric composition, corrections were carried out assuming an atmospheric composition for all blanks, which may not be always true especially at low temperatures.

Ages were calculated using Brereton formula (1970) and recommended decay constants (Steiger and Jäger 1977); errors reported are 2 σ deviations and correspond to the 95% confidence level.

Results and discussion

The results of the $^{40}Ar-^{39}Ar$ incremental release measurements are compiled in Table 2.

$^{40}Ar-^{39}Ar$ age spectra

The individual apparent ages are plotted against the cumulative percentage of ^{39}Ar released in Figs. 3 and 4.

The recrystallised phengite from the Gornergrat cover (ZT 11) yields a well-defined plateau age of 37.3±0.9 Ma for over 98% of the ^{39}Ar released (Fig. 3). The total gas age is concordant (37.7±0.9 Ma) although older ages are obtained in the first three steps. The 37–38 Ma age is a common result in the whole Western Alps and dates the temperature climax of the Tertiary, "Lepontine", Barrow-type metamorphism (Jäger 1973, Bocquet et al. 1974, Frey et al. 1976).

For MZ phengite (Fig. 4), the main result is that the 125–200 and 200–250 μm size fractions yield for over 96% of the ^{39}Ar released a group of ages at 108.9±2.5 and 111.4±2.6 Ma, respectively. The age spectrum of the 200–250 μm fraction does not strictly define a plateau in the sense of Fleck et al. (1977). Indeed, the larger micas exhibit a more irregular age pattern than the smaller ones for the high temperature steps. This might be an effect of grain size on argon migration within the mineral lattice during experimental heating or irradiation. Nevertheless the 111.4 mean value of the large size fraction is consistent within the 2 σ analytical error limits with the 108.9 plateau age of the smaller size fraction.

Another characteristic feature of the MZ age spectra is the existence for the first heating step of low apparent ages (67.9±4.5 and 74.9±9 Ma) which then progressively increase to the plateau value. We may first consider that these discordant low-temperature ages reflect a slight argon loss resulting from sample preparation, chiefly from the grinding and ultrasonic procedure and from the neutron irradiation. However, the comparison of irradiated and unirradiated samples has shown that the diffusion properties are not affected by the irradiation process (Kaneoka 1975, Roddick et al. 1980, Staudacher et al. 1982). Moreover the opposite trends in the low-temperature release patterns of the MZ and ZT 11 samples rule out the possibility of experimental artifacts. Therefore, although these low-temperature steps represent only a small percentage of the total argon release (3.4 and 1.7%, respectively) and have been usually ignored for interpretation, we have paid some attention to their possible geological significance as suggested by Roddick et al. (1980) and Harrison and McDougall (1980).

Isotope correlation diagrams

$^{40}Ar/^{36}Ar$ vs. $^{39}Ar/^{36}Ar$ diagram. Figure 5 represents the conventional $^{40}Ar/^{36}Ar$ vs. $^{39}Ar/^{36}Ar$ plot for the two size fractions of MZ phengite. Errors reported have been calculated according to York (1969). The plot shows no evidence for the incorporation of excess argon in the phengite lattice but it is in fact inconclusive since biotite containing proved excess argon may exhibit a reasonably well defined linear

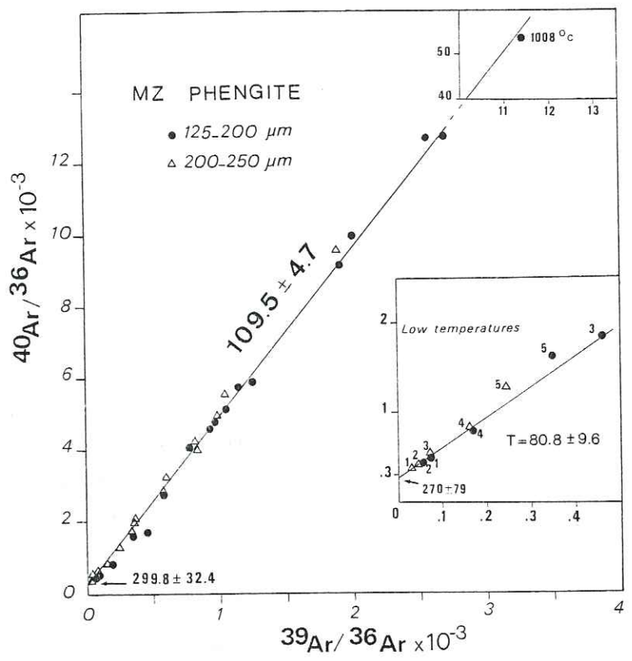

Fig. 5. $^{40}Ar/^{36}Ar$ vs. $^{39}Ar/^{36}Ar$ plot for two size-fractions of MZ phengite. The regression for the high-temperature steps does not include the 958° C step of the 200–250 µm fraction and yields an isochron age identical to the plateau ages. The first four low-temperature steps define a younger isochron age (inset). In both cases the intercept value is close to the atmospheric ratio. The higher representative point at 1,008° C is probably due to an inadequate blank correction moving this point too high along the isochron line but without a great incidence on the slope and intercept values

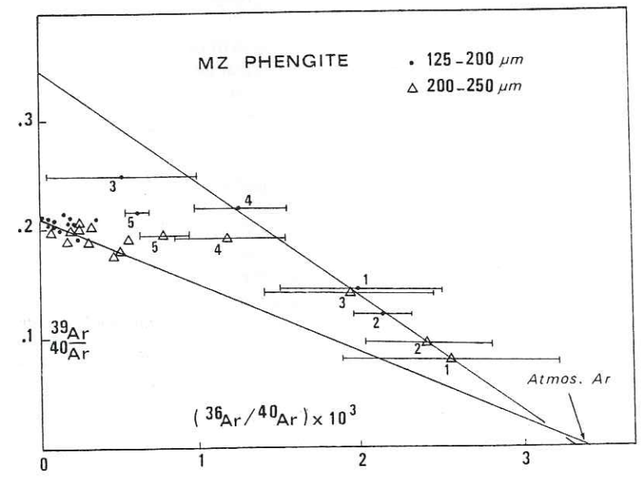

Fig. 6. $^{39}Ar/^{40}Ar$ vs. $^{36}Ar/^{40}Ar$ isotope correlation plot for the two size fractions of MZ phengite. The tight cluster of points for the high-temperature steps indicates constant proportions of ^{40}Ar, ^{39}Ar and ^{36}Ar in the argon released. The first low-temperature gas fractions define a good linear trend which can be interpreted as binary mixing with an argon of atmospheric composition (see text). The Y and X intercepts (0.3482 ± 0.0248 and $3.278 \pm 0.208.10^{-3}$ respectively) yield a 66.5 ± 4.5 Ma age and a 305 ± 20 initial ratio. The error bars drawn for the $^{36}Ar/^{40}Ar$ ratio include the uncertainty due to blank correction

correlation with a $^{40}Ar/^{36}Ar$ intercept close to 295.5 (Foland 1983, Dallmeyer and Rivers 1983) because of a constant proportion of excess ^{40}Ar relative to radiogenic ^{40}Ar in each step and of binary mixing with atmospheric argon (Roddick 1978). Therefore ^{40}Ar has been used as reference isotope in the graph of Fig. 6, as proposed by Roddick et al. (1980).

$^{39}Ar/^{40}Ar$ vs. $^{36}Ar/^{40}Ar$ diagram (Fig. 6). If the successive gas fractions plot on a line in this diagram the composition of trapped argon is given by the intercept on the abcissa while the intercept value on the ordinate yields the apparent age.

For the first temperature increments, MZ phengite displays a well defined linear trend which passes through air composition and which yields an apparent age of 66.5 ± 4.6 Ma. With increasing temperature the ^{36}Ar contribution becomes lower with respect to ^{40}Ar and ^{39}Ar. At high temperature, the tight cluster of points near the ordinate axis implies constant proportions of the three isotopes and a low atmospheric contribution in the argon release. The resulting pattern is quite characteristic. A loosely bound argon, which is a binary mixture between atmospheric argon and an argon reservoir with an apparent age of about 65–70 Ma, is released up to 660° C. From 760° C to fusion a tightly bound argon of constant isotopic composition is released by the phengite lattice.

Interestingly, the isotopic pattern obtained for ZT 11

phengite (not shown) is quite similar although the apparent age (about 80 Ma) of the argon released together with atmospheric argon at low temperature is higher than the apparent age (37 Ma) of the tightly bound, "lattice" argon. The latter undoubtedly dates the complete readjustment of the system to the conditions of the Tertiary, "Lepontine" metamorphism. This "lattice" argon is radiogenic, the 37 Ma age is a true one, the presence of detectable excess ^{40}Ar in the mineral lattice is ruled out by the ubiquity of similar 37–40 Ma ages in the Western Alps. The atmospheric component of the low-temperature release might have been adsorbed during sample preparation and irradiation, although our samples were sealed under vacuum before irradiation (see Roddick 1983). The second low-temperature argon component may represent excess argon located in the near-surface region of the crystals and having the composition of ambient argon in the rock. Indeed the $^{40}Ar/^{36}Ar$ ratio of ambient argon is likely to have been high because of the radiogenic argon expelled during the 38 Ma event and because of the immediately underlying gneissic basement which may act as a source of radiogenic argon. Small amounts of this ambient argon fixed on the less retentive sites of the mica can then account for the small low-temperature release with anomalously old ages obtained for ZT 11.

The isotopic pattern obtained for the MZ phengite may receive two alternative interpretations:

1. We may assume that the 110 Ma plateau is an anomalously old age due to uniform incorporation of excess ^{40}Ar within the phengite lattice. Whereas incorporation of excess argon yielding plateaux is now well documented for biotites (Pankhurst et al. 1973, Roddick et al. 1980, Foland 1983, Dallmeyer and Rivers 1983), this would be to our knowledge the first time it is reported in white mica. Admittedly, the unusually high crystallisation pressures are the sort of conditions under which excess argon would be expected to be absorbed. Then the model of argon evolution proposed by Roddick et al. (1980) for biotites known to contain excess argon could also be applied to the isotopic pattern of MZ phengite. According to this model only the 65–70 Ma apparent age of the low-temperatue argon fraction may have a geologic significance and may closely approach the time of argon retention. In this view such an age would be in agreement with that deduced by Chopin and Maluski (1980) for the high-pressure metamorphism in the Gran Paradiso massif.

2. Alternatively, we may consider that the high-temperature fraction essentially represents radiogenic argon (as in ZT 11), i.e. the 110 Ma plateau age dates the time of argon retention by the high-pressure phengite and is geologically meaningful. Then, the younger, discordant ages of the low-temperature steps may result from a loss of radiogenic argon from the less retentive sites during a later perturbation for which the first apparent ages would only yield an upper age limit. This perturbation may have occurred 65–70 Ma ago (under still high-pressure conditions?) or under low-pressure ones, most likely 38 Ma ago. Additional isotopic work has been undertaken to precise this point (Monié, in prep.). The only petrographic evidence for a perturbation of the system is the secondary formation of the low-pressure kyanite–chlorite assemblage from the high-pressure talc–chloritoid assemblage (see Petrography).

Unfortunately, the isotopic data yield no direct evidence to support or to reject either hypothesis. We favour the second one, i.e. 110 Ma as a true age, for the following reasons, even if, admittedly, none of these is sufficient to dismiss the excess argon hypothesis: i) the high-temperature gas release of MZ phengite shows a behaviour similar to that of ZT 11 in both isochron plots and these plots yield no evidence *for* the presence of excess argon; ii) the argon solubility in white mica is known to be low as compared, for instance, to that in biotite; iii) a 110 Ma age for the high-pressure metamorphism in the Monte Rosa massif is in agreement with the Rb–Sr whole-rock isochron obtained by Hunziker (1970) in that area, with Rb–Sr data obtained in the neighbouring Sesia zone (Oberhänsli et al. 1982) and also in the Central Alps (Steinitz and Jäger 1981).

In the structurally equivalent Gran Paradiso massif Chopin and Maluski (1980) have shown that high-pressure phengites unaffected by the 38 Ma event had become closed systems at various times in the range 60–75 Ma depending on several factors. These ages give only a minimum value for the age of phengite crystallisation and high-pressure metamorphism. A 110 Ma age for high-pressure metamorphism in the Monte Rosa is therefore not in formal contradiction with the Gran Paradiso data. It must be stressed that even the less deformed samples selected by Chopin and Maluski in the Gran Paradiso exhibited a distinct planar fabric. The latter must date back to high-pressure conditions since the oriented mica flakes are undeformed and have preserved their high-pressure chemical composition. In this respect the Monte Rosa sample studied here is indeed unique by the absence of preferred mineral orientation, and this may account for the difference in ages measured on assemblages which were *a priori* formed at the same time. Finding in the Gran Paradiso massif samples similar to MZ could show that high-pressure conditions might have lasted in this massif from about 110 Ma down to 60–75 Ma, as suggested by Oberhänsli et al. (1982) for the Sesia zone. Mineral growth would have taken place under static conditions 110 Ma ago and most of the systems would have recrystallised down to 60–75 Ma under non-static conditions. The problem remains to find such samples in the Gran Paradiso massif.

Conclusion

Early Alpine phengites extracted from an undeformed quartzose rock and having crystallised under high-pressure and low P_{H_2O} conditions yield a 110 Ma plateau age which either dates the time of argon retention or is due to uniform incorporation of excess argon, the true age then being about 65–70 Ma. Phengites from a strongly foliated quartzite sampled in the same, westernmost part of the Monte Rosa massif have been isotopically completely reset by the retrogressive greenschist metamorphism 38 Ma ago. Thermal conditions estimated near 400–450° C for the latter event (Frey et al. 1976) have thus obviously failed to reset the Ar system of the non foliated rock, whatever interpretation is chosen for the 110 Ma plateau age. Since the different Fe/Mg ratio of the two phengite samples is not likely to be responsible for such a contrasting behaviour with respect to argon retention, we suggest that recrystallisation and penetrative deformation have promoted the isotopic reequilibration of ZT 11, while the undeformed samples behave as a closed system even at temperatures higher than the usually assumed blocking temperature of white mica.

Acknowledgements. The continued support of H. Maluski, Montpellier, is gratefully acknowledged. Critical comments by J.M. Ferry on an earlier version of the manuscript and by two anonymous reviewers improved the presentation of this paper. The first author is also indebted to K. Abraham for microprobe facilities during a stay at Bochum.

Appendix: Data used for the thermodynamic calculations

	Components	Molar volume of the corresponding phase
Q	SiO_2	2.269 J/bar
Ky	$SiAl_2O_5$	4.409
Tc	$Mg_3Si_4O_{10}(OH)_2$	13.625
Ctd	$MgAl_2SiO_5(OH)_2$	6.874
Chl	$Mg_{4.75}Al_{2.5}Si_{2.75}O_{10}(OH)_8$	21.07

Reactions among the components

$$29\ \text{Ctd} + 3\ \text{Tc} = 8\ \text{Chl} + 19\ \text{Ky} \qquad (4)$$

$$12\ \text{Chl} + 58\ \text{Q} = 19\ \text{Tc} + 15\ \text{Ky} + 29\ H_2O \qquad (2')$$

The curve of reaction (4) has been linearly extrapolated in the $P-T$ range of interest from the experimental points 25 kbar, 600° C and 30.5 kbar, 710° C (Chopin, unpublished data which slightly modify those presented in Chopin and Schreyer 1983). The curve used for reaction (2′) is that experimentally determined by Massonne et al. (1981). The fact that both curves intersect with a high angle minimizes the uncertainty on the $P-T$ derivation. Mole fraction of the components in the minerals of sample MZ:

$$X_{Tc}^{talc} = 0.95 \qquad X_{Chl}^{chlorite} = 0.875 \qquad X_{Ctd}^{chloritoid} = 0.65$$

The isothermal pressure shift of a reaction curve due to modified activities in the solid and fluid phases is given by

$$\Delta V_S\,(\text{Pe}-P) = R\ \text{Te}\ \ln K + n(G_{H_2O,P,Te} - G_{H_2O,Pe,Te}) + n\ R\ \text{Te}\ \ln a_{H_2O}$$

with ΔV_S: standard molar volume change of the solids at Te, assumed to be equal to ΔV_S at 298 K

Pe, Te: define a (P, T) point on the reference equilibrium curve

n: stoichiometric coefficient for H_2O in the reaction

$G_{H_2O,P,T}$: standard molar Gibbs free energy of H_2O at specified P and T.

The system obtained for the two reaction curves is solved iteratively or graphically for Te and P assuming $a_{H_2O} = 1$ and ideal solid solutions. Alternatively, it yields the value of a_{H_2O} for which the curve of reaction (2) intersects that of reaction (4) at given T. G_{H_2O} data were taken from Halbach and Chatterjee (1982).

References

Alexander EC, Mickelson GM, Lanphere MA (1978) MM Hb−1: a new $^{40}Ar/^{39}Ar$ dating standard. US Geol Surv open file Rep 78–701:6–8

Bearth P (1952) Geologie und Petrographie des Monte Rosa. Beitr Geol Karte Schweiz, NF 96, 94 pp

Bearth P (1958) Über einen Wechsel der Mineralfazies in der Wurzelzone des Penninikums. Schweiz Min Petr Mitt 39:267–286

Bearth P (1967) Die Ophiolite der Zone von Zermatt-Saas Fee. Beitr Geol Karte Schweiz, NF 132, 130 pp

Bocquet J, Delaloye M, Hunziker JC, Krummenacher D (1974) K−Ar and Rb−Sr dating of amphiboles, micas and associated minerals from the Western Alps. Contrib Mineral Petrol 47:7–26

Brereton NR (1970) Corrections for the interfering isotopes in the $^{40}Ar/^{39}Ar$ dating method Earth Planet Sci Lett 8:427–433

Chinner GA, Dixon JG (1973) Some high-pressure parageneses of the Allalin gabbro, Valais, Switzerland. J Petrol 14:185–202

Chopin C (1979) De La Vanoise au massif du Grand Paradis: une approche pétrographique et radiochronologique de la signification géodynamique du métamorphisme de haute pression. Thèse 3ème cycle. Université Paris VI, 145 pp

Chopin C (1981) Talc-phengite: a widespread assemblage in high-grade pelitic blueschists of the Western Alps. J Petrol 22:628–650

Chopin C (1983) Magnesiochloritoid, a key-mineral for the petrogenesis of high-grade pelitic blueschists. Bull Mineral 106:715–717

Chopin C, Maluski H (1980) $^{40}Ar-^{39}Ar$ dating of high pressure metamorphic micas from the Gran Paradiso area (Western Alps): evidence against the blocking temperature concept. Contrib Mineral Petrol 74:109–122

Chopin C, Maluski H (1982) Unconvincing evidence against the blocking temperature concept? A reply. Contrib Mineral Petrol 80:391–394

Chopin C, Schreyer W (1983) Magnesiocarpholite and magnesiochloritoid: two index minerals of pelitic blueschists and their preliminary phase relations in the model system $MgO-Al_2O_3-SiO_2-H_2O$. Am J Sci, Orville volume 283A:72–96

Compagnoni R, Lombardo B (1974) The Alpine age of the Gran Paradiso eclogites. Rend Soc It Mineral Petrol 30:223–237

Dallmeyer RD, Rivers T (1983) Recognition of extraneous argon components through incremental release $^{40}Ar/^{39}Ar$ analysis of biotite and hornblende across the Grenvillian metamorphic gradient in Southwestern Labrador. Geochim Cosmochim Acta 47:413–428

Dal Piaz GV (1964) Il cristallino antico del versante meridionale del Monte Rosa: paraderivati a prevalente metamorphisme alpino. Rend Soc Mineral It 20:101–135

Dal Piaz GV (1965) La formazione mesozoica dei calcescisti con pietre verdi fra la Valsesia e la Valtournanche ed i suci rapporti strutturali con il ricoprimento Monte Rosa e con la zona Sesia-Lanzo. Boll Soc Geol It 83:1–40

Dal Piaz GV (1966) Gneiss ghiandoni, marmi ed anfiboliti antiche del ricoprimento Monte Rosa nell'alta Valle d'Ayas. Boll Soc Geol It 85:103–132

Dal Piaz GV (1971) Nuovi ritrovamenti di cianite alpina nel cristallino del Monte Rosa. Rend Soc It Mineral Petr 27:437–477

Dal Piaz GV, Lombardo B (1982) Early Alpine eclogitic overprinting in the penninic Monte Rosa – Gran Paradiso basement nappes, Italy. Abst first Eclogite conf. Terra Cognita 2:306

Dalrymple GB, Lanphere MA (1971) $^{40}Ar/^{39}Ar$ technique of K/Ar dating. A comparison with the conventional technique. Earth Planet Sci Lett 12:300–308

Ellenberger F (1958) Etude géologique du pays de Vanoise. Mém Serv carte géol Fr, 561 pp

Fleck RJ, Sutter JF, Elliot DH (1977) Interpretation of discordant $^{40}Ar/^{39}Ar$ age spectra of Mesozoic tholeiites from Antarctica. Geochim Cosmochim Acta 41:15–32

Foland KA (1983) $^{40}Ar/^{39}Ar$ incremental heating plateaus for biotites with excess argon. Isotope Geosc 1:3–21

Frey M, Hunziker JC, O'Neil JR, Schwander HW (1976) Equilibrium-disequilibrium relations in the Monte Rosa granite, Western Alps: petrological, Rb−Sr and stable isotope data. Contrib Mineral Petrol 55:147–179

Ganguly J (1972) Staurolite stability and related parageneses: theory, experiments and applications. Jour Petrology 13:335–365

Halbach H, Chatterjee ND (1982) An empirical Redlich-Kwong-type equation of state for water to 1,000° C and 200 kbar. Contrib Mineral Petrol 79:337–345

Harrison TM, McDougall I (1980) Investigations of an intrusive contact, northwest Nelson, New Zealand. II. Diffusion of radiogenic and excess ^{40}Ar in hornblende revealed by $^{40}Ar/^{39}Ar$ age spectrum analysis. Geochim Cosmochim Acta 44:2005–2020

Holland TJB (1979) High water activities in the generation of high-pressure kyanite eclogites of the Tauern Window, Austria. J Geol 87:1–27

Hunziker JC (1969) Rb−Sr Altersbestimmungen aus den Walliser Alpen. Hellglimmer- und Gesamtgesteinsalterswerte. Eclog Geol Helv 62:527–542

Hunziker JC (1970) Polymetamorphism in the Monte Rosa, Western Alps. Eclog Geol Helv 63:151–161

Hunziker JC (1974) Rb−Sr and K−Ar age determination and the Alpine tectonic history of the Western Alps. Mem Ist Geol Mineral Univ Padova 31, 55 pp

Hunziker JC, Bearth P (1969) Rb−Sr Altersbestimmungen aus den Walliser Alpen. Biotitalterswerte und ihre Bedeutung für die Abkühlungsgeschichte der alpinen Metamorphose. Eclog Geol Helv 62:205–222

Jäger E (1969) Colloquium on the geochronology of Phanerozoic Orogenic Belts. Zürich and Bern. Data compilation in Abstract volume

Jäger E (1973) Die alpine Orogenese im Lichte der radiometrischen Altersbestimmung. Eclog Geol Helv 66:11–21

Kaneoka I (1975) Non radiogenic argon in terrestrial rocks. Geochim J 9:113–124

Klein JA (1978) Post-nappe folding southeast of the Mischabel Rückfalte (Pennine Alps) and some aspects of the associated metamorphism. Leidse Geol Meded 51:233–312

Lacassin R (1983) Cisaillement ductile et déformation hétérogène du granite de la nappe du Mont-Rose dans la vallée de Saas (Suisse). CR Acad Sci Paris 296D:777–782

Laduron D (1976) L'antiforme de Vanzone, étude pétrographique et structurale dans la vallée d'Anzasca (Province de Novara, Italie). Mém Inst Géol Univ Louvain 28

Laduron D, Wittock R (1982) Chimisme et polytypisme des micas blancs de Vanzone (Alpes penniques italiennes). Abst 9è Réun Ann Sci Terre Paris, Soc Géol Fr édit, p 348

Maluski H (1977) Application de la méthode $^{40}Ar-^{39}Ar$ aux minéraux des roches cristallines perturbées par des événements thermiques et tectoniques en Corse. Thèse d'etat. Montpellier, 172 pp

Massonne HJ (1981) Phengite: eine experimentelle Untersuchung ihres Druck-Temperatur-Verhaltens im System $K_2O-MgO-Al_2O_3-SiO_2-H_2O$. Dissertation, Ruhr-Universität Bochum

Massonne HJ, Mirwald PW, Schreyer W (1981) Experimentelle Überprüfung der Reaktions Kurve chlorit + Quarz = Talk + Disthen im System $MgO-Al_2O_3-SiO_2-H_2O$. Fortschr Mineral 59:122–123

Mattauer M (1981) Plis en fourreau d'échelle plurikilométrique dans la zone interne des Alpes suisses (couverture nord de la Nappe du Mont-Rose). CR Acad Sci Paris 293D:929–932

Michard A (1967) Etudes géologiques dans les zones internes des Alpes Cottiennes. Thèse CNRS édit, Paris, 448 pp

Miller C (1977) Chemismus und phasenpetrologische Untersuchungen der Gesteine aus der Eklogitzone des Tauernfensterns. Österreich. Tschermaks Mineral Petrogr Mitt 24:221–277

Milnes AG, Greller M, Müller R (1981) Sequence and style of major post-nappe structures, Simplon-Pennine Alps. J Struct Geol 3:411–420

Mitchell JG (1968) The argon-40–argon-39 method for potassium-argon age determination. Geochim Cosmochim Acta 32:781–790

Newton RC (1972) An experimental determination of the high-pressure stability limits of magnesian cordierite under wet and dry conditions. J Geol 80:398–420

Oberhänsli R, Hunziker JC, Martinotti G, Stern WB (1982) Mucronites: an example of eo-Alpine eclogitisation of Permian granitoids, Italy. Abst first int Eclogite conf, Terra Cognita 2, p 325

Pankhurst RJ, Moorbath S, Rex DG, Turner G (1973) Mineral age pattern in ca. 3,700 m. y. old rocks from West Greenland. Earth Planet Sci Lett 20:157–170

Roddick JC (1978) The application of isochron diagrams in $^{40}Ar-^{39}Ar$ dating: a discussion. Earth Planet Sci Lett 41:233–244

Roddick JC (1983) High precision intercalibration of $^{40}Ar-^{39}Ar$ standards. Geochim Cosmochim Acta 47:887–898

Roddick JC, Cliff RA, Rex DC (1980) The evolution of excess argon in Alpine biotites. A $^{40}Ar-^{39}Ar$ analysis. Earth Planet Sci Lett 48:185–208

Staudacher Th, Jessberger EK, Dominik EB, Kirsten T, Schaeffer OA (1982) $^{40}Ar-^{39}Ar$ ages of rocks and glasses from the Nördlinger Ries Crater and the temperature history of impact breccias. J Geophys 51:1–11

Steiger RH, Jäger E (1977) Subcommission on geochronology: convention on the use of decay constants in geo and cosmochronology. Earth Planet Sci Lett 36:359–362

Steinitz G, Jäger E (1981) Rb−Sr and K−Ar studies on rocks from the Suretta nappe, Eastern Switzerland. Schweiz Mineral Petrogr Mitt 61:121–131

Turner G (1968) The distribution of potassium and argon in chrondrites. In: Ahrens LH (ed) Origin and distribution of the elements. Pergamon, New York, pp 387–398

Velde B (1965) Phengite micas: synthesis, stability and natural occurrences. Am J Sci 263:886–913

Vialette Y, Vialon P (1964) Etude géochronologique de quelques micas des formations du massif Dora-Maira, Alpes cottiennes piémontaines. Ann Fac Sci Univ Clermont 25:91–99

Vialon P (1966) Etude géologique du massif cristallin Dora Maira. Alpes cottiennes internes, Italie. Thèse Doctorat d'Etat, Univ Grenoble, 282 pp

Wetzel R (1972) Zur Petrographie und Mineralogie der Furgg-Zone (Monte Rosa-Decke). Schweiz Mineral Petrogr Mitt 52:161–236

York D (1969) Least squares fitting of a straight line with correlated errors. Earth Planet Sci Lett 5:320–324

Received January 26, 1984; Accepted July 16, 1984

Note added in proof

A wet-chemical analysis of sample MZ yields: SiO_2 65.99, Al_2O_3 17.95, MgO 5.84, total iron as FeO 2.46, Na_2O 0.27, K_2O 4.04, traces of TiO_2, P_2O_5, MnO and CaO, H_2O 3.78, sum 100.33 (N. Picot analyst).

Contrib Mineral Petrol (1984) 86:107–118

Contributions to Mineralogy and Petrology

Coesite and pure pyrope in high-grade blueschists of the Western Alps: a first record and some consequences*

Christian Chopin
ER 224, Laboratoire de Géologie, Ecole Normale Supérieure, 46 rue d'Ulm, 75005 Paris, France

Abstract. A pyrope-quartzite originally described by Vialon (1966) from the Dora Maira massif was resampled and reinvestigated. Garnet (up to 25 cm in size), phengite, kyanite, talc and rutile are in textural equilibrium in an undeformed matrix of polygonal quartz. The garnet is a pyrope-almandine solid solution with 90 to 98 mol % Mg end-member. It contains inclusions of coesite which has partially inverted to quartz, resulting in a typical radial cracking of the host garnet around the inclusions. Several lines of evidence show that coesite crystallised under nearly static pressure conditions and that the whole matrix has once been coesite.

The formidable pressures of formation implied ($\geqq$28 kbar) are independently indicated by i) the coexistence of nearly pure pyrope with free silica and talc, ii) the coexistence of jadeite with kyanite, iii) the high Si content of phengite. Water activity must have been low. The stability of talc-phengite and the presence of rare glaucophane inclusions in pyrope point to low formation temperatures (about 700 °C) and to a probable Alpine age for the assemblage.

This is evidence that low temperature gradients, how essentially transient they are, may nevertheless persist to considerable depths. Moreover, the upper crustal (evaporite-related?) origin of the quartzite and its interbedding within a continental unit implies that continental crust may also be subducted to depths of 90 km or more. The return back to the surface is problematic; the retrograde assemblages observed show that it must be tectonic. If the rocks remain at depth, new perspectives open for the genesis of intermediate to acidic magmas. Eventually, the role of continental crust in geodynamics may have to be reconsidered.

Introduction

Coesite, one of the high-pressure polymorphs of silica, was first synthesized and described by Coes (1953). The first natural occurrence was reported by Chao et al. (1960) from Meteor Crater, Arizona, and many similar occurrences have then been reported from impact structures. The high-pressure stability field of coesite, as investigated by many workers (from Mac Donald 1956, to Massonne and Mirwald 1981, with references), precluded the occurrence of this mineral in crustal rocks except at impact sites, but suggested that coesite is a stable phase in the upper mantle provided free silica exists there. Indeed, Sobolev et al. (1976) and Smyth and Hatton (1977) reported the first occurrences of coesite from a natural, static pressure environment, from xenoliths in diamond-bearing kimberlites, a now almost common type of occurrence (e.g. Lazko et al. 1983). Likewise very pyrope-rich garnet had exclusively been found in mantle-derived rocks, in accordance with its high-pressure stability field (Boyd and England 1959; Schreyer 1968).

At variance with the former results, an occurrence of coesite inclusions in nearly pure pyrope garnets is reported in this paper from a metasedimentary rock in high-grade blueschist terrane of the Western Alps. It implies that both coesite and pyrope may also be metamorphic products by burial of upper crustal material (cf. Chopin 1983).

Geological setting and the pioneering work of P. Vialon

The pyrope-bearing samples have been found in the Dora Maira massif which is, with Monte Rosa and Gran Paradiso, one of the three internal crystalline massifs of the Western Alps (Fig. 1). The massif consists of a Paleozoic basement and a Mesozoic cover series both of which underwent Alpine high-pressure, low-temperature metamorphism. The basement itself is composed of several volcanosedimentary series. One of them is polymetamorphic, intruded by granite bodies and unconformably overlain by the other series which are presumably of Late Paleozoic age (Fig. 1). This outline is made after Vialon (1966) who achieved the most comprehensive geologic and petrographic study of the massif to date.

Vialon noted, within the polymetamorphic series, a remarkable quartzite layer – probably mentioned as micascisti splendenti by Stella (1895) and Franchi (1900) – containing large phengite flakes and greenish or pale pink nodules up to 25 cm in size. He gave a detailed mineralogical description and established that the nodules were huge, monocrystalline, nearly pure pyrope garnets at various stages of chloritisation. He gave a wet chemical analysis of the garnet which, despite the probable presence of kyanite impurities, show that the garnet was indeed the closest to the pyrope end-member ever found (V16, Table 1). Vialon was also able to map the quartzite layer, which is a few metres thick, over about 15 kilometres and established that it was spatially associated with a sill (?) of metagranite on one side of which it systematically occurs. The surrounding rocks are a series of fine-grained felsic (para-?) gneisses with some marble and metabasite lenses, the latter occasionally containing relic assemblages of glaucophane eclogite (Franchi 1900; Vialon 1966).

The quartzite layer was resampled at Parigi, near Martiniana Po, Italy, in what is given by Vialon as the most spectacular out-

* This paper is dedicated to Pierre Vialon who first discovered these fascinating rocks

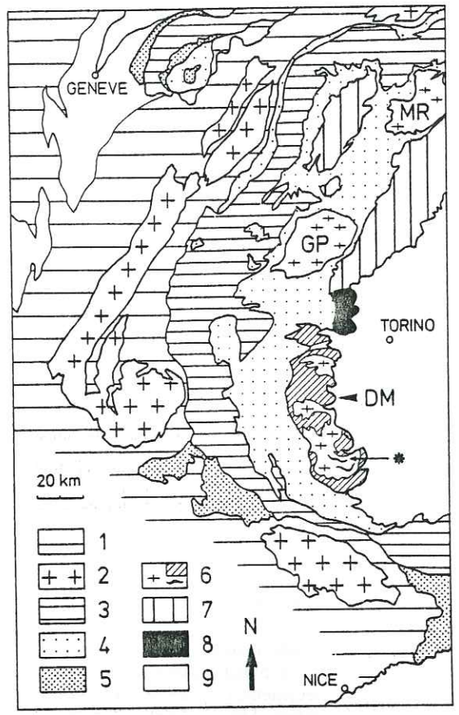

Fig. 1. Structural sketch map of the Western Alps. External zone: (1) folded post-Paleozoic cover; (2) External crystalline massifs (basement, Paleozoic and older). Penninic domain: (3) Briançonnais-St Bernard zone, basement and post-Paleozoic cover undifferenciated; (5) Upper Cretaceous Helminthoid flysch nappe; Piémont zone with (4) Schistes lustrés nappe (Mesozoic, mainly oceanic material) and (6) internal crystalline massifs, Monte Rosa (MR) and Gran Paradiso (GP) undifferenciated, in Dora Maira (DM) the cross-hatched area denotes the Late Paleozoic series, crosses the polymetamorphic, Early Paleozoic (?) basement with the pyrope quartzite layer (in black, the star showing the studied locality). Austroalpine units: (7) Sesia zone, Dent Blanche nappe and Monte Emilius klippe. (8) Lanzo ultramafic body. (9) Tertiary molassic basins

crop. Indeed the quartzite looks locally like an unsorted conglomerate with very pale pink rounded pebbles that could be mistaken for rose quartz were it not the higher density and occasional euhedral shapes. The size, the distribution and the alteration state of these "nodules" are quite variable, while the groundmass appears as a rather homogeneous quartzite containing up to one centimetre large white mica flakes which hardly show preferred orientation. The size of the garnets ranges from 0.2 to 25 cm. The garnets are evenly distributed in the groundmass regardless of their size but they may form impressive clusters that give the appearance of a conglomerate. The garnets are fresh, especially the larger ones, but they may also be completely transformed into a greenish phyllitic aggregate, these extreme states occurring nearly side by side. Rare, centimetre large kyanite crystals may also be found in the outcrop.

At the outcrop scale the minimum apparent thickness of the quartzite "layer" is about 30 metres. In fact, the quartzite occupies the core of a recumbent fold. This fold is a few hundred metres in magnitude, it has an E–W axis and an axial plane slightly dipping to the south. The very faint foliation of the quartzite is concordant with the axial plane foliation. These structures correspond to the first, main tectonic phase recognised by Vialon (1966) which created several-kilometre-large recumbent folds of northward vergence in this part of the massif. The only lithological variation consists of, rare, decimetre-thick layers (or veins?) of a weathered bluish rock devoid of mica. They occur twice (due to folding?) and are also concordant with the axial plane foliation. The contact between quartzite and surrounding gneisses can be well observed along the fold crest. It is sharp, there is no transitional lithology and the quartzite is nearly pure just below the contact. The gneisses are mostly phengite-, biotite-, albite- and garnet-bearing, and form a thick monotonous series. Some variational lithologies are reported to contain pseudomorphs after or even relics of glaucophane (Franchi 1900; Vialon 1966).

Another outcrop was visited at Brossasco, Val Maira. Here, the granite sill mentioned by Vialon occurs in the immediate vicinity but the only contacts observed are between quartzite and fine-grained gneiss, just as in Parigi. The structural situation is somewhat different, probably along the limb of a great fold, and the garnets have been completely transformed into a phyllitic aggregate.

Petrography

The present report is concerned with a single representative sample (2–39) in which garnet and the whole primary assemblage escaped any subsequent retrogression. The garnets are 2 to 10 mm large and nearly colourless, thus leaving the rock a white colour. The quartz groundmass shows a perfect, undeformed polygonal texture. White mica occurs as large, commonly up to 5 mm flakes, and talc as smaller ones (up to 1 mm) mostly on the rim of, or interlayered with the white mica. Both may be slightly bent and define a very faint foliation. Abundant kyanite is medium-sized (up to 2 mm). Rutile occurs as rounded grains, zircon is accessory. A sodic pyroxene was found twice in one out of four thin sections of the same sample. It is partly replaced by a rim of brownish, extremely fine-grained material but has formerly been in contact with kyanite. Chlorite is conspicuously absent. If one excepts pyroxene, all the matrix minerals mentioned coexist in contact with each other, and there is little doubt that the assemblage quartz-garnet-white mica-talc-kyanite-rutile was stable as quartz acquired its well recrystallised texture (Fig. 2).

The garnets contain mainly inclusions of kyanite, quartz and rutile, more rarely of talc sometimes associated with kyanite. The inclusions do not show any preferred orientation nor do they define a growth texture in the garnet. As in the matrix, the kyanite and rutile crystals are short prisms with smooth edges. In contrast the quartz inclusions have irregular shapes and a texture sharply differing from that of the matrix (see Fig. 3). Quartz is finely polycrystalline; on the inclusion boundary the grains or subgrains are strained elongated bands forming a radial pattern. The inner part of the inclusions looks like crosscut by "veinlets" also made of quartz, resulting in a very characteristic feathery texture (Fig. 3a–d). In each thin section several of these inclusions still contain relics of a colourless mineral with distinctly higher relief (Fig. 3). This mineral is obviously replaced by quartz as shown by the preservation of various replacement stages in different inclusions. The radial pattern on the inclusion rim corresponds to a peripheral transformation of the more highly refringent mineral; the "veinlets" in the middle part of the inclusion suggest a selective replacement along cleavages and cracks (Fig. 3). Another remarkable feature is the existence in the garnet of radial cracks around the quartz inclusions, which do not exist

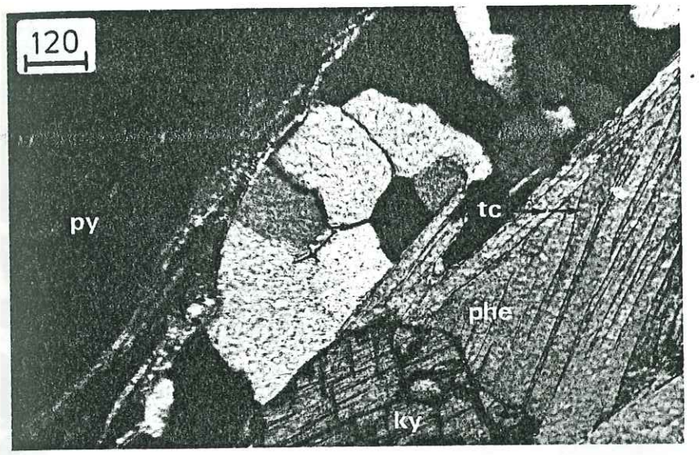

Fig. 2. The matrix assemblage quartz-pyrope-kyanite-phengite-talc. Note the polygonal texture of quartz. Crossed nicols, scale bar in μm

around the rutile and kyanite inclusions (Fig. 3). This unusual texture comparable with that sometimes observed around mineral inclusions undergoing metamictisation, suggests that the inclusions underwent a considerable volume change and overcame the mechanical strength of the garnet. This radial jointing, the high relief of the relic mineral and the nature of its transformation product (quartz!) suggested that it could be a high-pressure polymorph of silica, and this was confirmed by the electron microprobe giving pure SiO_2. The polymorph was further characterised as coesite by its Raman spectrum obtained in thin section using a MOLE microprobe, and by an electron diffraction study carried out by Ph. Gillet and M. Madon and on which will be reported elsewhere.

Beside the inversion of coesite to quartz and the partial breakdown of jadeitic pyroxene, the only other retrograde reaction has been observed between garnet and white mica. All the former contacts between garnet and mica have reacted to form a narrow rim of phlogopite, growing radially to garnet, and of kyanite (sometimes associated with minute talc flakes) on the white mica side (Fig. 4). The contacts between garnet and quartz matrix are sharp but, in the vicinity of mica flakes, both minerals may be separated by a very narrow rim of phlogopite on the garnet side and kyanite (±talc) on the quartz side, probably reflecting potassium migration along grain boundaries.

For the sake of completeness it should be mentioned that, in other pyrope-quartzite samples, the relative sizes and amounts of talc and white mica are quite variable, as well as the breakdown products of garnet. In some cases the latter are only chlorite, in other cases zoisite, margarite and an omphacitic pyroxene are also present, suggesting that the Ca content of garnet may have been quite variable from one sample to the other.

The bluish weathered rock interlayered within the pyrope quartzite deserves a further article for itself, but some of its features will be used here in the petrologic discussion. It is an almandine-kyanite-jadeite quartzite, and iron-rich chloritoid is produced by the retrogression of garnet.

Mineral chemistry

The microprobe analyses of *coesite*, of *quartz* in the matrix and of quartz in inclusions are undistinguishable, the main impurity being Al_2O_3 which amounts to near 0.1 wt %. Na lies near the detection limit, the other elements analysed (K, Mg, Ca, Ti, Fe) rather below it. Analyses of the other minerals making up this unusual rock are listed in Table 1.

Garnet is indeed nearly pure pyrope with 90 to 98 mol % of the end member, the rest being essentially almandine. Chromium is typically absent, and sodium is close to the detection limit. The smaller garnets are the more Mg-rich, their Fe content decreases toward the rim and their Ca content continuously increases but remains very low (Table 1, two first garnet analyses). The range of compositional variations is greater in the larger garnets and the zonation pattern is a little more complex, with a slight iron enrichment in the rim (Table 1, next three analyses).

The composition of *talc* is close to the ideal one. The iron content represents at most one mole per cent of the iron end member. The noticeable alumina content of about 0.45 wt.% is not linked to a sodium incorporation as in other cases (Råheim and Green 1974; Abraham and Schreyer 1976; Schreyer et al. 1980). It is probably in octahedral position and would represent about one mole per cent of the pyrophyllite end member (compare Newton 1972).

Kyanite is pure Al_2SiO_5, free of chromium and of iron. This together with the garnet analyses suggests that the iron in the rock might be essentially divalent.

The *white mica* analyses show a perfectly dioctahedral mica with a very important extent of the substitution $SiMg \rightleftharpoons AlAl$. It is thus a phengite, with 3.55 Si per 12 oxygen formula unit. This value remains constant throughout the thin section and also within a crystal, no matter whether phengite occurs in the matrix or in contact with garnet. The same holds for the $K \rightleftharpoons Na$ substitution, with a nearly constant value between 2.5 and 3 mol % of paragonite in phengite. Although always very small, the iron content is somewhat higher in phengite coexisting with garnet than in phengite in the matrix.

The rare *pyroxene* grains analysed have a jadeite content of over 70 mol %, they are thus close to the jadeite limb of the omphacite-jadeite solvus as drawn, for example, by Carpenter (1980). Noteworthy is the slight but systematic excess of Al over Na in the structural formula (Table 1). It is not clear as yet whether it reflects a peraluminous

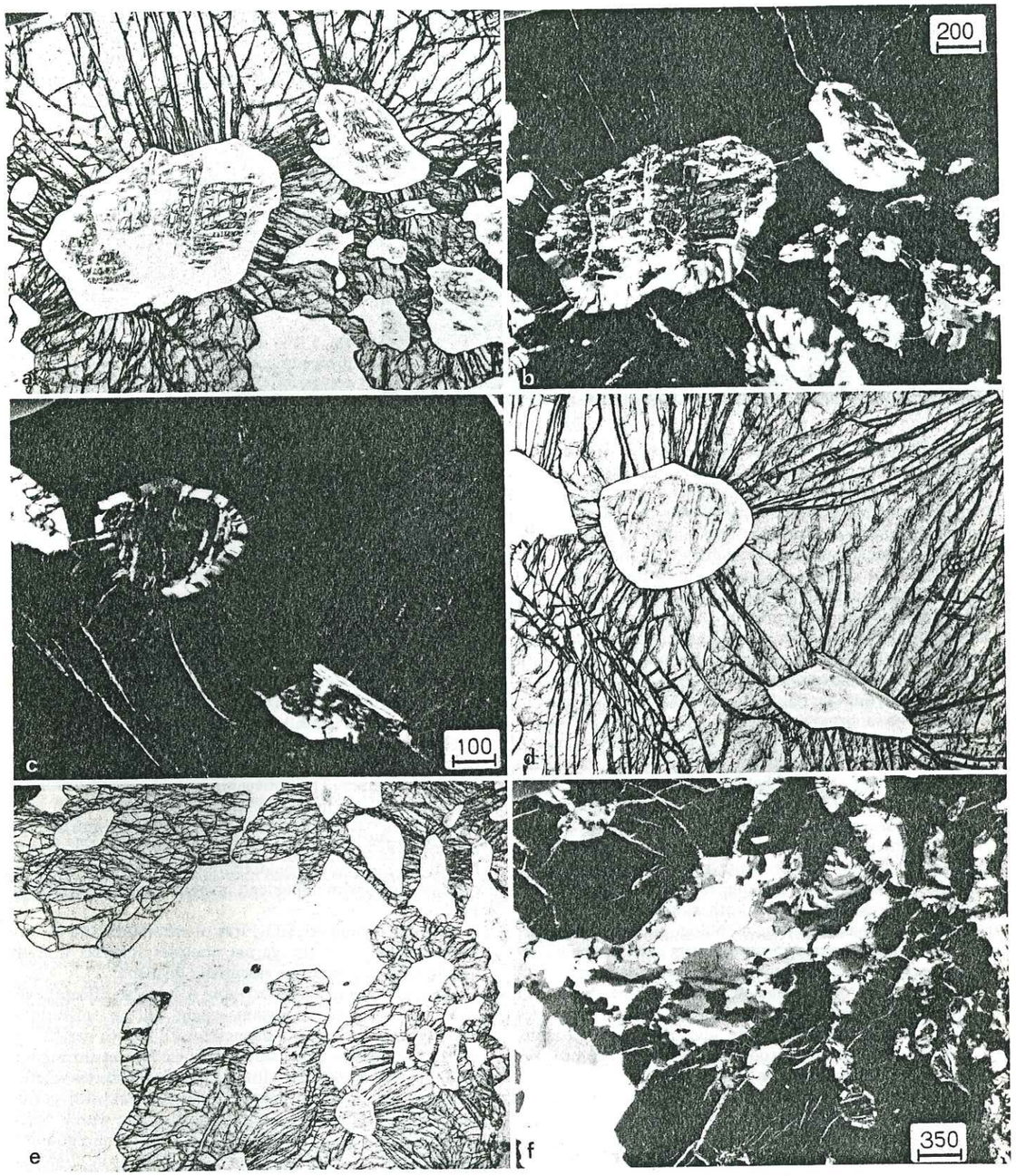

Fig. 3a–f. Microphotographs from sample 2–39. Scale bars in microns. **a–b, c–d** Relics of coesite (higher relief) partly inverted to quartz (lower relief), as inclusions in pyrope. Note the irregular shape of the inclusions, the absence of preferred orientation and of growth texture (also *E–F*), and the radial fractures of garnet around the inclusions. The replacement texture of coesite by quartz in garnet is characteristic with a radial growth of polycrystalline quartz around the inclusion rim (**c–d**) and a development along cleavages and cracks of coesite (**a–b**). Compare Smyth (1977). **e–f** The same texture of quartz pseudomorph after coesite exists in a part of matrix embayed in a poikilitic pyrope crystal (centre of the picture) but nowhere else in the matrix (lower left corner)

Fig. 4. Characteristic reaction rim between pyrope and phengite (in the matrix). Aluminous phlogopite grows on the garnet side, kyanite bundles (sometimes with talc) on the phengite side. Plane polarised light, scale bar in μm. This may illustrate the water-conserving reaction (8) discussed in the text but also, because of the occasional presence of talc, the quartz-absent hydration reaction pyrope + phengite + H_2O → phlogopite + kyanite + talc

Table 1. Mineral analyses

V 16 is a wet chemical analysis of pyrope concentrate (+kyanite?) given by Vialon (1966). The rest is microprobe analyses from sample 2–39. The first two garnet analyses are from a small garnet (about 2 mm), the three next ones from a large garnet (1 cm) containing coesite inclusions. The phengite analysed coexists with talc and garnet. Phlogopite is retrograde. Camebax electron microprobe (15 kV, 10 nA); standards used are forsterite (Mg), anorthite (Al, Ca), Fe_2O_3, $MnTiO_3$, K-feldspar (K), jadeite (Na). Forsterite was used for Si in most analyses, but quartz was used instead for the two first garnet analyses. The discrepancy in Si content between the two sets of garnet analyses does not allow any statement on a hydropyrope component (Ackermann et al. 1983)

	V 16	Garnet					Jadeite	Phengite	Talc	Phlogopite
		rim	core	rim		core				
SiO_2	41.90	45.21	45.13	44.46	44.85	43.84	58.26	53.81	63.54	40.13
TiO_2	tr.	0.00	0.02	0.01	0.00	0.01	0.07	0.25	0.00	0.02
Al_2O_3	29.15	25.55	25.39	25.35	25.52	25.15	18.87	24.12	0.46	20.61
FeO	1.87	0.91	1.35	1.89	1.58	4.20	0.17	0.19	0.35	0.52
MnO	tr.	0.02	0.03	0.00	0.03	0.09	0.02	0.00	0.00	0.02
MgO	26.05	28.83	28.98	29.26	29.83	27.10	5.04	5.66	30.55	23.10
CaO	0.30	0.28	0.09	0.26	0.11	0.23	5.81	0.06	0.02	0.27
Na_2O	0.45						11.03	0.19	0.02	0.43
K_2O	0.10						0.00	11.33	0.03	10.22
	100.35	100.80	100.99	101.23	101.92	100.62	99.27	95.61	94.97	95.32
Si		3.020	3.015	2.977	2.978	2.982	2.002	3.550	4.022	2.779
Ti			0.001	0.001		0.001	0.002	0.012		0.001
Al		2.012	2.000	2.001	1.997	2.017	0.765	1.876	0.034	1.683
Fe		0.051	0.075	0.106	0.088	0.239	0.005	0.010	0.019	0.030
Mn		0.001	0.002		0.002	0.005	0.001			0.001
Mg		2.870	2.885	2.920	2.951	2.748	0.258	0.557	2.882	2.384
Ca		0.020	0.006	0.019	0.008	0.017	0.214	0.004	0.001	0.020
Na							0.735	0.024	0.002	0.058
K								0.954	0.002	0.903
Σ cat.		7.974	7.984	8.022	8.024	8.009	3.981	6.988	6.963	7.859
Pyr		97.6	97.2	95.9	96.8	91.3				
Alm		1.7	2.5	3.5	2.9	7.9				
Gro		0.7	0.2	0.6	0.3	0.6				
Spe		–	0.1	–	–	0.2				

character of the pyroxene, as in the kimberlite xenolith described by Smyth and Hatton (1977), or 2 to 5 mol % of spodumene component in solid solution.

The secondary *phlogopite* is more aluminous than the ideal end member. The excess of octahedral Al is compensated by a deficiency of octahedral filling.

Petrologic discussion

The significance of coesite

Given the negligeable solid solutions in coesite and quartz and the independence of the phase transition relative to water activity and fluid composition, at least in the realm

of metamorphic conditions, the occurrence of coesite should be readily interpreted in terms of geobarometry. Under static conditions it would imply unusually high metamorphic pressure values, between 25 and 30 kbar, depending on temperature. However, it is crucial to know whether coesite crystallised under static conditions or not. It has been experimentally shown that coesite can grow from highly strained quartz as much as 10 kbar below the transition determined under static conditions (Hobbs 1968; Naka et al. 1972; Green 1974). It might then be questioned whether the beautiful, non deformed, hardly oriented texture of the sample does not result from a complete recrystallisation subsequent to the coesite breakdown, the coesite growth having taken place under high-stress conditions. However, it seems unconceivable that under such conditions 15 cm large garnets could grow developing euhedral faces and including monocrystalline coesite, talc and kyanite grains devoid of preferred orientation. Besides, the deviatoric stress in the experiments mentioned exceeded 10 kbar, i.e. was at least one order of magnitude larger than the usual estimates for geological processes. As stated by Green, "it probably is not possible to produce a dislocation density anywhere near that proposed here by natural means other than meteorite impact". Therefore, I favour the idea that coesite grew in this rock under nearly static pressure conditions.

The presence of coesite inclusions in garnet suggests that the whole groundmass now made of quartz has formerly also been coesite. The idea is supported by the fact that the very peculiar texture of quartz pseudomorph after coesite (Fig. 3 and Smyth 1977) has been observed, although in an advanced recrystallisation stage, in a part of the groundmass which had been nearly isolated within a cluster of small garnets. It has also been observed in quartz inclusions in kyanite and in a part of matrix embayed in garnet. In the latter case, even the radial growth pattern along the garnet rim is preserved (Fig. 3e–f), which I consider to be a definite evidence for a former coesite matrix. In fact, the same result may be obtained from mechanical considerations. On the basis of the much greater thermal expansion of quartz as compared to garnet, one might think that, if *quartz* inclusions are trapped in garnet on a *prograde* path, a considerable pressure will develop in the inclusions (and not in the matrix) upon further temperature increase, which may lead to coesite growth in the inclusions, and only in the inclusions. However, calculations performed using an elastic model (Gillet et al. 1984; compare Rosenfeld and Chase 1961) show that along metamorphic geotherms the pressure in the quartz inclusion reaches the transition value only if the external pressure does, the effect of the large thermal expansion of quartz being cancelled by its large compressibility. Therefore, if coesite is now present in garnet, it must have been present in the matrix.

Conversely, let us now consider a *coesite* inclusion in garnet (in a coesite matrix) on a *retrograde* metamorphic path starting within the coesite stability field. Upon pressure release, the coesite *matrix* will invert to quartz very quickly since it may be in contact with a fluid phase and since temperature is still rather high, two factors which are known to enhance the inversion kinetics (e.g. Boyd and England 1960). On the contrary, the inversion of coesite to quartz, which proceeds with a large volume increase, will be counteracted *in the garnet* by the low compressibility and the mechanical strength of the host mineral. Once initiated, for example by large overstepping of the phase transition, the inversion results in the development of a high pressure in the inclusion (which may explain the strained state of quartz) and eventually in the disruption of the garnet, i.e. radial jointing around the inclusion. This gives way to external fluids and makes possible the expansion of the inclusion; coesite inversion should therefore go to completion very quickly. The fact that relics are still preserved indicates that the fracturing of garnet around the inclusions must have occurred at very low temperatures and is thus quite a late process.

So, it is believed that this rock has endured unusually high lithostatic pressures which were then released at relatively low temperature. The preservation of coesite in garnet and the contrast in quartz texture between matrix and inclusions in garnet result from the fact that garnet acted during decompression as a pressure vessel on the inclusions and isolated them from any penetration of external fluids.

Phase relations of pyrope

The most Mg-rich garnets known so far were from xenoliths in kimberlite. They rarely exceeded 80 mol % pyrope and, if more Mg-rich, contained considerable amounts of chromium as knorringite component (e.g. Meyer and Boyd 1972). The chromium-free garnet analysed here must be of quite different origin and represents by far the closest approximation of the pyrope end-member.

Its coexistence with free silica is an important feature. It gives support to the experimental work of Hensen and Essene (1971) after which the pyrope-quartz pair has a stability field in the $MgO-Al_2O_3-SiO_2-H_2O$ system, a result which has been confirmed, refined and extended to the pyrope-coesite pair by Massonne (1983). As seen in the inset of Fig. 5, several alternative assemblages are possible, among which talc-Mg-chloritoid, talc-kyanite or enstatite-kyanite. The lower stability limit of pyrope + free silica can be approximately located using Massonne's data (1983 and pers. comm.) on the curve of the reaction

$$\text{pyrope} + \text{quartz} = \text{enstatite} + \text{kyanite}. \quad (1)$$

Its intersection with the upper stability limit of talc defines an invariant point (Fig. 6) from which emanates the curve of the reaction

$$\text{talc} + \text{kyanite} = \text{pyrope} + \text{quartz} + H_2O \quad (2)$$

which must have a steep negative slope. This invariant point lies close to the quartz-coesite transition and, considering the experimental uncertainties and the still poorly known influence of Al-incorporation on talc stability, it is in fact not clear whether it lies in the quartz or in the coesite field, i.e. whether it is stable or metastable. Whereas the existence of a talc-pyrope-coesite stability field is certain, that of a talc-pyrope-quartz stability field is thus still questionable and requires additional experimental work. At any rate, if such a stability field exists, it represents a very restricted P–T domain near 28 kbar and 800–830° C.

Considered in the system $MgO-FeO-Al_2O_3-SiO_2-H_2O$, reaction (2) or its equivalent with coesite instead of quartz is divariant and is relevant to our assemblage. Indeed, natural pyrope being more Fe-rich than talc, the Mg-enrichment of garnet proceeds through the reaction

$$\text{Mg}-\text{Fe}-\text{talc} + \text{kyanite} = \text{Mg}-\text{Fe}-\text{garnet} + SiO_2 + H_2O. \quad (2')$$

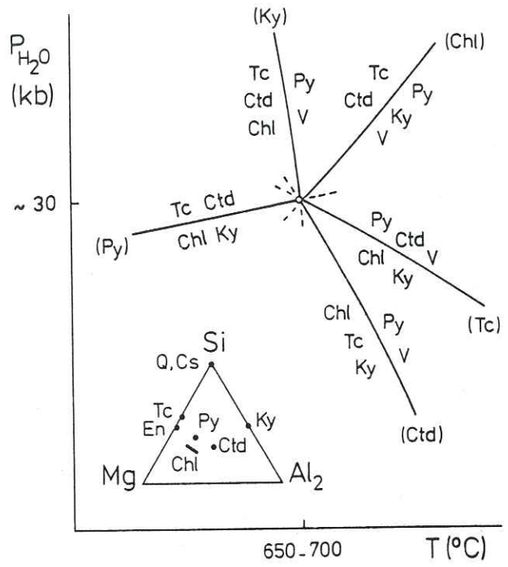

Fig. 5. The lower temperature stability limit of pyrope. The quartz-absent invariant point can be approximately located using the experimental data of Schreyer (1968) on the chloritoid-absent reaction and of Chopin and Schreyer (1983) on the pyrope-absent one. As inset the $MgO-Al_2O_3-SiO_2-H_2O$ system is projected on the water-free plane. Abbreviations used throughout this paper: *Ab* albite; *Alm* almandine; *Chl* chlorite; *Ctd* chloritoid; *Cs* coesite; *En* enstatite; *Jd* jadeite; *Ky* kyanite; *Par* paragonite; *Phe* phengite; *Phl* phlogopite; *Py* pyrope; *Q* quartz; *V* hydrous fluid

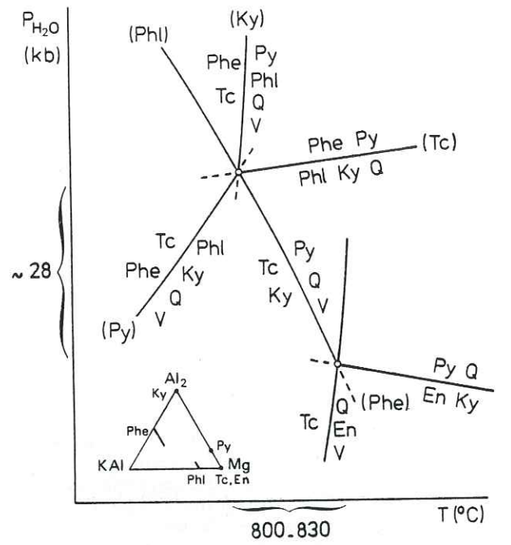

Fig. 6. High-pressure phase relations in the system $K_2O-MgO-Al_2O_3-SiO_2-H_2O$: a tentative outline. The invariant points have been located using the experimental data of Kitahara et al. (1966) for the talc breakdown, of Massonne (1983) for the reaction En + Ky = Py + Q, and of Massonne and Schreyer (pers. comm. 1983) for the reaction Tc + Phe = Phl + Ky + Q + V. See text for discussion. The main feature is the existence of a stability field for the assemblage free silica-pyrope-talc (± phengite) at very high pressure and on a rather narrow temperature interval (compare Fig. 8). The inset projection is made through SiO_2 and H_2O. Abbreviations: see Fig. 5

The trace of this reaction in the P–T plane depends both on the actual composition of the solid phases and on water activity. Iron incorporation in the system and lowered water activity will both shift the curve toward lower temperatures as compared to the Mg-end-member reaction curve drawn in Fig. 6. Since in our assemblage garnet and talc are close to the end-member composition, the position of the relevant curve is essentially dependent on water activity. However, calculations performed using the P–V–T data of H_2O from Halbach and Chatterjee (1982) show that even at very low water activity the curve cannot lie much below 700° C.

The phase relations observed in this sample may be compared with those observed in other high-pressure assemblages from Mg-rich metapelites of the Gran Paradiso and Monte Rosa massifs. There, the characteristic feature is the stable coexistence of talc with chloritoid, the chloritoid containing up to 74 mol % of the Mg end-member (Chopin 1979, 1981; Chopin and Schreyer 1983; Chopin and Monié 1984). Depending on metamorphic grade, chlorite may be stable in the presence of quartz in the critical assemblage talc-chloritoid-chlorite-quartz, or not, leading to the talc-chloritoid-kyanite assemblage (Fig. 7, GP and MR, respectively). In either case the coexistence of garnet with kyanite is forbidden in Mn- and Ca-free systems by the stability of Fe–Mg-chloritoid + quartz and by the talc-chloritoid tie-line. The phase relations observed in the Dora Maira sample (Fig. 7, DM) imply the instability of the talc-chloritoid join and of very Mg-rich chloritoid in the presence of quartz. In their experimental study of the pure magnesium system Chopin and Schreyer (1983) had already shown that Mg-chloritoid is not stable in the presence of quartz due to the greater stability of talc + kyanite or of Mg-carpholite, but they had not considered the pyrope-kyanite pair, which is also alternative to talc + chloritoid. Figure 5 shows the phase relations around the quartz-absent invariant point which is determined by the intersection of the lower stability limit of pyrope and of the lower pressure stability limit of talc + chloritoid. Respectively, the relevant reactions are

$$\text{chlorite} + \text{kyanite} + \text{talc} = \text{pyrope} + H_2O \quad (3)$$

and

$$\text{chlorite} + \text{kyanite} = \text{chloritoid} + \text{talc} \quad (4)$$

the latter being water-conserving (Chopin and Schreyer 1983). The pyrope-kyanite assemblage appears as a lower-pressure but essentially higher-temperature equivalent of the talc-chloritoid pair. Again, iron incorporation in the solids or low water activity will extend the field of pyrope + kyanite relative to the others.

Two other talc-kyanite-garnet-quartz occurrences have been reported, one from Kazakhstan (Udovkina et al. 1978, 1980) where, noteworthy, garnet contains inclusions of Mg-rich chloritoid (35 mol % Mg end-member), the other from Tasmania (Råheim and Green 1974). They may be referred to as "intermediate pressure whiteschists" (Chopin and

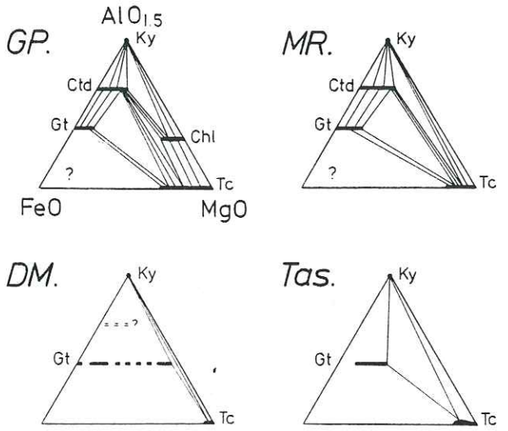

Fig. 7. Phase relations in some high-pressure, Mg-rich metapelites. *GP* Gran Paradiso massif, after Chopin (1979, 1981); *MR* Monte Rosa massif, overlying ophiolites of the Zermatt unit, or Hohe Tauern (Eastern Alps), after Chinner and Dixon (1963) and Miller (1977), respectively; *DM* Dora Maira massif, this paper; *Tas* Tasmania, after Råheim and Green (1974). The talc-chloritoid stability is a characteristic feature in GP and MR whereas the garnet-kyanite-talc coexistence suggests the instability of any chloritoid (+ quartz) in DM and Tas. The projection is made through SiO_2, H_2O and an eventual phengite component. Abbreviations as in Fig. 5

Schreyer 1983), the order of magnitude of the pressure estimates being 10 kbar. The Mg/(Mg+Fe) ratio of garnet, buffered according to reaction (2′), reaches about 0.4 in the former case and 0.5 in the latter. Given the steep negative slope of reaction (2), the much higher pyrope content of the Dora Maira garnet implies considerably higher pressures of formation, or higher temperatures, or lower water activity.

Phase relations with phengite

Considering now the K-bearing system, the coexistence of phengite with talc and pyrope and the absence of phlogopite in the primary assemblage are remarkable features. The talc-phengite pair has been shown to be a high-pressure assemblage (Abraham and Schreyer 1976; Schreyer and Baller 1977) and to be widespread in the Gran Paradiso area where it coexists with Mg-rich chloritoid (Chopin 1981). Since then it has also been found in the Monte Rosa where it coexists with magnesiochloritoid and kyanite (Chopin and Monié 1984). As shown by Fig. 6, the talc-phengite-pyrope-quartz assemblage is not only a very high-pressure assemblage but also a relatively low-temperature one, all the more because low water activity would favour the appearance of phlogopite according to the reaction

$$\text{talc} + \text{phengite} = \text{phlogopite} + \text{pyrope} + \text{quartz} + H_2O. \quad (5)$$

The extent of phengitic substitution is also quite meaningful. In the assemblage phengite-talc-kyanite-(pyrope)-quartz, it is buffered to relatively low values as compared to kyanite-free, phlogopite- or K-feldspar-bearing assemblages (see inset of Fig. 6). However the value reached by the substitution in this rock is among the highest recorded ($Si_{3.55}$), implying that the maximum possible value reached under the same conditions (in the assemblage phengite-phlogopite-K-feldspar-quartz) was exceptionnally high. According to Velde (1967) and Massonne (1981), this points again to unusually high pressure conditions and/or low temperatures. Noteworthy, water activity has no influence on the extent of phengitic substitution in the assemblage phengite-pyrope-kyanite-SiO_2 since the relevant buffering reaction

$$\text{pyrope} + \text{muscovite} + SiO_2 = \text{phengite} + \text{kyanite} \quad (6)$$

is water-conserving. In fact talc also participates to the natural assemblage and the high Si content of phengite may be also partly due to low water activity, through the reaction

$$\text{talc} + \text{muscovite} = \text{phengite} + \text{kyanite} + SiO_2 + H_2O. \quad (7)$$

Furthermore, if one assumes the less hydrated products to be on the high-temperature side, volume considerations show that the isopleths relevant to the latter reaction have a negative slope, i.e. phengite substitution in the assemblage talc-kyanite-quartz increases with pressure but, in contrast with phengite in the classical buffering assemblage K-feldspar-phlogopite-quartz, also increases with temperature. Thus the high Si content of phengite in this sample may result from three non exclusive factors: high pressure, relatively high temperature, or low water activity. For comparison, in the assemblage phengite-talc-kyanite-Mg-chloritoid-chlorite-quartz from the Monte Rosa (Chopin and Monié 1984; Chopin and Schreyer 1983) which is equivalent as far as the buffering of phengite substitution is concerned, phengites are between $Si_{3.35}$ and $Si_{3.42}$ and pressure has been independently estimated at 16 to 18 kbar for temperature and water activity varying between 500 and 560° C, 0.6 and 1, respectively.

The retrograde formation of phlogopite + kyanite from pyrope + phengite (Fig. 4) deserves particular attention. It corresponds to a univariant reaction in the pure magnesium system (Fig. 6), namely

$$\text{phengite} + \text{pyrope} = \text{phlogopite} + \text{kyanite} + \text{quartz}. \quad (8)$$

This reaction is water-conserving regardless of the extent of phengite substitution and it proceeds with a large positive volume change of 4 to 5%. It is therefore strongly dependent on pressure and insensitive to variations of water activity (see Fig. 6). Thus, the two main retrograde reactions observed, the inversion of coesite to quartz and the breakdown of pyrope + phengite, although they may not have proceeded at the same time, are both indicative of a pressure drop and are independent of the presence and composition of a fluid phase.

In this respect two other reaction curves have to be considered, that of reaction (2) and that of the reaction

$$\text{talc} + \text{phengite} = \text{phlogopite} + \text{kyanite} + \text{quartz} + H_2O \quad (9)$$

which has been experimentally determined by Massonne and Schreyer (pers. commun.). During isothermal decompression both curves are crosscut, the former in the hydration direction, the latter in the dehydration direction (Fig. 6 and 8). In the sample studied, the lack of evidence for reaction (2) proceeding in the retrograde direction implies a considerable overstepping of the reaction which may result both from a low water activity in the fluid (if any) and from the unfavourable kinetics of the hydration reaction. Conversely, a large overstepping of reaction (9) during decompression is very unlikely because dehydration is favoured both kinetically and by low water activity. Therefore, the stability of talc-phengite throughout the evolution of the rock implies that the curve of reaction (9) has not been crosscut and thus puts severe constraints on any decompressional path. The constraints are all the more severe as water activity is lower; for example calculations show that the curve of reaction (9) is shifted toward lower temperatures by about 100° for a water activity of 0.2.

Significance of sodic pyroxene

Although an accessory mineral, the jadeite-rich pyroxene is an important petrologic indicator because of its coexistence with kyanite and white mica. The reference reaction for the components is

$$\text{paragonite} = \text{jadeite} + \text{kyanite} + H_2O \quad (10).$$

It is very pressure-dependent and proceeds at 24–25 kbar water pressure for temperatures between 550 and 700° C, as experimentally determined by Holland (1979b). Its location in the P–T plane is dependent on water activity and on additional components in pyroxene and white mica, the effects of the latter counteracting each other. A calculation using the actual mineral compositions of the sample is made difficult by the very low paragonite content of mica (<3%) and the strong non-ideality of solid solutions on the jadeite-diopside and paragonite-muscovite joins. Assuming a jadeite activity of 0.7 in pyroxene, a paragonite activity of 0.1 in phengite and a water activity of 0.2, the calculation yields a pressure value of 26 kbar, which is nearly independent of the assumed temperature. If jadeite or water activities are in fact higher, or paragonite activity lower, this pressure estimate is only a minimum value. Moreover, the thin beds (?) of bluish rock occurring within the pyrope-quartzite layer also contain the equilibrium assemblage jadeite-kyanite-phengite (+quartz+almandine) with similar paragonite contents in phengite and 90 mol % end member in jadeite. Whatever temperature or water activity might have been, this assemblage implies formation pressures much in excess of any estimate ever made in the realm of regional metamorphism; it confirms the exceptional character of the sample studied.

Resulting evidence

The petrologic investigation and qualitative comparisons with other high-pressure assemblages yield a series of independent and consistent evidences concerning the petrogenetic conditions of this rock. High rock pressures are indicated by the occurrence of the assemblage free silica-pyrope-talc and of coesite, which cannot have crystallised under extreme shear-stress conditions, by the jadeite content of pyroxene coexisting with kyanite and white mica, and, accessorily, by the extent of phengite substitution. Even in the absence of coesite, minimum pressure estimates of 25 kbar are hardly avoidable. A relatively low temperature is implied by the stability of talc and the absence of primary phlogopite which yield an absolute upper limit of about 800° C for the pressures considered (compare Fig. 6 and 8). This upper limit depends on water activity, it is shifted down to about 700° C for a water activity reduced

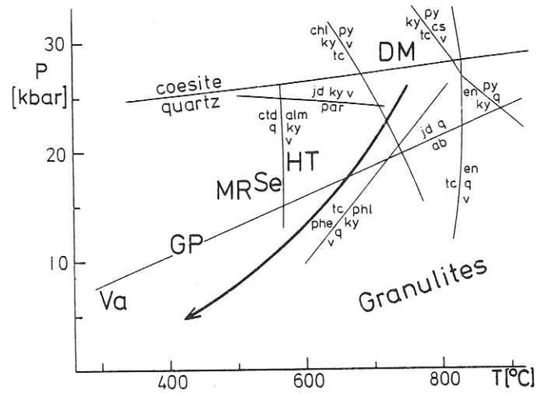

Fig. 8. The pyrope-coesite-talc assemblage as product of high-pressure, low-temperature metamorphism. P–T estimates from the highest-grade high-pressure assemblages from several areas of the Alpine chain: *Va* Vanoise (Goffé 1982; Goffé and Velde 1984); *GP* Gran Paradiso (Chopin and Maluski 1980, for T, P from phengite composition using Massonne's 1981 data); *MR* Monte Rosa (Chopin and Monié 1984); *Se* Sesia zone (Compagnoni 1977; Desmons and O'Neil 1978); *HT* Hohe Tauern (Holland 1979a; compare Miller 1977); *DM* Dora Maira, this study. For comparison with an other extreme of metamorphism, a granulite field is indicated. The originality of Alpine-type high-pressure metamorphism is obvious. The arrow drawn for the decompression path only represents an upper temperature limit for it (see text). The upper pressure stability limits of paragonite and albite are from Holland (1979b, 1980), the breakdown of chloritoid + quartz is derived from Ganguly (1969). See text for the other curves. All the curves drawn for $P_{H_2O} = P$. Abbreviations as in Fig. 5

to 0.2. The divariant assemblage pyrope-coesite-talc-kyanite also implies temperatures between about 700 and 800° C, depending on water activity and on the exact location of the relevant reaction curve (2). Actually, for temperatures close to 800° C and high water activity, melting would occur in K- or Na-bearing systems. The absence so far of evidence for melting in the sample studied and in the country-rocks supports the assumption of low water activity and thus the lower temperature estimates.

Therefore, the pyrope-coesite-talc-kyanite-phengite assemblage is thought to have formed under conditions of low water activity, at pressures in excess of 28 kbar and temperatures probably close to 700° C. This represents a very low thermal gradient and, together with the existence of rare glaucophane inclusions in huge pyrope crystals, confirms the definitely Alpine character of this rock. Obviously, blueschist facies metamorphism may reach extremely high grades and persist to considerable depths (Fig. 8).

The decompression path is well constrained on the high-temperature side by the stability of the talc-phengite pair, all the more as water activity is lower. Clearly, the uplift must proceed under decreasing temperature conditions and must therefore be of tectonic origin, the upward thrusting upon cooler units preventing a temperature rise. An additional evidence for rather low-temperature, high-pressure conditions prevailing during uplift is given by the retrograde breakdown of garnet in the almandine-kyanite-jadeite quartzite, which produces chloritoid and no staurolite, suggesting pressures above the staurolite-quartz stability field (compare Fig. 8 and Rao and Johannes 1979). Since the

uplift path remains poorly constrained on the low-temperature side, the possibility even arises that most of the decompression took place under P–T conditions corresponding to the blueschist facies, and thus that the blueschist assemblages observed in the terranes now juxtaposed in and on the Dora Maira massif were acquired in part on a prograde path, in part on a retrograde path.

Additional petrographic, experimental and field studies are clearly needed in order to define more accurately the evolution of the mineral assemblage described here. An investigation of the compositional variations and of the inclusions in the huge garnets, dating of phengite by the $^{40}Ar-^{39}Ar$ method, and an experimental determination of the equilibrium curves of the reactions (2) and (3) are presently undertaken.

Conclusions

Pressure values in excess of 28 kbar typically represent upper mantle conditions. Therefore, the problem arises of the origin of the pyrope-quartzite and of the enclosing series which do not have a mantle chemistry.

The protolith

The bulk composition of the sample studied is characterised by an extremely high Mg/Fe ratio, by a high silica content and by the virtual absence of Ca and Na, the latter point not holding true throughout the layer (see Petrography). This composition could be approximated by a mixture of quartz, Mg-chlorite and illite, and it reminds one of the highly magnesian, metaevaporitic whiteschists described and reviewed by Schreyer (1977). In the more restricted Alpine frame, very low Na and Ca contents and high Mg/(Mg+Fe) ratios (between 0.6 and 0.85) are characteristic for the layer of talc-chloritoid schist which occurs both in the Gran Paradiso (Chopin 1981) and the Monte Rosa massifs (Chopin and Monié 1984) as the first unit of a sedimentary and volcanic sequence of Paleozoic age transgressive on a granite and gneiss basement (see Bearth 1952). The highly magnesian character of this schist, its occasional contents of magnesite, dolomite and of the Ce–Al-phosphate florencite (Chopin 1979 and unpubl. data) suggest, together with its geological situation, an epicontinental, shallow-depth, possibly evaporitic origin. The correlation of the Dora Maira quartzite with this layer, and thus an evaporitic origin for it, is one of the most interesting working hypothesis as yet. The presence of metabasite and marble lenses in the series enclosing the quartzite is a common feature with the series overlying the magnesian layer in the Gran Paradiso and Monte Rosa massifs. However, neither carbonates nor florencite have been found in the Dora Maira quartzite and their is no obvious cover/basement distinction possible within the surrounding gneiss series. Besides, the Gran Paradiso and Monte Rosa series concerned are not affected by granite intrusions that they overlie discordantly. On the contrary, the Dora Maira series considered is intruded by granite bodies (and is much thicker). Vialon was even struck by the close spatial association of one of the granite sills and the quartzite layer, and he suggested that the latter might be genetically related to the granite intrusion as a sort of metasomatic marginal alteration. In fact, in Parigi as well as in Brossasco, the granite-quartzite association is not as close and as systematic as suggested by Vialon (1966). Furthermore, careful observation of the contacts between quartzite and surrounding gneiss supports the idea that the quartzite existed as such prior to granite intrusion in what would become the gneiss series. In any event these considerations make the crustal derivation of this material obvious.

The sedimentary origin of the series and the fact that the series acted as a basement during the Late Paleozoic sedimentation even imply that it probably remained at rather high levels of the continental crust up to Alpine times (Late Cretaceous?). Therefore, the generation of the high-pressure assemblage studied during the Alpine metamorphism implies a burial of upper crustal continental units of at least 90 km.

Plate tectonic consequences

Considering the contrasting densities of average continental and oceanic material, it was commonly accepted that oceanic material could be subducted to considerable depths under continental or oceanic plates while continental material always remained nearer to the earth's surface. It has been then realised that the overthrusting of oceanic crust on continental crust (obduction) was possible and able to generate at the edges of continental plates low-temperature, high-pressure mineral assemblages implying depths of 15 to 40 km. Besides, a crustal thickening resulting from continental collision, as that detected below Tibet, may lead to a Moho as deep as 60 to 70 km but is unlikely to produce a low-temperature metamorphism there. The fact that continental crust may be buried – necessarily rapidly in order to preserve a low temperature gradient – at such considerable depth as 90 km implies a revision of the current ideas on the relationships between oceanic and continental crust. A subduction process is not necessarily blocked by the collision of continental masses and continental lithosphere may be subducted as well.

In fact, a similar result seems to arise from geophysical work. According to Hamilton (1979), the Australian continental plate exists at depth below Timor and extends about 200 km north of the Timor through. In that case, however, it remains at shallow depth due to the gentle dip of the subducting plate (see also Silver et al. 1983). Besides, unpublished data presented by D.S. Cowan at the 1983 Penrose Conference illustrated the collision and partial subduction of a "microcontinental terrane" called Yakutak block, in the Gulf of Alaska. This terrane would extend about 300 km westward beneath the Alaskan continental margin.

Nevertheless, contrasting densities may result in a contrasted behaviour with regard to uplift: continental crust may return back to the surface more easily, sometimes perhaps more rapidly in order to preserve some exceptional high-pressure assemblages like that described here. In the case where the deeply subducted continental unit is not rapidly thrusted upward, thermal reequilibration results in advanced melting. Therefore, the evidence presented here for subducted continental material opens new possibilities for the genesis of acidic to intermediate magmas. In particular, the occurrence of an acidic igneous activity during early Alpine times must be envisaged.

Other occurrences

Even if several geologic processes exist which enable crustal rocks to be buried at depths sufficient for coesite to crystallise, their return back to the surface and the preservation of coesite imply a rapid and considerable uplift, therefore uncomfortable tectonic problems, and very peculiar circumstances such as inclusion in deformation-resistant minerals. The simultaneous fulfilment of these conditions is rather unlikely and, accordingly, the occurrence of preserved metamorphic coesite should remain exceptional. An indication or even an evidence for its presence or former presence may be the existence of radial jointing around quartz inclusions in other minerals. Thus, after having examined thin sections of the Dora Maira quartzite, D.C. Smith (pers. comm.) found these features in a Norwegian eclogite, which led him to the discovery of relic coesite in small quartz inclusions in pyroxene. In fact, as early as 1965, Chesnokov and Popov had drawn attention to the existence of radial cracks around quartz inclusions in eclogites of crustal derivation and had proposed as the most likely explanation that these inclusions formerly were coesite, now inverted to quartz. The discovery reported here and that of Smith give considerable support to their hypothesis. According to their observations coesite might have been present in eclogites from southern Ural and from the Münchberger Gneissmasse, Bavaria, among other regions. A careful search for coesite in these regions is a very desirable step for our understanding of the origin of high-pressure assemblages. Several of the geobarometers used for high-pressure assemblages often yield minimum pressure estimates due to the absence of a buffered assemblage; the range of pressure endured by crustal rocks of continental derivation might be in fact much wider than presently thought. Some of our present concepts about earth tectonics might have to be modified by these coesite discoveries and other possible ones to come.

Acknowledgements. H.-J. Massonne, Bochum, provided many unpublished experimental results which promoted the interpretation of the mineral assemblage. Sincere thanks are also due to W. Schreyer for critical comments on an earlier version of the manuscript and for the many facilities offered in his institute, and to D.S. Cowan, T.J.B. Holland, P.W. Mirwald, R.C. Newton and D.C. Smith for stimulating discussions. An anonymous reviewer, O. Medenbach who contributed most of the pictures, E. Grew and A. Mottana who have drawn my attention to Russian literature are also gratefully acknowledged.

References

Abraham K, Schreyer W (1976) A talc-phengite assemblage in piemontite schist from Brezovica, Serbia, Yugoslavia. J Petrol 17:421–439

Ackermann L, Cemič L, Langer K (1983) Hydrogarnet substitution in pyrope: a possible location for "water" in the mantle. Earth Planet Sci Lett 62:208–214

Bearth P (1952) Geologie und Petrographie des Monte Rosa. Beitr Geol Karte Schweiz NF 132:p 130

Boyd FR, England JL (1959) Pyrope. Carnegie Inst Washington Yearb 58:83–87

Boyd RF, England JL (1960) The quartz-coesite transition. J Geophys Res 65:749–756

Carpenter MA (1980) Mechanisms of exsolution in sodic pyroxenes. Contrib Mineral Petrol 71:289–300

Chao ETC, Shoemaker EM, Madsen BM (1960) First natural occurrence of coesite. Science 132:220–222

Chesnokov BV, Popov VA (1965) Increase in the volume of quartz grains in South Urals eclogite. Dokl Akad Nauk SSSR 162:176–178

Chinner GA, Dixon J (1973) Some high-pressure parageneses of the Allalin gabbro, Valais, Switzerland. J Petrol 14:185–202

Chopin C (1979) De la Vanoise au massif du Grand Paradis. Thèse 3ème cycle Univ P et M Curie Paris:p 145

Chopin C (1981) Talc-phengite: a widespread assemblage in high-grade pelitic blueschists of the Western Alps. J Petrol 22:628–650

Chopin C (1983) High-pressure facies series in pelitic rocks: a review. Terra Cognita 3:183 (abstr)

Chopin C, Maluski H (1980) $^{40}Ar-^{39}Ar$ dating of high-pressure metamorphic micas from the Gran Paradiso area (Western Alps): evidence against the blocking temperature concept. Contrib Mineral Petrol 74:109–122

Chopin C, Monié P (1984) A unique Mg-chloritoid-bearing, high-pressure assemblage from the Monte Rosa, Western Alps: a petrologic and $^{40}Ar-^{39}Ar$ radiometric study. (Submitted to Contrib Mineral Petrol)

Chopin C, Schreyer W (1983) Magnesiocarpholite and magnesiochloritoid: two index minerals of pelitic blueschists and their preliminary phase relations in the model system $MgO-Al_2O_3-SiO_2-H_2O$. Am J Sci Orville vol:72–96

Coes L (1953) A new dense crystalline silica. Science 118:131–152

Compagnoni R (1977) The Sesia-Lanzo zone: high-pressure, low-temperature metamorphism in the Austroalpine continental margin. Rend Soc Ital Mineral Petrol 33:325–374

Desmons J, O'Neil JR (1978) Oxygen and hydrogen isotope compositions of eclogites and associated rocks from the eastern Sesia zone (Western Alps, Italy). Contrib Mineral Petrol 67:79–85

Franchi S (1900) Sopra alcuni giacimenti di roccie giadeitiche nelle Alpi occidentali e nell'Appennino ligure. Boll R Comit Geol Ital (IV) 1:119–158

Ganguly J (1969) Chloritoid stability and related parageneses: theory, experiments and applications. Am J Sci 267:910–944

Gillet P, Ingrin J, Chopin C (1984) Coesite in subducted continental crust: (P, T) history deduced from an elastic model. (Submitted to Earth Planet Sci Lett)

Goffé B (1982) Définition du faciès à Fe-Mg-carpholite-chloritoïde, marqueur du métamorphisme de haute pression-basse température. Thèse d'état Univ P et M Curie Paris

Goffé B, Velde B (1984) Contrasted metamorphic evolutions in thrusted cover units of the Briançonnais zone (French Alps): a model for the conservation of HP–LT metamorphic mineral assemblages. Earth Planet Sci Lett (in press)

Green HW (1974) Metastable growth of coesite in highly strained quartz. J Geophys Res 77:2478–2482

Halbach H, Chatterjee ND (1982) An empirical Redlich-Kwong type equation of state for water to 1000° C and 200 kbar. Contrib Mineral Petrol 79:337–345

Hamilton W (1979) Tectonics of the Indonesian region. US Geol Survey Prof Paper 1078

Hensen BJ, Essene EJ (1971) Stability of pyrope-quartz in the system $MgO-Al_2O_3-SiO_2$. Contrib Mineral Petrol 30: 72–83

Hobbs BE (1968) Recrystallization of single crystals of quartz. Tectonophysics 6:353–401

Holland TJB (1979a) High water activities in the generation of high-pressure kyanite eclogites of the Tauern Window, Austria. J Geol 87:1–27

Holland TJB (1979b) Experimental determination of the reaction paragonite = jadeite + kyanite + water, and internally consistent thermodynamic data for part of the system $Na_2O-Al_2O_3-SiO_2-H_2O$, with applications to eclogites and blueschists. Contrib Mineral Petrol 68:293–301

Holland TJB (1980) The reaction albite = jadeite + quartz determined experimentally in the range 600–1200° C. Am Mineral 65:129–134

Kitahara S, Takenouchi S, Kennedy GC (1966) Phase relations in the system $MgO-SiO_2-H_2O$ at high temperatures and pressures. Am J Sci 264:223–233

Lazko YY, Koptil VI, Serenko VP, Tsepin AI (1983) Fassaite

clinopyroxenes from diamond-bearing kyanite eclogite xenoliths. Dokl Earth Sci Section 258:138–142
MacDonald GJF (1956) Quartz-coesite stability relations at high temperatures and pressures. Am J Sci 254:713–721
Massonne HJ (1981) Phengite: eine experimentelle Untersuchung ihres Druck-Temperatur-Verhaltens im System $K_2O-MgO-Al_2O_3-SiO_2-H_2O$. Dissertation Ruhr-Universität Bochum
Massonne HJ (1983) Experiments on melting to 50 kbar in the system $MgO-Al_2O_3-SiO_2-H_2O$ (MASH) with excess SiO_2 and H_2O (abstract). EOS Trans AGU 64:875
Massonne HJ, Mirwald PW, Schreyer W (1981) Experimentelle Überprüfung der Reaktionskurve Chlorit + Quarz = Talk + Disthen im System $MgO-Al_2O_3-SiO_2-H_2O$. Fortschr Mineral 59:122–123
Meyer HOA, Boyd FR (1972) Composition and origin of crystalline inclusions in diamonds. Geochim Cosmochim Acta 36:1255–1273
Miller C (1977) Chemismus und phasenpetrologische Untersuchung der Gesteine aus der Eklogitzone des Tauernfensters, Österreich. Tschermaks Mineral Petrogr Mitt 24:221–277
Mirwald PW, Massonne HJ (1980) The low-high quartz and quartz-coesite transition to 40 kbar between 600° C and 1600° C and some reconnaissance data on the effect of $NaAlO_2$ component on the low quartz-coesite transition. J Geophys Res 85:6983–6990
Naka S, Ito S, Inagaki M (1972) Effect of shear on the quartz-coesite transition. J Am Ceramic Soc 55:323–324
Newton RC (1972) An experimental determination of the high-pressure stability limits of magnesian cordierite under wet and dry conditions. J Geol 80:398–420
Råheim A, Green DH (1974) Talc-garnet-kyanite-quartz schist from an eclogite-bearing terrane, Western Tasmania. Contrib Mineral Petrol 43:223–231
Rao BB, Johannes W (1979) Further data on the stability of staurolite + quartz and related assemblages. Neues Jahrb Mineral Monatsh 10:437–447
Rosenfeld JL, Chase AB (1961) Pressure and temperature of crystallisation from elastic effects around solid inclusions in minerals. Am J Sci 259:519–541
Schreyer W (1968) A reconnaissance study of the system $MgO-Al_2O_3-SiO_2-H_2O$ at pressures between 10 and 25 kbar. Carnegie Inst Wash Yearb 66:380–392
Schreyer W (1977) Whiteschists: their compositions and pressure-temperature regimes based on experimental, field, and petrographic evidence. Tectonophysics 43:127–144
Schreyer W, Abraham K (1976) Three stage metamorphic history of a whiteschist from Sar e Sang, Afganistan, as part of a former evaporite deposit. Contrib Mineral Petrol 59:111–130
Schreyer W, Abraham K, Kulke H (1980) Natural sodium phlogopite coexisting with potassium phlogopite and sodian aluminian talc in a metamorphic evaporite sequence from Derrag, Tell Atlas, Algeria. Contrib Mineral Petrol 74:223–233
Schreyer W, Baller T (1977) Talc-muscovite: synthesis of a new high-pressure phyllosilicate assemblage. Neues Jahrb Mineral Monatsh 9:421–425
Silver EA, Reed D, McCaffrey R (1983) Back arc thrusting in the Eastern Sunda arc, Indonesia: a consequence of arc-continent collision. J Geophys Res 88:7429–7448
Smyth JR (1977) Quartz pseudomorphs after coesite. Am Mineral 62:828–830
Smyth JR, Hatton CJ (1977) A coesite-sanidine grospydite from the Roberts Victor kimberlite. Earth Planet Sci Lett 34:284–290
Sobolev NV et al. (1976) Coesite, garnet and omphacite inclusions in Yakut diamonds – first finding of coesite paragenesis. Dokl Akad Nauk SSSR 230:1442–1444 (in Russian) Abstr in Mineral Abstr 78–818
Stella A (1895) Sul rilevamento geologico eseguito nel 1894 in Valle Varaita (Alpi Cozie). Boll R Comit Geol Ital 26:283–313
Udovkina NG, Muravitskaya GN, Laputina IP (1978) Phase equilibria in the talc-garnet-kyanite rocks of the Kokchetav block, Northern Kazakhstan. Isvestiya Akad Nauk SSSR Geol section 7:55–64 (in Russian)
Udovkina NG, Muravitskaya GN, Laputina IP (1980) Talc-garnet-kyanite rocks of the Kokchetav block, Northern Kazakhstan. Dokl Earth Sci section 237:202–205
Velde B (1967) Si content of natural phengites. Contrib Mineral Petrol 14:250–258
Vialon P (1966) Etude géologique du massif cristallin Dora-Maira, Alpes cottiennes internes, Italie. Thèse d'état Univ Grenoble

Earth and Planetary Science Letters, 70 (1984) 426–436
Elsevier Science Publishers B.V., Amsterdam – Printed in The Netherlands

[5]

Coesite in subducted continental crust: *P-T* history deduced from an elastic model

Ph. Gillet [1], J. Ingrin [2] and C. Chopin [3]

[1] *Centre Armoricain d'Étude Structurale des Socles (C.N.R.S.), Université de Rennes, 35042 Rennes Cedex (France)*
[2] *Institut de Physique du Globe de Paris, 4 place Jussieu, 75230 Paris Cedex (France)*
[3] *Laboratoire de Géologie, Ecole Normale Supérieure, 46 rue d'Ulm, 75005 Paris (France)*

Received January 25, 1984
Revised version accepted May 23, 1984

Coesite has been found in a metasedimentary rock in a continental unit of the Western Alps (Dora Maira massif). The rock preserves the high-pressure, low-temperature assemblage of nearly pure pyrope–talc–phengite–kyanite in a quartz matrix; coesite exclusively occurs as inclusions in pyrope and is partly inverted to quartz. Textural observations and mechanical considerations suggest that the rock crystallised in the coesite stability field. A simple elastic model for a coesite inclusion in pyrope explains why coesite has been exclusively preserved in the inclusions and not in the matrix. Combined with petrological data the model constrains the crystallisation conditions of the pyrope–coesite rock ($P > 28$ kbar, $650 < T < 830$ °C) and possible uplift paths. The paths derived suggest a mechanism of rapid decompression without any temperature increase, which must be related to tectonic processes.

This finding has an important bearing on the significance of *P-T* conditions estimated from minerals occurring as inclusions and on the actual behaviour of continental crust in collision zones.

1. Introduction

The dense high-pressure silica phase coesite was first synthesized by Coes [1] at 35 kbar. Its stability field and kinetic aspects of its transformation have been experimentally investigated by MacDonald [2], Boyd and England [3] and, more recently, by Mirwald and Massonne [4]. The stability data could seem to preclude the occurrence of coesite in crustal rocks metamorphosed under static conditions, but coesite could be expected to be a stable phase in the mantle provided free silica exists there [3]. Indeed the natural occurrences are mainly impact-metamorphosed rocks [5] and kimberlite xenoliths [6–8]. The recent discovery of coesite as inclusions in pyrope from buried continental rocks [9,10] raises a number of questions:

—How can coesite be preserved while the experimental studies indicate that it breaks down rapidly when held outside its stability field?

—What may be the crystallisation conditions of such a coesite-pyrope assemblage?

—What actual role of continental crust in geodynamic processes such as subduction-collision may be inferred from the presence of coesite?

In order to answer these questions we have developed an elastic model for the *P-V-T* behaviour of coesite crystals included in pyrope when the rock is brought back to the surface, i.e., when pressure and temperature decrease around the garnet.

2. Sample description

The samples studied were collected at Parigi, near Martinania Po, Western Italian Alps, in the Dora Maira massif. The rocks belong to a Paleozoic polymetamorphic complex which underwent Alpine high-pressure, low-temperature metamorphism [11].

0012-821X/84/$03.00

Chopin [10] gives a detailed petrologic description. The present report is concerned with the same representative quartzite sample, in which the primary assemblage shows no evidence of retrogression. The garnets are 3–10 mm in section and nearly pure pyrope (90–98 mole% of the end member). The quartz groundmass shows a perfect polygonal texture. Phengite occurs as large flakes (up to 5 mm), talc as smaller ones mostly on the rim of, or interlayered with phengite. Kyanite is abundant, rutile and zircon are also present. All the matrix minerals coexist in contact with each other, suggesting that the assemblage quartz–garnet–phengite–talc–kyanite–rutile was stable when the quartz acquired its well-recrystallised texture [10].

The garnets contain, beside kyanite and rutile inclusions, high-relief SiO_2 inclusions which were further characterised as coesite by Raman spectroscopy (using a MOLE microprobe) and by TEM (Ingrin and Gillet, unpublished data) (Fig. 1a). Coesite is invariably surrounded by an inversion rim of polycrystalline quartz (Fig. 1b). Some of the inclusions consist only of quartz but show the same typical radiating texture as the coesite-bearing inclusions, suggesting that they are now quartz pseudomorphs after coesite (Fig. 1b). Similar textures have been described by Smyth and Hatton [6] and Smyth [7] but, in their samples, the coesite grains are surrounded by a matrix mainly composed of a peraluminous omphacite.

Another unusual feature is apparent: fractures radiate from all the quartz–coesite inclusions and reach the outer rim of garnet (Fig. 1c). These fractures are clearly tension fractures and are distinct from the fractures usually occurring in garnet. Reaching the edge of the garnet, the fractures have two types of behaviour depending on the nature of the minerals in contact with garnet: reaching a quartz–garnet interface they are perpendicular to the interface, whereas they turn and tend to be parallel to the interface when they reach a mica–garnet interface. This alternative behaviour is related to the contrast between the elastic properties of the mineral species in contact [12]. The tension fractures originate from the tip regions of the inclusions where stress concentrations can be expected, which eventually exceed the tensile strength of garnet. No radiating fractures emerge

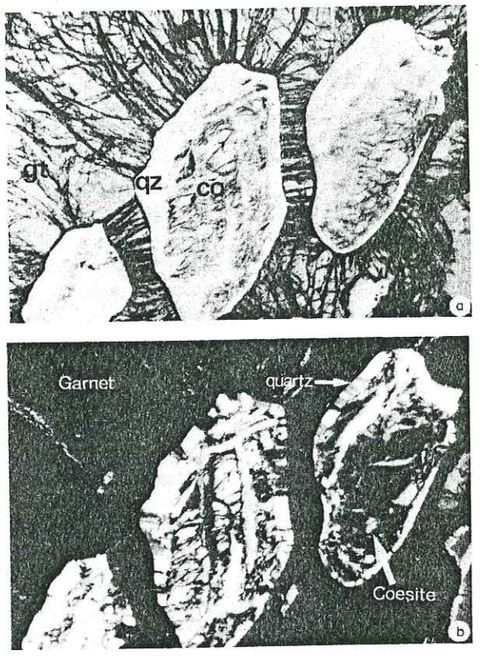

Fig. 1. (a) Thin section microphotograph showing inclusions in pyrope (*gt*). Relic coesite (high relief, *co*) is corroded by quartz (low relief, *qz*). Length of the picture is 2 cm. (b) Same photograph under crossed nicols. The coesite grains are surrounded by inversion rims of polycrystalline quartz showing a radiating texture. (c) Schematic features of the included minerals in pyrope. Garnet is always fractured around the silica inclusions, fractures being absent around the other inclusions (see text).

from the kyanite or rutile inclusions.

Most of the silica inclusions exhibit clearly two quartz generations. The first type consists of well-crystallised and strained quartz grains or subgrains at the rim of the inclusions. Between this rim and the preserved coesite and along cleavages or cracks within the coesite crystals there exists a more diffuse quartz (Fig. 1c). This second type of quartz can be in some cases related to large radial fractures in garnet filled with phyllites and so attributed to the fracturing stage of garnet (Fig. 1c).

Some authors have pointed out the importance of elastic effects around solid inclusions in minerals [13–15]. Williams [16] shows microphotographs of eclogite containing garnet with kyanite inclusions surrounded by radial fractures as the result of pressure exerted on the surrounding host crystal by the inclusions. Our observations suggest that the pressure inside the coesite inclusions (now called internal pressure, P_i) exceeded the pressure in the whole rock (external pressure, P_e), which led to garnet fracturing. In the following we will show that this internal pressure rise is due to the elastic contrast between garnet and coesite and to the inversion of coesite to quartz which implies an important volume change, thus allowing coesite conservation by keeping the inclusion pressure on the coesite–quartz equilibrium curve.

3. Elastic model for a coesite inclusion in a pyrope crystal

It is a necessity that pyrope grew around coesite and not around quartz. Indeed, the negative volume change during the transformation of quartz into coesite prevents the coesite growth from a quartz inclusion in the elastic garnet, and the differential elasticity of quartz and garnet cannot alone produce the internal pressure required to stabilize coesite. The possibility that coesite may have been produced metastably under conditions of high strain [17] has been discussed at length by Chopin [10] and has been ruled out. So our elastic model will start from a coesite inclusion in a pyrope crystal in the coesite stability field. To solve the problem analytically some simplifying assumptions have to be made. We consider a unique inclusion located at the centre of a spherical garnet, which is a good approximation to the shapes of most of the actual garnets (in which most of the inclusions are localized near the garnet centre).

We suppose that the included mineral and its host are perfect elastic isotropic bodies. The assumption is justified for the garnet which is an isotropic mineral (index of anisotropy $A = (C_{11} - C_{12})/2C_{44} \simeq 1$) and can be considered as elastic in all the pressure-temperature range that may be encountered by a metamorphic rock. Indeed, the elastic limit of garnet of various compositions is very high, even at high temperatures (3–4 kbar at 1400 °C) [18]. In order to simplify the calculations both coesite and the narrow rim of type 1 quartz are also considered as isotropic and elastic. Preliminary TEM observations have shown that coesite is free of dislocation thus corroborating the assumption of an elastic behaviour for it.

Pyrope grows around coesite at the initial conditions (P_0, T_0) which are identical outside the garnet and in the inclusion. At this point, the radius of the garnet hole (r_0) and the inclusion radius (r_0') are equal (Fig. 2). When pressure and

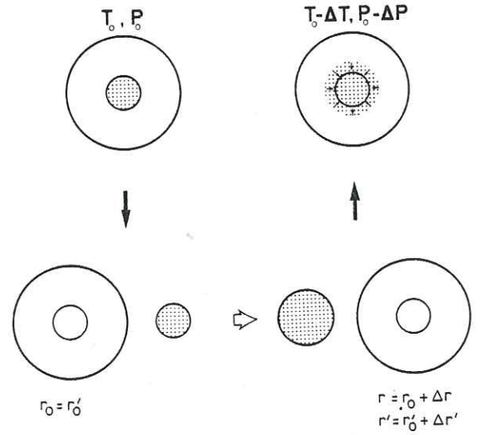

Fig. 2. Schematic presentation of the elastic model for the host–inclusion assemblage. At the origin both radii r_0 and r_0' are equal. For each pressure and temperature decrease we consider separately the evolution in size of hole and inclusion. The inclusion expands more than the hole and we derive the inclusion pressure by forcing the inclusion to occupy the hole volume.

temperature decrease, the volume of each species changes as a function of the elastic parameters α (thermal expansion), β (isothermal compressibility) and μ (shear modulus). In fact, when pressure and temperature decrease, the volume of the inclusion is always larger than that of the garnet hole. Then constraining the inclusion to occupy the volume of the garnet hole leads to an overpressure in the inclusion with respect to the whole-rock pressure (Fig. 2).

The solution of the Navier equation for the sphere-in-hole problem leads to the general formulation of the displacement (u) and stresses (σ_{ij}) in coesite and garnet (see Appendix 1)—

for garnet:

$$u(\rho) = B\rho + C/\rho^2$$

$$\sigma_{\rho\rho} = \frac{3B}{\beta} - \frac{4\mu C}{\rho^3}$$

$$\sigma_{\theta\theta} = \sigma_{\phi\phi} = \frac{3B}{\beta} + \frac{2\mu C}{\rho^3}$$

for coesite:

$$u(\rho) = A\rho$$

$$\sigma_{\rho\rho} = \sigma_{\phi\phi} = \sigma_{\theta\theta} = \frac{3A}{\beta'}$$

where A, B, and C are constants and ρ, θ, ϕ the spheric coordinates. The diagonal terms of the stress tensor ($\sigma_{\rho\rho}$, $\sigma_{\theta\theta}$, $\sigma_{\phi\phi}$) yield the hydrostatic pressures in garnet and in coesite which differ from one another but have a constant value within each mineral. The temperature distribution is assumed to be uniform throughout the system.

The three following boundary conditions allow the determination of A, B and C for each species, and of the pressures in coesite and pyrope:

—the normal stress continuity at the coesite–garnet interface

—continuity between radial stress and external hydrostatic pressure at the garnet–matrix interface

—displacement continuity at the host–inclusion interface.

In the range of pressure and temperature variations considered α, β and μ change considerably and so we have to take into account derivative terms. The elastic constants can be written:

$$a_i(T, P) = (a_i)_0 + (\partial a_i/\partial T)\cdot T + (\partial a_i/\partial P)\cdot P$$

with $a_i = \alpha, K, \mu$

where $K = 1/\beta$ is the bulk modulus. Data concerning these elastic constants are presented in Table 1.

Another circumstance must be taken into account in the evolution of the internal pressure: the volume change occurring at the coesite–low quartz transition. For the P_e-T paths considered $\Delta V/V$ varies between 7.4% at 50 °C, 20 kbar and 13% at 800 °C, 30 kbar. As we are basically interested in the final amount of quartz formed in the inclusion and since this final amount is independent of the P-T path chosen (see below), the lower $\Delta V/V$ value has been used throughout the calculations.

Using this elastic model we decrease external pressure and temperature from the initial point

TABLE 1

Data used for the elastic model (the values in parentheses represent uncertainties)

Coefficient	Units	Pyrope [a]	Coesite [c]
K_0	Pa	$1.5(0.2)\times10^{11}$	$0.96(0.03)\times10^{11}$
$\partial K/\partial P$		5.3(0.8)	8.4(1.6)
$\partial K/\partial T$	Pa K^{-1}	$-2.0(0.3)\times10^{7}$	-2.0×10^{7} [e]
α_0 [a]	K^{-1}	$21.4(2.0)\times10^{-6}$	$7.3(1.0)\times10^{-6}$
$\partial\alpha/\partial P$	$Pa^{-1}\,K^{-1}$	$-2.0(0.3)\times10^{7}\beta^2$	$-2.0\times10^{7}\beta'^2$ [f]
$\partial\alpha/\partial T$ [a]	K^{-2}	$1.1(0.1)\times10^{-8}$	$8.5(0.5)\times10^{-9}$
μ_0 [b]	Pa	$9.0(0.2)\times10^{10}$	
$\partial\mu/\partial P$ [b]		1.5(0.1)	
$\partial\mu/\partial T$ [b]	Pa K^{-1}	$-1.0(0.1)\times10^{7}$	

Inclusion radius $r_0 = r_0' = 3\times10^{-4}$ m

Garnet radius $R = 2.5\times10^{-3}$ m

Clapeyron's curve: $P = 2.07\times10^{9} + 10^{6}\,T$ (Pa) [d]

Volume change: $\Delta V/V = 7.4\%$

[a] Clark [26], cf. Hazen and Finger [30].
[b] Lieberman et al. [28].
[c] Levien and Prewitt [29].
[d] Mirwald and Massonne [4].
[e] Estimated value. Considering quartz and other minerals we have, $-2\times10^{7} < \partial K/\partial T < -0.8\times10^{7}$ Pa K^{-1} (see text for discussion).
[f] Coefficient obtained using the relation: $\partial\alpha/\partial P = \beta^2(\partial K/\partial T)$.

(P_0, T_0) according to different paths (Fig. 3) and compute variations in the inclusion pressure due to small decrements in (P_e, T) along these paths. When the (P_i, T) conditions depart from the coesite–low quartz equilibrium curve we assume that a few percent of coesite transforms into quartz (or vice versa) so that, because of the volume change, the pressure and temperature of the inclusion are constrained to stay on the low quartz–coesite equilibrium curve as long as there is some coesite left.

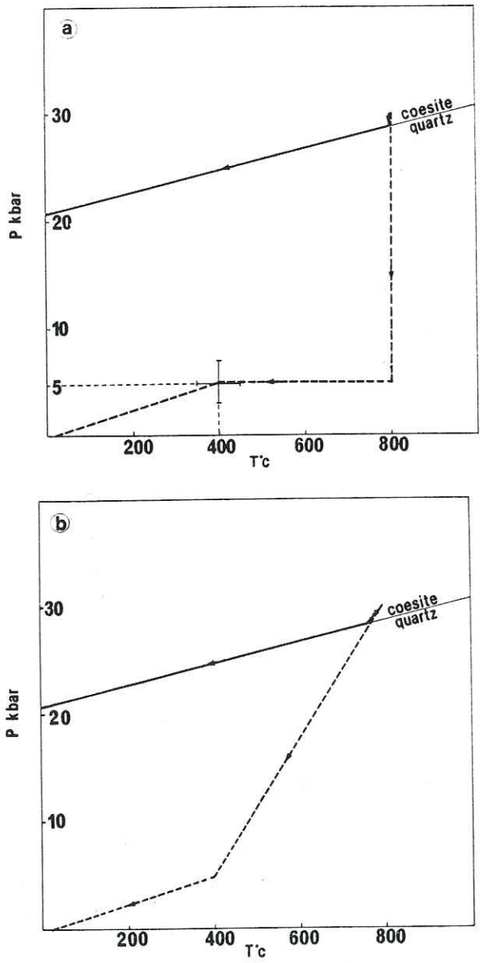

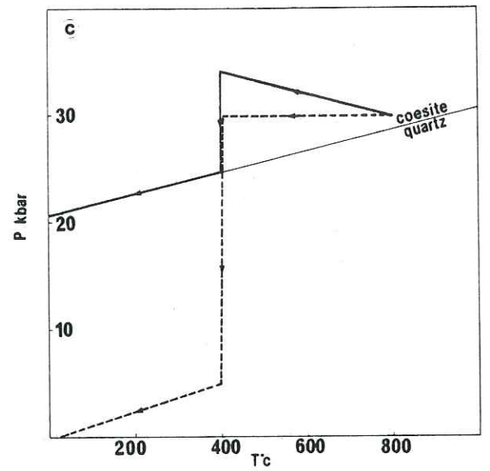

Fig. 3. P_i-T conditions in the inclusion (full line) as a function of the P_e-T path followed by the whole rock (dashed line). The starting (P, T) point of the host-inclusion assemblage lies in the coesite stability field. Three types of retrogressive path (1, 2, 3) are envisaged constrained through the point (5 kbar, 400 °C) because the surrounding rocks exhibit a greenschist overprint. (a) Path 1, (b) path 2, (c) path 3.

4. Computational results

4.1. Examples of computation

We have computed the inclusion pressure and the volume of retrogressive quartz formed along three different P_e-T paths which represent extreme possibilities: isothermal decompression followed by isobaric cooling (Fig. 3a); isobaric cooling followed by isothermal decompression (Fig. 3c), and an intermediate path (Fig. 3b). We suppose that the inclusion and the pyrope host have grown at $P = 30$ kbar and $T = 800$ °C, i.e., within the coesite stability field. Moreover, the three paths are constrained to pass through the point $P = 5 \pm 2$ kbar, $T = 400 \pm 50$ °C, representing the estimated conditions for a greenschist overprint which is well

expressed in rocks surrounding the sample studied. For each of the paths the inclusion pressure is always larger than the external hydrostatic pressure. Along path 1 (Fig. 3a) the difference between inclusion (P_i) and external pressure (P_e) increases and reaches a maximum value of 24 kbar during the isothermal part ($T = 800\,°C$). Along path 3 (Fig. 3c) the same pressure difference increases sharply also during the isothermal event, but at 400 °C. In path 2 (Fig. 3b) the behaviour is intermediate between the two others. Fig. 4 shows that along the intermediate path 2 the amount of quartz formed in the inclusion shows a maximum at 5 kbar, 400 °C. Performed under the assumption that garnet remains unfractured, the calculations show that the amounts of quartz formed are different at the end of each path but quite close to a value of about 23% of the inclusion volume. In fact, elastic deformation is a reversible process and thus the amount of quartz produced in the inclusion only depends on the initial and final conditions, it is independent of the P_e-T path followed. The observed discrepancies ($\simeq 1\%$) are mainly attributed to the errors on the elastic constants which were determined by various authors in different devices.

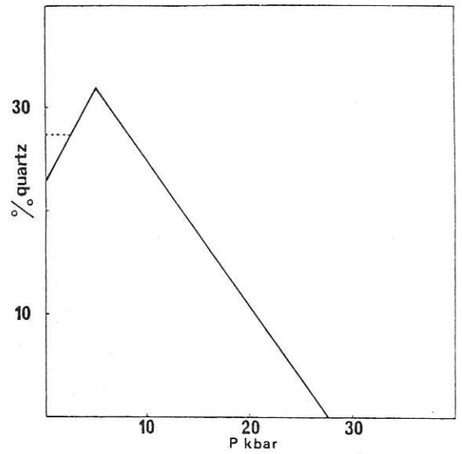

Fig. 4. Variations of the amount of quartz in the inclusion for a path of type 2. From the starting point to the point corresponding to $P = 5$ kbar coesite is transformed into quartz and from this point until the surface quartz must be retransformed into coesite. The full curve is drawn assuming a transformation active down to room temperature. The dashed curve represents the amount of quartz when the system is quenched at 200 °C.

4.2. Inverse problem

For each final amount of retrogressive quartz in the inclusion there exists a specific (P, T) curve representing the possible conditions of formation of the assemblage. We have calculated isopercentage curves of quartz in the inclusion under the assumption that the coesite–low quartz transformation proceeds down to room temperature without fracturing of the garnet (Fig. 5, thin full line). Thus, by measuring the amount of quartz in

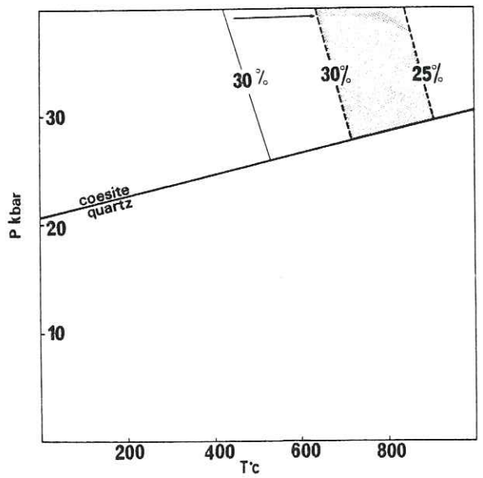

Fig. 5. Final amount of quartz (in percent of the inclusion volume) as a function of the crystallisation conditions. Each curve represents possible crystallisation conditions for an inclusion containing the specified percentage of quartz at present time. The thin full line is drawn assuming that the low quartz–coesite transition proceeds down to surface conditions. The dashed lines are drawn under the assumption that the transformation stops at 200 °C (Fig. 4). Thick full line: coesite–quartz equilibrium curve. The dotted area represents the formation conditions derived from the amount of quartz measured in the most coesite-rich inclusions (see text for discussion).

the inclusion the formation conditions may be approached.

5. Application of the model: discussion

5.1. Kinetics of the low quartz–coesite transition

The crucial point of the model is that the (P_i, T) conditions in the inclusion remain on the low quartz–coesite equilibrium curve as long as coesite can transform into quartz (or vice versa). Obviously the final percentage of quartz in the inclusion will depend on the kinetics of the transformation. No systematic study exists for the kinetics of the coesite–low quartz transition, but it may be assumed that the reaction rate becomes very slow at low temperature and in the vicinity of the equilibrium curve, a fact which is confirmed by the lack of experimental data below 400 °C. For this reason the rate of the coesite–quartz transition may be taken as effectively zero below 200 °C. The calculations performed in the preceding section for the amount of quartz formed (Fig. 4, full line) and for the isopercentage lines (Fig. 5, thin full line) were done assuming a transition operative until the sample reaches the surface. Taking the above kinetic restriction into account, i.e., quenching the system at 200 °C, leads to higher values of the final quartz amount (Fig. 4, dashed line) and thus shifts the isopercentage curves toward higher temperatures (Fig. 5, dashed lines).

5.2. Garnet fracture and P-T path

The inclusions show two types of retrogressive quartz. The first type at the inclusion rim is most likely due to coesite inversion while garnet is unfractured. The stresses generated within the inclusion during the uplift are reflected by the deformation features such as undulatory extinctions observed in the grains of this rim quartz. The second type of quartz may be related to a rapid breakdown of coesite after the garnet fracture. One can now explain why some inclusions are totally inverted while some other retain coesite. Garnet fracturing releases the inclusion pressure; the later the fracture, the more coesite will be conserved because of the slow inversion rate at low temperatures.

Depending on the P_e-T path chosen, the maximum pressure difference ($P_i - P_e$) is reached at different (P, T) conditions and so garnet fracturing occurs at different (P, T) conditions. Along a path of type 1 (Fig. 3a) the difference between internal and external pressure reaches its maximum at the end of the isothermal decompression, garnet fracture would then occur at high temperature (700–800 °C) and lead to a complete breakdown of coesite. For this reason such a path and a fortiori an uplift path implying a temperature increase can be precluded for the rock considered. Since a path of type 3 is geologically difficult to account for, the path followed by our sample is probably close to a type 2 one.

Computations made for the kyanite and zircon inclusions also present in pyrope show that these inclusions are still subjected to 10 kbar of hydrostatic pressure at the present surface conditions. The absence of fractures around these inclusions suggests that pyrope can sustain 10 kbar without fracturing. Since garnet is fractured around all the silica inclusions for a maximum pressure difference ($P_i - P_e$) of 24 kbar, this puts limits on the tension strength of pyrope.

5.3. Amount of retrogressive quartz: derivation of the formation conditions

The amount of type 1 quartz is relatively constant for all the inclusions examined and thus will be taken as representative of the amount of quartz formed by coesite inversion in the unfractured garnet. The quartz content in the most coesite-rich inclusions was measured to be $27 \pm 3\%$ in volume (see Appendix 1). This value mainly represents rim type quartz and for kinetic reasons already pointed out, is likely to represent the quartz amount formed along the path down to 200 °C.

Before deriving the formation conditions from this value, we must keep in mind the assumptions made, in particular: (1) the choice of a minimum value for $\partial K/\partial T$ of coesite; (2) the choice of a two-medium assemblage (pyrope–coesite) instead of a three-medium one (pyrope–coesite–quartz); and (3) the linear extrapolation down to room

temperature of the low quartz– coesite equilibrium curve.

Approximate calculations made for a three-medium assemblage show the little role played by the difference between the elastic constants of quartz and coesite and justify the two-body simplification. Actually all the assumptions can only result in an overestimation of the calculated amount of quartz formed in the inclusion. Therefore the measured amount of quartz and the corresponding isopercentage curve (Fig. 5) yield in fact not a (P, T) curve for possible formation conditions but rather a lower (P, T) limit for these conditions which must then lie in the dotted area of Fig. 5.

6. Petrologic considerations, geodynamic inferences

According to the petrologic study of Chopin [10] the main constraints on the crystallisation conditions of this rock are given by the stability of the paragenesis talc–pyrope–free silica which imposes, even in the absence of coesite, a minimum pressure of 28 kbar and a temperature between about 700 and 820 °C, depending on water activity. The agreement with the conditions derived from the elastic model is thus excellent (Fig. 6).

Moreover, the elastic model and petrologic considerations yield similar constraints on the return path. There is petrographic evidence that the curve of the reaction:

$$\text{talc} + \text{phengite} = \text{phlogopite} + \text{kyanite} + \text{quartz} + H_2O$$

has never been crosscut during decompression [10]. The uplift path is thus severely constrained on the high-temperature side (Fig. 6), all the more as water activity is lower, since a lower activity shifts the curve toward lower temperatures [10]. Thus a return path beginning with isothermal decompression (cf. type 1 in Fig. 3) and a fortiori a path implying temperature increase are precluded on petrologic grounds. As already pointed out, they are also ruled out by the elastic model since they would result in a high-temperature fracturing of garnet and thus in a complete breakdown of coesite.

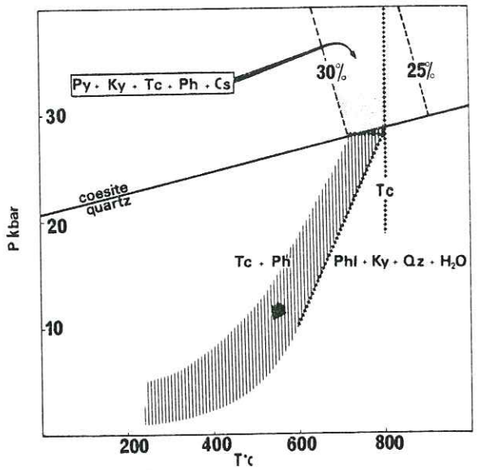

Fig. 6. Crystallisation conditions and uplift path of the rock studied as constrained by mechanical and petrologic data. The dotted area represents the formation conditions of the assemblage pyrope (Py)–kyanite (Ky)–talc (Tc)–phengite (Ph)–coesite (Cs) obtained by combining the results of the elastic model (Fig. 5) and the upper stability limit of talc (+ + +) [19] which sets an upper temperature limit to the whole P-T evolution. The uplift path (hatched area) is constrained by the reaction talc + phengite → phlogopite + kyanite + quartz + H_2O (as experimentally determined by Massonne and Schreyer, personal communication) and by mechanical and kinetic considerations (see text).

Therefore, we are led both by mechanical and petrologic considerations to a two-fold conclusion. The first point is that the rock must have been buried to depths of about 100 km. The temperature reached there implies that low-temperature gradients, how essentially transient they are, may nevertheless persist to considerable depth [10]. This carries also far-reaching implications for the role of continental crust in geodynamic processes. Indeed, considering the upper crustal, probably meta-evaporitic origin of the quartzite [10] and its interbedding within a continental unit [10,11], we must admit that continental crust may also be subducted to depths of 100 km or more.

The second point concerns the uplift of the rock which must have proceeded without temperature increase. This is a rather unusual feature which has already been suggested and reported from high-

pressure terranes of the Western Alps [23,24]. It is at variance with thermal models of uplift by denudation which all predict temperature increase during decompression [20–22]. For instance, a rock buried to a depth corresponding to $P = 32$ kbar and $T = 750$ °C would reach a temperature of 900 °C during an erosion-controlled uplift. In order to preserve a coesite-bearing assemblage, other mechanisms than erosion alone have to be invoked; in our opinion they must be tectonic. Intracrustal upward thrusting upon cooler units [24] is the most likely mechanism. Nevertheless, even if the geologic setting does not suggest it (cf. [10]), a diapiric rise [25] may be envisaged in the absolute. The important density change (from 2.9 to 2.6 g/cm^3) during the coesite–quartz transition could indeed be a driving force for the uplift, as far as silica-rich rocks are concerned.

7. Concluding remarks

A simple elastic model derived from the sphere-in-hole problem and applied to coesite inclusions in the garnets of a pyrope-quartzite accounts for all the textural features observed and for the selective preservation of coesite in the inclusions. Through the derivation of crystallisation conditions implying that continental crust may also be subducted, this model has very important bearings on some basic concepts of geodynamics. Besides, it carries also important petrologic consequences. Indeed, calculations performed during the course of this study showed that pressure differences of several kilobars may exist between the matrix and the inclusions in garnet. This recalls that applying geobarometers to crystalline inclusions may be fraught with error if the mechanical aspect of the problem is not considered.

Acknowledgements

The authors wish to thank J.P. Poirier for introducing to the sphere-in-hole problem and for comments of an earlier version of the manuscript. Stimulating discussions with J.C. Mercier, R.C. Lieberman and R.C. Newton, and the constructive reviews of J.C. Doukhan, P.W. Mirwald and an anonymous reviewer are gratefully acknowledged.

This is Institut de Physique du Globe Contribution No. 759.

Appendix 1

Problem of the sphere-in-hole [25]

Navier's equation in spherical symmetry for an isotropic medium is:

$$\text{div}\,\vec{u} = \frac{\mathrm{d}}{\mathrm{d}\rho}\left(\frac{\mathrm{d}\vec{u}}{\mathrm{d}\rho} + \frac{2\vec{u}}{\rho}\right) = 0$$

where ρ is the radial coordinate, $\vec{u}$ the displacement vector.

Its general solution is:

$$u = I\rho + \frac{J}{\rho^2}$$

where I, J are constants.

According to Hooke's law, the stress tensor for each species is given by:

$$\sigma_{ij} = \lambda\delta_{ij}\Sigma e_{ij} + 2\mu e_{ij}$$

where e_{ij} are the strain tensor coefficients.

For coesite:

$$u'(\rho) = A\rho$$

$$\sigma_{\phi\phi} = \sigma_{\theta\theta} = \sigma_{\rho\rho} = 3A/\beta'$$

For garnet:

$$u(\rho) = B\rho + \frac{C}{\rho^2}$$

$$\sigma_{\rho\rho} = \frac{3B}{\beta} - \frac{4\mu C}{\rho^3}$$

$$\sigma_{\theta\theta} = \sigma_{\phi\phi} = \frac{3B}{\beta} + \frac{2\mu C}{\rho^3}$$

where A, B, C are constants.

The boundary conditions are:

—at $R = \rho$

$$\sigma_{\rho\rho} = -P_e = \frac{3B}{\beta} - \frac{4\mu C}{R^3}$$

where P_e is the external pressure which is supposed to be hydrostatic and R the garnet radius (Fig. A-1).

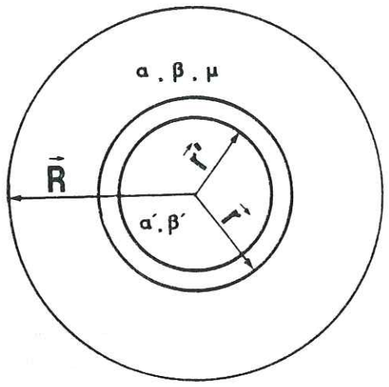

Fig. A-1. Geometry of the problem. r = hole radius, r' = inclusion radius, α, β, μ = elastic constants of garnet, α', β' = elastic constants of coesite.

—normal stress continuity at the coesite–garnet interface:

$$\sigma_{\rho\rho}\left[r' + u'(r')\right] = \sigma_{\rho\rho}\left[r + u(r)\right] = -P_i$$

where P_i is the pressure in the coesite inclusion (internal pressure).

—displacement continuity at the interface:

$$r' + u'(r') = r + u(r)$$

Pressure in the inclusion does not depend on the hole radius but on the relative size of hole and garnet. When $R > 5r'$ the garnet can be considered as an infinite medium. Assuming that this relation is satisfied, which is evidenced by the thin sections, the constants may be written (neglecting the small terms):

$$A = -\left(\frac{4\beta'\mu C}{3r'^3} + \frac{\beta' P}{3}\right)$$

$$B = \left(\frac{4\mu\beta C}{3R^3} - \frac{\beta P}{3}\right)$$

$$C = \frac{(r'-r)r^2}{4\beta'\mu r'/3r + 1}$$

The three equations are solved by iteration. At each P and T incremental decrease we compute A, B and C, the elastic constants α, α', β, β', μ and then the corresponding value of internal pressure and the quartz amount needed to keep the P-T conditions of the inclusion on the low quartz–coesite equilibrium curve.

The radius variations due to temperature are calculated according to:

$$r = r_0\left[\exp(\alpha\Delta T)\right]^{1/3}$$

Determination of the amount of retrogressive quartz

We have measured the amount of coesite in surface from thin section microphotographs and then derived the volumic amount assuming a spherical inclusion:

$$(S_{coes}/S_{incl})^{3/2} = V_{coes}/V_{incl}$$

Alternative approach

As suggested by J.C. Doukhan the problem may also be solved considering the energetic budget of the system.

A rigorous thermodynamic treatment should take into account the variations of the deviatoric stress tensor $\sigma(r)$ when $\mathrm{d}n$ molecules of coesite are transformed into quartz. The energy associated to the stress variation is introduced in the free-energy equation as follows:

$$\delta G = (-\mu_1 \mathrm{d}n + \mu_2 \mathrm{d}n) + V\mathrm{d}P$$

$$-\iiint \epsilon(r)\cdot \mathrm{d}\sigma(r)\cdot \mathrm{d}r$$

i.e. $\delta G = \mathrm{d}G_1 + \mathrm{d}G_2 + \mathrm{d}G_3$

where $\mathrm{d}G_1$ and $\mathrm{d}G_2$ denote the free energy variations due to the coesite–quartz phase transformation and to hydrostatic variations, respectively. ($\mathrm{d}G_3$) is due to deviatoric stress variations. μ_1 and μ_2 are the chemical potentials of coesite and quartz, respectively, and ϵ the deformation tensor.

A rough calculation shows that $\mathrm{d}G_3/\mathrm{d}G_2$ is less than 10^{-2}, which supports the assumption implicitly made in our elastic model that the coesite–quartz equilibrium curve is not strongly affected by the deviatoric stresses developed in the quartz rim.

References

1 L. Coes, A new dense crystalline silica, Science 118, 131–152, 1953.
2 G.J.F. MacDonald, Quartz–coesite stability relations at high temperatures and pressures, Am. J. Sci. 254, 713–721, 1956.
3 F.R. Boyd and J.L. England, The quartz–coesite transition, J. Geophys. Res. 65, 749–756, 1960.
4 P.W. Mirwald and H.J. Massonne, The low-high quartz and quartz–coesite transition to 40 kbar between 600 °C and 1600 °C and some reconnaissance on the effect of $NaAlO_2$ component on the low quartz-coesite transition, J. Geophys. Res. 85, 6983–6990, 1980.
5 E.C.T. Chao, E.M. Shoemaker and B.M. Madsen, First natural occurrence of coesite, Science 132, 220–222, 1960.
6 J.R. Smyth and C.J. Hatton, A coesite–sanidine grospydite from the Roberts-Victor Kimberlite, Earth Planet. Sci. Lett. 34, 284–288, 1977.
7 J.R. Smyth, Quartz pseudomorphs after coesite, Am. Mineral. 62, 828–830, 1977.
8 N.V. Sobolev et al., Coesite, garnet and omphacite inclusions in Yakut diamonds. First finding of coesite paragenesis, Dokl. Akad. Nauk SSSR 230, 1442–1444, 1976 (in Russian, quoted from Mineral. Abstr. M.A. 78–818).
9 C. Chopin, High-pressure facies series in pelitic rocks: a review, Terra Cognita 3, 183, 1983.
10 C. Chopin, Coesite and pure pyrope in high-grade blueschists of the Western Alps: a first record and some consequences, Contrib. Mineral. Petrol., in press, 1984.
11 P. Vialon, Etude géologique du massif cristallin de Dora Maira, Alpes cottiennes internes, Italie, 282 pp., Thèse, Fac. Sci., Grenoble, 1966.
12 J. Bouchez, Comportement des fissures de traction au voisinage d'interfaces matérielles, 141 pp., Thèse, Ecole Centrale des Arts et Manufactures, Paris, 1983.
13 J.L. Rosenfeld and A.B. Chase, Pressure and temperature of crystallisation from elastic effects around solid inclusions in minerals, Am. J. Sci. 259, 519–541, 1961.
14 J.L. Rosenfeld, Stress effects around quartz inclusions in almandine and the piezothermometry of coexisting aluminium silicates, Am. J. Sci. 267, 317–351, 1969.
15 H.G. Adams, L.W. Cohen and J.L. Rosenfeld, Piezothermometry, II. Geometric basis, calibration for the association quartz-garnet, and application to some pelitic schists, Am. Mineral. 60, 584–598, 1975.
16 A.F. Williams, The Genesis of the Diamond, Vols. 1 and 2, 636 pp., Ernest Benn, 1932.
17 H.W. Green II, Metastable growth of coesite in highly strained quartz, J. Geophys. Res. 77, 2478–2482, 1972.
18 J. Rabier, Dissociation des dislocations dans les oxydes de structures grenat. Application à l'étude de la déformation plastique du grenat de fer et d'yttrium (YIG), 182 pp., Thèse, Université de Poitiers, 1979.
19 S. Kitahara, S. Takenouchi and G.C. Kennedy, Phase relations in the system $MgO\text{-}SiO_2\text{-}H_2O$ at high temperature and pressure, Am. J. Sci. 264, 223–233, 1966.
20 P.C. England and S.W. Richardson, The influence of erosion upon the mineral facies of rocks from different metamorphic environments, J. Geol. Soc. London 134, 201–213, 1977.
21 A.B. Thompson, The pressure and temperature (P, T) plane viewed by geophysicists and petrologists, Terra Cognita 1, 11–16, 1981.
22 G. Draper and R. Bone, Denudation rates, thermal evolution and preservation of blueschist terrains, J. Geol. 89, 601–613, 1981.
23 J.M. Lardeaux, G. Gosso, J.R. Kienast and B. Lombardo, Relations entre le métamorphisme et la déformation dans la zone Sésia-Lanzo (Alpes Occidentales) et le problème de l'éclogitisation de la croûte continentale, Bull. Soc. Géol. Fr. 7, 793–800, 1982.
24 B. Goffé and B. Velde, Contrasted metamorphic evolutions in the thrusted cover units of the Briançonnais zone (French Alps): a model for the conservation of HP-LT metamorphic mineral assemblages, Earth Planet. Sci. Lett. 68, 351–360, 1984.
25 P.C. England and T.B.J. Holland, Archimedes and the Tauern eclogites: the role of buoyancy in the preservation of exotic blocks, Earth Planet. Sci. Lett. 44, 287–294, 1979.
26 A.E.H. Love, The Mathematical Theory of Elasticity, 643 pp., Dover, New York, N.Y., 1944.
27 S.P. Clark, Handbook of Physical Constants, Geol. Soc. Am. Mem. 97, 587 pp., 1966.
28 R.C. Lieberman, B.J. Leitner and P.J. Lellis, Elasticity of minerals relevant to geophysics, Rev. Geophys. Space Phys., in press, 1983.
29 L. Levien and C. Prewitt, High pressure crystal structure and compressibility of coesite, Am. Mineral. 66, 324–333, 1981.
30 R.M. Hazen and L.W. Finger, The crystal structure and compressibilities of pyrope and grossular to 60 kbar, Am. Mineral. 63, 297–303, 1978.

Ellenbergerite, a new high-pressure Mg-Al-(Ti,Zr)-silicate with phosphatian varieties and a novel structure based on face-sharing octahedra

Christian Chopin[1], Rolf Klaska[2], Olaf Medenbach[2], Dominique Dron[1]

1) Laboratoire de Géologie, Ecole Normale Supérieure, 46 rue d'Ulm, 75005 PARIS, France

2) Institut für Mineralogie, Ruhr-Universität, 4630 BOCHUM 1, Federal Republic of Germany

ABSTRACT

Ellenbergerite occurs as purple millimetre-size grains associated with talc, kyanite, clinochlore, rutile and zircon in composite inclusions within decimetre-large pyrope crystals (90-98 mole percent end-member) in the quartzite layer of the Dora Maira massif, Western Alps, from which coesite has been recently reported (Chopin, 1984). It is hexagonal, a = 12.229(4), c = 4.919(3) Å, Z = 1, space group $P6_3$. Mohs hardness 6.5 ; D_{mes} 3.15, D_{cal} 3.12 ; no cleavage. Uniaxial negative and vividly pleochroic, ω colourless, ε colourless to deep lilac with colour zoning. The intensely coloured variety has ω 1.6789(5), ε 1.670(1) ; microprobe analysis yields SiO_2 39.09, P_2O_5 0.44, Al_2O_3 25.12, TiO_2 4.01, MgO 22.19, FeO 0.20, sum 99.05 wt. % including H_2O 8.0 (coulometrically). The formula calculated on a $O_{28}(OH)_{10}$ basis (implying 7.5 wt. % H_2O) is

$Mg_{6.71}\ Fe_{0.03}\ Ti_{0.61}\ Al_{6.00}\ Si_{7.92}\ P_{0.08}\ O_{28}(OH)_{10}$

The colour zoning is due to nearly complete Ti=Zr substitution. In addition ellenbergerite may contain more than 8 wt.% P_2O_5 with strictly correlated changes of Si, Mg, Al and Ti+Zr contents, over 80% of which represent the SiAl = PMg substitution.

The structure has been refined from 1049 independent reflections to R = 0.036, R_w = 0.033. It builds up rods of face-sharing octahedra along the six-fold screw axes and pairs of face-sharing octahedra which are linked over edge-sharing to form zig-zag chains parallel to the two-fold screw axes, all interconnected by SiO_4 tetrahedra. The structural formula is

$(Mg,Ti,Zr,\square)_2\ Mg_6(Al,Mg)_6\ (Si,P)_2\ Si_6\ O_{28}(OH)_{10}$

The interconnection of the octahedra proceeds mainly by face-sharing. This unusual feature and the resulting density of the structure reflect, considering the common bulk composition, the uncommon high-pressure formation conditions

(about 25-30 kbar, 700-800°C). In the absence of tetrahedral aluminium, the consistent positive departure of the P/Si substitution from the 1/1 ratio even suggests that up to 1.5 % of the Si atoms could be accommodated in six-fold coordination with increasing P content. Ti^{4+}-Fe^{2+} charge transfer between face-sharing octahedra on the six-fold screw axes most likely accounts for the absorption scheme.

INTRODUCTION

The phengite quartzite layer of the Dora Maira crystalline massif, Western Alps, from which coesite has been recently reported (Chopin, 1984) is also remarkable for the size and the composition of the garnet crystals it contains (Vialon, 1966). Indeed, some large, euhedral crystals may exceed 20 cm in diameter and are the most pyrope-rich ever recorded with 95 to 98 mole percent end member. In contrast with the more typical centimetre-size garnets of the quartzose matrix, the large garnets do not contain coesite but numerous mineral inclusions among which a conspicuous purple mineral, probably mentioned as piemontite by Vialon (1966). Our investigations show this mineral to be a new hydrated Mg-Al-Ti-silicate with very unusual crystal chemistry and structure. Indeed, in addition to an extensive Ti = Zr substitution and an ability to incorporate phosphorus which makes this mineral one of the most P-rich silicates known, its dense nesosilicate structure based on face-sharing octahedra cannot be related to any known structure. The present paper is concerned with the description and crystal chemistry of the new species, petrologic implications are discussed elsewhere (Chopin, 1985). We take pleasure in naming this mineral in honour of Professor François Ellenberger, Paris, in recognition of his geological work in the internal Western Alps. Incidentally, his epoch-making "Etude géologique du pays de Vanoise" (1958) contains the first records of two high-pressure minerals to be described years later, namely deerite (p. 261, compare Agrell et al., 1965) and magnesiocarpholite (p. 282 and plate 17-6, compare Goffé et al., 1973). The type material is preserved at the Galerie de Minéralogie, Université P. et M. Curie, Paris ; cotype specimens are preserved at the Ecole Nationale des Mines, Paris, and at the Institut für Mineralogie, Ruhr-Universität, Bochum.

The description and name have been approved by the IMA commission on New Minerals and Mineral Names.

OCCURRENCE

Ellenbergerite was found at Parigi, near Martiniano Po, Italy, in the very phengite-pyrope-quartzite outcrop from which coesite has been reported (Chopin,

1984). It exclusively occurs as inclusions within large, 2 to 25 cm pyrope crystals in which it apparently stably coexists with kyanite, talc, clinochlore, rutile, zircon, a sodic amphibole close to glaucophane, and the host garnet (Fig. 1). Even if not present in all the large garnets, ellenbergerite is rather abundant and may represent up to a few modal percent of the pyrope crystals. These rocks were formed during Alpine times by unusually deep burial of continental crust along a low temperature gradient. Indeed, formation conditions estimated from the matrix assemblage phengite-talc-kyanite-pyrope-quartz/coesite are 25 to 30 kbar, 700 to 800°C (Chopin, 1984), and the lower range of this estimate probably pertains to the ellenbergerite-bearing relic assemblage preserved within the large garnets (Chopin, 1985). Extensive overprinting of the high-pressure assemblages occurred during the subsequent uplift and metamorphic evolution. This is the reason why, although numerous other outcrops of the phengite-quartzite exist - the layer has been mapped over 15 km by Vialon -, no other ellenbergerite occurrence and few other occurrences of fresh pyrope have been found in the area, between Val Po and Val Varaita.

PHYSICAL AND OPTICAL PROPERTIES

Ellenbergerite crystals are typically millimetre-sized and anhedral, they rarely form elongated, up to 10 mm prisms with hexagonal cross-section. The mineral is transparent with a purple to lilac colour, a few grains showing a pink core. There is no cleavage, the fracture is easy and brittle, the lustre vitreous. Extremely fine, channel-like fluid (?) inclusions often materialize the c axis direction. Repeated density measurements in heavy liquids yield 3.15 g/cm^3 for most grains, up to 3.22 for a few grains. The Mohs hardness is 6.5. The mineral is not fluorescent in ultraviolet light but displays a faint, bluish cathodoluminescence under the electron beam.

Ellenbergerite is uniaxial negative and vividly pleochroic, colourless perpendicular to c , colourless to deep lilac parallel to c . Most grains are colour-zoned and, although complex zonation patterns exist, the general trend is from pale pink with low birefringence in the core to purple or lilac with higher birefringence on the rim. High-precision spindel stage measurements (Medenbach, 1985) have been carried out on five grains (I to V) about 200 μm large and showing a wide range of refractive indices and chemical compositions. The results reported in Table 1 show that n_o is well correlated with the Ti/(Ti + Zr) ratio, while n_e is more dependent on the phosphorus content.

The very distinctive optical properties, i.e. the uniaxial character and the pleochroic scheme, should avoid any confusion with other species, in particular

with the epidotes thulite and piemontite.

CELL PARAMETERS

Single crystal work with Weissenberg and precession camera established the hexagonal symmetry of ellenbergerite with the space group $P6_3$ ($P6_{3/m}$ precluded by the refined structure). The cell parameters refined from a powder diffractogram (Table 2) using Si as internal standard are a = b = 12.229(4), c = 4.919(3) Å, V = 637.1 $Å^3$, Z = 1. The calculated density for a common, Ti-rich and P-poor composition is 3.125.

CHEMISTRY

Ellenbergerite was analysed using a Cameca Microbeam electron probe (40° take off angle) with an operating voltage of 15 kV and a beam current of 15 or 20 nA. In addition to the five single crystals optically measured, about 30 grains have been investigated in thin sections cut from four large garnets (samples 3-64, 3-65, 4-18/19 and 4-55). The only elements detected with atomic number greater than 8 are Mg, Al, Si, P, Ti, Fe and Zr. Wavelength dispersive analysis was carried out using the standards forsterite (Mg,Si), anorthite (Al), Fe_2O_3, $MnTiO_3$(Ti), apatite (P) and zircon (Zr), care being taken to avoid PKα, ZrLα and CaKβ(2) interferences. The ZAF correction programme supplied by the manufacturer having proved unsatisfactory (altering the relative proportions of the light elements and undercorrecting the heavier ones), the data were corrected using the ZAF correction programme MISO written by K. Abraham, Bochum (pers. comm., 1979), following the procedure of Sweatman and Long (1969, compare Springer, 1976) and using the Theisen and Vollath (1965) absorption coefficients.

The analyses (Table 1) reveal a Mg-Al-Ti-silicate with low analytical totals and two major chemical variations, the Ti/Zr ratio and the P incorporation. The most intensely coloured ellenbergerite contains about 4 wt. percent TiO_2, no zirconium and little or no phosphorus. It forms the outer part of zoned grains and also a few homogeneous, smaller grains (as crystal V). The less coloured zones are Ti-poor and correlatively Zr-rich. They are usually P-poor, rarely P-free, but may contain up to 8.3 wt. percent P_2O_5 in a few strongly zoned grains as crystal IV (Table 1). The iron contents are consistently low resulting in a Mg/(Mg + Fe) ratio higher than 0.98 in sample 4-55 and higher than 0.99 in all the others. Iron is believed to be in the divalent state in the absence of any evidence for trivalent iron in the mineral assemblage,

considering in particular the absence or very low contents of iron in kyanite (Fe_2O_3 < 0.05 wt.%).

The analytical totals typically amount to 90-92 %. Application of the Gladstone-Dale relationship suggested that the difference must be entirely accounted for by H_2O. This has been confirmed by ion microprobe scans which showed insignificant amounts of Li, Be and B. Since talc and clinochlore analysed with the electron probe under the same conditions as ellenbergerite show consistently low analytical totals of 93-94 and 84-85 %, respectively, a water content near 7 wt. percent could be derived for ellenbergerite. A coulometric determination performed at the Ruhr-Universität (details in Johannes and Schreyer, 1981) on a ca. 6 mg sample baked at 110°C yields 8.0 ± 0.4 wt. percent H_2O.

Structural formula :

The refined structure to be described below contains per unit cell 8 tetrahedral cation sites, 14 octahedral cation sites, 38 oxygen atoms among which at least 8, probably 10 are involved in OH groups. The analyses have thus been recalculated on a 33 oxygen anhydrous basis (Table 1). The resulting atomic contents of Si, Al, Ti + Zr and Mg + Fe are plotted as a function of P contents in Figure 2 and show very regular variations. A linear extrapolation yields the following formula for the P-free end-member :

$$(Mg,Fe)_{6.69}(Ti,Zr)_{0.61}Al_{6.05}Si_{8.01}O_{28}(OH)_{10}$$

Considering that aluminium is overestimated by about one percent relative in pyrope analyses performed using the same standards (Chopin, 1985), the P-free end-member may be ideally written :

$$Mg_{6.74}Ti_{0.63}Al_{6.0}Si_{8.0}O_{28}(OH)_{10}$$

This formula implies a water content of 7.5 wt. percent, which agrees well with the measured one and that deduced from the analytical totals. It also implies the absence of tetrahedrally coordinated aluminium, which is likely in such a high-pressure mineral. The sum of the octahedrally coordinated cations, 13.37 as compared to the 14 possible ones, implies octahedral vacancies.

The substitutions :

The substitution having the most conspicuous effects is that of titanium by zirconium which results in colour zoning. Molecular Ti contents are plotted as a

function of Zr contents in Fig.3, in which only P-poor grains are considered in order to keep the sum Ti + Zr to a nearly constant value (compare Fig.2). The substitution obviously proceeds on a one to one atomic ratio and may be nearly complete, which, incidentally, is evidence for the tetravalent state of titanium in this structure.

With up to 8.3 wt. percent P_2O_5, ellenbergerite appears as the most phosphatian silicate ever reported, with the possible exception of a few yttrian zircons if the latter are true zircon-xenotime solid solutions. High phosphorus contents have been reported in various terrestrial silicates, mostly nesosilicates (Koritnig, 1965) : 4.1 wt. % P_2O_5 in spessartine (3.6% corrected for impurities, Mason and Berggren, 1941), 0.5 % in sodian garnets (Thompson, 1975), 6.5 % in allanite (Iimori et al., 1931), 0.3 to 0.5 % in yoderite (Abu-Eid et al., 1978) and davreuxite (Langer et al., 1984), 2.5 % in olivine and pyroxene (Goodrich, 1984). The P^{5+} ion substitutes for Si^{4+} in tetrahedral site and various substitutional mechanisms have been proposed in order to insure charge balance, e.g. NaP = CaSi in garnet (Thompson, 1975), $Fe^{2+}P = Fe^{3+}Si$ in andalusite (Langer et al., 1984), or $SiMg = P\,\square_{0.5}Mg_{0.5}$ in olivine (Buseck, 1977). The complete range from P-free to very P-rich ellenbergerite compositions provides a good opportunity to study the substitutional mechanisms involved by phosphorus incorporation into this nesosilicate structure.

Noteworthy, Table 1 shows that the sum of the cations calculated on the 33 oxygen anhydrous basis remains constant regardless of P content. P incorporation is thus entirely balanced by the other cations considered and does not involve OH groups nor vacancies. Neglecting the Ti = Zr and Mg = Fe substitutions for the present purpose, Fig. 2 shows that P incorporation proceeds through a single, bulk substitution involving all the cations except H^+. From the slopes of the plots of Fig. 2, this substitution may be written

$$1\ P + 0.86\ Mg = 0.90\ Si + 0.75\ Al + 0.22\ Ti \qquad (1)$$

in which the cation number and electric charges are virtually balanced.

A puzzling point is that the Si/P substitution deviates by about 10 % from the 1/1 ratio to be expected since Si and P are the only tetrahedrally coordinated elements. In the structural formulae Si + P increases from 8.00 to 8.13 when P increases from 0 to 1.4. An analytical artefact was first suspected, partly because P is the analysed element with the largest correction factor. This factor varies with increasing P content from 1.30 to 1.28, it is in fact in excellent agreement with the 1.27 mean value given by Bishop et al. (1978) for small P amounts in various structures analysed with an apatite standard and comparable operating conditions but a higher take-off angle, which minimizes the

correction. Furthermore, using lazulite as alternative P standard reduces the correction factor to 1.12 but yields strictly identical results. As to Si, it is hardly affected by varying P contents, its correction factor ranging between 0.98 and 0.99. Therefore we see here no reason to suspect that either the P content or the Si content must be in error. An alternative possibility is that the Si/P substitution actually proceeds with the 1/1 ratio, i.e. P incorporation does in fact imply an increase of the number of OH groups and a correlative decrease of the number of cations (other than H^+). In this event the constancy, regardless of P content, of the sum of the cations calculated on an anhydrous basis would have to be purely fortuitous. If this seems unlikely, one has to assume that about 1.5 percent of the Si atoms are accommodated in six-fold coordination in the most P-rich crystal. Although this would be a novelty among terrestrial minerals formed under static conditions, this is perhaps less shocking when considering how unusual the structure and formation pressure of this mineral are. The structure refinement of such a P-rich crystal is presently undertaken.

Whatever the issue of this debate, the bulk substitution responsible for P incorporation may be decomposed into several independent ones, which are essentially SiAl = PMg (for over 80 percent) and TiMg = AlAl or, alternatively, SiTi = PAl. The extent of these individual substitutions are in fact strictly correlated so that the composition of ellenbergerite is entirely defined by the three independent parameters : P content, Ti/Zr ratio and, accessorily, Mg/Fe ratio. Whereas the Mg/Fe ratio of ellenbergerite shows little variations between and within grains in a given garnet, the Ti/Zr ratio may vary considerably within a grain, even if the latter coexists with both rutile and zircon. Likewise the P_2O_5 content may decrease from 8.3 wt. percent in the core of a crystal containing a relic grain of apatite to 0.2 on the rim, while other grains even containing apatite inclusions show rather constant P_2O_5 values, between 2 and 3 wt. percent. This suggests that the availabilities of the elements obey local controls, the scale of which may be quite different and variable.

AN OUTLINE OF THE STRUCTURE

Only a few outstanding features are addressed here, a complete report being published elsewhere (Klaska, in prep.). From 1049 independent observed reflections the structure of a crystal with optical properties identical to those of crystal II (Table 1) has been refined in the $P6_3$ space group to an R value of 0.036 (R_w = 0.033) using anisotropic temperature factors. The structure as seen along c is represented in Fig. 4 which emphasizes the

coordination polyhedra. It consists of rods of regular, face-sharing octahedra extending along the six-fold screw axes, and of zig-zag chains consisting of stacked, edge-sharing pairs of distorted face-sharing octahedra. Three such chains extending parallel to c define a sort of channel around the three-fold axes. At a given z level the three pairs of octaheda closer to a three-fold axis share common corners and are interconnected by a tetrahedron situated on the three-fold axis (Fig. 4). The overlying pairs of octahedra do not share corners but are interconnected by three tetrahedra in non-special position. One of the remaining vertices of such a tetrahedron is the shared corner of the underlying octahedral pairs, the other belongs to the octahedral rod running along the six-fold axis. The connection between the octahedral rods and chains is thus achieved by six tetrahedra.

The Si(1) tetrahedra situated on the three-fold axis all point in the same direction and their free vertex is occupied by an OH group. Their nevertheless smaller size as compared to the six Si(2) tetrahedra (1.62 vs 1.64 Å for the mean Si-O bond distance) suggests that the smaller phosphorus ion is partitioned into Si(1).

In the beams, the face-sharing octahedra of each pair are not equivalent. Al occupies the smaller one with an average Al-O bond length of 1.93 Å ; Mg occupies the larger, more distorted one, now referred to as Mg(1) octahedra, with an average Mg-O bond length of 2.08 Å. Local bond valences deduced from observed bond lengths imply that 6 OH groups per unit cell occupy the corners common to four octahedra of the beam.

The regular Mg(2) octahedra situated on the six-fold screw axis are only partly filled, with a mean cation-oxygen bond length of 2.07 Å. Mg and Ti+Zr account each for one third, leaving one third of the sites vacant.This makes likely the existence of cooperative ordering of Mg, Ti or Zr, and vacancies within each rod. However, their arrangement over the whole structure is disordered as shown by the absence of superstructure in the c direction and of violation of the extinction rules. Bond strength considerations for the oxygen atoms forming the Mg(2) polyhedra suggest the presence of one OH group per octahedron, which cannot be symmetry-related and must be considered as delocalized.

The cell contains thus 10 OH groups, 2 on the three-fold axes, 6 in zig-zag chains forming like the back-bone of the octahedral beams, and 2 around the six-fold screw axes. The presence of OH groups is confirmed but not further resolved by the IR powder absorption spectrum which shows a broad band near 3500 cm^{-1} with a prominent shoulder at 3600 cm^{-1}. The polar structure described here implies that ellenbergerite is optically active and piezoelectric, which could not be directly evidenced. Phosphorus incorporation

can also be reconsidered in the light of this structure. If P is exclusively present in the Si(1) site, it is somewhat surprising that charge balance involves Ti atoms in the remote Mg(2) site. A possibility is that a small fraction of P (20 percent or less as suggested by equation (1)) substitutes for Si in the Si(2) site, charge balance being achieved by substitution of Al for Ti in the Mg(2) site.

The most interesting structural feature is yet that the interconnection of the octahedra proceeds mainly by face-sharing, which is very uncommon if not unique among the nesosilicate and even silicate structures. This feature implies quite a dense packing, which is undoubtedly linked to the unusually high pressure of formation of ellenbergerite. Indeed, even if the hexagonal close packing of the oxygen atoms is not realized throughout the whole structure, the "packing efficiency" in ellenbergerite approaches that in pyrope, with less than 17 $Å^3$ per oxygen, as compared to less than 16 $Å^3$ in pyrope.

THE ORIGIN OF COLOUR IN ELLENBERGERITE

Microprobe work has shown that the colour zoning of ellenbergerite is related to variations of the Ti/Zr ratio, the absorption increasing with Ti content. Furthermore ellenbergerite shows for a same Ti content a much stronger absorption in sample 4-55 (the absorption seems nearly complete along ε for the most Ti-rich grains!),the only chemical pecularity in this sample being FeO contents two to three times higher than in all others : 0.6 to 0.7 wt. percent FeO against 0.2 to 0.4, respectively. Besides the pleochroic scheme shows the absence of absorption along ω. Both the dependence of absorption on the FeO and TiO_2 concentrations and its orientation relative to the c axis can be readily and entirely accounted for by charge transfer between Fe^{2+} and Ti^{4+} ions occupying neighbouring, face-sharing Mg(2) sites on the six-fold screw axis (Fig. 4). As shown by the structure refinement, the Ti atoms lie off centre in the octahedra, resulting in a long Mg-Ti (or Fe-Ti) distance of 2.73 Å. After the relation given by Smith and Strens (1976), this distance should result in an absorption near 15,000 cm^{-1}, which is in fair agreement with the observed colour.The simplicity of the working hypothesis and the unusual structure make thus ellenbergerite an interesting candidate for an optical absorption spectroscopic study. The results will have to be compared with those on corundum in which Ti^{4+}-Fe^{2+} charge transfer occurs (Smith and Strens, 1976), also between face-sharing octahedra.

CONCLUSION

Were it for its structure based on face-sharing polyhedra, for its crystal chemistry with P incorporation and the possibility of octahedrally coordinated Si, or for its optical absorption properties, ellenbergerite is obviously a fascinating material to study at the atomic scale. Nevertheless it must be kept in mind that its very existence carries far-reaching consequences near the other end of the scale spectrum, concerning the role of continental crust in earth tectonics. Indeed the chemical components necessary to form ellenbergerite are utterly common and available in any magnesian pelitic rock. The very restricted occurrence and the dense structure of ellenbergerite necessarily testify for unusual formation conditions. They lend considerable support to the conclusion drawn from the occurrence of coesite and pure pyrope in the enclosing continental unit, namely that continental crust as well can be buried to depths approaching 100 km.

REFERENCES

Abu-Eid RM, Langer K, Seifert F (1978) Optical absorption and Mössbauer spectra of purple and green yoderite, a kyanite-related mineral. Phys Chem Minerals 3 : 271-289

Agrell SO, Brown MG, McKie D (1965) Deerite, howieite and zussmanite, three new minerals from the Franciscan of the Laytonville district, Mendocino Co., California. Am Mineral 50 : 278

Bishop FC, Smith JV, Dawson JB (1978) Na, K, P and Ti in garnet, pyroxene and olivine from peridotite and eclogite xenoliths from African kimberlites. Lithos 11 : 155-173

Buseck PR (1977) Pallasite meteorites - mineralogy, petrology, and geochemistry. Geochim Cosmochim Acta 41 : 711-740

Chopin C (1984) Coesite and pure pyrope in high-grade blueschists of the Western Alps : a first record and some consequences. Contrib Mineral Petrol 86 : 107-118

Chopin C (1985) Phase relationships of ellenbergerite, a new high-pressure Mg-Al-Ti-silicate in coesite-pyrope quartzite from the Western Alps. Geol Soc America Special Papers, Blueschist Volume, in press

Ellenberger F (1958) Etude géologique du pays de Vanoise. Mém exp Serv carte géol France, 561 p.

Goffé B, Goffé-Urbano G, Saliot P (1973) Sur la présence d'une variété magnésienne de ferrocarpholite en Vanoise (Alpes françaises). Sa signification probable dans le métamorphisme alpin. C R Acad Sci Paris D 277 : 1965-1968

Goodrich CA (1984) Phosphoran pyroxene and olivine in silicate inclusions in natural iron-carbon alloy, Disko Island, Greenland. Geochim Cosmochim Acta 48 : 1115-1126

Iimori T, Yoshimara J, Hata S (1931) A new radioactive mineral found in Japan. Sci Papers Inst Phys Chem Research Tokyo 15 : 83 (quoted in Deer WA, Howie RA Zussman J (1962) Rock-forming minerals vol 1, Longmans, London)

Johannes W, Schreyer W (1981) Experimental introduction of CO_2 and H_2O into Mg-cordierite. Am J Science 281 : 299-317

Koritnig S (1965) Geochemistry of Phosphorus. I. The replacement of Si^{4+} by P^{5+} in rock-forming silicate minerals. Geochim Cosmochim Acta 29 : 361-371

Langer K, Hålenius E, Fransolet AM (1984) Blue andalusite form Ottré, Venn-Stavelot Massif, Belgium : a new example of intervalence charge-transfer in the aluminium silicate polymorphs. Bull Minéral 107 : 587-596

Mason B, Berggren T (1941) A phosphate-bearing spessartite garnet from Wodgina, Western Australia. Geol Fören Förh Stockholm 63 : 413-418

Medenbach O (1985) A new refractometer spindel-stage and its application. Fortschr Miner 63 : in press

Smith G, Strens RGJ (1976) Intervalence transfer absorption in some silicate, oxide and phosphate minerals. In : The Physics of Minerals and Rocks, Strens RGJ ed, Wiley, New York, pp 584-612

Springer G (1976) Correction procedures in electron-probe analysis. In : Mineral Assoc Canada Short Course in microbeam techniques, Smith DGW ed, pp 45-62

Sweatman TR, Long JVP (1969) Quantitative electron-probe micro-analysis of rock-forming minerals. J Petrol 10 : 332-379

Theisen R, Vollath D (1967) Tables of X-ray mass attenuation coefficients. Verlag Stahleisen, Düsseldorf

Thompson RN (1975) Is upper-mantle phosphorus contained in sodic garnet ? Earth Planet Sci Lett 26 : 417-424

Vialon P (1966) Etude géologique du massif cristallin Dora Maira, Alpes cottiennes internes, Italie. Thèse d'Etat, Univ Grenoble

FIGURE CAPTIONS

Figure 1 : Microphotographs

Figure 2 : Compositional variations related to phosphorus incorporation in ellenbergerite. The molecular contents of Si, Al, Ti + Zr, Mg + Fe are plotted against P molecular contents. On the diagram Ti and Mg stand for Ti + Zr and Mg + Fe, respectively. Note that the ordinate scale is doubled for Ti. The lines drawn were obtained by least square regression ; int , r and sl represent intercept on the ordinate axis, correlation coefficient and slope, respectively. Source of data is Table 1.

Figure 3 : Ti vs. Zr molecular contents in ellenbergerite. The line drawn represent ideal Ti = Zr substitution with Ti + Zr = 0.60. The filled circles represent low-P analyses from sample 4-18/19 and show nearly complete Ti/Zr substitution. The few P-rich analyses represented (open circles) may suggest that Ti/Zr replacement proceeds independently of P incorporation, although Zr-free, very P-rich crystals have not been found so far.

Figure 4 : The coordination polyhedra in the ellenbergerite structure as seen along c . Tetrahedra located on the three-fold axes are referred to as Si(1) sites in the text, the six others as Si(2). The octahedra situated on the six-fold screw axes are referred to as Mg(2). In the pairs of face-sharing octahedra forming the beams around and parallel to the three-fold axes, the smaller octahedron is referred to as Al site, the larger more distorted one as Mg(1) site. The figure was drawn using the ORTEP programme written by C.K. Johnson.

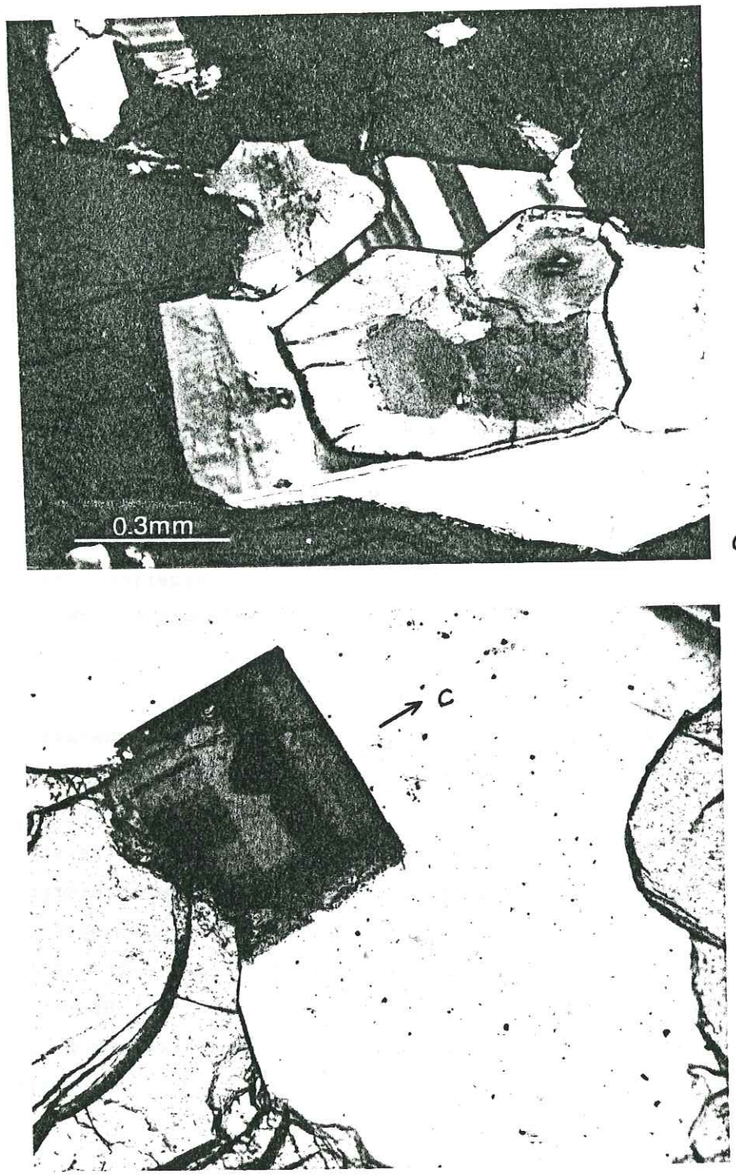

Figure 1

a - Zoned ellenbergerite crystal ($\sim\perp$c) with talc and chlorite as composite inclusion in pyrope. Crossed nicols.

b - Termination of a zoned ellenbergerite prism ($\parallel$c) grown on pyrope and surrounded by chlorite.

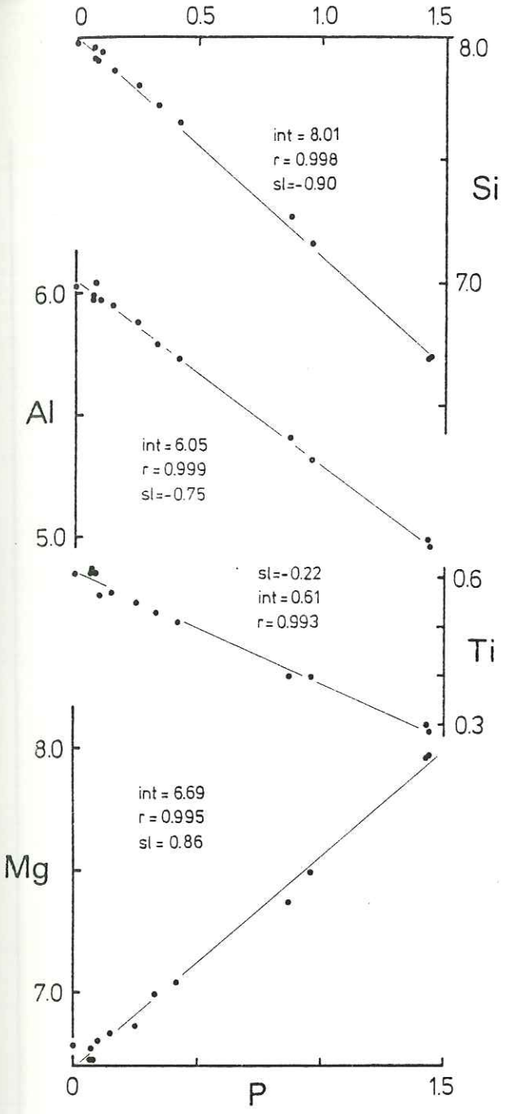

Fig. 2

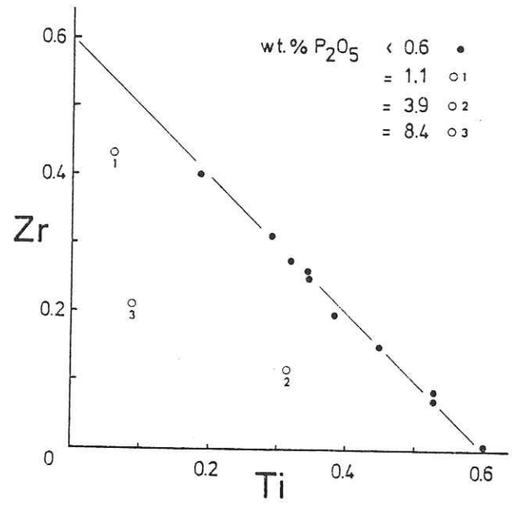

Fig. 3

Fig. 4

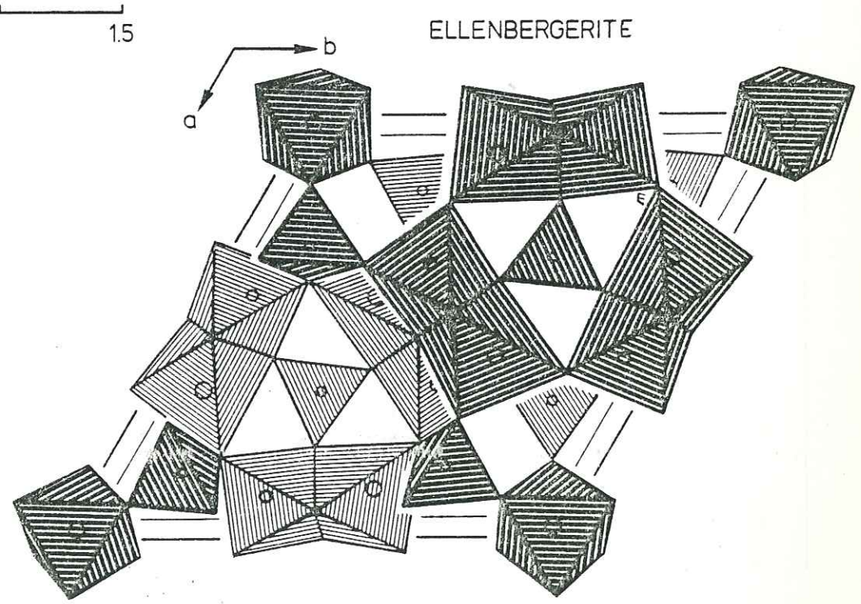

	4-18/19	V			I		II	III		IVb		IVa	
ω		1.6789(5)			1.6687(5)		1.6719(5)	1.6671(5)		1.6553(5)			
ε		1.6697(10)			1.6645(10)		1.6666(10)	1.6617(10)		1.6538(10)			
SiO_2	38.61	39.13	39.30	38.83	38.77	38.56	38.53	37.30	37.08	35.53	35.07	32.61	32.51
P_2O_5	0.00	0.42	0.44	0.48	0.55	0.89	1.46	1.90	2.39	4.99	5.55	8.26	8.27
Al_2O_3	24.79	24.91	25.24	25.21	24.71	24.79	24.62	23.74	23.56	22.42	22.09	20.64	20.41
TiO_2	2.67	3.96	4.10	3.96	2.39	1.73	2.52	2.06	1.48	1.04	1.03	0.58	0.52
ZrO_2	1.92	0.00	0.00	0.00	1.95	3.10	1.65	2.11	2.82	2.43	2.42	2.13	2.10
MgO	21.80	22.05	22.48	22.04	22.09	22.33	22.58	22.57	22.76	23.94	24.38	25.80	25.72
FeO	0.40	0.19	0.20	0.20	0.30	0.25	0.24	0.15	0.23	0.39	0.41	0.41	0.43
	90.19	90.66	91.76	90.72	90.76	91.65	91.60	89.83	90.32	90.74	90.95	90.43	89.96
Si	7.98	7.96	7.91	7.90	7.94	7.86	7.80	7.72	7.65	7.27	7.16	6.69	6.70
P	–	0.07	0.07	0.08	0.10	0.15	0.25	0.33	0.42	0.87	0.96	1.43	1.44
Si + P	*7.98*	*8.03*	*7.98*	*7.98*	*8.04*	*8.01*	*8.05*	*8.05*	*8.07*	*8.14*	*8.12*	*8.12*	*8.14*
Al	6.03	5.97	5.99	6.04	5.97	5.95	5.88	5.79	5.73	5.41	5.32	4.99	4.96
Ti	0.42	0.61	0.62	0.61	0.37	0.26	0.39	0.32	0.23	0.16	0.16	0.09	0.08
Zr	0.19	–	–	–	0.19	0.31	0.16	0.21	0.28	0.24	0.24	0.21	0.21
Ti + Zr	*0.61*	*0.61*	*0.62*	*0.61*	*0.56*	*0.57*	*0.55*	*0.53*	*0.51*	*0.40*	*0.40*	*0.30*	*0.29*
Mg	6.71	6.69	6.74	6.69	6.75	6.79	6.82	6.96	7.00	7.30	7.43	7.89	7.90
Fe	0.07	0.03	0.03	0.03	0.05	0.04	0.04	0.03	0.04	0.07	0.07	0.07	0.08
Mg + Fe	*6.78*	*6.72*	*6.77*	*6.72*	*6.80*	*6.83*	*6.86*	*6.99*	*7.04*	*7.37*	*7.50*	*7.96*	*7.98*
Σ cat.	21.40	21.33	21.36	21.35	21.37	21.36	21.34	21.36	21.35	21.32	21.34	21.37	21.37

PHASE RELATIONSHIPS OF ELLENBERGERITE, A NEW HIGH-PRESSURE Mg-Al-Ti-SILICATE IN PYROPE-COESITE-QUARTZITE FROM THE WESTERN ALPS

Christian CHOPIN
ER 224, Laboratoire de Géologie, Ecole Normale Supérieure,
46 rue d'Ulm, 75005 Paris, France

ABSTRACT

The new Mg-Al-Ti-silicate ellenbergerite occurs among abundant inclusions within decimetre-size garnets in the pyrope-quartzite layer of the Dora Maira massif, Western Alps, from which coesite relics have been reported. It is associated with pyrope (95 to 98 mol. percent end-member), kyanite, talc, chlorite, rutile, zircon, and minor sodic amphibole, which all formed an apparently stable assemblage now exclusively preserved within large garnets.

A petrologic analysis shows that the new mineral, which has the formula

$(Mg_{2/3},Ti_{2/3},\square)_2Mg_6Al_6Si_8O_{28}(OH)_{10}$

with extensive Ti ⇌ Zr substitution, is a high-pressure phase with a lower pressure stability limit above 20 kbar and an upper temperature limit near 800°C or less. Its stability field extends from the Mg-carpholite field to the pyrope field and broadly overlaps that of Mg-chloritoid. The high-pressure phase relationships in the magnesian pelitic system are thus considerably modified, in particular through the reactions

chlorite + talc + kyanite + rutile + H_2O = ellenbergerite

and

chlorite + kyanite + rutile + H_2O = ellenbergerite + Mg-chloritoid

which provide new upper pressure limits for two important chlorite-bearing assemblages.

The different assemblages preserved within the garnets and in the matrix record variations of pressure, temperature and water activity along a prograde metamorphic path passing near 25 kbar, 700°C, and reaching the coesite field. This finding confirms the unusual depth reached by the enclosing continental unit along a low-temperature metamorphic gradient.

INTRODUCTION

A phengite quartzite layer reported by Vialon (1966) in the crystalline basement of the Dora Maira massif, Western Alps, is remarkable for the composition and size of the garnet crystals it contains. The garnet is indeed nearly pure pyrope (90 to 98 mole % end member) and individual crystals may reach 25 cm in diameter. Recently, the mineral assemblage of the matrix was reinvestigated and the typically centimetre-size garnets of the quartzose matrix were found to preserve coesite relics as inclusions (Chopin, 1984). Considering the far-reaching consequences of this finding, especially in a blueschist and eclogite-bearing crustal terrane, the present study of the larger garnet porphyroblasts and their inclusions has been initiated in order to shed more light on the evolution of these fascinating rocks.

The large garnets are crowded with mineral inclusions. Among them are a conspicuous purple mineral, a sodic amphibole and chlorite that are characteristically absent from the matrix and the smaller matrix garnets. The purple pleochroic mineral proved to be a new hydrated, Ti-bearing Mg-Al silicate with hexagonal symmetry and has been described as **ellenbergerite** (Chopin et al., 1985). The present work is an outline of its phase relationships and relevance to the high-pressure metamorphism of pelitic rocks.

GEOLOGICAL AND PETROLOGICAL SETTING

The reader is referred to Vialon (1966) for a description of the regional geology and to Chopin (1984, Fig. 1) for an outline of it. The quartzite layer is a few metres thick but has been mapped by Vialon (1966) over 15 km within a polymetamorphic, Early (?) Paleozoic series of fine-grained felsic gneisses and of schists with some marble and eclogite lenses (Fig. 1). They were intruded by granite bodies and sills, and later underwent Alpine high-pressure, low-temperature metamorphism. The samples to be discussed here have been collected near Parigi, Martiniana Po, Italy, in the same quartzite outcrop as the coesite-bearing samples described by Chopin (1984) and for which P-T estimates of about 28 kbar and 700°C have been proposed. Recent field work by Chopin and Monié shows that the quartzite layer is closely associated with garnet-kyanite schists, thin marble layers, and amphibolite or eclogite lenses. The whole is a few hundred metres thick and represents, with the metagranites, the only lithologic variations in the monotonous gneiss series. Typical K_D values for Fe-Mg partitioning between garnet and omphacite in eclogites are between 8 and 10. Quartz - kyanite - phengite - eclogite is rather common and a typical pseudomorph of quartz after coesite has been observed in an omphacite grain. Furthermore, centimetre-size garnet porphyroblasts of the garnet-kyanite schists contain in their inner part numerous tiny inclusions of staurolite and magnesian chloritoid and, on their rim, silica inclusions with coesite relics

which also occur in kyanite porphyroblasts (Chopin, unpub. data, see Fig. 1). This provides an important record of the prograde metamorphic evolution and leaves little doubt that the whole series enclosing the quartzite layer also experienced unusually high pressures.

PETROGRAPHY

The quartzite layer is rather homogeneous in appearance, usually with evenly distributed centimetre-size garnets. Locally, however, fist-size garnets or even larger ones, mostly euhedral, are clustered within a more micaceous matrix, these clusters defining a very rough layering concordant with the regional foliation. Their matrix is often devoid of quartz and consists of kyanite and centimetre-large phengite flakes. The kyanite grains and sometimes abundant rutile are often concentrated along the garnet rims, as if they had been pushed aside during garnet growth. Kyanite and rutile are nevertheless by far the most abundant mineral inclusions within the garnets. Among the included species, talc and zircon are also always present while chlorite, ellenbergerite and, to a lesser extent, a sodic amphibole are common (up to a few modal percent) but may be missing in some samples. It is noteworthy that the three latter minerals are absent in the immediately surrounding micaceous matrix, as well as in the quartzose matrix and its smaller garnets. Phengite, which is ubiquitous in the matrix, has not been observed as an inclusion, either in the large garnets or in the smaller ones. The only two other minerals observed in thin section are corroded grains of Cl-rich apatite in the core of two ellenbergerite crystals, and a unique grain of arsenopyrite in the core of the large garnet specimen 4-18/19.

Large, isolated garnets also sporadically occur directly within the quartzose matrix. They often show an outer, 1 to 2 cm thick shell nearly devoid of inclusions, thus sharply contrasting with the inner part of the porphyroblasts, which contains the same included minerals as the other large garnets. The inner part of such a euhedral 22 cm diameter crystal (sample 4-18/19) shows a distinct orientation of inclusions. The lineation is defined by abundant elongated prisms of ellenbergerite which have a constant orientation throughout the inner part of the crystal. The outer shell contains only a few oriented kyanite inclusions which tend to parallel the garnet rim during the very last stages of garnet growth. Thus it seems, as will also be shown by the chemical study, that such garnet porphyroblasts have grown first very quickly, without rotation and including numerous minerals, then more slowly under somewhat changing physical conditions. However, it has proved impossible so far to establish a correlation between the nature of the matrix, the existence or lack of an outer shell or an oriented texture, and the presence or absence of ellenbergerite. For instance, a fist-size garnet found in a quartz-bearing

matrix is devoid of outer shell and of ellenbergerite inclusions but contains centimetre-size kyanite blades without any preferred orientation. Conversely, large ellenbergerite-rich garnet crystals in a quartz-free matrix may also lack any oriented texture. A further confusing point presently investigated is that, within a cluster of large garnets, some of the porphyroblasts are obviously zoned in their colour and inclusion repartition, while others are apparently not.

Apart from orientation, the textural relationships among the different minerals within the garnets show little variation from one sample to the other. Monomineralic inclusions consist nearly exclusively of kyanite or rutile. Ellenbergerite, chlorite and amphibole occur consistently within polymineralic inclusions containing any combination of these minerals with talc, kyanite, rutile and zircon. The typical included assemblage is kyanite - talc - chlorite $\pm$ ellenbergerite $\pm$ rutile $\pm$ zircon (Figs. 2-5). With perhaps some restriction for zircon, the minerals mentioned may be found in contact with each other and the textural evidence suggests equilibrium among these phases. Ellenbergerite may show euhedral faces, particularly toward the phyllosilicates (Fig. 2), and might have some crystallographic relationship to garnet (Fig. 2). It may also be completely anhedral (Fig. 4). Thus, petrographic evidence suggests that most ellenbergerite is coeval with, or predates garnet growth. However, in the smallest (2 cm) garnet found to contain it, ellenbergerite is interstitial to pyrope and seems to postdate garnet growth.

The main retrogressive textures observed within garnet are the replacement of ellenbergerite either by a sericitic aggregate or, along rims and cracks, by a nearly opaque aggregate (Fig. 2 and 3). In addition, of the often abundant cracks existing in the garnet, a few broader ones have acted as channelways for the penetration of external fluids during retrogression and are now filled by secondary chlorite. Where such fractures reach a polymineralic inclusion containing talc and kyanite, the local breakdown of talc + kyanite to form secondary chlorite and minute (up to 20 μm) quartz grains was, in a few instances, observed.

The possible presence of silica inclusions and of coesite relics in the large garnets was of course of particular interest to this study, and attention was paid to every silica grain. In fact, individual silica inclusions such as those occurring in the smaller matrix garnets (see Chopin, 1984) are completely absent in the larger ones, even in those residing in a quartz-bearing matrix. The few tiny quartz grains mentioned above are obviously secondary and, in fact, were never seen in contact with pyrope or ellenbergerite. A unique quartz grain, 400-100 μm in size, was found in a talc - kyanite - chlorite inclusion in the core of the large garnet 4-18/19. Although some secondary chlorite is also present, the amount of quartz compared to chlorite seems too large to be a

breakdown product of talc + kyanite, so that this grain might be primary. If this holds true, it may have been trapped as quartz or as coesite. In the former case, it should have remained quartz throughout the whole metamorphic evolution ; in the latter, coesite would have been completely converted to quartz. Both behaviours are easily explained by considering that the silica grain is isolated from the host garnet by much more compressible talc and chlorite (compare Gillet et al., 1984), but the textural evidence does not favour either possibility.

MINERAL CHEMISTRY

From 12 thin sections cut through large garnets, six, representing four garnet crystals (3-64, 3-65, 4-18/19, 4-55), have been selected for microprobe work.

Analytical technique : The analyses were obtained with a Cameca Microbeam electron probe (40° take-off angle) using wavelength dispersive techniques and ZAF correction with the X-ray absorption coefficients of Theisen and Vollath (1967) instead of Heinrich's (1966) coefficients used in the normal Cameca programme (see Chopin et al., 1985). Typical operating conditions were 15 kV and 15 nA beam current. Standards used were forsterite (Mg,Si), anorthite (Ca,Al), K-feldspar and albite (K,Na), Fe_2O_3, $MnTiO_3$ (Mn,Ti), apatite (P) and zircon (Zr). With this combination of standards the Al/Si ratio tends to be overestimated in garnet, which is particularly obvious for one batch of analyses (Table 1, analyses 8 and 9 for garnet, 4 and 5 for ellenbergerite). Since no particular care was taken for the analysis of trace elements, the routinely obtained values of less than 0.04 wt. percent reported in Table 1 must be regarded with caution. In the absence of any mineralogic evidence for trivalent iron, total iron is reported as FeO. This view is supported by the near-absence of iron in kyanite and by the colour of ellenbergerite which is much probably due to Fe^{2+}-Ti^{4+} charge transfer (Chopin et al., 1985).

Ellenbergerite : The crystal chemistry of ellenbergerite has been discussed by Chopin et al. (1985) and only a few points essential to the petrologic discussion are addressed here. Ellenbergerite has the general structural formula

$$(Mg,Ti,Zr,\square)_2Mg_6(Al,Mg)_6(Si,P)_2Si_6O_{28}(OH)_{10}$$

in which about one percent of the Mg atoms may be replaced by Fe. Accordingly, the formulae given in Table 1 have been calculated on a 33 oxygens anhydrous basis. Of importance is the high water content of about 7.5 wt. percent, whereas fluor has not been detected. Ellenbergerite composition is entirely defined by three independent parameters, namely Ti/Zr ratio, P content and, accessorily, Mg/Fe ratio. The Ti = Zr substitution may be nearly complete and is responsible for the colour zoning. The most intensely coloured ellenbergerite contains about

4 wt. percent TiO_2, no zirconium and little or no phosphorus. It forms the outer part of zoned grains and also a few homogeneous, smaller grains (Analysis 1). The less coloured, most often core zones are Ti-poor and correlatively Zr-rich. They are usually P-poor, rarely P-free, but may contain up to 1.4 P atom p.f.u. as observed in a strongly zoned crystal containing an apatite inclusion.

Compositional variations, mainly of the Ti/Zr ratio, are more important within a single crystal than between crystals from different parts of a large garnet. This fact is documented in Table 1, in which analyses 2 and 3 are from a single grain in the outer part of the inclusion-rich zone of the garnet crystal 4-18/19, and analyses 4 and 5 from a single grain in the core of this zone. The same holds true for crystals from different garnets, although some garnets (3-64, 3-65) seem to have on the whole more Ti-rich ellenbergerite than others. Also, the P content of ellenbergerite, which is in general rather uniform within a single garnet, may show some variation from garnet to garnet (P_2O_5 between 0 and 0.6 wt. percent in 4-18/19, between 0.4 and 2.9 wt. percent in 4-55).

Garnet : The analyses of the large garnets confirm their extreme pyrope contents (Vialon, 1966) and show a very limited compositional range within and between crystals. The pyrope content varies only between 95 and 98 mol. percent in 3-64, 3-65 and 4-18/19. These garnets are free of Cr and Zr ; Mn, Ti and Na remain close to the detection limit and the P_2O_5 content never exceeds 0.16 wt. percent (Table 1). Their FeO and CaO contents range between 0.5 and 2.5, and 0 and 0.8 wt. percent, respectively. In a given garnet, the range of CaO variations is in fact much smaller, about 0.2 wt. percent. The same holds true for FeO which varies somewhat erratically throughout the whole garnet, local variations often exceeding those from core to rim, if any. This is in particular the case throughout the inclusion-rich part of garnet 4-18/19 (analyses 8 and 9) whereas FeO decreases and CaO increases towards the rim in the inclusion-poor and ellenbergerite-free outer zone (analyses 6 and 7). This pattern and this compositional range compare well with those of the smaller, millimetre- to centimetre-size matrix garnets, which have pyrope contents from 91 to 97 mol. percent (Chopin, 1984).

Talc is close to the ideal end-member composition, with small amounts of Al, which seems to be partitioned between octahedral and tetrahedral sites (Table 1).

Chlorite shows little compositional variations and is close to ideal clinochlore, with typical Si contents of 2.85 to 2.90 p.f.u. (Table 1). No

systematic variation was observed with the mineral in contact with chlorite nor with its location in the garnet.

Amphibole : analyses 14 and 16 in Table 1 represent extreme compositions among the six inclusions analysed in three different garnets. These amphiboles referred to as glaucophane by Chopin (1984) on the basis of optics are definitely sodic, but actually deviate from ideal glaucophane by a Na-deficiency and the presence of tetrahedral Al, which are compensated by an excess of Mg over the ideal value of 3 and by the presence of some Ca. In addition, the number of cations may show a small deficiency (analysis 15) and indirect evidence suggests that this might be due to Li incorporation. Indeed, the rare jadeite-rich pyroxene of the quartzose matrix and that of a jadeite - kyanite - almandine quartzite from the same locality both show a slight but consistent excess of Al over Na (Chopin, 1984) relative to a jadeite standard. One of the possibe explanations for this is the presence of a few percent of spodumene component in solid solution. The definite identification of ephesite, $NaLiAl_4Si_2O_{10}(OH)_2$, among the breakdown products of jadeite + kyanite in the almandine quartzite substantiates the latter hypothesis and, consequently, the presence of Li at least in the matrix of the pyrope quartzite.

Rutile : small amounts of Nb have been detected in rutile grains which, in a few instances, show clearer, Nb-free rims.

Kyanite is pure $SiAl_2O_5$, with iron near the detection limit (0 to 0.05 wt. percent Fe_2O_3).

Fe-Mg partitioning : in spite of the extreme Mg-richness of the studied rocks and the very tight clustering of Fe/Mg ratios, a quite consistent picture arises from the iron partitioning among coexisting phases, with iron preference decreasing in the order garnet > amphibole > chlorite > ellenbergerite > talc (Fig. 6). The least Mg-rich and most Mg-rich mineral assemblages in garnet 4-18/19 (Fig. 6) were analysed a few millimetres apart in the outermost part of the inclusion-rich zone. All the assemblages analysed in the core of this garnet fall between these two, showing that a systematic variation of Fe/Mg ratio throughout the garnet, if any, is of lesser extent than very local variations. This suggests that the growth of the inclusion-rich part of the garnet has proceeded under rather constant physical conditions, or rapidly, possibly after a large overstepping of the equilibrium reaction.

ANALYSIS OF THE PHASE RELATIONSHIPS :

The preceding section has shown that P-poor to P-free ellenbergite compositions are the most common. Thus the role of phosphorus will not be further considered and the discussion will first focuse on the P-, Fe- and Zr-free ellenbergerite, i.e. on the TiO_2-MgO-Al_2O_3-SiO_2-H_2O (Ti-MASH) system.

1) The TiO_2-MgO-Al_2O_3-SiO_2-H_2O system

The ellenbergerite formula may then be simplified to

$(Mg_{2/3},Ti_{2/3},\square)_2\ Mg_6Al_6Si_8O_{28}(OH)_{10}$

This corresponds to the proportions 2:20:9:24:15 in the Ti-MASH system, which are used throughout the following discussion. A projection of the system through H_2O and TiO_2 (Fig. 7) reveals the most important phase relationships of ellenbergerite which, lyke pyrope and yoderite, projects within the talc-kyanite-chlorite triangle. The most simple ellenbergerite forming reaction is thus

chlorite + talc + kyanite + rutile + H_2O = ellenbergerite (1)

A Schreinemakers analysis of the system has been performed considering the solid phases ellenbergerite (Eb), pyrope (Py), chlorite (Chl), talc (Tc), kyanite (Ky), rutile (Ru) and either quartz or coesite (Q), and taking into account three experimentally determined curves, namely

chlorite + quartz = talc + kyanite + H_2O (2)

chlorite + talc + kyanite = pyrope + H_2O (3)

talc + kyanite = pyrope + SiO_2 + H_2O (4)

(Massonne et al., 1981, for reaction 2 ; unpublished data of the author for reactions 3 and 4). The analysis leads to two alternative chemographies which both satisfy the criterion that less hydrated products are on the high-temperature side. In one case, ellenbergerite displays an upper pressure stability limit, in the other a lower pressure stability limit. Additional consideration of the volume criterion (Table 2) unequivocally defines the latter case as the unique solution, which is represented in Fig. 8. The 386 cm^3 molar volume of ellenbergerite used in the calculations is the average of several cell parameters determinations. The volume changes calculated for the reactions (Table 2) must be regarded as only indicative since a constant value is given to the molar volume of H_2O (corresponding to 25 kbar, 580°C or 30 kbar, 800°C), and the compressibility and thermal expansion of the solids is ignored. However the resulting picture remains unchanged for a larger molar volume of H_2O, or by considering coesite instead of quartz. Thus it may be confidently deduced from Fig. 8 that ellenbergerite is a high-pressure phase.

Interestingly, the ellenbergerite-forming reaction (1) closes the talc - chlorite - kyanite - rutile stability field on the high-pressure side ; it

proceeds with a significant volume change of about 6 percent (Table 2) and should thus be quite pressure-dependent. Likewise the curve for the reaction

ellenbergerite + SiO_2 = talc + kyanite + rutile + H_2O (5)

yields an upper pressure limit for the talc - kyanite - rutile stability field.

Among the stable invariant points of Fig. 8, the "quartz"-absent one is of particular relevance to this study since it involves all the phases present in the natural assemblage, and it should actually be stable. It lies on the curve of reaction (3) which has been approximatively located by Schreyer (1968) and is presently being refined by the author. This curve extends stably from near 20 kbar, where Mg-staurolite or yoderite may become stable, to about 30 kbar, where it reaches the upper pressure stability limit of chlorite + kyanite, which react to talc + magnesiochloritoid. This creates an invariant point (Chopin, 1984, Fig. 5), which can now be more precisely located between about 30 and 31 kbar, 700 and 720°C, according to the experimental data given by Chopin and Schreyer (1983) and in Chopin and Monié (1984) for the reaction

chlorite + kyanite = talc + magnesiochloritoid (6).

Since magnesiochloritoid is absent and chlorite + kyanite obviously stable in the natural assemblages studied here, the [Q] invariant point of Fig. 8 must lie at pressures lower than 30 kbar water pressure and be stable.

Moreover, magnesian, talc-kyanite-rutile-bearing rocks metamorphosed at pressures approaching 20 kbar are known from the Eastern Alps (Holland, 1979 ; cf. Miller, 1977) and, for somewhat lower pressures, from the Western Alps (Chopin and Monié, 1984). In neither case has ellenbergerite been observed, in spite of favourable bulk compositions. This suggests that the lower-pressure part of the ellenbergerite field as limited by the invariant points [Q] and [Py] lies at water pressures in excess of 20 kbar. Considering the positive slope of the curve of the quartz- and pyrope-absent reaction (1), these few constraints allow an approximate location of the invariant points in the P_{H_2O}-T plane. The [Py] invariant point would lie between 20 and 25 kbar at temperatures near 500°C, and the [Q] invariant point at about 25 kbar (the maximum possible value being 30 kbar) at temperatures between 700 and 750°C. The reaction connecting the [Q] and [Chl] invariant points, namely

ellenbergerite = pyrope + talc + kyanite + rutile + H_2O (7)

proceeds with a very small volume change (Table 2) and should be nearly pressure-independent. Its curve should therefore intersect the steep curve of reaction (4) at quite high-pressure, creating the [Chl] invariant point well within the coesite field, at temperatures near 800°C or less. Reaction (7) thus represents the upper temperature stability limit of ellenbergerite, making it unlikely that this mineral is involved in melting reactions.

This first attempt at deciphering the phase relations of ellenbergerite concerns the phases present in the natural assemblage. In fact, in the P-T range deduced, other high-pressure phases such as Mg-carpholite, Mg-chloritoid, Mg-staurolite and yoderite have also to be considered. It is assumed in the following that ellenbergerite displays no stable phase relations with yoderite because this phase is stable only at temperatures in excess of 700°C and probably has an upper pressure limit near 25 kbar (Schreyer and Seifert, 1969, p. 423). The same assumption is made with the Al-rich phase Mg-staurolite, although only limited data are available on its lower stability limit (Schreyer and Seifert, 1969). Mg-carpholite and Mg-chloritoid deserve more attention, since the stability field of ellenbergerite as outlined above broadly overlaps that of Mg-chloritoid and, in its lower-temperature part, that of Mg-carpholite.

The curve of reaction (2) extends stably up to 18 kbar, 540°C where it reaches the stability field of Mg-carpholite (Chopin and Schreyer, 1983). If we correctly assume that the [Py] invariant point, which lies on this curve, is in excess of 20 kbar, it must then be metastable. This implies a new set of low-temperature phase relations involving Mg-carpholite, which are shown in a tentative manner in Fig. 9. The [Q] invariant point of Fig. 8 remains unaffected and lies, as deduced in the preceding section, on the curve of reaction (3) at a lower pressure than the invariant point involving the solid phases pyrope, Mg-chloritoid, chlorite, talc and kyanite (Chopin, 1984, Fig. 5). The latter invariant point thus becomes metastable in the presence of excess TiO_2. The resulting phase relations are also depicted in Fig. 9. An interesting feature is that the curve of reaction (6), which is so important for barometry in high-grade pelitic blueschists (Chopin and Schreyer, 1983 ; Chopin and Monié, 1984), becomes in fact entirely metastable in the presence of rutile. Indeed, the upper pressure limit of chlorite + kyanite + rutile is now given by the reaction

chlorite + kyanite + rutile + H_2O = ellenbergerite + Mg-chloritoid (8)

which involves little H_2O but proceeds with a significant volume decrease of about 7 percent. Another important point is that the main ellenbergerite-forming reaction remains unchanged ; it is still reaction (1), the curve of which extends stably from the Mg-carpholite field to the pyrope field, as that of reaction (8) does.

Thus, this chemographic analysis reveals that the high-pressure phase relations in the Ti-MASH system, hitherto essentially the same as in the MASH system, are considerably modified by the existence of ellenbergerite. Reactions (1) and (8) represent new upper pressure stability limits for the assemblages chlorite - talc - kyanite - rutile and chlorite - kyanite - rutile, respectively.

2) Zr-ellenbergerite :

The role of Zr-ellenbergerite is conveniently discussed in the Zr-MASH system. Projected through $ZrSiO_4$ and H_2O, ellenbergerite plots within the talc-kyanite-chlorite triangle, so that a ZrO_2 phase does not need to be considered in the analysis, which is basically the same as in Ti-MASH. The most important ellenbergerite-forming reaction is

chlorite + talc + kyanite + zircon + H_2O = ellenbergerite (9)

which is very similar to reaction (1) and proceeds with a volume decrease of about 6 percent. Again, the existence of ellenbergerite makes reaction (6) metastable in the Zr-bearing system and, for the same reasons as those developed for reaction (1), reaction (9) must take place at pressures higher than 20 kbar (on the low-temperature side) and lower than 30 kbar (on the high-temperature side).

One may speculate on the position of reaction (9) relative to its Ti-counterpart reaction (1), by considering the relative stabilities of end-members in isomorphous series, such as the Mg, Fe and Mn end-members of carpholite, chloritoid, cordierite and garnet, among others. The systematics arising is that the lower pressure stability limit is shifted toward higher pressure as the size of the substituting cation decreases. Therefore, one may tentatively conclude that Zr-ellenbergerite becomes stable at lower pressure than Ti-ellenbergerite, an important point for interpreting the zoning pattern.

3) A new phase of the $MgO-Al_2O_3-SiO_2-H_2O$ system ?

Considering the crystal structure of ellenbergerite (Chopin et al., 1985), it is quite tempting to speculate on a Mg Mg = (Ti, Zr) substitution within the Mg(2) site, which would lead to the hypothetical Mg-Al-silicate $Mg_8Al_6Si_8O_{28}(OH)_{10}$, compositionally close to pyrope + H_2O. A chemographic analysis essentially similar to that developed above shows that this end-member would be a high-pressure phase of the MASH system, in which reaction (6) and the invariant point involving the solid phases pyrope, chloritoid, talc, chlorite and kyanite would become metastable. Again, on the basis of ionic radius alone, one would expect this "Mg-ellenbergerite" to become stable at higher pressure than Ti-ellenbergerite.

However, as long as ellenbergerite has not been found in a TiO_2- and ZrO_2-undersaturated rock, or as a specific experimental study has not been undertaken in the MASH system, this event remains purely conjectural and is thus not further discussed here. It may be merely noticed that the presence of rutile and zircon in the natural assemblages studied here sets the Ti + Zr contents of ellenbergerite at the maximum value.

THE METAMORPHIC EVOLUTION

In the natural assemblages, the phases relevant to the systems discussed in the preceding section are talc, kyanite, chlorite, pyrope, ellenbergerite, rutile and zircon. Obviously, it is hardly possible to find in thin section a small area in which seven minerals show contacts one to each other, so that actual equilibrium among the seven phases is difficult to demonstrate. Whereas garnet inclusions containing all the phases but zircon are rather common, less inclusions contain zircon in addition to the six phases. In such cases, zircon is usually included within ellenbergerite and probably does not participate any more to the equilibrium.

The role of iron must also be considered (see Fig. 6), this component providing one more degree of freedom. An assemblage represented by an invariant point in the pure magnesian system becomes univariant. The locus of its representative points in the P_{H_2O}-T plane is a curve emanating from the invariant point of the magnesian system, in every point of which the mineral compositions are uniquely defined. The orientation of this curve relative to the univariant curves of the magnesian system (Fig. 8, inset) is deduced from the data on Fe-Mg partitioning (Fig. 6), considering the shift of the Mg-curves after iron incorporation. The univariant curves of the Fe-Mg-system converge into an invariant point of higher order which has been qualitatively located on the inset of Fig. 8. Nevertheless, even if the role of iron is important with regard to the phase rule, the actual mineral compositions are so Mg-rich that the iron contents do not materially affect P-T estimates that could be derived from the magnesian system. Indeed, calculations made to approximate the shift of the curve of reaction (3) due to Fe incorporation show it to be negligible as compared to the experimental uncertainty on the location of the curve.

The mineral assemblages preserved in the large garnet porphyroblasts, even in the core zones, do not record a history any earlier than that of the incoming of ellenbergerite. Only the possible presence of relic quartz can be an indication that the chlorite-quartz pair was formerly present in these rocks. Nevertheless the main stages of the mineral evolution which led to the actual state can be reconstructed. With increasing pressure (and temperature), the compositional field of chlorite coexisting with quartz narrows to form either talc + garnet on the Fe-rich side (cf. Chopin, 1981 ; Chopin and Schreyer, 1983), or talc + kyanite on the Mg-rich side, until the univariant reaction

chlorite + quartz = talc + kyanite + garnet + H_2O (10)

is reached. This reaction which is fundamental to the understanding of the few talc - kyanite - garnet assemblages reported so far (Råheim and Green, 1974 ; Udovkina et al., 1978) is actually by-passed here because of the highly magnesian bulk-rock composition. Indeed, talc and kyanite are formed and quartz is exhausted before reaction (10) is reached. The incoming of pyropic garnet

occurs at a higher pressure from the talc - kyanite - chlorite assemblage through reaction (3'), the divariant equivalent of reaction (3). Upon further pressure increase, more pyrope is produced by the divariant breakdown of chlorite + talc + kyanite, all the mafic phases becoming increasingly Mg-rich until the conditions of ellenbergerite formation are reached. If the assumption that Zr-ellenbergerite has the lower stability limit holds true, the zoning pattern observed in ellenbergerite is prograde. The univariant ellenbergerite forming reaction is then

talc + kyanite + chlorite + pyrope + H_2O = Zr-ellenbergerite (11)

As soon as Zr-ellenbergerite is formed, rutile participates to the reaction instead of zircon and ellenbergerite composition continuously evolves toward Ti-ellenbergerite. These large variations of Ti/Zr ratio, as compared to those of Mg/Fe ratio in ellenbergerite and garnet, suggest that the stability limits of Ti- and Zr-ellenbergerite do not significantly differ.

The coexistence in garnet of the six solid phases talc, kyanite, chlorite, pyrope, rutile and, as discrete grains and rims, Ti-ellenbergerite apparently implies that the conditions of ellenbergerite formation have not been overstepped, i.e. that this relic paragenesis records exactly the univariant formation of ellenbergerite, according to the reaction

talc + kyanite + chlorite + pyrope + rutile + H_2O = Ti-ellenbergerite (12)

This may not be as unlikely as it seems. First, the curve of reaction (12), which emanates from the [Q] invariant point of Fig. 8 (inset), has a gentle positive slope, forming a small angle with metamorphic gradients, thus making the preservation of nearly univariant conditions by a metamorphic rock more likely. Second, the development of the hydration reaction (12) may result in a lowering of the water activity, which would allow the coexistence of the six solid phases over a divariant field. The Mg end-member of the water-conserving reaction

talc + kyanite + chlorite + rutile = ellenbergerite + pyrope (13)

is shown in Fig. 8 as reaction (V). Very importantly, this reaction is the only one which produces pyrope together with ellenbergerite, and, as suggested by textural evidence, the considerable growth of pyrope must be accounted for along with the appearance and growth of ellenbergerite. Thus, this may be evidence for a decrease of water activity after the incoming of ellenbergerite.

The absence of ellenbergerite in the outer zone of the large garnets, and of ellenbergerite and chlorite in the surrounding matrix shows that these more hydrated phases have disappeared during the later metamorphic evolution, while garnet has grown further. This should mainly reflect a temperature increase, since the divariant ellenbergerite- and chlorite-consuming reactions

ellenbergerite + chlorite + talc = garnet + H_2O (14')

ellenbergerite + chlorite = garnet + kyanite + H_2O (15')

and especially reaction (7'), which leads to the matrix assemblage talc - kyanite - pyrope, have a rather steep slope (Fig. 8). These reactions, too, conveniently account for the Mg enrichment in the outer zone of large garnets (Table 1, 4-18/19). As shown by the assemblage found in the quartzose matrix, the conditions of the equilibrium

talc + kyanite = garnet + SiO_2 + H_2O (4')

are finally reached within the coesite field (Chopin, 1984). As compared to the conditions of equilibrium (3') preserved within the large garnets, equilibrium (4') implies higher temperatures and/or pressures, even for very different water activities. Calculations made using unpublished experimental data of the author on reactions (3) and (4) (see Fig. 9) and the water data of Halbach and Chatterjee (1982) show that, if a water activity of 1.0 prevails for reaction (3) and of 0.2 for reaction (4), the two curves still differ in temperature by about 50°C at pressures near the quartz-coesite transition. This result leads to a reevaluation of the temperature estimate made for the matrix assemblage, which, unless water activity was extremely low, is probably closer to 750°C than to 700°C as originally proposed in Chopin (1984), for the same minimum pressure of 28 kbar.

An estimate of the conditions recorded by the assemblage preserved in garnet can only be tentative, yet is constrained to be close to the conditions of equilibrium (3), for an initially high water activity. The latter point is suggested by the presence of the hydrated phases ellenbergerite, chlorite and sodic amphibole among the inclusions, whereas talc - kyanite - pyrope and sodic pyroxene occur instead in the matrix. In addition to the occurrence of ellenbergerite, the composition of chlorite and amphibole suggests unusually high pressures of formation. Inasmuch as the decrease of tetrahedral Al through the AlAl = SiMg substitution is likely to be favoured by a pressure increase, the unusual Si content of chlorite (2.9 p.f.u.) in this kyanite-bearing assemblage suggests higher pressures than the 2.7 to 2.8 values known in talc - chloritoid - quartz $\pm$ kyanite, high-pressure assemblages from the Gran Paradiso (Chopin, 1981) and Monte Rosa massif (Chopin and Monié, 1984). Likewise, the departure of amphibole composition from ideal glaucophane suggests that the upper stability limit of glaucophane was approached as the large garnets crystallised (compare Carman and Gilbert, 1983 ; Koons, 1982), bearing in mind that the highest-pressure talc - kyanite-bearing assemblages known until recently contain pure glaucophane (Holland, 1979). These are reasons why pressures near 25 kbar or more, and thus temperatures near 700°C, seem likely for the formation of the ellenbergerite-bearing assemblage.

These conditions are rather close to those of the supposed metamorphic maximum recorded in the matrix and, therefore, much of the prograde history of

these rocks still remains conjectural. Nevertheless, this study strengthens the results obtained during the study of the matrix and further enhances the importance of these rocks, which indicate that continental material may be subducted to depths of about 100 km along very low temperature gradients.

CONCLUSION

Titanium and zirconium being present in every pelitic rock, the present analysis applies to one of the most common rock types. It provides at least a general framework for interpreting the petrographic observations and for a forthcoming experimental study, even if a few puzzling points remain, such as the absence of phengite inclusions in garnet, or the juxtaposition of silica-saturated and undersaturated systems.

More generally speaking, it is noteworhty that the pelitic system which has been so extensively studied in nature and in experiment may still yield new rock-forming silicates. This reflects of course very unusual metamorphic conditions but is in keeping with the trend of metamorphic petrology during the last decade(s). Indeed, the wealth of new minerals or mineral assemblages recently reported from common, pelite-like compositions - ferro- and magnesiocarpholite (De Roever, 1951 and Goffé et al., 1973, respectively), yoderite and talc-kyanite (McKie, 1959), magnesiochloritoid and talc-chloritoid (Bearth, 1963 ; Miller, 1977), talc-phengite (Abraham and Schreyer, 1976 ; Chopin, 1981), sudoite (Fransolet and Bourguignon, 1978), pure pyrope and coesite (Chopin, 1984), very Mg-rich staurolite (Schreyer et al., 1984 ; Ward, 1984), and finally ellenbergerite - shows that progress is being made primarily in the area of high-pressure assemblages. Interestingly, several of these discoveries were anticipated by the experimental reconnaissance work of Schreyer (1968), covering P-T conditions which, at that time, were not clearly known to have existed in nature.

ACKNOWLEDGEMENTS

Helpful reviews and comments by B.W. Evans, W. Maresch, R.C. Newton and W. Schreyer on an earlier version of the manuscript are gratefully acknowledged. O. Medenbach, Bochum, contributed the photomicrographs.

REFERENCES

Abraham, K., and Schreyer, W., 1976, A talc-phengite assemblage in piemontite schist from Brezovica, Serbia, Yugoslavia: Journal of Petrology, v. 17, p. 421-439.

Bearth, P., 1963, Chloritoid und Paragonit aus der Ophiolith-Zone von Zermatt-Saas Fee: Schweizerische mineralogische und petrographische Mitteilungen, v. 43, p. 269-286.

Carman,J.H., and Gilbert, M.C., 1983, Experimental studies on glaucophane stability: American Journal of Science, v. 283-A, p. 414-437.

Chernosky, J.V., 1974, The upper stability of clinochlore at low pressure and the free energy of formation of Mg-cordierite: American Mineralogist, v. 59, p.496-507.

Chopin, C., 1981, Talc-phengite: a widespread assemblage in high-grade pelitic blueschists of the Western Alps: Journal of Petrology, v. 22, p. 628-650.

Chopin, C., 1984, Coesite and pure pyrope in high-grade blueschists of the Western Alps: a first record and some consequences: Contributions to Mineralogy and Petrology, v. 86, p. 107-118.

Chopin, C., and Monié, P., 1984, A unique magnesiochloritoid-bearing high-pressure assemblage from the Monte Rosa, Western Alps: petrologic and ^{40}Ar-^{39}Ar radiometric study: Contributions to Mineralogy and Petrology, v. 87, p. 388-398.

Chopin, C., and Schreyer, W., 1983, Magnesiocarpholite and magnesiochloritoid: two index minerals of pelitic blueschists and their preliminary phase relations in the model system MgO-Al_2O_3-SiO_2-H_2O: American Journal of Science, v. 283-A, p. 72-96.

Chopin, C., Klaska, R., Medenbach, O., and Dron, D., 1985, Ellenbergerite, a new high-pressure Mg-Al-(Ti,Zr)-silicate with phosphatian varieties and with a novel structure based on face-sharing octahedra. Submitted to Contibutions to Mineralogy and Petrology.

Fransolet, A.-M., and Bourguignon, P., 1978, Di/trioctahedral chlorite in quartz veins from the Ardenne, Belgium: Canadian Mineralogist, v. 16, p. 365-373.

Gillet, Ph., Ingrin, J., and Chopin, C., 1984, Coesite in subducted continental crust: P-T path deduced from an elastic model: Earth and Planetary Science Letters, v. 70, p. 426-436.

Goffé, B., Goffé-Urbano, G., and Saliot, P., 1973, Sur la présence d'une variété magnésienne de la ferrocarpholite en Vanoise (Alpes francaises)-Sa signification probable dans le métamorphisme alpin. Académie des Sciences Paris, Comptes rendus, v. 277, serie D, p. 1965-1968.

Halbach, H., and Chatterjee, N.D., 1982, An empirical Redlich-Kwong type equation of state for water to 1000°C and 200 kbar: Contributions to Mineralogy and Petrology, v. 79, p. 337-345.

Heinrich, K.F.J., 1966, X-ray absorption uncertainty. In The electron microprobe. New-York, John Wiley and sons, p. 296-377.

Holland, T.J.B., 1979, High water activities in the generation of high-pressure kyanite eclogites of the Tauern Window, Austria: Journal of Geology, v. 87, p. 1-27.

Koons, P.O.,1982,An experimental investigation of the behavior of amphibole in the system Na_2O-MgO-Al_2O_3-SiO_2-H_2O at high pressure: Contributions to Mineralogy and Petrology, v. 79, p. 258-267.

Massonne, H.-J., Mirwald, P.W., and Schreyer, W., 1981, Experimentelle überprüfung der Reaktionskurve Chlorit+Quarz=Talk+Disthen im System MgO-Al_2O_3-MgO-SiO_2-H_2O: Fortschritte der Mineralogie, v. 59, p. 122-123.

McKie, D., 1959, A new hydrous magnesium iron aluminosilicate from Mautia Hill, Tanganyika: Mineralogical Magazine, v. 32, p. 282-307.

Miller, C., 1977, Chemismus und phasenpetrologische Untersuchungen der Gesteine aus der Eklogitzone des Tauernfensterns, Österreich: Tschermaks mineralogische und petrographische Mitteilungen, v. 24, p. 221-277.

Råheim, A., and Green, D.H., 1974, Talc-garnet-kyanite-quartz schist from an eclogite-bearing terrane, Western Tasmania. Contributions to Mineralogy and Petrology, v. 43, p. 223-231.

Robie, R.A., Hemingway, B.S., and Fisher, J.R., 1978, Thermodynamic properties of minerals and related substances at 298.15 K and 1 bar pressure and at higher temperature: Geological Survey Bulletin 1452.

Roever, W.P. de, 1951, Ferrocarpholite, the hitherto unknown ferrous iron analogue of carpholite proper: American Mineralogist, v. 36, p. 736-745.

Schreyer, W., 1968, A reconnaissance study of the system MgO-Al_2O_3-SiO_2-H_2O at pressures between 10 and 25 kbar: Carnegie Institution of Washington, Yearbook, v. 66, p. 380-392.

Schreyer, W., and Seifert, F., 1969, High-pressure phases in the system MgO-Al_2O_3-SiO_2-H_2O: American Journal of Science, v. 267-A, p. 407-443.

Schreyer, W., Horrocks, P.C., and Abraham, K., 1984, High-magnesium staurolite in a sapphirine-garnet rock from the Limpopo Belt, Southern Africa: Contributions to Mineralogy and Petrology, v. 86, p. 200-207.

Theisen, R., and Vollath, D., 1967, Tables of X-ray mass attenuation coefficients. Düsseldorf, Verlag Stahleisen.

Udovkina, N.G., Muravitskaya, G.N., and Laputina, I.P., 1978, Phase equilibria in the talc-garnet-kyanite rocks of the Kokchetav Block, Northern Kazakhstan. Isvestiya Akademia Nauk SSSR, Geological Section, v. 7, p. 55-64 (in Russian).

Vialon, P., 1966, Etude géologique du massif cristallin Dora Maira, Alpes cottiennes internes, Italie [Thèse d'état] Université de Grenoble. 282 p.

Ward, C.M., 1984, Magnesium staurolite and green chromian staurolite from Fjordland, New Zealand. American Mineralogist, V. 69, p. 531-540.

FIGURE CAPTIONS

Figure 1:

Geological map of the southern Dora Maira massif (after Vialon, 1966)

(1)- Paleozoic augen gneisses and metagranites

(2)- Paleozoic fine-grained gneisses and schists with eclogite lenses and marble layers. The outcrops of the pyrope-quartzite are denoted by full circles. Coesite relics occur throughout the pyrope-quartzite layer ; the two stars drawn limit the area in which, so far, coesite relics have been found in the country-rock.

(3)- Dronero and Sampeyre formations: Late Paleozoic (?) schists and meta-arkoses.

(4)- Mesozoic: Carbonated cover series and Schistes lustrés undifferentiated.

(5)- Alluvium.

The inset locates the area in the Western Alps, showing the external crystalline massifs, the Penninic Front, the internal crystalline massifs, the Sesia zone and its Dent Blanche outlier. Ge: Geneva, Ni: Nice, To: Torino.

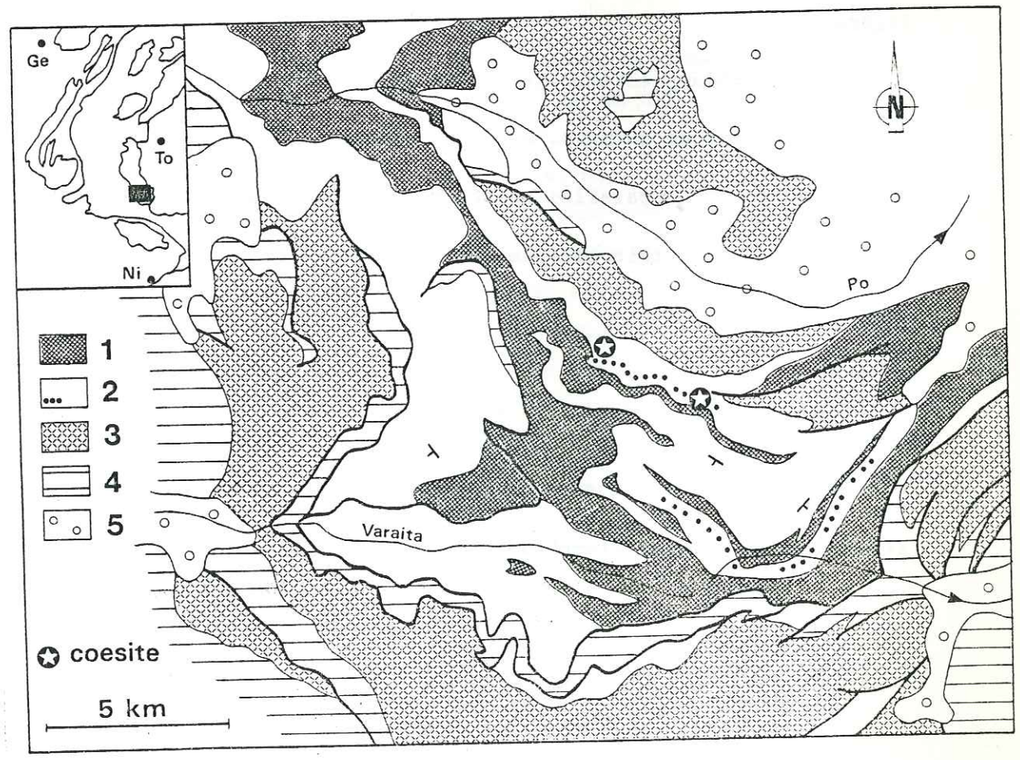

Figure 2:

The assemblage ellenbergerite(el)-chlorite(chl)-talc(tc)-kyanite(ky) in garnet porphyroblast 3-64. Note the absence of preferred orientation, the association of ellenbergerite and pyrope suggesting topotactic relationships, and the opaque rim of ellenbergerite which is absent on the garnet side. Plane polarised light.

Figure 3:

Polymineralic inclusion in garnet porphyroblast 3-64. A zoned ellenbergerite crystal is associated with talc, kyanite and minor chlorite (left hand side of the photograph). Plane polarised light.

Figure 4:

The assemblage ellenbergerite-chlorite-talc-kyanite-rutile(ru)-zircon(zr) in pyrope megacryst 4-18/19. Note the anhedral shape of ellenbergerite and the mineral orientation parallel to the main fracture system of the garnet. Zircon is surrounded by a thin selvage of both fresh and sericitised ellenbergerite. Nearly crossed nicols.

Figure 5:

Polymineralic inclusion in garnet megacryst 4-18/19, with the typical assemblage ellenbergerite-chlorite-talc-kyanite-pyrope. Crossed nicols.

Figure 6:

Fe-Mg partitioning between ellenbergerite and the coexisting phases talc, chlorite and garnet, in the four garnet porphyroblasts 3-64, 3-65, 4-18/19 and 4-55.

Figure 7:

The system TiO_2-MgO-Al_2O_3-SiO_2-H_2O and phases of interest projected from the H_2O and TiO_2 components.

Figure 8:

Chemographic analysis of the system TiO_2-MgO-Al_2O_3-SiO_2-H_2O involving the solid phases pyrope, talc, chlorite, kyanite, quartz (or coesite), ellenbergerite and rutile. The construction is based on the volume data of Table 2 and on the assumption that dehydration proceeds with temperature increase. Abbreviations: see Table 2. The inset shows the position of the relevant Fe-Mg-univariant curves (double lines) relative to the main univariant curves (simple lines) of the pure Mg system.

Figure 9:

Phase relations of ellenbergerite in the system TiO_2-MgO-Al_2O_3-SiO_2-H_2O with excess TiO_2: a tentative outline.
The grid used as basis for the MASH subsystem is drawn after Chopin and Schreyer (1983) for the relations of Mg-carpholite (Car) and Mg-chloritoid (Ctd), after Massonne et al. (1981) for reaction (2), and after unpublished experimental results of the author for reactions (3) and (4). The curve of the reaction Eb+Q=Tc+Ky+V is unconstrained on the high-pressure side; it may lie at still higher, geologically unrealistic pressures. For clarity, the curves of reactions (1), (8) and (6) have been drawn to converge toward the lower temperatures, whereas they should converge on the high-temperature side. The stability field of Mg-chloritoid is merely outlined; the assemblages alternative to chloritoid are, with increasing temperature, carpholite+chlorite+diaspore, kyanite+chlorite+diaspore, kyanite+chlorite+corundum and pyrope+corundum. Mg-staurolite and the quartz-coesite(cs) transition have been ignored.

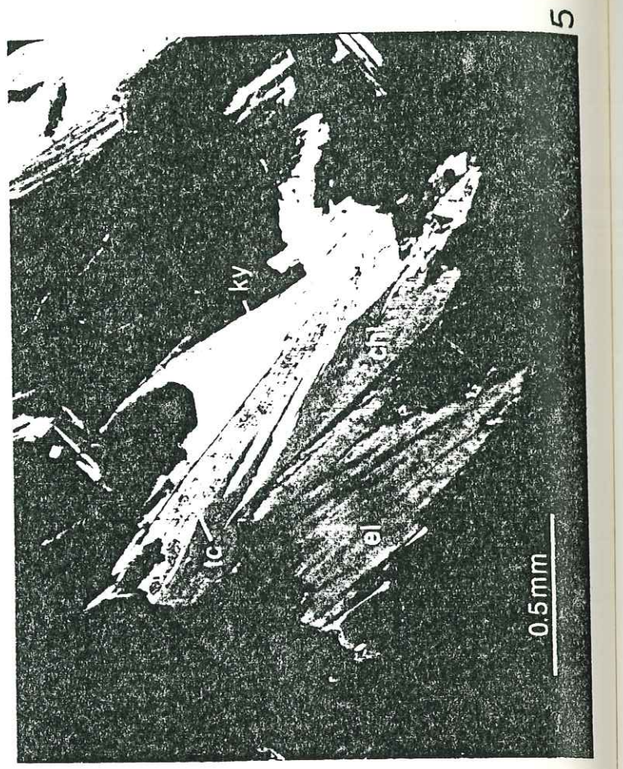

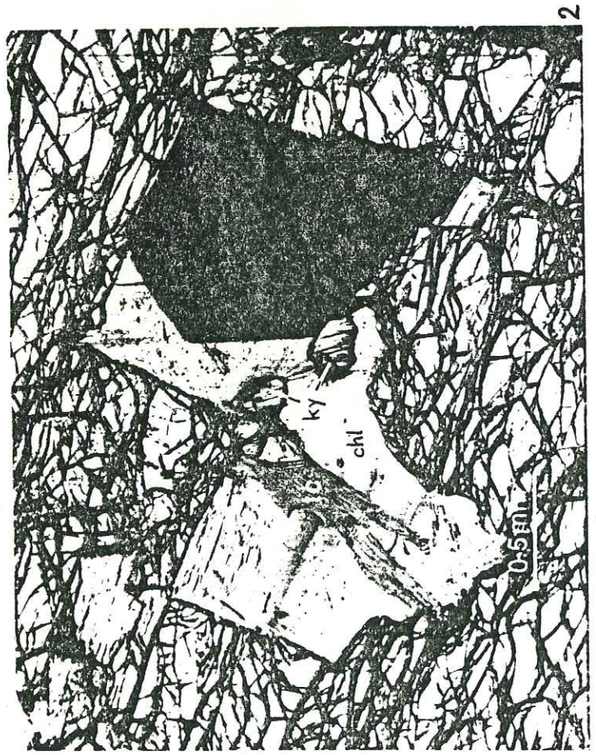

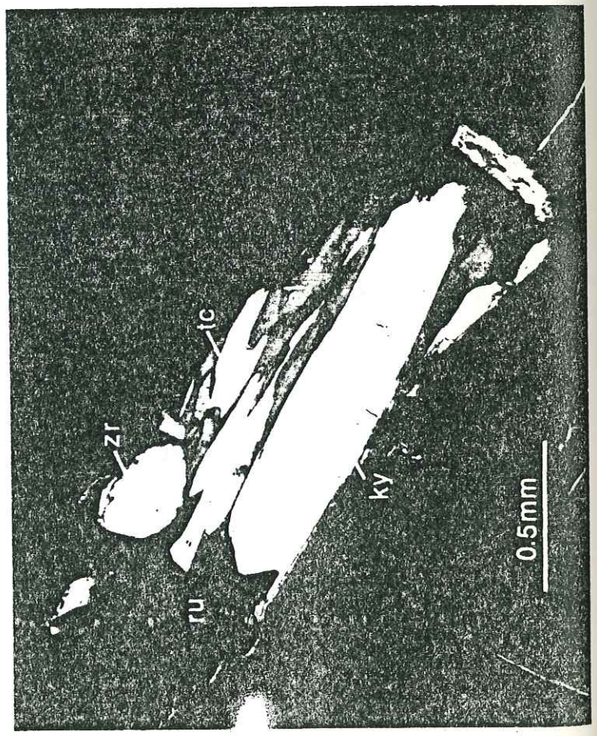

Fig. 6

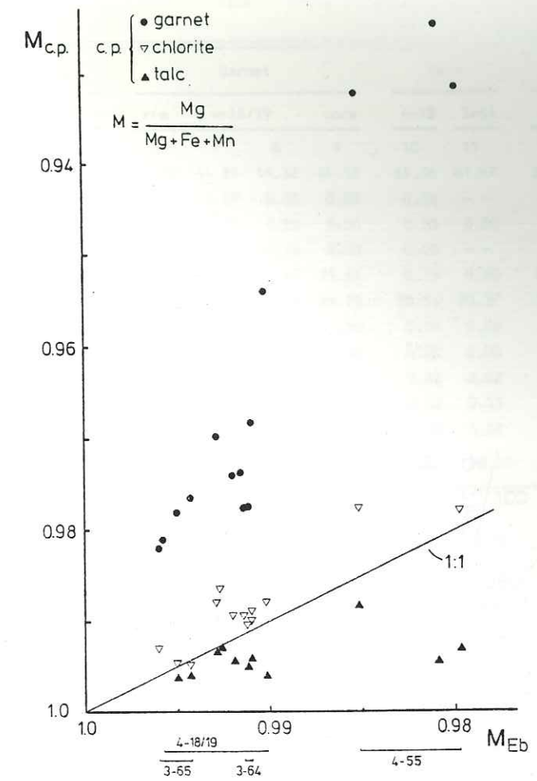

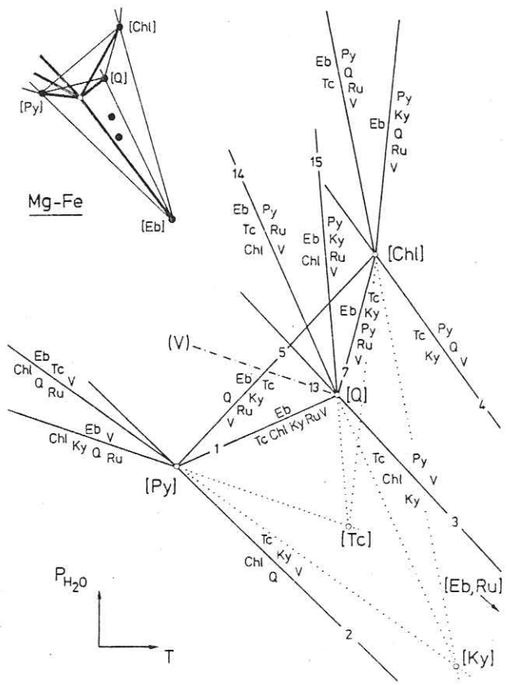

Fig. 8

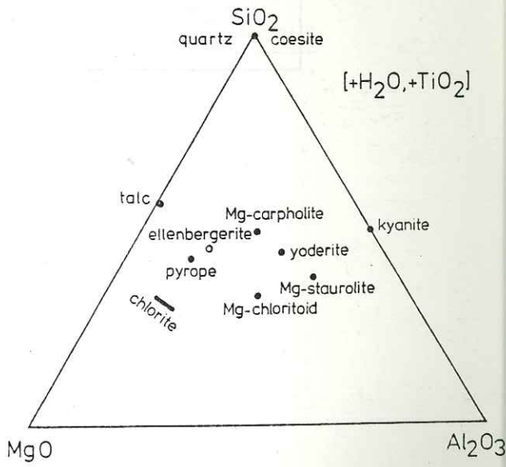

Fig. 7

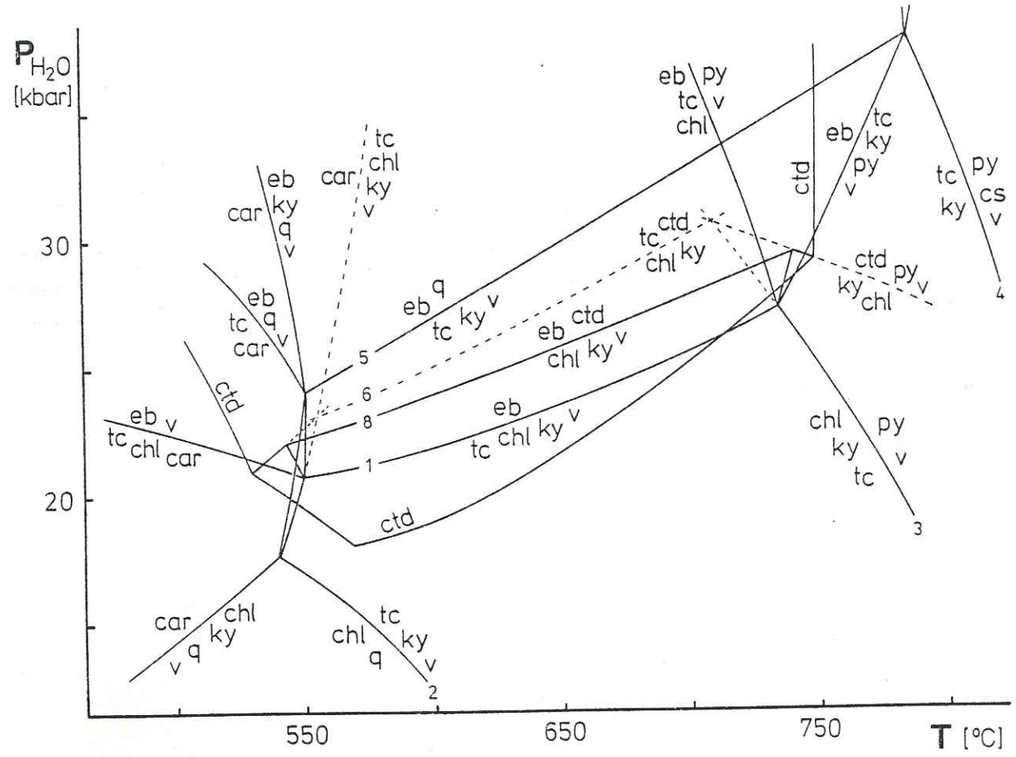

Figure 9

TABLE 1. MINERAL ANALYSES

	Ellenbergerite					Garnet				Talc		Chlorite		Amphibole		
	3-64	4-18/19				rim	4-18/19		core	4-18	3-64	4-18	3-64	4-18	3-64	4-55
	1	2	3	4	5	6	7	8	9	10	11	12	13	14	15	16
SiO_2	39.09	38.97	38.26	38.52	38.61	44.68	44.89	44.32	44.62	61.06	61.47	29.73	30.06	55.62	58.28	56.41
P_2O_5	0.44	0.15	0.19	0.05	0.00	0.10	0.09	0.03	0.05	0.06	- -	0.02	- -	0.03	- -	0.01
TiO_2	4.01	3.43	1.17	2.23	2.67	0.06	0.00	0.02	0.06	0.00	0.00	0.03	0.04	0.06	0.08	0.03
ZrO_2	0.00	0.81	3.91	2.69	1.92	0.00	0.00	0.02	0.00	0.00	- -	0.00	- -	0.03	- -	0.04
Al_2O_3	25.12	24.92	24.53	24.83	24.79	25.41	25.42	25.43	25.61	0.73	0.80	20.68	20.40	14.64	14.37	13.45
MgO	22.19	21.92	21.74	21.76	21.80	29.02	28.96	28.53	28.73	30.54	30.37	33.93	33.13	17.71	16.26	15.79
FeO	0.20	0.21	0.27	0.29	0.40	0.54	0.95	1.79	1.50	0.19	0.32	0.21	0.68	1.11	0.75	1.04
MnO	- -	0.00	0.02	0.02	0.00	0.02	0.01	0.02	0.00	0.00	0.00	0.03	0.00	0.01	0.03	0.00
CaO	- -	0.02	0.02	0.03	0.00	0.41	0.14	0.20	0.15	0.02	0.02	0.04	0.02	1.87	0.75	1.15
Na_2O	- -	0.00	0.00	0.00	0.00	0.03	0.00	0.07	0.03	0.02	0.03	0.01	0.04	4.31	5.60	6.32
K_2O	- -	0.00	0.00	0.02	0.00	0.00	0.00	0.00	0.00	0.00	0.02	0.00	0.06	0.21	0.12	- -
Total	91.05	90.43	90.11	90.95	90.19	100.27	100.46	100.43	100.75	92.62	93.03	84.65	84.43	95.60	96.24	94.24
	33 oxygens					24 oxygens				11 oxygens		14 oxygens		23 oxygens		
Si	7.92	7.98	7.97	7.96	7.98	6.00	6.02	5.98	5.98	3.97	3.98	2.84	2.88	7.49	7.74	7.70
P	0.08	0.03	0.03	0.01	-	0.01	0.01	-	0.01	-	-	-	-	-	-	-
Ti	0.61	0.53	0.18	0.35	0.42	0.01	-	-	-	-	-	-	-	-	-	-
Zr	-	0.08	0.40	0.27	0.19	-	-	-	-	-	-	-	-	-	-	-
Al	6.00	6.02	6.02	6.05	6.03	4.02	4.01	4.04	4.05	0.05	0.06	2.32	2.30	2.32	2.25	2.16
Mg	6.71	6.69	6.74	6.70	6.71	5.81	5.78	5.73	5.74	2.96	2.93	4.82	4.73	3.56	3.22	3.21
Fe	0.03	0.04	0.05	0.05	0.07	0.06	0.11	0.20	0.17	0.01	0.02	0.02	0.05	0.12	0.08	0.12
Ca	-	-	-	-	-	0.06	0.02	0.03	0.02	-	-	-	-	0.27	0.11	0.17
Na + K	-	-	-	-	-	-	0.01	0.02	-	-	-	-	0.02	1.16	1.46	1.67
Σ cat	21.35	21.37	21.39	21.39	21.40	15.97	15.96	16.00	15.97	6.99	6.99	10.00	9.98	14.92	14.86	15.03
M	0.995	0.995	0.993	0.993	0.990	0.989	0.982	0.968	0.972	0.997	0.994	0.996	0.989	0.966	0.975	0.965

TABLE 2. VOLUME CHANGE OF THE REACTIONS

Absent phases	Reaction	Label in text	ΔV/V
(Q, Py)	6 Eb = 5 Tc + 5 Chl + 13 Ky + 4 Ru + 5 V	(1)	+ 6%
(Q, Chl)	18 Eb = 35 Py + 5 Tc + 19 Ky + 12 Ru + 85 V	(7)	+ 0
(Q, Ky)	24 Eb + 6 Tc + 19 Chl = 91 Py + 16 Ru + 202 V	(14)	- 4
(Q, Tc)	12 Eb + 5 Chl = 35 Py + 6 Ky + 8 Ru + 80 V	(15)	- 2
(Q, Eb, Ru)	3 Chl + 2 Tc + 4 Ky = 7 Py + 14 V	(3)	- 8
(Q, V)	80 Tc + 35 Chl + 202 Ky + 56 Ru = 84 Eb + 35 Py	(13)	- 6
(Chl, Py)	9 Eb + 35 Q = 20 Tc + 27 Ky + 6 Ru + 25 V	(5)	+ 3
(Chl, Ky)	9 Eb + 7 Tc = 27 Py + 18 Q + 6 Ru + 52 V		- 2
(Chl, Tc)	9 Eb = 20 Py + 7 Ky + 5 Q + 6 Ru + 45 V		- 0
(Chl, Eb, Ru)	Tc + Ky = Py + 2 Q + V	(4)	- 4
(Py, Ky)	27 Chl + 91 Q + 6 Ru = 9 Eb + 25 Tc + 38 V		- 6
(Py, Tc)	4 Chl + 5 Ky + 7 Q + 2 Ru = 3 Eb + V		- 7
(Py, Eb, Ru)	3 Chl + 14 Q = 5 Tc + 3 Ky + 7 V	(2)	- 4

Abbreviations, formulae and molar volumes (in cm^3)

Chl : chlorite	$Mg_5Al_2Si_3O_{10}(OH)_8$	211.5*
Ky : kyanite	$SiAl_2O_5$	44.1†
Py : pyrope	$Mg_3Al_2Si_3O_{12}$	113.3†
Ru : rutile	TiO_2	18.8†
Tc : talc	$Mg_3Si_4O_{10}(OH)_2$	136.2†
Q : quartz	SiO_2	22.7†
V : fluid	H_2O	14.8§
Eb : ellenbergerite	$Mg_{6.67}Ti_{0.66}Al_6Si_8O_{28}(OH)_{10}$	386.0§

Data sources :

* Chernosky (1974)
† Robie et al. (1978)
§ see text

RESUME

L'étude des métapélites de haute pression des Alpes occidentales révèle une variété considérable de degrés métamorphiques, depuis un domaine à Fe-Mg-carpholite, un domaine intermédiaire à chloritoïde magnésien-talc-phengite, jusqu'à un domaine où sont stables la coesite, le pyrope et l'ellenbergerite, $(Mg,Ti,\square)_2Mg_6Al_6Si_8O_{28}(OH)_{10}$, nouveau mineral du système pélitique.

L'étude expérimentale du système $MgO-Al_2O_3-SiO_2-H_2O$ a permis la synthèse de Mg-carpholite, Mg-chloritoïde et pyrope, et la détermination de leur stabilité et relations de phases entre 480 et 800°C, 15 et 40 kbar.

Appliquées aux systèmes naturels et associées à de nouvelles datations (^{39}Ar-^{40}Ar), ces données sont intégrées dans un schéma évolutif de la chaîne alpine impliquant l'enfouissement de croûte continentale à près de 100 km de profondeur.

MOTS-CLES : métapélites, haute pression, Alpes occidentales, pétrologie, étude expérimentale, système $MgO-Al_2O_3-SiO_2-H_2O$, Mg-carpholite, Mg-chloritoïde, pyrope, coesite, ellenbergerite.